

3A  
12-20-79

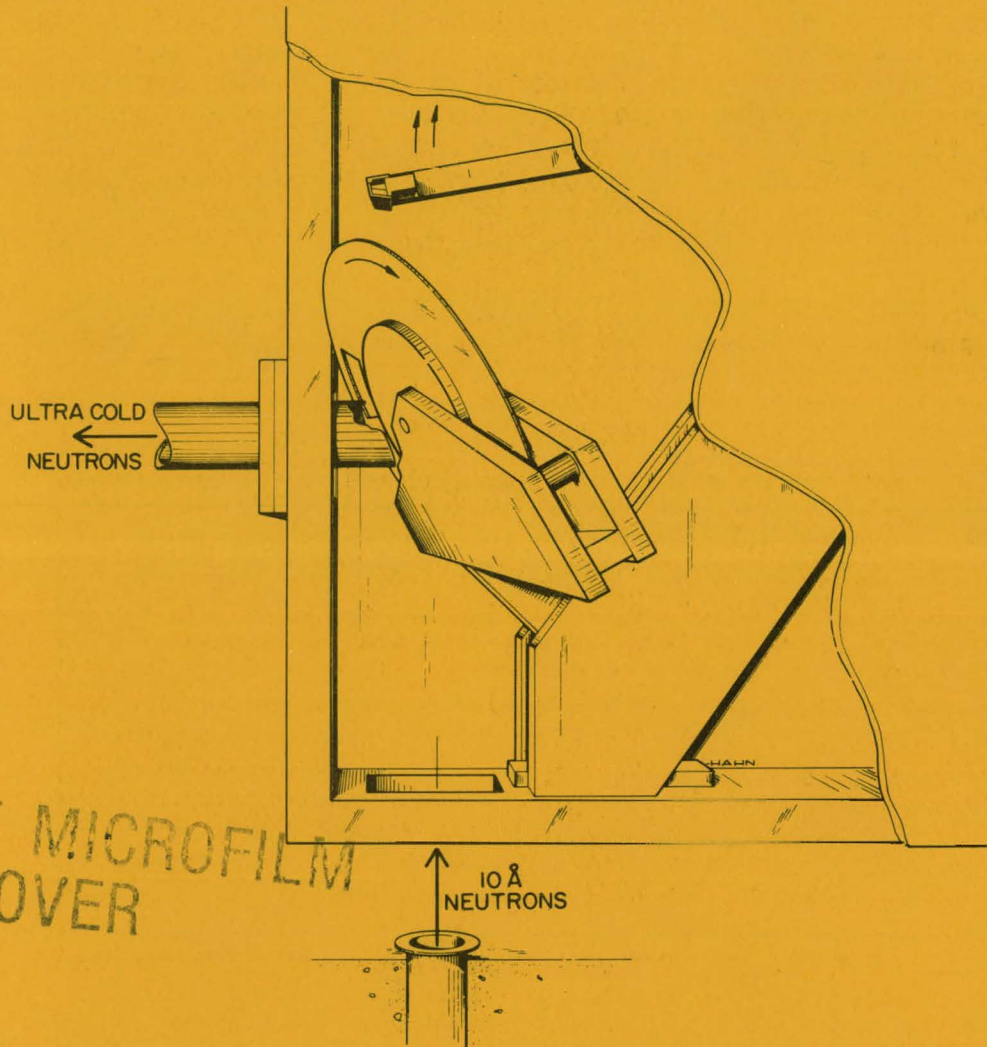
ANL-79-40

**MASTER**

14.435

ANL-79-40

**PHYSICS DIVISION  
ANNUAL REVIEW  
1 April 1978—31 March 1979**



**ARGONNE NATIONAL LABORATORY, ARGONNE, ILLINOIS**

**Prepared for the U. S. DEPARTMENT OF ENERGY  
under Contract W-31-109-Eng-38**

**DISTRIBUTION OF THIS DOCUMENT IS UNLIMITED**

## **DISCLAIMER**

**This report was prepared as an account of work sponsored by an agency of the United States Government. Neither the United States Government nor any agency Thereof, nor any of their employees, makes any warranty, express or implied, or assumes any legal liability or responsibility for the accuracy, completeness, or usefulness of any information, apparatus, product, or process disclosed, or represents that its use would not infringe privately owned rights. Reference herein to any specific commercial product, process, or service by trade name, trademark, manufacturer, or otherwise does not necessarily constitute or imply its endorsement, recommendation, or favoring by the United States Government or any agency thereof. The views and opinions of authors expressed herein do not necessarily state or reflect those of the United States Government or any agency thereof.**

## **DISCLAIMER**

**Portions of this document may be illegible in electronic image products. Images are produced from the best available original document.**

# DO NOT MICROFILM COVER

The facilities of Argonne National Laboratory are owned by the United States Government. Under the terms of a contract (W-31-109-Eng-38) among the U. S. Department of Energy, Argonne Universities Association and The University of Chicago, the University employs the staff and operates the Laboratory in accordance with policies and programs formulated, approved and reviewed by the Association.

## MEMBERS OF ARGONNE UNIVERSITIES ASSOCIATION

The University of Arizona	The University of Kansas	The Ohio State University
Carnegie-Mellon University	Kansas State University	Ohio University
Case Western Reserve University	Loyola University of Chicago	The Pennsylvania State University
The University of Chicago	Marquette University	Purdue University
University of Cincinnati	The University of Michigan	Saint Louis University
Illinois Institute of Technology	Michigan State University	Southern Illinois University
University of Illinois	University of Minnesota	The University of Texas at Austin
Indiana University	University of Missouri	Washington University
The University of Iowa	Northwestern University	Wayne State University
Iowa State University	University of Notre Dame	The University of Wisconsin-Madison

## NOTICE

This report was prepared as an account of work sponsored by an agency of the United States Government. Neither the United States nor any agency thereof, nor any of their employees, makes any warranty, expressed or implied, or assumes any legal liability or responsibility for any third party's use or the results of such use of any information, apparatus, product or process disclosed in this report, or represents that its use by such third party would not infringe privately owned rights. Mention of commercial products, their manufacturers, or their suppliers in this publication does not imply or connote approval or disapproval of the product by Argonne National Laboratory or the United States Government.

Printed in the United States of America  
Available from  
National Technical Information Service  
U. S. Department of Commerce  
5285 Port Royal Road  
Springfield, VA 22161

NTIS price codes  
Printed copy: A13  
Microfiche copy: A01

Distribution Category:  
Physics—General (UC-34)

ANL--79-40

ARGONNE NATIONAL LABORATORY  
9700 South Cass Avenue  
Argonne, Illinois 60439

PHYSICS DIVISION ANNUAL REVIEW  
1 APRIL 1978—31 MARCH 1979

Murray Peshkin, Acting Division Director

Preceding Annual Reviews:

ANL-76-96, Annual Review 1975—1976  
ANL-77-60, Annual Review 1976—1977  
ANL-78-66, Annual Review 1977—1978

**DISCLAIMER**

This report was prepared as an account of work sponsored by an agency of the United States Government. Neither the United States Government nor any agency thereof, nor any of their employees, makes any warranty, express or implied, or assumes any legal liability or responsibility for the accuracy, completeness, or usefulness of any information, apparatus, product, or process disclosed, or represents that its use would not infringe privately owned rights. Reference herein to any specific commercial product, process, or service by trade name, trademark, manufacturer, or otherwise does not necessarily constitute or imply its endorsement, recommendation, or favoring by the United States Government or any agency thereof. The views and opinions of authors expressed herein do not necessarily state or reflect those of the United States Government or any agency thereof.

*[Signature]*

## FOREWORD

The Physics Division Annual Review presents a broad but necessarily incomplete view of the research activity within the Division for the year ending in April 1979.

At the back of this report a complete list of publications along with the Divisional roster can be found.

## TABLE OF CONTENTS

	<u>Page</u>
NUCLEAR PHYSICS RESEARCH	1
INTRODUCTION	1
I. THE SUPERCONDUCTING LINAC	3
INTRODUCTION	3
A. HEAVY-ION ENERGY BOOSTER	4
1. MAIN FEATURES OF THE DESIGN	4
2. STATUS OF THE PROJECT	7
3. BOOSTER OPERATIONAL EXPERIENCE	10
4. NEAR-TERM PLANS	13
B. INVESTIGATIONS OF SUPERCONDUCTING LINAC TECHNOLOGY	16
1. LOW- $\beta$ RESONATOR	16
2. RESONATOR PERFORMANCE	18
3. RESONATOR DIAGNOSTIC TECHNIQUE	19
4. FAST TUNER	19
5. ASYMMETRY IN ACCELERATING FIELD	20
6. BEAM-DYNAMICS COMPUTER PROGRAMS	20
C. PROPOSAL FOR ATLAS	21
II. MEDIUM-ENERGY PHYSICS	23
INTRODUCTION	23
a. <u>Properties of Pion Single-Charge-Exchange Reactions in Nuclei</u>	24
b. <u>Study of Pion Absorption Mechanisms in <math>^4\text{He}</math> and Other Nuclei</u>	25
c. <u>Gamma-Ray Study of Pion-Induced Reactions on the Nickel Isotopes</u>	26

	<u>Page</u>
<u>d. Scattering of Pions by Complex Nuclei</u>	27
<u>e. Inelastic Pion Scattering from Light Nuclei: <math>^{10}\text{B}</math>, <math>^{11}\text{B}</math>, <math>^{14}\text{N}</math></u>	29
<u>f. Excitation of High-Spin Particle-Hole States in <math>^{28}\text{Si}</math></u>	30
<u>g. Pion Double-Charge-Exchange Reactions</u>	30
<u>h. Low-Energy Pion Elastic Scattering from the Proton and Deuteron at <math>180^\circ</math></u>	32
 <b>III. HEAVY-ION RESEARCH AT THE TANDEM AND SUPERCONDUCTING LINAC ACCELERATORS</b>	 35
<b>INTRODUCTION</b>	35
<b>A. RESONANT STRUCTURES IN HEAVY-ION REACTIONS</b>	36
<u>a. Resonant Effects in the <math>^{24}\text{Mg}(^{16}\text{O}, ^{12}\text{C})^{28}\text{Si}</math> Reaction at Forward Angles</u>	36
<u>b. Resonant Effects in the <math>^{24}\text{Mg}(^{16}\text{O}, ^{12}\text{C})^{28}\text{Si}</math> and <math>^{24}\text{Mg}(^{16}\text{O}, ^{16}\text{O})^{24}\text{Mg}</math> Reactions at Backward Angles</u>	38
<u>c. Analysis of the <math>^{24}\text{Mg}(^{16}\text{O}, ^{12}\text{C})^{28}\text{Si}</math> Reaction</u>	39
<u>d. Search for Resonant Structures in the Excitation Functions of the <math>^{26}\text{Mg}(^{16}\text{O}, ^{14}\text{C})^{28}\text{Si}</math>, <math>^{48}\text{Ca}(^{16}\text{O}, ^{14}\text{C})^{50}\text{Ti}</math>, and <math>^{26}\text{Mg}(^{16}\text{O}, ^{12}\text{C})^{30}\text{Si}</math> Reactions</u>	39
<u>e. Search for Resonant Structure in the <math>^{24}\text{Mg}(^{16}\text{O}, ^{12}\text{C})</math> Reaction to States in <math>^{28}\text{Si}</math> Between 5 and 12-MeV Excitation Energy</u>	41
<b>B. FUSION CROSS SECTIONS</b>	43
<u>a. Systematics of <math>^{12}\text{C}</math> and <math>^{16}\text{O}</math> Induced Fusion on Targets <math>12 \leq A \leq 19</math></u>	43
<u>b. The Fusion of <math>^{12}\text{C} + ^{24}\text{Mg}</math> and <math>^{12}\text{C} + ^{26}\text{Mg}</math></u>	45
<u>c. The Fusion Cross-Section Behavior for <math>^{15}\text{N} + ^{27}\text{Al}</math></u>	47
<u>d. Fusion of <math>^{16}\text{O} + ^{40}\text{Ca}</math> at <math>E_{\text{lab}} = 315</math> MeV</u>	48
<b>C. HIGH ANGULAR MOMENTUM STATES IN NUCLEI</b>	49
<u>a. Yrast Traps Near the Closed Neutron Shell <math>N = 82</math></u>	49

	<u>Page</u>
b. <u>Very-High-Spin States in <math>^{152}\text{Dy}</math></u>	50
c. <u>Recoil-Distance-Lifetime and Linear-Polarization Measurements of <math>^{152}\text{Dy}</math></u>	51
d. <u>High-Spin Yrast States in <math>^{151}\text{Dy}</math></u>	51
e. <u>(<math>^{12}\text{C}</math>, xn) Studies of <math>^{151,152}\text{Dy}</math></u>	53
f. <u>High-Spin States in <math>^{150}\text{Dy}</math></u>	53
g. <u>Spectroscopic Studies of High-Spin States in <math>^{148,149}\text{Dy}</math> and <math>^{148}\text{Tb}</math></u>	56
<b>D. OTHER HEAVY-ION EXPERIMENTS</b>	<b>58</b>
a. <u>Energy Dependence of the Inelastic Scattering of <math>^{16}\text{O}</math> on <math>^{40}\text{Ca}</math></u>	58
b. <u>Interactions of <math>^{32}\text{S}</math> Beam from the Argonne Superconducting Post Accelerator with <math>^{40,48}\text{Ca}</math> Target Nuclei</u>	61
c. <u>Energy-Loss Straggling Measurements for <math>^{16}\text{O}</math> and <math>^{32}\text{S}</math> Ions in Thin Carbon Foils</u>	61
d. <u>Radioisotope Dating with the FN Tandem Accelerator</u>	63
e. <u>Pd(<math>^{16}\text{O}</math>, xn)Xe</u>	65
f. <u>Heavy-Ion Coulomb Excitation in <math>^{148,150,152,154}\text{Sm}</math></u>	66
g. <u>Radiation-Damage Enhanced Trapping of Hydrogen in Molybdenum</u>	67
h. <u>Radiative Capture of <math>^{12}\text{C}</math> by <math>^{12}\text{C}</math> Near the Coulomb Barrier</u>	67
<b>IV. CHARGED-PARTICLE RESEARCH</b>	<b>69</b>
<b>INTRODUCTION</b>	<b>69</b>
<b>A. CHARGED-PARTICLE RESEARCH AT THE DYNAMITRON</b>	<b>70</b>
a. <u>Interpretation of <math>d + ^6\text{Li}</math> Reactions at Low Energies</u>	70
b. <u>Absolute Cross Sections for Three-Body Breakup Reactions <math>^6\text{Li}(d, n ^3\text{He}) ^4\text{He}</math> and <math>^6\text{Li}(d, p ^3\text{H}) ^4\text{He}</math></u>	71

	<u>Page</u>
c. <u>The <math>^6\text{Li}(p, ^3\text{He})^4\text{He}</math> and Other Reactions of Light Ions with <math>^6\text{Li}</math> at Low Energies</u>	71
d. <u>Cross Sections for Three-Body Breakup in <math>^3\text{He} + ^6\text{Li}</math> Reactions at Low Energy</u>	73
e. <u><math>^8\text{Li}(\beta^-, a)a</math> and <math>^8\text{B}(\beta^+, a)a</math> Angular Correlations</u>	75
f. <u>Parity Violation in the 5.1-MeV <math>J=2</math> Doublet of <math>^{10}\text{B}</math></u>	76
g. <u>Measurement of the Direct Capture Reaction <math>^2\text{H}(^4\text{He}, \gamma)^6\text{Li}</math></u>	78
h. <u>Search for Neutral Currents in <math>^6\text{Li}</math></u>	79
i. <u>Search for Neutral Currents in <math>^{20}\text{Ne}</math></u>	79
j. <u>Measurement of the <math>T=2</math> Level in <math>^{24}\text{Al}</math></u>	80
 B. CHARGED-PARTICLE RESEARCH AT THE TANDEM ACCELERATOR	 81
a. <u>Coulomb Shifts in Mirror Nuclei of the <math>f_{7/2}</math> Shell</u>	81
b. <u>Gamma Decay in <math>^{45}\text{V}</math></u>	82
c. <u>States in <math>^{47}\text{Cr}</math></u>	84
d. <u>Magnetic Moment of the First Excited State of <math>^{99}\text{Mo}</math></u>	84
e. <u>Measurements of Astrophysical Interest</u>	84
 V. ACCELERATOR OPERATIONS AND DEVELOPMENT	 95
INTRODUCTION	95
 A. OPERATION OF THE TANDEM-LINAC ACCELERATOR	 96
1. RECENT OPERATING EXPERIENCE FOR THE TANDEM	96
2. OPERATION OF THE SUPERCONDUCTING LINAC	96
3. UPGRADING OF THE TANDEM	97
a. <u>Ion Sources</u>	97
b. <u>Vacuum Systems</u>	98
c. <u>Terminal Box</u>	99
d. <u>Stripping Foils</u>	99

	<u>Page</u>
e. <u>Beam Bunching</u>	100
4. INSTALLATION OF THE BOOSTER	100
5. PLANNED ACCELERATOR-SYSTEM IMPROVEMENTS	100
a. <u>Tandem Improvements</u>	100
b. <u>Linac Improvements</u>	101
6. EXPERIMENTAL FACILITIES DEVELOPMENT AT THE SUPERCONDUCTING-LINAC BOOSTER	102
a. <u>New Beam Line for the Superconducting Linac Booster</u>	102
b. <u>Layout and Installation of the Zero-Degree Beam Line in the New Experimental Area</u>	103
c. <u>Beam Optics Calculations</u>	103
d. <u>65-in. Scattering Chamber in New Target Area</u>	104
e. <u>Split-Pole Spectrograph in the New Experimental Area</u>	104
f. <u>Sum/Multiplicity Detector for <math>\gamma</math> Rays</u>	105
g. <u>Nuclear Target Making and Development</u>	105
7. UNIVERSITY USE OF THE TANDEM ACCELERATOR	106
B. DYNAMITRON OPERATIONS	109
1. OPERATIONAL EXPERIENCE OF THE DYNAMITRON	109
2. UNIVERSITY USE OF THE DYNAMITRON	112
 VI. NEUTRON AND PHOTONUCLEAR PHYSICS	117
INTRODUCTION	117
A. MEASUREMENT OF THE ELECTRIC DIPOLE MOMENT OF THE NEUTRON	119
B. PHOTONUCLEAR PHYSICS	121
a. <u>NaI Spectrometers</u>	121
b. <u>Photon Scattering by the Giant Dipole Resonance</u>	121
c. <u>Photodisintegration of the Deuteron</u>	122
d. <u>R-Matrix Analysis of the <math>^{13}\text{C}(\gamma, n_0)^{12}\text{C}</math> Reaction             Below an Excitation of 9.3 MeV</u>	125

	<u>Page</u>
e. <u>Effects of Channel and Potential Radiative Transitions in the <math>^{17}\text{O}(\gamma, n_0)^{16}\text{O}</math> Reaction</u>	125
f. <u>Doorway Resonances in <math>^{29}\text{Si}</math></u>	127
g. <u>The Giant M1 Resonance in <math>^{119}\text{Sn}</math></u>	128
h. <u>Absence of Large M1 Excitations in <math>^{208}\text{Pb}</math> Below 8.4 MeV</u>	128
i. <u>Polarization in Nuclear Reactions Involving Photons</u>	131
j. <u>Background Photoneutrons from <math>W(\gamma, n)</math> at Radiation Therapy Centers</u>	131
k. <u>Study of the <math>^6\text{Li} + n</math> System Below 4 MeV</u>	132
l. <u>Neutron Interaction with <math>^{12}\text{C}</math> in the Few-MeV Region</u>	132
 VII. THEORETICAL PHYSICS	 133
INTRODUCTION	133
A. HEAVY-ION DIRECT REACTIONS	135
a. <u>Heavy-Ion Coupled-Channel Calculations — Sequential Iteration</u>	136
b. <u>Heavy-Ion Coupled-Channel Calculations — Coulomb Excitation</u>	136
c. <u>Ptolemy: A Computer Program for Heavy-Ion Direct Reactions. Light-Ion Version</u>	137
d. <u>Ingoing-Wave Boundary-Condition Model for Heavy-Ion Elastic Scattering</u>	138
e. <u>The "Sensitive Radius" in Heavy-Ion Elastic Scattering</u>	138
B. NUCLEAR SHELL THEORY AND NUCLEAR STRUCTURE	140
a. <u>Interpretive Model for <math>^{10}\text{B}</math></u>	140
b. <u>Transition Densities in the 1p Shell</u>	140
c. <u>Transverse E2 Form Factor for <math>^{12}\text{C}(e, e')</math></u>	142
d. <u>Forbidden Beta Decay in <math>^{205}\text{Tl}</math></u>	142
e. <u>The Isotensor Term in the Isobaric-Mass-Multiplet Equation</u>	143

	<u>Page</u>
f. <u>Isospin Mixing Between T=0 and T=1 States in the 1p Shell</u>	144
g. <u>Isospin Mixing in <math>^{19}\text{F}</math></u>	144
h. <u>The <math>f_{7/2}</math> Nuclei</u>	145
C. NUCLEAR MATTER	146
a. <u>Solution of the Three-Body Equations in Nuclear Matter</u>	146
b. <u>Model Bose Gases</u>	148
D. INTERMEDIATE-ENERGY PHYSICS	150
a. <u>Phenomenological Determination of the Baryon-Baryon Interactions from N-N and <math>\pi</math>-d Scattering Data</u>	151
b. <u>Reaction Theory for Pion Nucleus Interaction</u>	151
c. <u>Momentum-Space DWIA Studies of Pion-Nucleus Inelastic Scattering</u>	152
d. <u>Momentum-Space Coupled-Channel Calculations of Pion-Nucleus Inelastic Scattering</u>	153
E. DENSE NUCLEAR MATTER AND CLASSICAL CALCULATIONS OF THE HIGH-ENERGY COLLISIONS OF HEAVY IONS	154
a. <u>Nonrelativistic CEOM Calculations with Static and Momentum-Dependent Potentials</u>	154
b. <u>Programs to Analyze the Physical Content of the CEOM Calculations</u>	156
c. <u>Relativistic CEOM Calculations</u>	157
d. <u>Macroscopic and Microscopic Descriptions of High-Energy Heavy-Ion Collisions</u>	157
e. <u>Dense Nuclear Matter</u>	157
F. RADIATIVE TRANSITIONS AND NUCLEAR RESONANCE REACTIONS	159
a. <u>A Theoretical Description of Quantum Beats of Recoil-Free Gamma Radiation</u>	159
b. <u>Resonance Peak Shapes in Molecular Photo-ionization Mass Spectroscopy</u>	162

	<u>Page</u>
c. <u>Effects of Channel and Potential Radiative Transitions in the <math>^{17}\text{O}(\gamma, n_0)^{16}\text{O}</math> Reaction</u>	162
d. <u>Nuclear Mass Relations</u>	163
e. <u>Absolute Cross Sections for Three-Body Breakup Reactions <math>^6\text{Li}(d, n)^3\text{He}4\text{He}</math> and <math>^6\text{Li}(d, p)^3\text{H}4\text{He}</math></u>	163
f. <u>Low-Energy <math>d + ^6\text{Li}</math> Reactions</u>	164
EXPERIMENTAL ATOMIC AND MOLECULAR PHYSICS RESEARCH 167	
INTRODUCTION	167
VIII. EXPERIMENTAL ATOMIC AND MOLECULAR PHYSICS 169	
A. DISSOCIATION AND OTHER INTERACTIONS OF ENERGETIC MOLECULAR IONS IN SOLID AND GASEOUS TARGETS	169
a. <u>Dissociation of Fast Molecular Ions in Gases</u>	170
b. <u>Modifications to the Apparatus</u>	171
B. BEAM-FOIL RESEARCH AND COLLISION DYNAMICS OF HEAVY IONS 175	
a. <u>Excitation of Hydrogen by a Thin Carbon Foil</u>	176
b. <u>An Analysis of the Time Evolution of Atomic Observations</u>	177
c. <u>Temperature Dependence of Alignment Production in HeI by Beam-Foil Excitation</u>	177
d. <u>Fine Structure of Doubly-Excited States of 3-Electron Ions</u>	178
e. <u>Lamb Shift and Fine Structure of <math>n = 2</math> in Cl XVI</u>	178
f. <u>Spectroscopy of 3-, 4-, and 5-Electron Ions</u>	178
g. <u>Energies and Lifetimes of Excited States of Kr VIII</u>	179
h. <u>Charge-Changing Cross Section of Xe on Xe</u>	179

	<u>Page</u>
C. PHOTOIONIZATION-PHOTOELECTRON RESEARCH	182
1. ONE-METER PHOTOIONIZATION MASS SPECTROMETER	183
a. <u>Photoionization Mass Spectrometry of UF<sub>6</sub></u>	183
b. <u>Production of Doubly-Charged Ions in Vacuum-Ultraviolet Photoionization</u>	184
2. THREE-METER PHOTOIONIZATION MASS SPECTROMETER	185
a. <u>Collisional Ionization in Argon</u>	185
b. <u>Comparison of Single-Photon and Multiphoton Ionization Near Threshold</u>	186
c. <u>Detailed Study of Molecular Autoionization</u>	186
3. PHOTOELECTRON SPECTROSCOPY	188
a. <u>Photoelectron Spectroscopy of Higher Temperature Vapors</u>	188
b. <u>Partial Photoionization Cross Sections of Atomic Iodine: Irreducible Tensor Analysis of Intensities</u>	192
c. <u>Photoelectron Spectroscopy of Phthalocyanine Vapors</u>	192
d. <u>Photoelectron Spectroscopy of Trinuclear Metal Complexes</u>	193
e. <u>Photoelectron Spectroscopy of Sulfur Nitrides</u>	194
4. PHOTOELECTRON-PHOTOION COINCIDENCE SPECTROSCOPY	194
a. <u>Improved Apparatus for Fixed Wavelength Photoelectron-Photoion Coincidence Spectroscopy</u>	194
b. <u>Predisociation of C<sub>2</sub>H<sub>2</sub><sup>+</sup>, H<sub>2</sub>S<sup>+</sup>, and D<sub>2</sub>S<sup>+</sup> Ions</u>	195
c. <u>Angular Distributions of Photoelectrons from Orientated Molecules</u>	197
D. SPECTROSCOPY OF FREE ATOMS	200
1. HIGH-RESOLUTION SPECTROSCOPY WITH TUNABLE LASERS AND ATOMIC BEAMS	200
a. <u>High-Precision Studies of the hfs of <sup>51</sup>V</u>	200

	<u>Page</u>
b. <u>Ultrahigh Precision Measurements of the hfs of Several Levels of <math>^{235}\text{U}</math></u>	201
c. <u>Enhancement of Isotope Separation Efficiency</u>	204
d. <u>Identification of Previously Unclassified Spectral Lines in Terbium</u>	205
2. STUDY OF HIGH-RYDBERG ATOMS	205
E. MÖSSBAUER EFFECT RESEARCH	207
1. GENERATION OF DELAYED ULTRASOUND IN LOW TEMPERATURE COPPER	207
2. QUANTUM BEATS OF RECOIL-FREE $\gamma$ RAYS	208
<u>Measurement of the Second-Order Doppler Shift in Beryllium Doped with Iron by the Method of Harmonic Ratio of Gamma-Ray Quantum Beats</u>	210
3. IODINE IN UNIDIMENSIONAL, MIXED-VALENCE SOLIDS	211
a. <u>Charge Transfer and Partial Oxidation in the Conductive Hydrocarbon-Iodine Complex "2perylene.3I<sub>2</sub>"</u>	211
b. <u>Rational Synthesis of Unidimensional, Mixed-Valence Solids. Structure-Oxidation State-Charge Transport Relationships in Iodinated Nickel and Palladium Bisbenzoquinonedioximates</u>	212
F. MONOCHROMATIC X-RAY BEAM PROJECT	213
APPLIED PHYSICS	
INTRODUCTION	215
IX. APPLIED PHYSICS	217
A. INTERACTION OF ENERGETIC PARTICLES WITH SOLIDS	217
1. THE EFFECT OF DOSE ON THE EVOLUTION OF CAVITIES IN 500-keV $^4\text{He}^+$ -ION IRRADIATED NICKEL	219

	<u>Page</u>
2. SURFACE EFFECTS INDUCED BY SIMULATED PLASMA	225
a. <u>Temperature Dependence of the Relationship Between Blister Diameter and Blister Skin Thickness for Helium-Ion-Irradiated Nb</u>	225
b. <u>Surface Damage of TFTR Protective Plate Candidate Materials by Energetic D<sup>+</sup> Irradiation</u>	227
c. <u>Damage of Niobium Surfaces Caused by Bombardment with <sup>4</sup>He<sup>+</sup> Ions of Different Energies Typical for T-20</u>	230
B. SCANNING SECONDARY-ION MICROPROBE	236
MICROSCOPIC LOCATION OF TRACER ISOTOPES	236
PUBLICATIONS FROM 1 APRIL 1978 THROUGH 31 MARCH 1979	239
STAFF MEMBERS OF THE PHYSICS DIVISION	263

# NUCLEAR PHYSICS RESEARCH

## INTRODUCTION

The research program in nuclear physics concerns itself with gaining understanding of the properties of atomic nuclei, their structures, and their reactions with different probes. Work is carried out under different subprograms: heavy-ion, medium-energy, theory, charged-particle, and neutron physics. Those categories do not reflect sharp divisions between people; the same individuals participate in several subprograms more often than not. This flexibility allows scientific problems to be addressed as they come up with reasonable resources, without having to define people as being members of a given group.

The Physics Division operates two major accelerators—the FN tandem with the developing superconducting booster, and the 4-MV Dynamitron. The tandem is used almost entirely for nuclear research by Argonne staff and university users. About 30% of the time on the Dynamitron is used in nuclear studies. Photonuclear research is carried out at the Chemistry Division's electron linac and, during the past year, at the University of Illinois Urbana microtron. The medium-energy program is centered on the LAMPF facility at Los Alamos.

### Highlights

In heavy-ion research the chief accomplishment during the past year has been the successful operation of the superconducting linac booster. Beams of  $^{16}\text{O}$  and  $^{32}\text{S}$  were accelerated by superconducting resonators with an equivalent accelerating field in excess of 5 MV. These beams were sufficiently stable and well behaved that they were used in prototype experiments. In other heavy-ion work the investigation of sharp resonances has been continued and a rather sophisticated program of their analysis is being carried out. The investigations of very high angular momentum states in heavy nuclei have continued to be very active and fruitful.

In medium-energy physics two inclusive measurements were carried out—one of  $(\pi^+, \pi^0)$  reactions and the other of high-energy protons produced by pions in nuclei. Both measurements covered a range of energies and target nuclei, and help to substantially constrain our understanding of pion interaction modes with nuclei. High-resolution studies of inelastic pion scattering at EPICS have probed the isospin impurities of nuclei.

In nuclear theory the culmination of a ten-year study of nuclear matter has been achieved and important results obtained on the detailed influence of internal nuclear structure on inelastic pion scattering from light nuclei. For nuclear matter it is now possible to start from a given nucleon-nucleon interaction and to compute the ground-state energy with an accuracy of 1 to 2 MeV/nucleon and the equilibrium density to about 5%. It has been shown that DWIA, with nuclear wave functions and effective multipole operators that accurately reproduce known electromagnetic multipole transition rates, gives a good account of the systematics of the inelastic scattering of pions of near-resonant energy from 1p-shell nuclei.

In charged-particle research considerable progress has been made in fabricating a polarized  $^6\text{Li}$  target for the study of  $\Delta T=1$ , parity violation in the  $^6\text{Li}(\alpha, \gamma)^{10}\text{B}$  reaction through the 5.11- and 5.16-MeV states of  $^{10}\text{B}$ . The spectroscopy of  $1f_{7/2}$ -shell nuclei is continued. The  $N=Z$  nuclei  $^{66}\text{As}$  and  $^{70}\text{Br}$  have been produced and attempts are being made to measure the endpoint energies and half-lives of their  $0^+ \rightarrow 0^+$  decays.

In neutron physics an ANL-university collaboration is attempting an experiment, using magnetically-bottled ultracold neutrons, to improve the limits on (and perhaps to measure) the electric dipole moment of the neutron. This would provide a critical test of a number of theories by exploring the limits of the expected breakdown of CP invariance. The photoneutron program has continued—a measurement of inelastic photon scattering through the giant resonance was carried out by a collaboration with the University of Illinois group.

## I. THE SUPERCONDUCTING LINAC

R. Benaroya, L. M. Bollinger, K. W. Shepard, T. P. Wangler,  
J. Aron, \* B. E. Cliff, \* A. H. Jaffey, \* K. W. Johnson, \*  
P. Markovich, \* and J. M. Nixon \*

### INTRODUCTION

The Superconducting Linac Project has two main components, both of which are developmental in nature. One is the specific task of designing, building, and testing a small superconducting linac to serve as an energy booster for heavy ions from the present FN tandem electrostatic accelerator. The second, more general part, consists of investigations of various aspects of superconducting rf technology. Although most of these investigations are now aimed at the immediate needs of the booster, many of them are of fairly general interest for accelerator technology.

Both parts of the Superconducting Linac Project are jointly supported and administered by the Chemistry and Physics Divisions.

---

\* Chemistry Division, ANL.

## A. HEAVY-ION ENERGY BOOSTER

The booster project, started in mid-1975, is concerned with the design, construction, installation, and testing of a small superconducting linear accelerator (linac) to serve as an energy booster for heavy-ion beams from the FN tandem accelerator. The principal objective of the project is to develop a new accelerator technology and to build the prototype for a heavy-ion energy booster that can be used to upgrade the performance of any tandem accelerator. The overall design is highly modular in character in order to provide maximum flexibility for future modifications and/or improvements. Two sections of the planned booster went into operation in 1978, and the installation of a third section will be completed by the end of 1979. A fourth section will be added in 1980.

The highlight of the work reported here is the initial testing and use of the partly completed booster. Heavy-ion beams were first accelerated in June 1978, followed by increasingly long operating periods in September and December 1978 and in March-April 1979. By the time of the last period, the operation was aimed primarily at providing beams for nuclear-physics experiments.

### 1. MAIN FEATURES OF THE DESIGN

A schematic representation of the booster as it is expected to be in 1980 is shown in Fig. I-1. The heart of the system is the split-ring resonator, a three-gap structure made of superconducting niobium. Superconducting solenoids at frequent intervals confine the radial excursions of the beam. The basic accelerating section of the linac consists of a linear array of these resonators and solenoids within a cryostat that can be isolated from the others both with respect to vacuum and cryogenics. The general characteristics of an accelerator section may be judged from Fig. I-2, which shows section C during assembly.

The four sections of the booster make use of resonators that have two lengths. One type is 35.6 cm long and is optimized for a projectile velocity  $\beta \equiv v/c = 0.105$  (sections C and D). A second type is 20.3 cm long and is optimized for  $\beta = 0.060$  (sections A and B). The

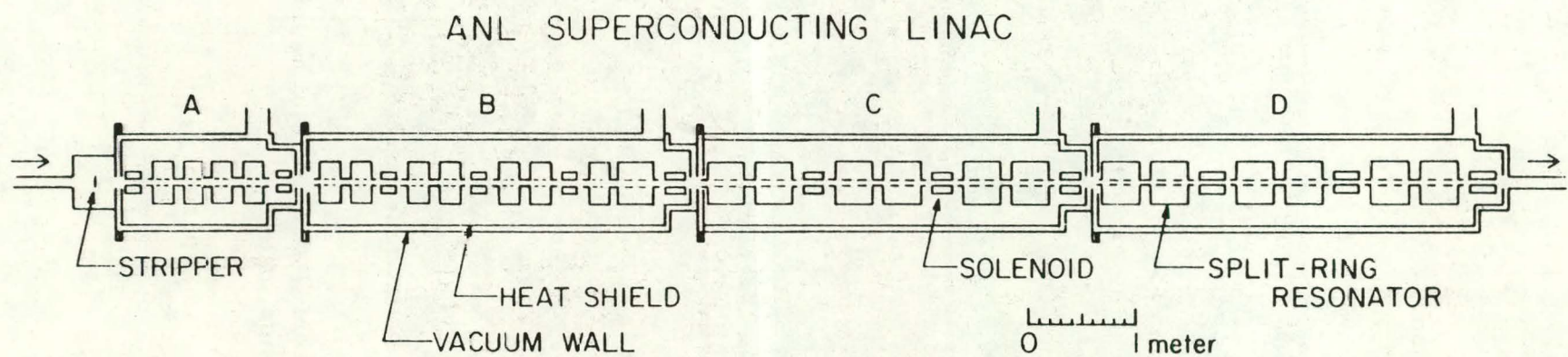


Fig. I-1. Schematic representation of the heavy-ion booster ABCD.

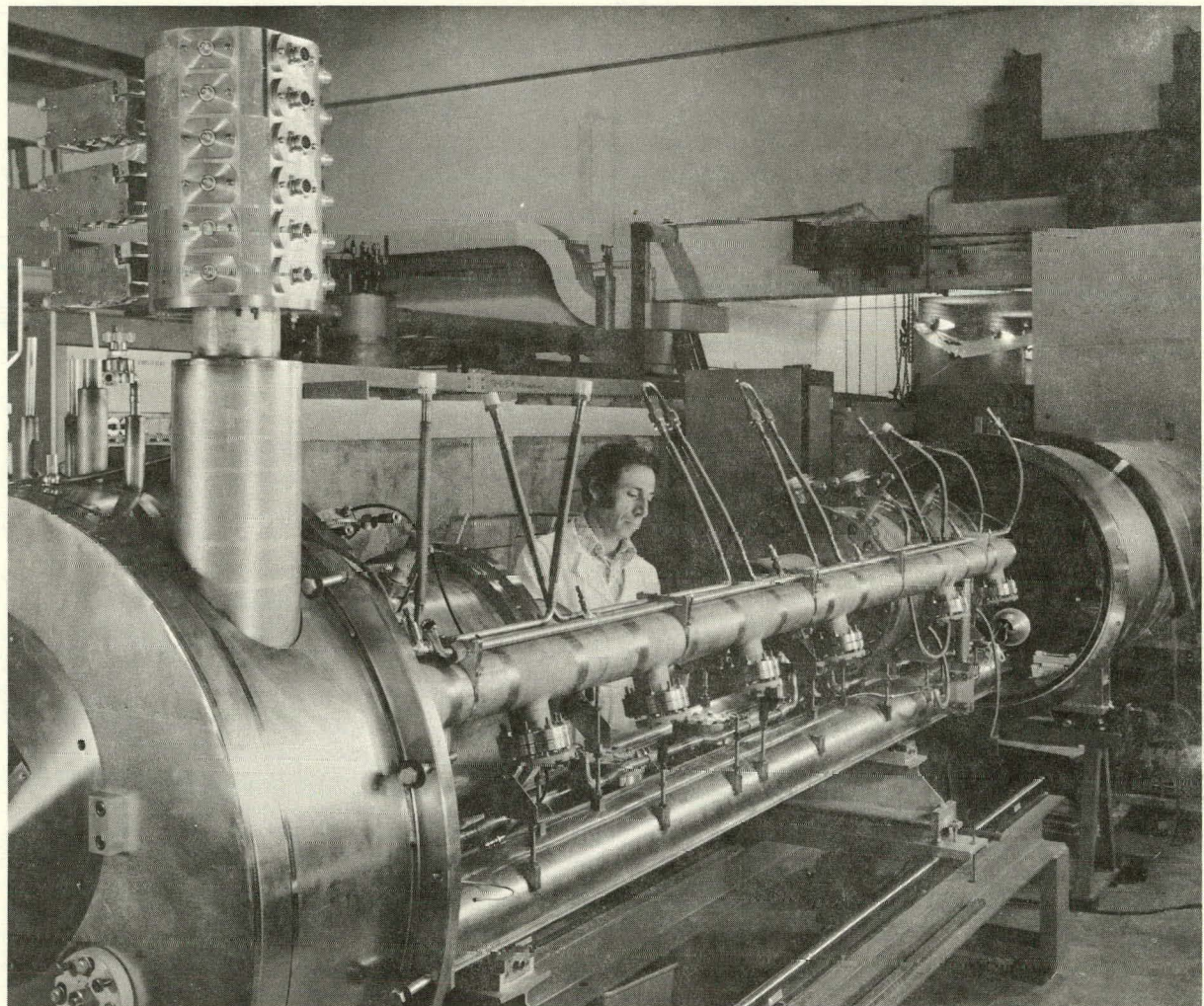


Fig. I-2. Accelerator section C at a stage of assembly when four of six high- $\beta$  resonators have been installed.

resonators are cooled to a temperature of  $4.7^{\circ}\text{K}$  by forced-flow, two-phase helium from a 95-watt refrigerator.

The total rf power required for the linac is only 2.4 kW. This is to be compared with a need for at least 1.3 MW of rf power for an equivalent room-temperature linac. The control of the linac as a whole is accomplished with the assistance of a dedicated small computer. This approach allows rapid tune-up of the accelerator.

The beam from the linac passes into a small new target room that will house a large scattering chamber, an existing magnetic spectrograph, and various specialized reaction chambers. The layout of the area is planned so that a debunching/rebunching resonator can be added (in 1980) to manipulate the phase ellipse of the output beam to meet the needs of the experimenter.

For ions in the lower half of the periodic table, the 4-section booster will be equivalent to that of a very large ( $\sim 30\text{-MV}$  terminal) tandem. A sophisticated beam-bunching system will allow the beam out of the linac to have the same good quality as the beam from the tandem. The beam energy can be varied easily by changing the phase and/or amplitude of the last resonator.

## 2. STATUS OF THE PROJECT

In general terms, the status of the project in March 1979 is that the heavy-ion booster is a working reality, with two of the accelerator sections in operation: section C is functional with its full complement of 6 high- $\beta$  resonators, whereas section A is being used temporarily with two high- $\beta$  resonators rather than with low- $\beta$  units planned ultimately. This 8-resonator system is being operated for long periods of time with the dual objectives of thoroughly testing performance and of providing beams for nuclear-physics experiments. An overall view of this system is pictured in Fig. I-3.

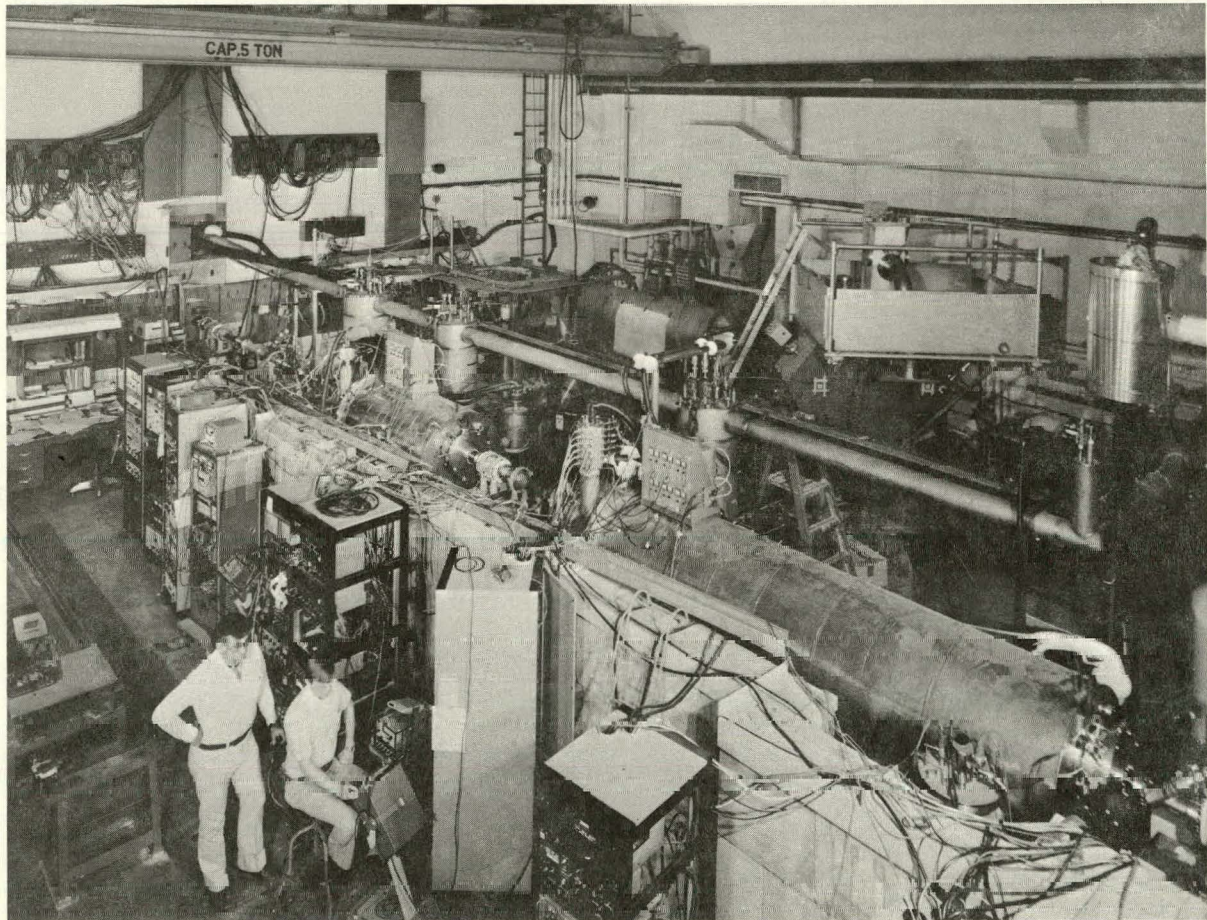


Fig. I-3. Overall view of the linac area in early 1979. The rf power and control electronics is in the foreground and section A and C are on line in the background.

### High- $\beta$ Resonators

Eight resonators are in operation and the fabrication of four additional units is nearing completion.

The techniques of resonator fabrication have been perfected to the point where new units usually perform well without developmental effort. The maximum field gradient for individual resonators now averages 3.9 MV/m, when the resonators are tested in an off-line cryostat. For a variety of reasons, the useful fields obtainable in the beam-line cryostats are somewhat lower on the average ( $\sim 3.0$  MV/m), but the beam-line performance is being steadily improved.

### Low- $\beta$ Resonator

A prototype of the low- $\beta$  resonators required for section A has been completed, and an initial test shows that its design is successful.

### Cryostats

Cryostats A and C are in use, and their main design features are proving to be excellent. In particular, the end-loading design is making it exceptionally easy to assemble resonators and to make improvements in the system. The assembly of cryostat D has started and the work will be completed by mid-1979.

### Helium Refrigeration and Distribution System

The helium system is fully functional and is being used routinely to cool the booster and to provide liquid helium for precooling operations and for the operation of a test cryostat.

Although the helium system operates well, the refrigeration capacity is inadequate for routine operation of the full booster as a research tool. The inadequate capacity of a 95-watt refrigerator was recognized from the inception of the booster project, but it was judged that it would

be advantageous to have a small, easily-operated system during the developmental phase of the booster project. In order to provide the capacity needed for long-term operation, we hope to be able to add a second helium refrigerator soon.

#### rf Control System

The rf-control system consists of two major parts: a local hard-wired control for each resonator and a computer-based system to monitor and control the booster as a whole. The hard-wired circuitry has by now been extensively used and has proven to be generally effective. A number of detailed changes have been made on the basis of operational experience, and little additional work is planned.

The computer-based control system is functional, and it effectively performs the most elementary operations of booster control. Additional effort is still required to develop the software to the point where more complex operations can be carried out.

### 3. BOOSTER OPERATIONAL EXPERIENCE

Beam-acceleration tests were carried out in June, September, and December of 1978, and in March-April 1979. These tests involved use of the complete bunching system and various combinations of resonators in sections A and C, which were configured in the way shown in Fig. I-4. The accelerated beam was studied by means of a surface-barrier detector in a scattering chamber after the booster. Initially, the primary purpose of the tests was to investigate the accelerator system, but in the later tests increasing emphasis was placed on providing beams for nuclear-physics experiments.

In the June 1978 tests, two resonators were used to accelerate a beam of  $^{19}\text{F}^{6+}$  ions. The voltage gain provided by the booster was 1.6 MV. These first tests demonstrated that tuning the linac is straightforward,

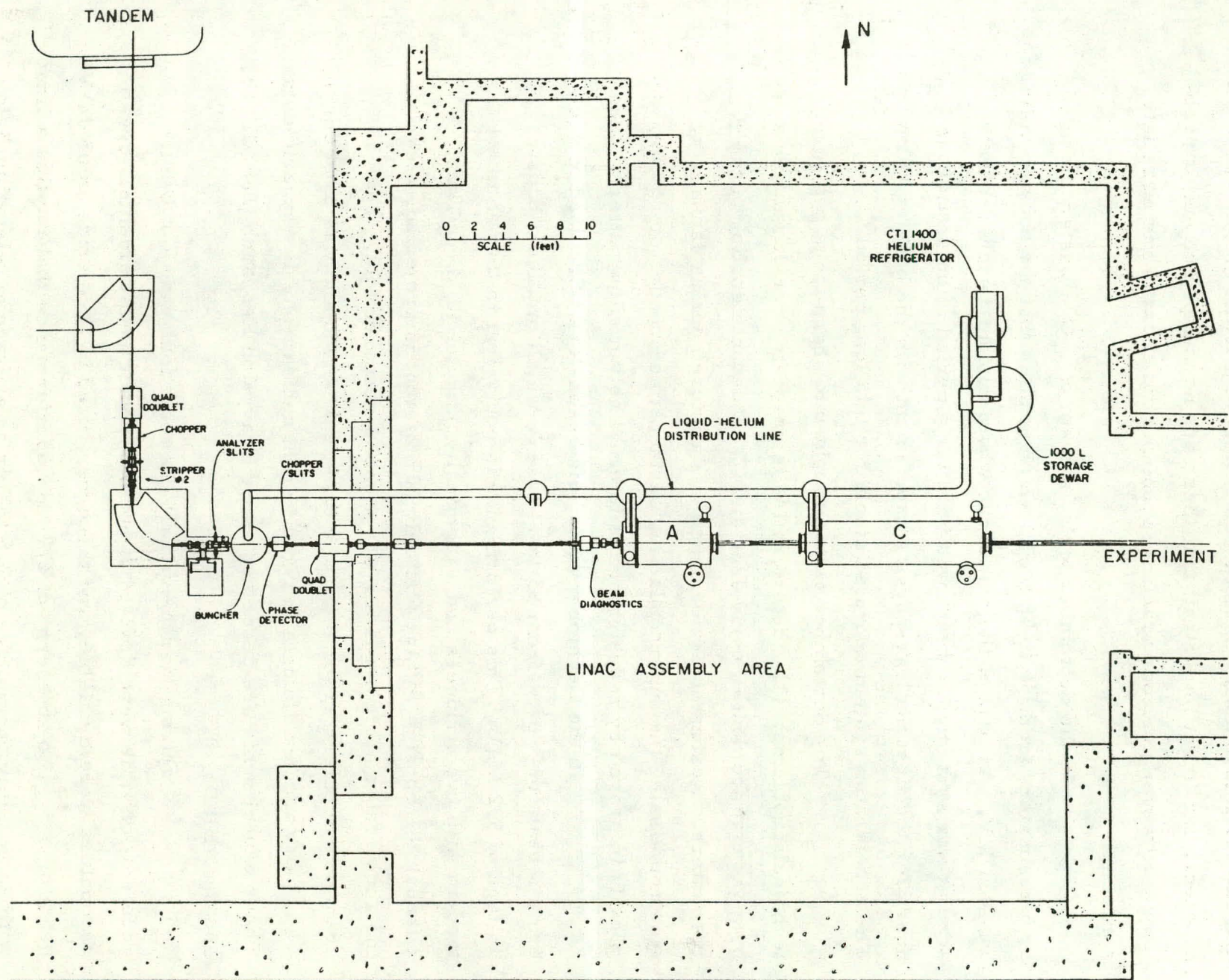


Fig. I-4. Booster configuration for the beam acceleration tests of 1978 and early 1979.

that the axial asymmetry in the accelerating field is not an important problem, and (most important) that there are no unexpected major problems. However, various practical problems did show up and were later corrected.

In the September tests, a beam of  $^{16}\text{O}^{6+}$  was accelerated by 5 resonators from 56 to 78 MeV, which implies that the booster voltage was 4.1 MV. As part of the test of the whole tandem-buncher-booster accelerator system, the beam was used for a period of 56 continuous hours for the first nuclear-physics experiment with the booster beam. The accelerator system operated stably for this long period.

The September tests brought into sharp focus two severe technical problems: (1) a deterioration in resonator performance caused by a vacuum accident in early June and (2) inadequate cooling of the resonators. Resonator performance was restored during January by electropolishing the superconducting surfaces; and resonator cooling was greatly improved by redesigning the internal helium-flow pattern.

In the December tests, six resonators were used to accelerate a beam of  $^{32}\text{S}^{14+}$  from 85 to 148 MeV, which implies a booster voltage of 5.2 MeV. This performance is equivalent to that of an MP tandem with two strippers and a terminal voltage of 12 MV. Thus, although the booster voltage was only 20% of what is projected, clearly the accelerator system was already a useful research tool. The  $^{32}\text{S}$  beam was accelerated for most of a two-week period and was used during  $\sim$ 6 days to accumulate data in two different nuclear-physics experiments. These experiments are described under Heavy-Ion Research (Sec. III. Cf, g and Sec. III. Db, c).

During March-April 1979, about four weeks of beam-acceleration time were devoted to nuclear-physics experiments. Seven resonators were available, and these were used to accelerate an 85-MeV beam of  $^{32}\text{S}^{14+}$  to an energy of 177 MeV, performance that implies a linac with an accelerating voltage of 7.6 MV or an average accelerating field of 3.0 MV/m.

The overall reliability of the booster was substantially greater than it had been in the earlier runs. As a result, it was not necessary to have an operator in the area most of the time. The linac-development crew were available on an on-call basis, but the experimenters using the beam were easily able to fix most of the occasional malfunctions. It is increasingly clear that the booster is going to be an easy machine to operate.

#### 4. NEAR-TERM PLANS

During the remainder of 1979, the booster will continue to be operated with the dual objectives of developing the technology and of providing a useful beam for nuclear-physics experiments. The booster will be operated approximately one-third of the time, with the periods between operation being devoted to the installation of new components and to the removal of various technical defects. Both the accelerating power of the booster and the reliability of its operation are expected to increase substantially during the coming year. The performance at various stages of completion is given in Fig. I-5.

Three major additions to the booster are planned for the near-term future. The first is to complete and install the third accelerator section (D) by late 1979. The enlarged system will contain at least 12 resonators and will provide an accelerating voltage in the range 12-14 MV. For ions with  $A < 40$ , this performance will provide a beam energy that is roughly equivalent to that of an 18-MV tandem with two strippers.

The second major task is to install a rebuncher/debuncher resonator on the beam line from the booster. Its function will be to deliver to the experimenter either very short ( $< 100$  ps) beam pulses or, alternatively, to improve the energy resolution. This system is expected to be functional in early 1980.

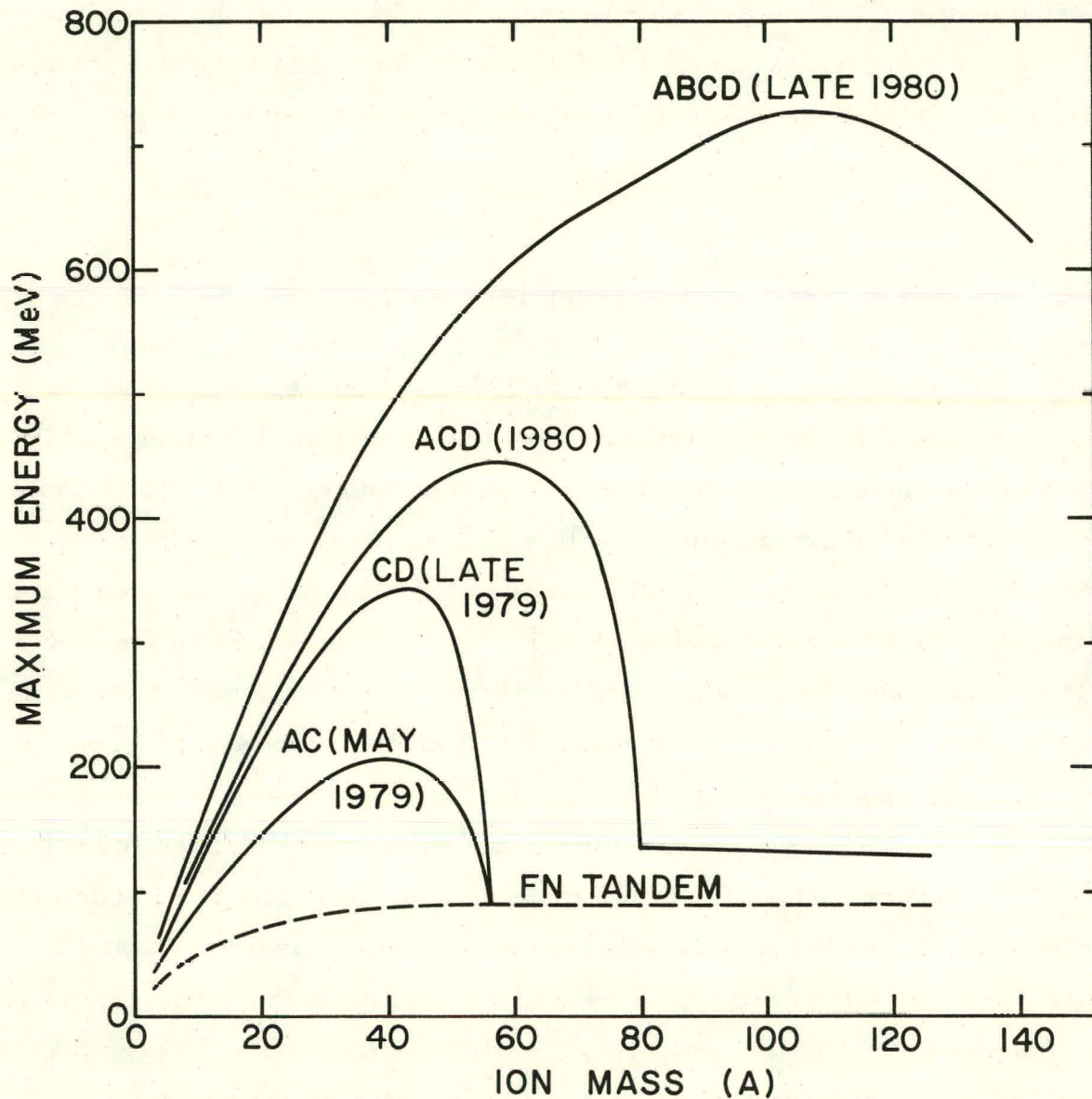


Fig. I-5. Booster performance at various stages of completion.

The third task is to remove the present restriction on the projectile mass by installing low- $\beta$  resonators in section A (late 1979) and then in B (late 1980), thus completing the four-section booster described by Fig. I-1.

## B. INVESTIGATIONS OF SUPERCONDUCTING LINAC TECHNOLOGY

This research program, carried out jointly by the Chemistry and Physics Divisions, is concerned with investigations of the general aspects of applications of superconducting technology to the acceleration of heavy ions. Most of the recent activities have been related to the development of an accelerating structure of the split-ring type made of niobium. Investigations of this type will continue, but the program will gradually be broadened to include developmental work on other aspects of accelerator technology, including the development of superconducting magnets for use in bending and analyzing heavy-ion beams.

### 1. LOW- $\beta$ RESONATOR

Sections A and B of the heavy-ion booster require a type of resonator designed to give optimum acceleration for ions with a relative velocity  $\beta = 0.06$ . The design of a low- $\beta$  resonator of this kind was started in 1978, and the fabrication of the prototype was completed in late December 1978. The drift-tube assembly of the resonator is pictured in Fig. I-6.

In all essentials, the low- $\beta$  resonator is similar to the fully-developed high- $\beta$  resonators now in use in section C. However, design of the unit involved the new problem of matching the rf frequency accurately to the 97 MHz of the high- $\beta$  resonator. This was achieved by a combination of modeling and calculation.

Only preliminary tests on the low- $\beta$  prototype have been carried out to date. The unit worked well on the first attempt, giving an accelerating field of 3.4 MV/m for 4 watts of rf power dissipation. At this field level, the main source of power loss is electron loading, and it is expected that the field level will be pushed higher by reducing this loading.

In view of the good performance of the low- $\beta$  prototype, the fabrication of production-model units will start soon without any significant changes in design.

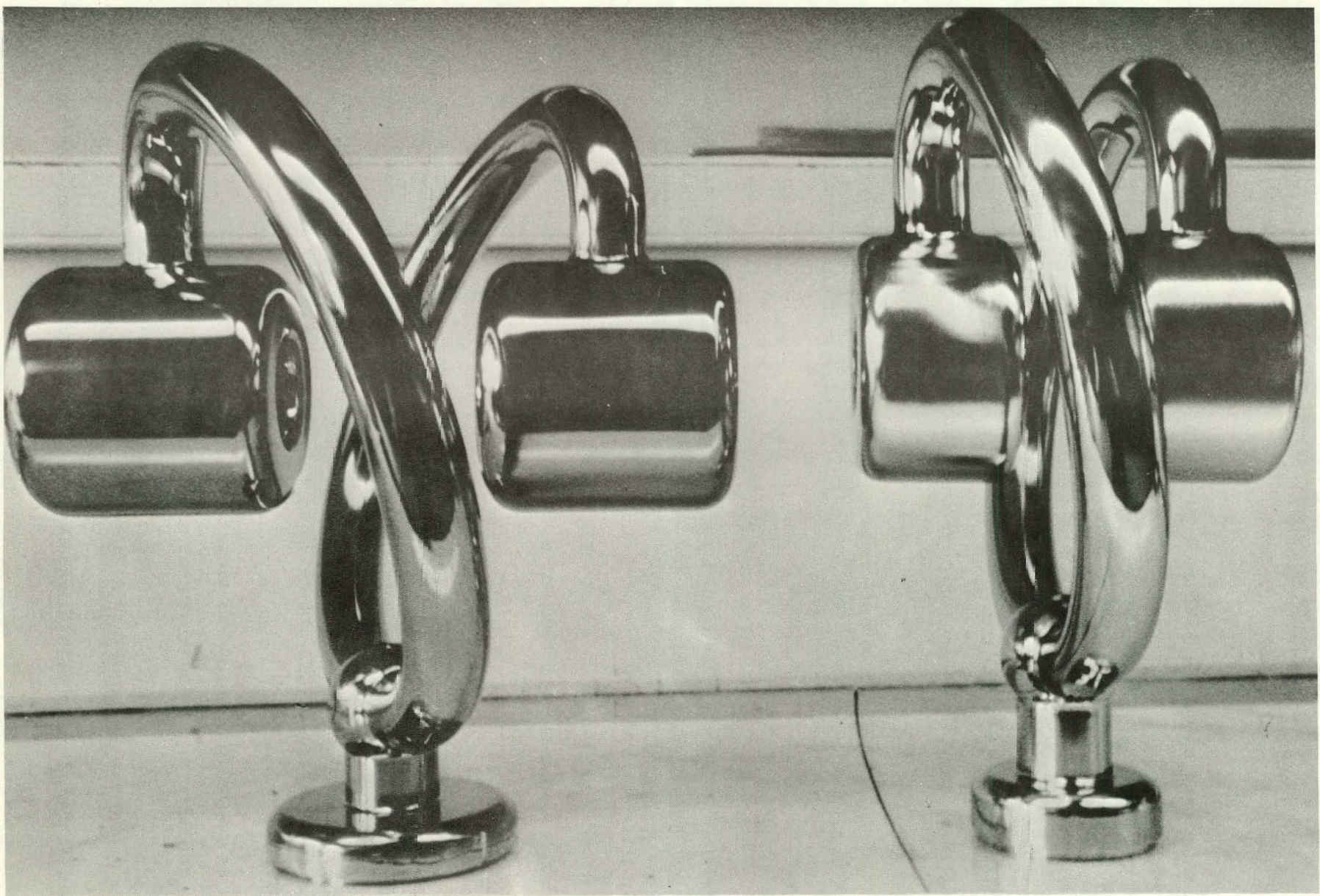


Fig. I-6. Comparison of the drift-tube assemblies of high- $\beta$  (left) and low- $\beta$  resonators.

## 2. RESONATOR PERFORMANCE

Investigations aimed at understanding and pushing back the limitations on the performance of superconducting resonators have started. This work, which will extend over several years, is expected to lead to significant improvements in the performance of superconducting heavy-ion linacs. The work initiated recently includes (1) the development of techniques for conditioning superconducting resonators, (2) the study of the stability of resonator performance, especially under beam-line conditions, and (3) the development of techniques for restoring resonators whose performance has been degraded.

Substantial progress has been made in the development of conditioning techniques that increase the maximum accelerating field of the split-ring resonator. The basic approach is the technique of "helium conditioning," introduced several years ago. The effectiveness of this technique has been enhanced recently by exciting the resonators with a high-power pulsed amplifier rather than, as previously, with CW power. In this way and with our present 400-W amplifier, it is usually feasible to extend the field limit by about 15%. On the basis of the results obtained to date, it seems possible that electron loading can be removed as the primary limitation on the accelerating field of the high- $\beta$  split-ring resonator.

A systematic effort is being made to monitor resonator performance over long periods of time and under various conditions in order to establish the conditions needed to ensure stable long-term performance. It has not yet been established with certainty whether or not resonator performance remains unchanged as a result of normal beam-line operation, but it has been shown that the change (if any) is small during a month of high-power operation.

Certain abnormal conditions, such as a vacuum explosion that occurred in beam-line cryostat C in June 1978, can degrade resonator performance to a significant degree. Thus, it is important to know how to

restore degraded resonators to good performance. We have found that each of six resonators involved in the vacuum accident mentioned above was easily restored to at least its original performance by electropolishing away about  $40 \mu$  of material from its superconducting niobium surface.

### 3. RESONATOR DIAGNOSTIC TECHNIQUE

Until recently, we have been unable to obtain quantitative information about the performance of resonators in the beam-line cryostats because of an inability, in these cryostats, to determine the quality factor  $Q$  from rf measurements. This problem has now been partially solved by the development of a technique in which the heat dissipated by a resonator in liquid helium (a few watts) is measured directly. In this technique, the whole helium refrigeration and distribution system is used, in effect, as a calorimeter. Even though the total power dissipated in the refrigeration system is 75 kW, a change of heat input as small as  $\frac{1}{2}$  W can be detected with ease.

The new diagnostic technique is being used for two purposes:  
(1) to study and monitor the performance of the helium system itself and  
(2) to measure the rf power that resonators dissipate into helium. This latter function will be used to monitor resonator performance over long periods of time.

### 4. FAST TUNER

Development of the special voltage-controlled reactance (VCX) used as a fast tuner for the split-ring resonators has continued. This device consists of an air-gap condenser that can be shorted out by a PIN-diode switch. The compact size of the device is a controlling feature of the whole linac design.

Since the fast tuner associated with each resonator is inside the cryostat, a resonator can be eliminated from useful phase-controlled operation if any one of six parallel PIN diodes in its fast tuner is shorted out. This kind of failure has happened occasionally. The problem has now been largely removed by fusing each individual diode in such a way that, if it shorts out, it can be eliminated from the circuit by blowing its fuse from outside the cryostat. This arrangement has been used successfully under beam-line operating conditions.

## 5. ASYMMETRY IN ACCELERATING FIELD

Because the split-ring accelerating structure is not axially symmetrical, the electrical field along the beam axis necessarily has a transverse component, and this component tends to steer the beam off axis. During 1978, the magnitude of the transverse field was measured by means of the dielectric-bead technique, and the effect was found to be unimportant for our resonators. This result has now been confirmed by a direct measurement of the beam steering caused by the high- $\beta$  resonators.

## 6. BEAM-DYNAMICS COMPUTER PROGRAMS

The development of computer programs is continuing. Our earlier work resulted in programs suitable for studying the basic properties of acceleration through a system of independently-phased resonators, and these programs were used in the design of the booster. We have now undertaken the additional task of making a program that is convenient and cost-effective enough to permit the linac operator to use it routinely and interactively as the main guide as to how to tune the linac for optimum performance.

### C. PROPOSAL FOR ATLAS

The Argonne Tandem-Linac Accelerator System (ATLAS) is a proposed heavy-ion accelerator that would be formed by enlarging the booster now being assembled and by adding a large new target area, as shown in Fig. I-6. The resulting system, consisting of the existing tandem and a 7-section linac, will have a performance that is approximately equivalent to that of a 50-MV tandem with two strippers.

ATLAS is aimed squarely at the needs of precision nuclear-structure physics, providing beam energies up to 25 MeV/A, easy energy variability, and beams of exceptionally good quality. The short-pulse character of the beam will be emphasized so as to maximize its usefulness for time-of-flight and other timing measurements. An unusual feature of the facility is the capability of providing beams simultaneously for two independent experiments without a loss of intensity to either.

The ATLAS proposal has been resubmitted to the Department of Energy for funding in fiscal year 1981. The proposal was reviewed by the Facilities Subcommittee of DOE/NSF Nuclear Science Advisory Committee (NUSAC) in March 1979, following which the parent committee strongly recommended that the project be funded. Quoting from the NUSAC report: "The demonstrated successful performance of the vital components of this system is the basis for a confident recommendation to proceed with the accelerator construction project described in this proposal. By utilizing breakthroughs in the technology of superconducting rf cavities the facility will be able to provide a unique research capability, equivalent to that of a 50 MV tandem Van de Graaff, which will permit the precision study of heavy-ion reactions in an unexplored energy regime. The subcommittee is unanimous in its recommendation that the ATLAS proposal be given highest priority for early funding based on its cost effectiveness, the technical feasibility of its innovative design and the scientific merit of the research program which it will make possible."

THIS PAGE  
WAS INTENTIONALLY  
LEFT BLANK

## II. MEDIUM-ENERGY PHYSICS

## INTRODUCTION

Medium-energy research in the Argonne Physics Division continued to develop and flourish in the past year and the ANL staff assumed new obligations as participants in the LAMPF research program. In one area of study, efforts of the Argonne group focused on measurements of "inclusive" spectra of charged particles, neutral pions from nuclear charge-exchange reactions, and nuclear-decay  $\gamma$  rays. Recently, the Argonne group demonstrated and easily implemented a simple new technique for direct observation of neutral pions. These  $(\pi^+, \pi^0)$  measurements provided a body of qualitatively new data; and the trends displayed in the first results suggest, quite unexpectedly, that the bulk of this reaction proceeds through a quasi-free scattering process favoring large momentum transfer. These measurements were continued in the past year with the acquisition of a comprehensive body of data for a range of targets and beam conditions. The results make clear the need for similar studies of inelastic pion scattering. To that end, the Argonne group has undertaken primary responsibility for construction of a Large Acceptance Pion Spectrometer (ALAS) at LAMPF, to be developed as a multipurpose instrument eventually available to all LAMPF users. In addition, studies of high-energy particle spectra, which probe the initial phases of pion-nucleus reactions have continued, as part of our program to contribute to the data base necessary to the development of a coherent theory of pion-nucleus interactions.

High-resolution studies of elastic and inelastic pion scattering using the EPICS spectrometer are a second major component of the program. The studies of elastic scattering provide information on the average pion-nucleus interaction and its description in terms of the optical model. Measurements of inelastic scattering are made for nuclei where details of the nuclear structure are well understood, and the data can be used to obtain information about features of the pion-nucleus reaction mechanism such as isospin dependence. The results, together with data from other laboratories at lower energies will provide a complete picture of pion-nucleus scattering, and will be of major importance in the development of precise optical-model descriptions of pion-nucleus interactions.

Several experiments directed at an understanding of the pion-nucleon interaction have also been prepared in the last year. Direct measurements of pion-nucleon scattering at  $180^\circ$  using the LAMPF Low Energy Pion Channel as a spectrometer are planned. Data at  $180^\circ$  are

particularly useful in constraining global phase-shift solutions to pion-nucleon scattering. A proposal to study doubly-radiative pion capture was also submitted for consideration of the LAMPF program committee. The latter experiment would explore the character of the pion-nucleon coupling for kinematic conditions "off the energy shell." Argonne participation continued in the LAMPF collaboration on measurement of double-charge exchange of pions, a uniquely mesonic reaction. Analysis of a substantial body of data collected in earlier runs has continued and a substantial theoretical effort has demonstrated that the details of the nuclear structure of the targets studied can explain puzzling trends in the data.

a. Properties of Pion Single-Charge-Exchange Reactions in Nuclei

T. J. Bowles, D. F. Geesaman, R. J. Holt, H. E. Jackson, R. M. Laszewski, J. R. Specht, E. J. Stephenson, R. E. Segel,\* R. P. Redwine,<sup>†</sup> M. A. Yates-Williams,<sup>†</sup> and J. Julien<sup>‡</sup>

Pion single-charge-exchange reactions initiated by  $\pi^+$  and  $\pi^-$  beams have been surveyed on targets ranging from Be to Pb with the use of a back-angle  $\gamma$ -ray spectrometer. The beam energy varied from 50 to 200 MeV, and the  $\pi^0$  spectra were recorded at 6 angles from 25° to 150°. This experiment was an extension of earlier measurements at  $T_{\pi} = 100$  MeV and  $\theta = 40^\circ$  and  $120^\circ$ . The 2- $\gamma$  decay of the  $\pi^0$  was detected colinearly with the  $\pi^0$  momentum. The substantial Doppler shifts of the two  $\gamma$  rays allowed the low-energy photon to be detected with good resolution in a large volume NaI(Tl) spectrometer while the presence of the high-energy photon was observed in a Pb-glass Cerenkov counter. The  $\pi^0$  spectrum was obtained by transforming the NaI  $\gamma$ -ray spectrum. The efficiency of the detector system was calibrated using the  $\pi^- + p \rightarrow \pi^0 + n$  reaction observed in a  $\text{CH}_2 - \text{C}$  difference spectrum. The effects of the NaI response function were removed from the  $\pi^0$  spectra. The more complete angular distributions determine the total charge-exchange cross section, whose dependence on pion charge and target mass can be

---

\* Northwestern University, Evanston, Illinois.

<sup>†</sup> Los Alamos Scientific Laboratory, Los Alamos, New Mexico.

<sup>‡</sup> CEN, Saclay, France.

investigated. The similarity of the angular distribution of the  $T_{\pi} = 100$  MeV measurements to that for the free nucleon suggested by earlier observations is confirmed. Compared to the shape of the free-nucleon cross section, the observed angular distributions show forward-angle enhancement at 50 MeV, indicating the importance of other reaction mechanisms. Integrated charge-exchange cross sections are larger than values estimated from optical-model calculations.

b. Study of Pion Absorption Mechanisms in  $^4\text{He}$  and Other Nuclei

H. E. Jackson, R. D. McKeown, K. E. Rehm, L. L. Rutledge, Jr.,\*  
J. P. Schiffer, R. E. Segel,\* S. J. Sanders, S. L. Tabor, R. P.  
Redwine,† and M. A. Yates-Williamst

Even though pions are one of the basic building blocks of nuclear matter, our understanding of how pions propagate, lose energy, and are absorbed inside a nucleus is still inadequate. To obtain experimental information on these processes, we have studied the energetic protons produced when pions are incident on nuclei. In the first measurements using the LAMPF LEP channel, protons produced by 60, 100, and 220-MeV  $\pi^+$  and  $\pi^-$  on targets of  $^4\text{He}$ ,  $^{12}\text{C}$ ,  $^{62}\text{Ni}$ , and  $^{181}\text{Ta}$  were measured at  $45^\circ$  and  $90^\circ$ . The data on  $^4\text{He}$  were especially informative. Clear evidence, in the form of a distinct peak of high-energy protons, was seen for a two-body absorption mechanism in which the pion deposits its rest mass and kinetic energy onto two nucleons. This mode becomes relatively much weaker in  $^{12}\text{C}$  and heavier nuclei. The spectra from heavier targets at  $45^\circ$  for 220-MeV positive pions are shown in Fig. II-1. There is a pronounced difference in the shapes of the spectra for  $^4\text{He}$  and  $^{12}\text{C}$ ; the ratio of proton yields at high energy is about 1.4, while the ratio at lower energy is much larger. Evidence was also seen for a possible multinucleon-absorption mode in all nuclei. Preparations were made during the past

---

\* Northwestern University, Evanston, Illinois.

† Los Alamos Scientific Laboratory, Los Alamos, New Mexico.

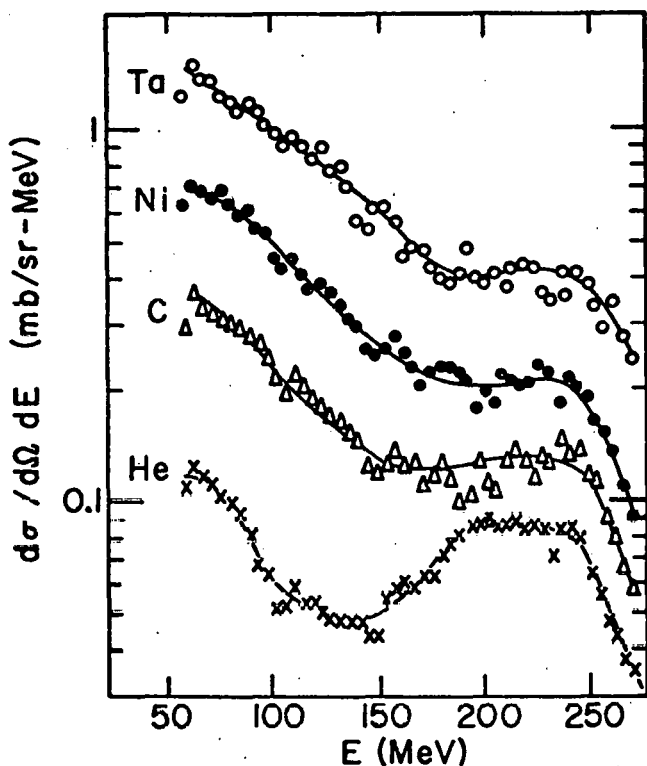


Fig. II-1. Proton spectra at 45° from 220-MeV  $\pi^+$  on various targets.

year for an extensive study of the angular distribution of protons and the behavior of the inelastic charged-particle yield as a function of target mass.

c. Gamma-Ray Study of Pion-Induced Reactions on the Nickel Isotopes

H. E. Jackson, S. B. Kaufman,\* D. G. Kovar, L. Meyer-Schützmeister, K. E. Rehm, J. P. Schiffer, S. L. Tabor, S. E. Vigdor, T. P. Wangler, L. L. Rutledge, Jr.,† R. E. Segel,† R. L. Burman,‡ P. A. M. Gram,‡ R. P. Redwine,‡ and M. A. Yates-Williams‡

The spectra of residual nuclides following 100-, 160-, and 220-MeV  $\pi^+$  and  $\pi^-$  bombardment of  $^{58,60,62,64}\text{Ni}$  have been measured by detecting prompt and, at 220 MeV,  $\beta$ -delayed gamma rays. During the past year the data analysis was completed and a summary paper<sup>1</sup> describing the conclusions was published. A wide spectrum of residual nuclides

\* Chemistry Division, ANL.

† Northwestern University, Evanston, Illinois.

‡ Los Alamos Scientific Laboratory, Los Alamos, New Mexico.

<sup>1</sup> H. E. Jackson et al., Phys. Rev. C 18, 2656 (1978).

extending along the valley of stability down to Ca was seen. Where radioactivities were measured, the total (prompt + delayed) observed cross section amounted to  $\approx 900$  mb. The mean number of nucleons removed increased from about 5 for the  $^{58}\text{Ni}$  target to about 8 for  $^{64}\text{Ni}$ . The residual-nuclide spectrum depends sensitively on the target neutron excess but is essentially independent of pion charge or pion energy in the range observed. A Monte-Carlo cascade-evaporation calculation involving an intermediate  $\Delta$  resonance reproduces the yield of residual nuclides far (more than about eight nucleons) removed from the target, but it fails to reproduce the yield of nearer nuclides which is a more sensitive measure of the early stages of the reaction. The discrepancies for the near nuclides suggest that our current understanding of the pre-equilibrium phase of pion-nucleus interactions is inadequate.

#### d. Scattering of Pions by Complex Nuclei

D. F. Geesaman, C. Olmer, B. Zeidman, G. R. Burleson,\* M. Devereux,\* R. L. Boudrie,<sup>†</sup> C. L. Morris,<sup>‡</sup> H. A. Thiessen,<sup>‡</sup> R. E. Segel,<sup>§</sup> R. H. Siemssen,<sup>||</sup> and L. W. Swenson<sup>¶</sup>

Elastic and inelastic scattering of both  $\pi^+$  and  $\pi^-$  by  $^9\text{Be}$ ,  $^{28}\text{Si}$ ,  $^{58}\text{Ni}$ , and  $^{208}\text{Pb}$  has been studied at  $E_\pi = 162$  and 291 MeV. The experiment was performed with the EPICS system at LAMPF. The initial analysis of the elastic scattering at 162 MeV using the pion optical-model program PIPIT yielded reasonable agreement with the data, but improved agreement was obtained for small reductions in the nuclear radii. No evidence for different proton- and neutron-matter distributions was indicated

\* New Mexico State University, Las Cruces, New Mexico.

<sup>†</sup> University of Colorado, Boulder, Colorado.

<sup>‡</sup> Los Alamos Scientific Laboratory, Los Alamos, New Mexico.

<sup>§</sup> Northwestern University, Evanston, Illinois.

<sup>||</sup> K. V. I., Groningen, Netherlands.

<sup>¶</sup> Oregon State University, Corvallis, Oregon.

in this analysis. These results have been published.<sup>1</sup> The data for <sup>9</sup>Be elastic and inelastic scattering at 162 MeV also provided an unambiguous demonstration of the strong effects of quadrupole scattering, i. e., contributions to elastic scattering directly attributed to the quadrupole moment of the target. These results have also been published.<sup>2</sup> Additional analyses of the data have utilized optical models in both configuration and momentum space and DWBA calculations for inelastic scattering in both representations.

In configuration space, fits to the elastic data were achieved for matter distributions consistent with proton distributions obtained from electron scattering. The corresponding DWBA calculations for inelastic scattering are in reasonable agreement with the data, but require deformation parameters approximately 50% larger than obtained with other probes.

The calculations in momentum space have no free parameters since they are based upon measured pi-nucleon phase shifts and nuclear-matter distributions. Better agreement with the elastic data is observed if binding energy, and Coulomb effects are included in the pion nucleon interaction energies. The corresponding calculations for inelastic scattering are also in good agreement with the data for deformation parameters consistent with those measured with other probes. Both types of analysis indicate a selective sensitivity to protons and neutrons by  $\pi^+$  and  $\pi^-$ , respectively. In <sup>58</sup>Ni the deformation parameters for  $\pi^-$  are about 10% greater than those required for  $\pi^+$ , reflecting the extra two neutrons. The deformation parameter for the 3<sup>-</sup> state in <sup>208</sup>Bi is much larger for  $\pi^-$  than  $\pi^+$  in the momentum space analysis, but is roughly equal in the

---

<sup>1</sup> B. Zeidman, C. Olmer, D. F. Geesaman, R. L. Boudrie, R. H. Siemssen, J. F. Amann, C. L. Morris, H. A. Thiessen, G. R. Burleson, M. J. Devereux, R. E. Segel, and L. W. Swenson, Phys. Rev. Lett. 40, 1539 (1978).

<sup>2</sup> D. F. Geesaman, C. Olmer, B. Zeidman, R. L. Boudrie, R. H. Siemssen, J. F. Amann, C. L. Morris, H. A. Thiessen, G. R. Burleson, M. J. Devereux, R. E. Segel, and L. W. Swenson, Phys. Rev. C 18, 2223 (1978).

configuration space analysis. The origins of these discrepancies require further study. The analysis of the 291-MeV data is partially completed. It is anticipated that the constraints imposed by the data at both 162 and 291 MeV will yield new insight into the pion-nucleus interaction.

e. Inelastic Pion Scattering from Light Nuclei:  $^{10}\text{B}$ ,  $^{11}\text{B}$ ,  $^{14}\text{N}$

D. F. Geesaman, C. Olmer, E. J. Stephenson, B. Zeidman, G. C. Morrison,\* G. Blanpied,† G. R. Burleson,† R. Anderson,‡ R. L. Boudrie,‡ C. L. Morris,‡ and L. W. Swenson§

A proposal to measure complete angular distributions for the elastic and inelastic scattering of both  $\pi^+$  and  $\pi^-$  from  $^{10}\text{B}$ ,  $^{11}\text{B}$ , and  $^{14}\text{N}$  was submitted. The experiment is to be performed at LAMPF with the EPICS system with pion energies of 170 and 230 MeV. The emphasis is upon studies of the low-lying  $T=0$  and  $T=1$  states in  $^{10}\text{B}$  and  $^{14}\text{N}$  and the low-lying states of  $^{11}\text{B}$ . The proposal was approved and scheduled for beam time during the first cycle in 1979.

The objective of this proposal is to obtain information about reaction mechanisms in pion-nucleus interactions under conditions where the details of nuclear structure are well understood. To date, in the two cases where  $\Delta T=1$  transitions have been observed (see  $^{28}\text{Si}$  summary) discrepancies between comparable  $T=0$  and  $T=1$  transitions are noted. In this experiment, the nuclear structure has been extensively probed with other strongly-absorbed particles so that reaction mechanism remains as the only major issue. Analysis will use realistic microscopic calculations developed by theorists in the Physics Division.

---

\* University of Birmingham, Birmingham, England.

† New Mexico State University, Las Cruces, New Mexico.

‡ Los Alamos Scientific Laboratory, Los Alamos, New Mexico.

§ Oregon State University, Corvallis, Oregon.

f. Excitation of High-Spin Particle-Hole States in  $^{28}\text{Si}$

D. F. Geesaman, C. Olmer, B. Zeidman, R. E. Segel,\* L. W. Swenson,† R. L. Boudrie,‡ C. L. Morris,‡ and H. A. Thiessen‡

Inelastic scattering of 162-MeV  $\pi^+$  by  $^{28}\text{Si}$  has been investigated with the EPICS facility at LAMPF. An overall resolution of  $\sim 270$  keV was achieved. Particular emphasis was placed upon obtaining high quality spectra at large scattering angles ( $40^\circ - 110^\circ$ ) so that high-spin particle-hole states which peak at large momentum transfer ( $\sim 300$  MeV/c) could be observed. Among the states seen in Fig. II-2 are the predominantly  $(1f_{7/2} \times 1d_{5/2})^{-1}6^-$   $T=0$  and  $T=1$  states at excitation energies of 11.58 and 14.36 MeV, respectively. The ratio of cross sections  $\sigma(T=0)/\sigma(T=1) = 1.5 \pm 0.2$ , as compared to the value of 4 expected from estimates based upon 3,3 resonance dominance. Other states with angular distributions indicative of large spin transfer,  $\geq 4$ , are also observed. Microscopic calculations, in progress, should help to define the spin-flip amplitudes of the effective pion-nucleon amplitude as well as test the nuclear-structure dependence of the inelastic-scattering models.

g. Pion Double-Charge-Exchange Reactions

R. J. Holt, B. Zeidman, M. P. Baker,‡ R. L. Burman,‡ M. D. Cooper,‡ R. H. Heffner,‡ D. M. Lee,‡ R. P. Redwine,‡ J. E. Spencer,‡ D. J. Malbrough,§ T. Marks,§ and B. M. Freedman§

Analysis of the cross-section data at  $0^\circ$  for pion double-charge exchange on targets of  $^9\text{Be}$ ,  $^{12}\text{C}$ ,  $^{24}\text{Mg}$ ,  $^{26}\text{Mg}$ ,  $^{28}\text{Si}$ ,  $^{40}\text{Ca}$ , and  $^{58}\text{Ni}$  has been completed. These reactions were induced by 140-MeV  $\pi^+$  from the LEP channel at LAMPF. The final cross sections, listed in order of increasing mass, are:  $80 \pm 50$ ,  $650 \pm 200$ ,  $670 \pm 200$ ,  $180 \pm 100$ ,

\* Northwestern University, Evanston, Illinois.

† Oregon State University, Corvallis, Oregon.

‡ Los Alamos Scientific Laboratory, Los Alamos, New Mexico.

§ University of South Carolina, Columbia, South Carolina.

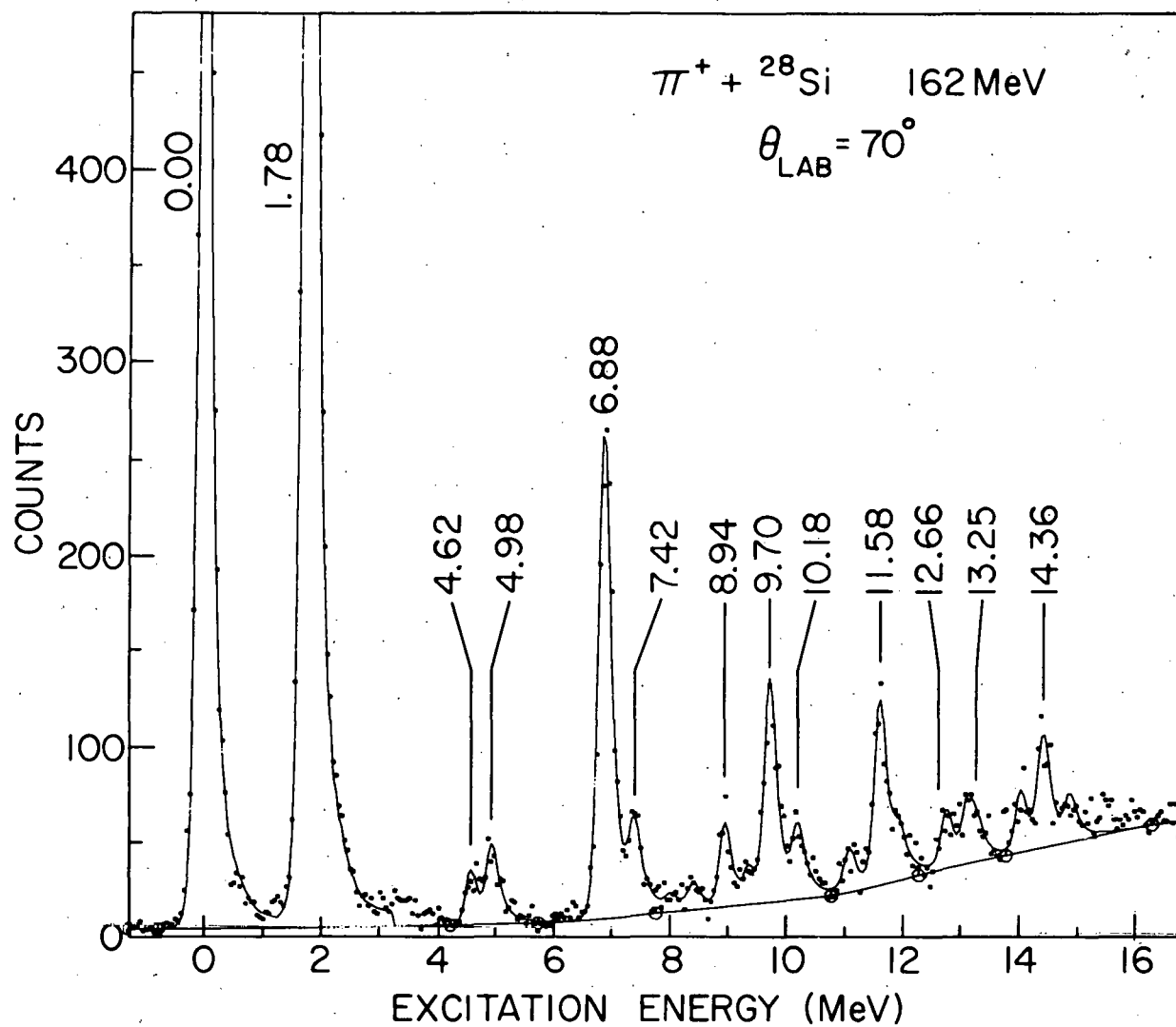


Fig. II-2. Spectrum for  $\pi^+$  scattering by  ${}^{28}\text{Si}$  at  $70^\circ$ . The lines are the result of peak shape fitting with AUTOFIT after subtraction of a background (marked by the open circles).

$350 \pm 100$ ,  $<300$  and  $<100$  nb/sr. The cross sections for  $^9\text{Be}$ ,  $^{24}\text{Mg}$ , and  $^{26}\text{Mg}$  clearly demonstrate nuclear structure effects. For  $^9\text{Be}$ , the recoupling of nucleon orbitals produces a predominant  $L=2$  transition which is small at  $0^\circ$ . The small cross section for  $^{26}\text{Mg}$  compared to that for  $^{24}\text{Mg}$  has not as yet been explained. A priori expectations were that the  $^{26}\text{Mg}$  cross section would greatly exceed that of  $^{24}\text{Mg}$  since an analog transition is expected to be favored.

II. Low-Energy Pion Elastic Scattering from the Proton and Deuteron at  $180^\circ$

R. J. Holt, J. R. Specht, E. J. Stephenson, B. Zeidman, R. L. Burman,\* J. Frank,\* M. Leitch,\* J. D. Moses,\* R. P. Redwine,\* M. A. Yates-Williams,\* and R. M. Laszewskit

The goal of this experiment is to observe the energy dependence of the  $\pi$ -p and  $\pi$ -d cross section at a scattering angle of  $180^\circ$ , throughout the energy range 30—150 MeV by using the unique features of the low-energy-pion (LEP) channel at the Los Alamos Meson Physics Facility. In addition, we hope to observe the tensor polarization of the deuteron at  $180^\circ$  for  $\pi$ -d elastic scattering. The advantages of studying these pion cross sections are manifold: (i) the spin-flip amplitudes vanish at  $180^\circ$  and the theoretical calculations are greatly simplified; (ii) the momentum transfer is largest at this angle and high momentum components of the interaction should be enhanced; (iii) the calculated  $\pi^-$ -p cross section at this angle shows a high sensitivity to the isoscalar, s-wave  $\pi$ -N amplitude; (iv) theoretical calculations indicate that the tensor polarization in  $\pi$ -d elastic scattering is sensitive to the D-state admixture in the deuteron wave function; and (v) the Coulomb effects are at a minimum for  $180^\circ$  scattering. Since the LEP channel was not designed with these specific measurements in mind, a feasibility study must be made. A formal proposal for this experiment was approved and the feasibility study was

\* Los Alamos Scientific Laboratory, Los Alamos, New Mexico.

<sup>†</sup> University of Illinois, Urbana, Illinois.

scheduled for the first LAMPF run cycle in 1979. A novel polarimeter for use in medium-energy reactions was designed and is under construction. The essential features of this polarimeter design are (i) high efficiency, (ii) large tensor analyzing power, (iii) a large energy acceptance ( $\sim 6$  MeV at 40 MeV), and (iv) a wide aperture. We plan to calibrate this polarimeter using the polarized deuteron beam available at the Berkeley cyclotron.

THIS PAGE  
WAS INTENTIONALLY  
LEFT BLANK

### III. HEAVY-ION RESEARCH AT THE TANDEM AND SUPERCONDUCTING LINAC ACCELERATORS

#### INTRODUCTION

The heavy-ion research program in the Argonne Physics Division is concerned principally with the connections between heavy-ion interactions and nuclear structure. To this end measurements are needed that concentrate on the precision that is required in order that specific effects of nuclear structure be clearly determined. Hitherto, the research program has been carried out with the FN tandem, but during FY 1979 sections of the superconducting booster became available for research use, providing beams of increased energies.

The study of high-angular-momentum states through gamma-ray spectroscopy has been a very fruitful endeavor. Argonne work has concentrated on nuclei where high-spin isomers, the so-called yrast traps, are prevalent. Using the additional handle provided by time-delayed measurements, it has been possible to sort out transitions and to determine the properties of states up to spin 37  $\hbar$ —a current record. Rather pronounced differences are found between nuclei differing by only one neutron.

The study of fusion reactions has continued. The variation in fusion cross sections between different nuclear systems has been confirmed though no simple pattern is apparent. It is clear that rather drastic changes can occur when the configurations of valence nucleons differ only very slightly. Resonant effects appear to have been found in the fusion cross sections for additional systems.

Resonant effects have been studied in the  $^{24}\text{Mg}(\text{O}, \text{C})^{28}\text{Si}$  reactions. Pronounced oscillations are found in the excitation functions, with energy widths and spacings so large that they suggest a simple underlying explanation. Strong correlations are seen between transitions to different final states. Methods of analysis are being developed that show promise of constraining the parameters of the resonant structures.

A major activity during this time has been concerned with the development of a small new target area for the superconducting linac booster. In addition to new beam lines, optical and diagnostic elements and a clean high-vacuum system, a new 65-in. scattering chamber is under construction and a new type of gamma-ray sum/multiplicity detector is under development for use with the linac booster.

### A. RESONANT STRUCTURES IN HEAVY-ION REACTIONS

With the observation of resonance-like structures in the backward-angle elastic-scattering excitation functions of the  $^{16}\text{O} + ^{28}\text{Si}$  and  $^{12}\text{C} + ^{28}\text{Si}$  reactions, new attention has been focused on the question of the energy dependence of heavy-ion reactions which before were believed to be direct and to occur on a rapid time scale. At Argonne, work has concentrated on heavy-ion-transfer reactions, where nonresonant contributions are expected to be well described by the conventional distorted-wave Born approximation. The experiments carried out at Argonne have identified strong correlated resonant structures in several channels, all involving  $^{24}\text{Mg} + ^{16}\text{O}$  as the entrance channel. The major question now is to attempt to classify these resonant structures, as to their quantum numbers and dominant configurations. Only then may one hope to formulate reasonable hypotheses as to their origin. Considerable progress has been made in developing the analysis of these structures in terms of interfering direct and resonant amplitudes.

#### a. Resonant Effects in the $^{24}\text{Mg}(\overset{16}{\text{O}}, \overset{12}{\text{C}}) \overset{28}{\text{Si}}$ Reaction at Forward Angles

M. Paul, S. J. Sanders, J. Cseh, D. F. Geesaman, W. Henning, D. G. Kovar, C. Olmer, and J. P. Schiffer

Excitation functions at  $0^\circ$  and at the second maxima of the angular distributions ( $\sim 11^\circ$ ) have been measured for the reaction  $^{24}\text{Mg}(\overset{16}{\text{O}}, \overset{12}{\text{C}}) \overset{28}{\text{Si}}$  to the ground and first excited states of  $^{28}\text{Si}$ . In the range  $23 \text{ MeV} \leq E_{\text{c.m.}} \leq 38 \text{ MeV}$ , covered in this study, resonance-like structures were found in both excitation functions with pronounced maxima at center-of-mass energies of 26, 28, 31, and 34 MeV. The peak-to-valley ratio for these structures was typically 3 to 1. (See upper box in Fig. III-1.) Our measurements are the first to reveal structure in the energy dependence of the forward-angle transfer cross sections for any system where the composite system has  $A > 32$ . Angular distributions measured at the maxima of the excitation function are fitted rather well with the square of a single Legendre polynomial of order close to that of the grazing partial wave. An excitation function was also measured at  $\sim 90^\circ$  in the center of mass. This last measurement, which should be sensitive only to even partial waves, showed some, but not complete, correlation with the  $0^\circ$

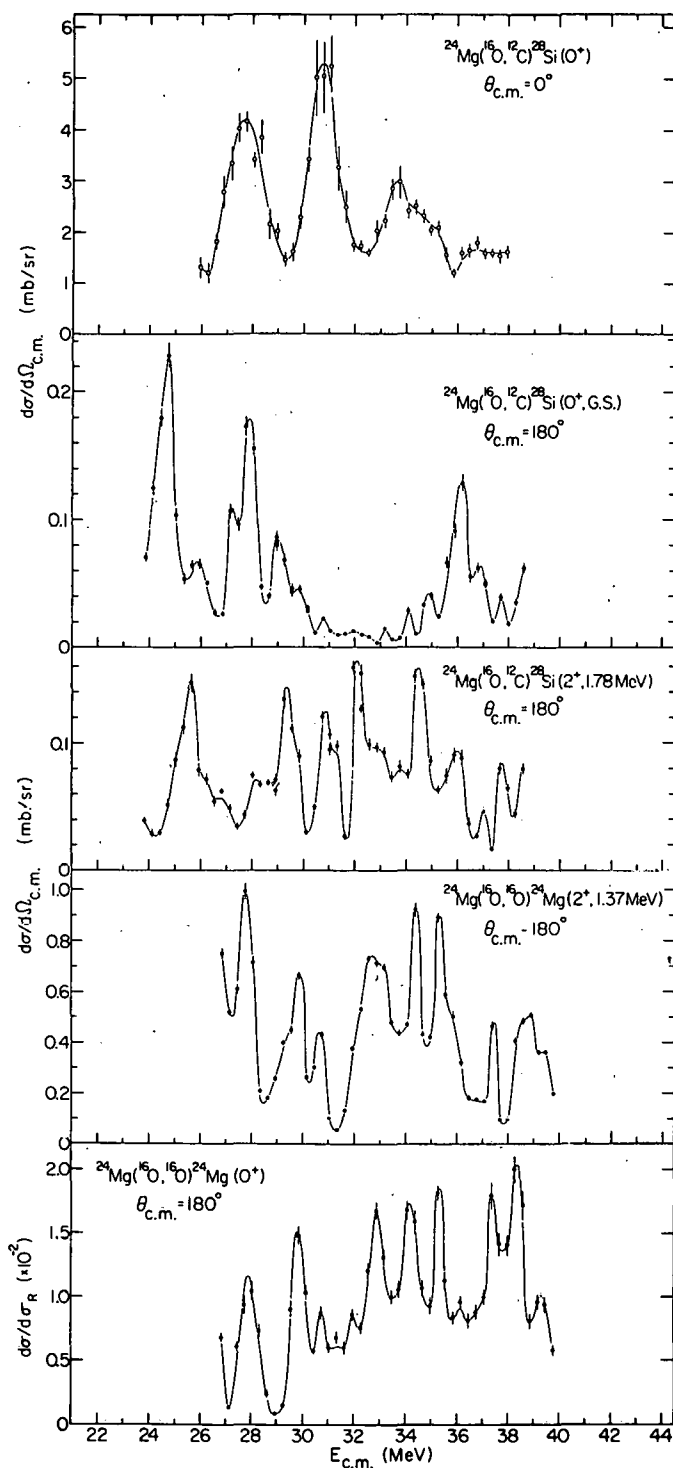


Fig. III-1. Excitation functions for the  $^{24}\text{Mg}(^{16}\text{O}, ^{12}\text{C})^{28}\text{Si}$  and  $^{24}\text{Mg}(^{16}\text{O}, ^{16}\text{O})^{24}\text{Mg}$  reactions at  $180^\circ$ . The upper box shows for comparison the excitation function of the  $^{24}\text{Mg}(^{16}\text{O}, ^{12}\text{C})^{28}\text{Si}$  measured at  $0^\circ$ . The solid lines connect smoothly the experimental points to guide the eye.

excitation function. The structure in the forward-angle transfer data is also not clearly correlated with that seen in the back-angle elastic scattering,  $^{12}\text{C} + ^{28}\text{Si}$ , excitation function.

b. Resonant Effects in the  $^{24}\text{Mg}(^{16}\text{O}, ^{12}\text{C})^{28}\text{Si}$  and  $^{24}\text{Mg}(^{16}\text{O}, ^{16}\text{O})^{24}\text{Mg}$  Reactions at Backward Angles

M. Paul, S. J. Sanders, J. Barrette,\* D. F. Geesaman, W. Henning, D. G. Kovar, M. J. LeVine,\* C. Olmer, and J. P. Schiffer

To complement our study of the forward angle  $^{24}\text{Mg}(^{16}\text{O}, ^{12}\text{C})^{28}\text{Si}$  reaction, we have measured excitation functions at  $180^\circ$  for the  $^{24}\text{Mg}(^{16}\text{O}, ^{12}\text{C})^{28}\text{Si}$  reaction to the ground state and first excited state of  $^{28}\text{Si}$  and the elastic  $^{24}\text{Mg}(^{16}\text{O}, ^{16}\text{O})^{24}\text{Mg}$  scattering and the inelastic scattering to the first  $2^+$  state in  $^{24}\text{Mg}$ . These measurements, performed on the Brookhaven National Laboratory MP tandem, using a  $^{24}\text{Mg}$  beam on  $\text{Al}_2\text{O}_3$  targets and detecting the  $^{16}\text{O}$  or  $^{12}\text{C}$  ions at  $0^\circ$ , covered the energy range  $24 < E_{\text{c.m.}} < 39$  in 0.3-MeV increments. All four reactions show quite strong resonant structures with widths  $\sim 0.6$  to  $1.2$  MeV, and a spacing approximately one-half of that seen in the forward-angle excitation functions (Fig. III-1). Angular distributions were measured at  $27.8$ ,  $30.7$ , and  $36.2$  MeV for the  $^{24}\text{Mg}(^{16}\text{O}, ^{12}\text{C})^{28}\text{Si}$  reactions and at  $27.8$  and  $36.2$  MeV for the  $^{24}\text{Mg}(^{16}\text{O}, ^{16}\text{O})$  elastic and inelastic scattering. These angular distributions were adequately fit by the square of a single Legendre polynomial.

The excitation function for the  $(^{16}\text{O}, ^{12}\text{C})$  reaction to  $^{28}\text{Si}$  ground state has a broad minimum at  $E_{\text{c.m.}} \sim 31$  MeV, where the forward-angle excitation function has a maximum. If nonresonant transfer is negligible at  $180^\circ$ , these results imply that two overlapping resonances must be interfering destructively at  $180^\circ$  and constructively at  $0^\circ$ , and therefore have opposite parity. This interpretation suggests that the structure underlying these resonances is more complicated than was previously assumed.

\* Brookhaven National Laboratory, Upton, L.I., New York.

c. Analysis of the  $^{24}\text{Mg}(\text{O}, \text{C})^{28}\text{Si}$  Reaction

S. J. Sanders, D. F. Geesaman, W. Henning, D. G. Kovar, C. Olmer, M. Paul, and J. P. Schiffer

Angular distributions were measured at  $6^\circ \leq \theta_{\text{c.m.}} \leq 50^\circ$  for the  $^{24}\text{Mg}(\text{O}, \text{C})^{28}\text{Si}$  reaction at  $E_{\text{c.m.}} = 26.3, 26.9, 27.8, 29.4, 30.1, 31.6, 32.4$ , and  $33.8 \text{ MeV}$ . These data (see Fig. III-2), along with corresponding data from the  $0^\circ, 90^\circ$ , and  $180^\circ$  excitation functions, have been analyzed in terms of a DWBA amplitude plus a resonant term at each energy. The energy dependence of the amplitude and phase of the resonant term extracted in this manner have been compared to that expected for a single resonance or a sum of two resonances. The results of this analysis confirm the hypothesis that two overlapping resonances are required to fit the data around  $E_{\text{c.m.}} = 31 \text{ MeV}$ ; at  $28 \text{ MeV}$  one resonant amplitude seems to be sufficient. The partial waves of the resonant amplitudes at present are uncertain to  $\sim 3 \%$ . This analysis demonstrates that the structures observed at forward and backward angles can be explained in terms of interfering direct and resonant amplitudes. Further work is in progress to study the sensitivity of these calculations to the choice of DWBA amplitudes, to refine the fits, and to get a consistent fit to the whole excitation function and the angular distributions.

d. Search for Resonant Structures in the Excitation Functions of the  $^{26}\text{Mg}(\text{O}, \text{C})^{28}\text{Si}$ ,  $^{48}\text{Ca}(\text{O}, \text{C})^{50}\text{Ti}$ , and  $^{26}\text{Mg}(\text{O}, \text{C})^{30}\text{Si}$  Reactions

W. Henning, D. G. Kovar, R. L. Kozub,\* C. Olmer, M. Paul, F. W. Prosser, Jr.,† S. J. Sanders, and J. P. Schiffer

With the observation of resonant structures in the  $^{24}\text{Mg}(\text{O}, \text{C})^{28}\text{Si}$  reaction, it is important to learn whether  $\alpha$ -particle transfer or the  $\alpha$ -particle structure of the target and projectile are essential in the underlying mechanism for the resonances. We have

\* Tennessee Technological University, Cookeville, Tennessee.

† University of Kansas, Lawrence, Kansas.

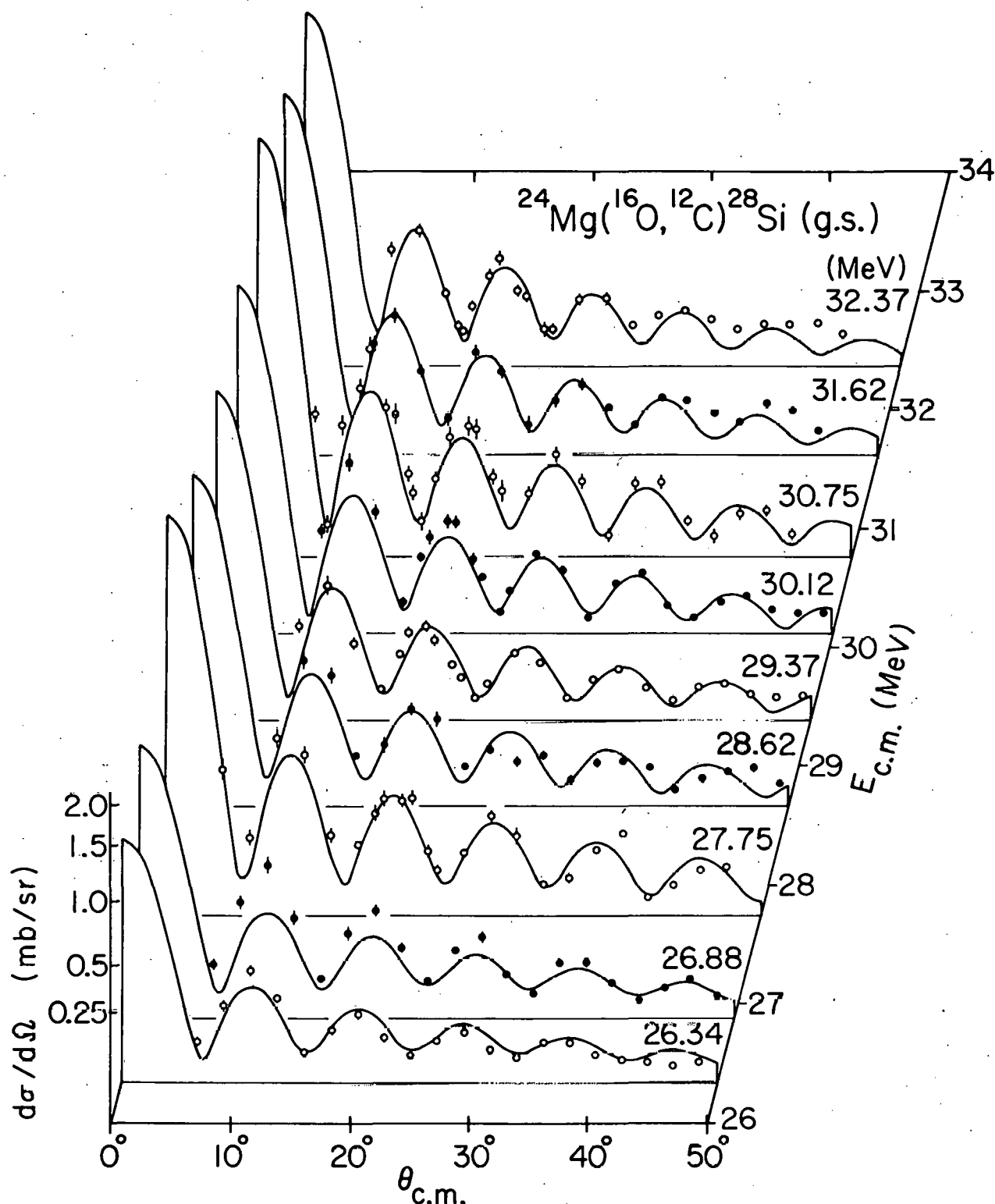


Fig. III-2. Angular distributions for the  $^{24}\text{Mg}(^{16}\text{O}, ^{12}\text{C})^{28}\text{Si}$  (g. s.) reaction at forward angles. The curves show a two-resonance Breit-Wigner (plus DWBA background) fit to the data.

measured ( $^{16}\text{O}$ ,  $^{14}\text{C}$ ) excitation functions from  $41 \leq E_{\text{lab}} \leq 53$  MeV on a  $^{26}\text{Mg}$  target and from  $54.3 \leq E_{\text{lab}} \leq 59$  MeV on a  $^{48}\text{Ca}$  target. Both of these reactions, to the ground states of  $^{28}\text{Si}$  and  $^{50}\text{Ti}$ , respectively, have strongly oscillatory angular distributions at forward angles, close in shape to a single Legendre-polynomial squared of order near the grazing partial wave. No evidence of structure in the excitation functions was observed. Data on the  $^{26}\text{Mg}(^{16}\text{O}, ^{12}\text{C})^{30}\text{Si}$  reaction show some evidence of a broad  $\sim 10$  MeV wide structure. DWBA calculations are under way to interpret the energy dependence of the cross sections.

e. Search for Resonant Structure in the  $^{24}\text{Mg}(^{16}\text{O}, ^{12}\text{C})$  Reaction to States in  $^{28}\text{Si}$  Between 5 and 12-MeV Excitation Energy

S. J. Sanders, D. F. Geesaman, W. Henning, D. G. Kovar, C. Olmer, M. Paul, and J. P. Schiffer

In extending our attempts to understand the underlying mechanism of the observed resonant structure in the  $^{24}\text{Mg}(^{16}\text{O}, ^{12}\text{C})^{28}\text{Si}$  reaction, we have measured excitation functions at laboratory angles of 10.5, 12.0, and 13.5 degrees for this reaction to final states between 5 and 12-MeV excitation energy. Preliminary analysis reveals that the excitation functions for at least the three strongest states,  $3^-$  (6.88 MeV),  $5^-$  (9.70 MeV), and the  $3^-$  (10.18 MeV) show evidence of structure at the  $\sim 50\%$  level, somewhat lower than that observed for the ground state and  $2^+$  (1.78 MeV) state (see Fig. III-3); the structure seems to show some correlation in energy with that for the lower states. These observations suggest that the resonance strength may be shared between several channels. Further analysis is under way to determine whether the excitation functions of the weaker states also show structure.

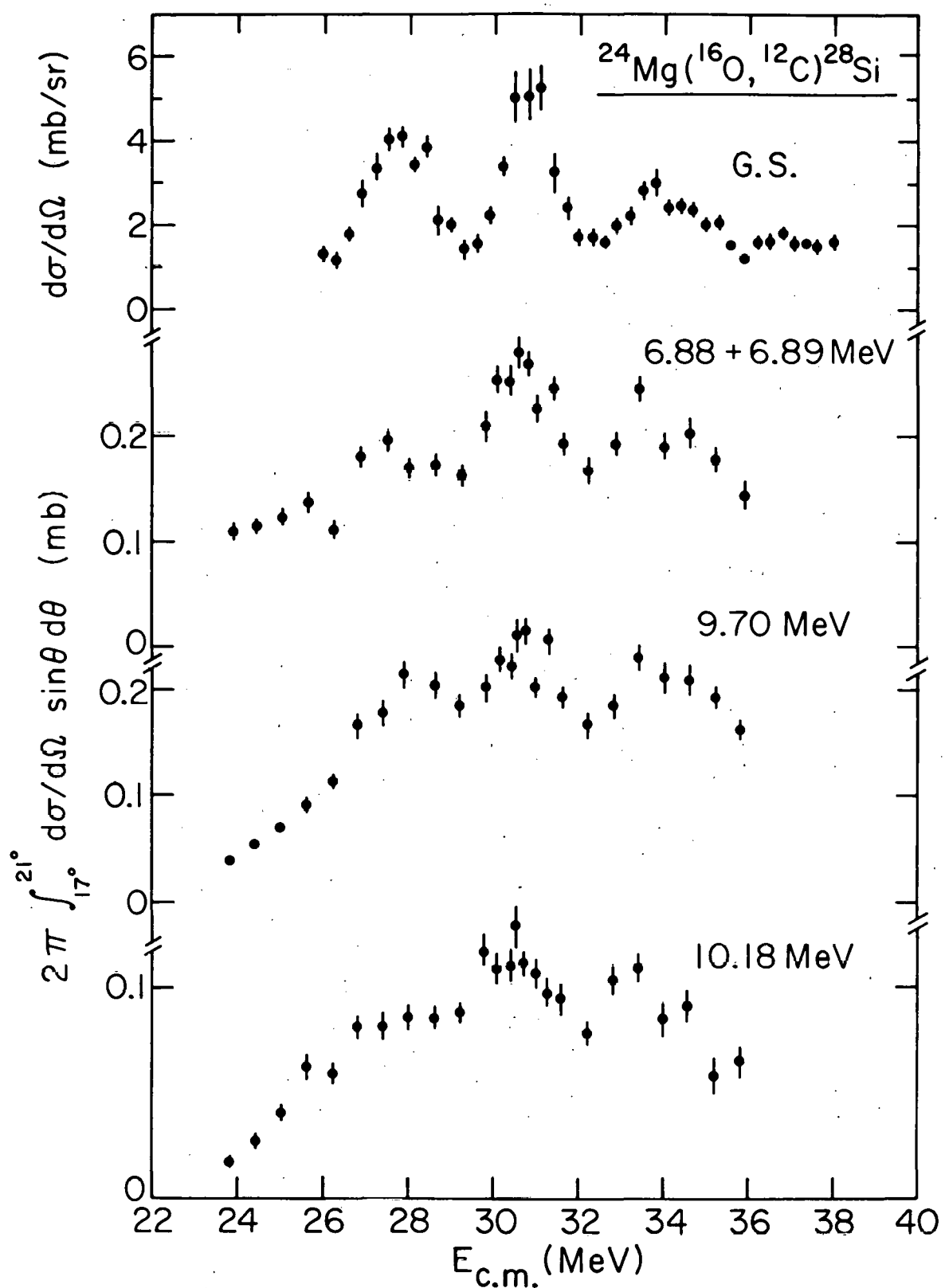


Fig. III-3. Excitation functions for states in  $^{28}\text{Si}$  populated through the  $^{24}\text{Mg}(^{16}\text{O}, ^{12}\text{C})^{28}\text{Si}$  reaction.

## B. FUSION CROSS SECTIONS

Over the past three years a program of measurements has been carried out in the Argonne Physics Division to explore systematic trends in the fusion cross sections of heavy ions. A survey of this process among light nuclei has been completed and various nuclear structure effects have been established. Oscillatory behavior is evident in several systems suggesting resonance effects. Variations in the maximum cross sections for fusion are found in systems differing in only one or two nucleons—the reasons for such variations are still not understood.

a. Systematics of  $^{12}\text{C}$  and  $^{16}\text{O}$  Induced Fusion on Targets  $12 \leq A \leq 19$

D. G. Kovar, D. F. Geesaman, W. Henning, M. Paul, S. J. Sanders, and J. P. Schiffer

Measurements were completed during the past year on a total of seven light systems and the accumulated data have been analyzed. A careful study has been carried out based on the ANL data as well as on measurements published from other laboratories. In the lower-energy region, the fusion cross sections seem to be dominated by the interaction barrier. It is apparent that while the barrier radii deduced have a smooth dependence on  $A$ , this  $A$  dependence does not follow the same trend as do the heavier systems. This is shown in Fig. III-4, where the barrier radii  $R_B$  and heights  $V_B$  [as determined from fitting the data using the classical equation  $\sigma_{\text{fus}} = \pi R_B^2 (1 - V_B/E)$ ] are plotted versus  $A_1^{1/3} + A_2^{1/3}$  for the systems of this study as well as those reported in the literature. At higher energies, the fusion cross sections are found to saturate at magnitudes which differ significantly for systems which differ by only a nucleon or two. This, together with the observation of resonant structures present in the fusion-excitation functions for the  $^{12}\text{C} + ^{12}\text{C}$ ,  $^{12}\text{C} + ^{16}\text{O}$ , and  $^{16}\text{O} + ^{16}\text{O}$  systems [see, for example, P. Sperr *et al.*, Phys. Rev. Lett. 37, 321 (1976)], but not for other light systems, constitutes evidence for nuclear structure effects in the fusion process. Further measurements at higher energies would be of great interest and such measurements are planned with the beams produced by the linac booster.

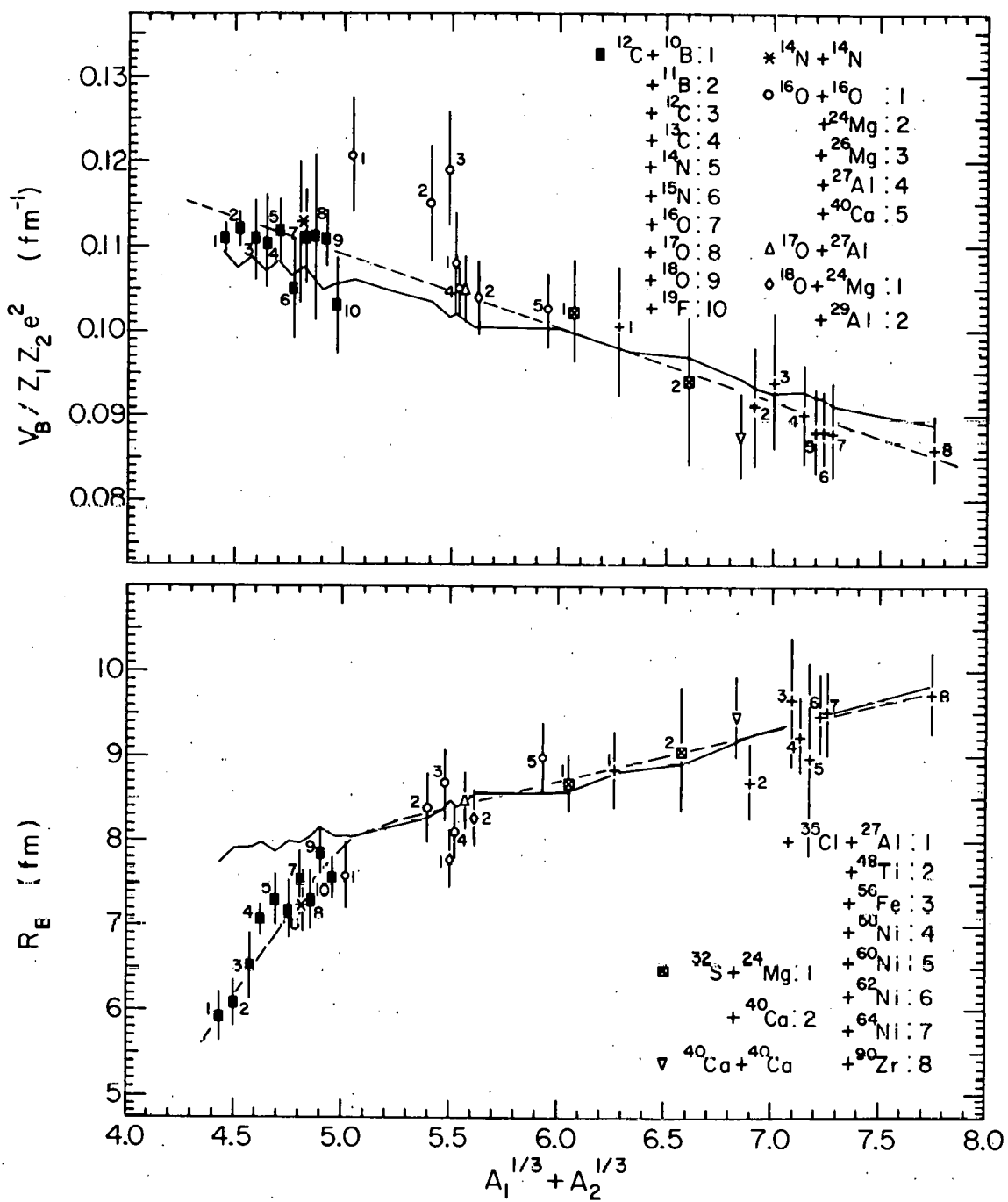


Fig. III-4. The barrier parameters  $R_B$  and  $V_B$  ( $V_B / Z_1 Z_2 e^2$ ) extracted from fits to the fusion data of this study and data reported in the literature are plotted versus  $(A_1^{1/3} + A_2^{1/3})$ . The dashed curves represent the averaged behavior and the solid lines are the predictions of the model of Krappe and Nix [H. J. Krappe and J. R. Nix, in Proceedings of the Third International Atomic Energy Symposium on Physics and Chemistry of Fission, Rochester, 1973 (International Atomic Energy Agency, Vienna, 1974), p. 159].

b. The Fusion of  $^{12}\text{C} + ^{24}\text{Mg}$  and  $^{12}\text{C} + ^{26}\text{Mg}$

K. Daneshvar and D. G. Kovar

The fusion cross-section excitation functions for "a-cluster" light heavy-ion systems (namely,  $^{12}\text{C} + ^{12}\text{C}$ ,  $^{12}\text{C} + ^{16}\text{O}$ , and  $^{16}\text{O} + ^{16}\text{O}$ ) have been found to exhibit resonance-like structure, while similar systems with an excess of a nucleon or two appear smooth. [See for example, P. Sperr *et al.*, Phys. Rev. Lett. 37, 321 (1976).] To establish whether similar behavior exists for somewhat heavier systems, the detailed energy dependences of the total fusion cross sections  $\sigma_{\text{fus}}(E)$  for  $^{12}\text{C} + ^{24}\text{Mg}$  and  $^{12}\text{C} + ^{26}\text{Mg}$  have been measured. Data were obtained for  $20 \leq E_{\text{lab}} \leq 60$  MeV by measuring the evaporation residues in the  $\Delta E$ -E gas-ionization-chamber/silicon-detector system. Single-angle measurements ( $\theta_{\text{lab}} = 8^\circ$ ) were made in 500-keV steps and full angular distributions were measured at several energies over the region studied. The results indicate the presence of structure of  $\leq 5-10\%$  in  $\sigma_{\text{fus}}(E)$  for  $^{12}\text{C} + ^{24}\text{Mg}$ , while that for  $^{12}\text{C} + ^{26}\text{Mg}$  shows a smoother behavior; moreover,  $\sigma_{\text{fus}}(E)$  for the two systems differ significantly. The fusion cross sections for the  $^{12}\text{C} + ^{24}\text{Mg}$  system are shown plotted versus  $E_{\text{c.m.}}$  in Fig. III-5, where evidence for structure can clearly be seen. To study the distribution of reaction strength in more detail, the strongest direct channel (i. e., inelastic scattering) was measured with the split-pole magnetic spectrograph. The results of the fusion measurements show that for heavier systems (i. e., involving targets in the sd shell) the specific structure of the nuclei interacting indeed does significantly affect the fusion cross-section behavior. Further studies involving  $\gamma$ -ray and spectrograph measurements are underway to establish the detailed distribution of reaction strength in the hope that this will provide a better understanding of the reaction process.

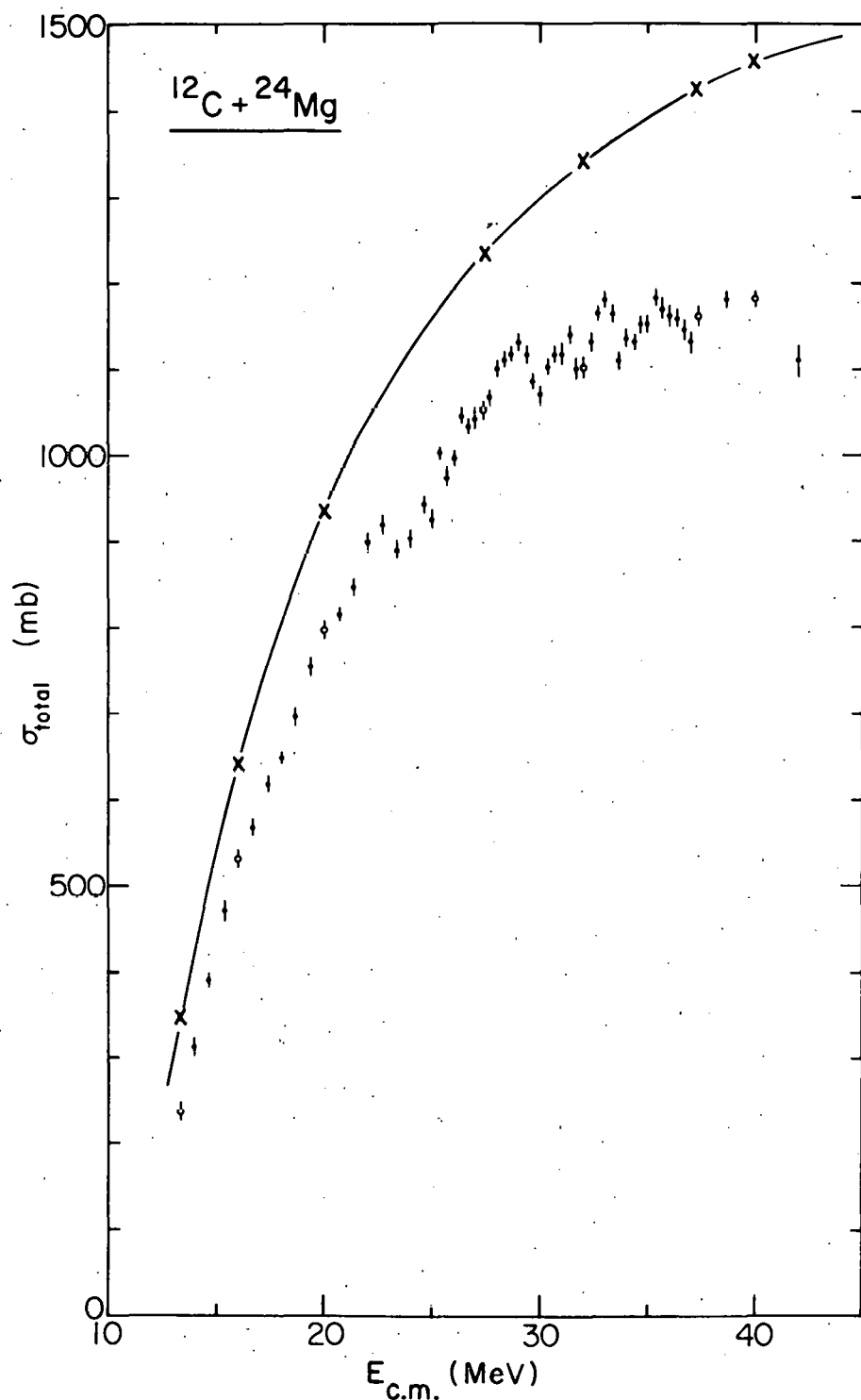


Fig. III-5. Plot of total fusion cross sections versus  $E_{\text{c.m.}}$  for the system  $^{12}\text{C} + ^{24}\text{Mg}$ ; the open dots represent full angular distributions and the solid dots represent single angle measurements. The crosses represent the total reaction cross sections as predicted by PTOLEMY from fits to elastic scattering.

c. The Fusion Cross-Section Behavior for  $^{15}\text{N} + ^{27}\text{Al}$

F. W. Prosser, Jr.,\* R. A. Racca,\* K. Daneshvar, D. F. Geesaman, W. Henning, D. G. Kovar, K. E. Rehm, and S. L. Tabor

The behavior of the total fusion cross sections observed for systems with  $10 \leq A_{\text{proj.}, \text{targ.}} \leq 19$  indicates that the detailed structure of the interacting nuclei plays a significant role in the fusion process.

[See for example, P. Sperr et al., Phys. Rev. Lett. 37, 321 (1976).]

The question of whether such a dependence on structure is present in the fusion cross section for heavier systems has not been conclusively answered. In this study, the fusion of  $^{15}\text{N} + ^{27}\text{Al}$ , forming the compound nucleus  $^{42}\text{Ca}$ , has been measured for comparison with that observed in the previously reported study [S. L. Tabor, D. F. Geesaman, W. Henning, D. G. Kovar, K. E. Rehm, and F. W. Prosser, Jr., Phys. Rev. C 17, 2136 (1978)] of  $^{18}\text{O} + ^{24}\text{Mg}$  and  $^{16}\text{O} + ^{26}\text{Mg}$  which form the same compound nucleus. Measurements for  $27 \leq E_{\text{lab}} \leq 70$  MeV were made by detecting the evaporation residues in a  $\Delta E$ -E gas-ionization-chamber/silicon-detector system. Elastic-scattering and evaporation-residue angular distributions were measured at 6 energies; single-angle ( $\theta_{\text{lab}} = 6^\circ$ ) measurements were performed at several intermediate energies. Comparison of  $\sigma_{\text{fus}}(E)$  for the three systems shows evidence of a dependence on the specific entrance channel. In particular, parameterization of the fusion data in terms of the Glas and Mosel model shows that, while  $^{15}\text{N} + ^{27}\text{Al}$  and  $^{18}\text{O} + ^{24}\text{Mg}$  systems have interaction barrier radii which are very nearly identical, the barrier radius for the  $^{16}\text{O} + ^{26}\text{Mg}$  system is  $\sim 12-15\%$  larger. This difference is not understood at this time and further measurements would be of interest to see whether similar anomalies exist for other systems which form the same compound nucleus.

---

\* University of Kansas, Lawrence, Kansas.

d. Fusion of  $^{16}\text{O} + ^{40}\text{Ca}$  at  $E_{\text{lab}} = 315 \text{ MeV}$

D. G. Kovar, H. C. Britt,\* R. DeVries,\* E. R. Flynn,\* D. L. Hendrie,<sup>†</sup> F. Plasil,<sup>‡</sup> K. VanBibber,<sup>§</sup> and M. Zisman<sup>§</sup>

The  $^{16}\text{O} + ^{40}\text{Ca}$  fusion cross section was measured at  $E_{\text{lab}} = 315 \text{ MeV}$  (8.4 times the Coulomb barrier height) at the LBL 88-inch cyclotron using a  $\Delta E$ - $E$  gas-ionization-chamber/silicon-detector system. While the analysis is still at a preliminary stage, it is already clear that the distribution of reaction strength has changed rather dramatically from that seen at  $E_{\text{lab}} = 214 \text{ MeV}$ , the highest energy previously measured [S. E. Vigdor, in Proceedings of the Symposium on Macroscopic Features of Heavy-Ion Collisions, Argonne National Laboratory, 1-3 April 1976, Vol. I - Invited Papers, ANL Physics Division Report ANL-PHY-76-2 (1976), p. 95]. The reaction products are spread much more, in both energy and  $Z$ , and the separation between evaporation residues and deep inelastic or fission events is not distinct. However, if "reasonable" assumptions are made in identifying the fusion products, the fusion cross section appears to be significantly lower than at 214 MeV. This energy dependence of the fusion cross section is a critical element in understanding the reaction mechanism; it can, for instance, be used to test the recent TDHF calculations [see for example, H. Flocard, S. E. Koonin, and M. S. Weiss, Phys. Rev. C 17, 1682 (1978)] in which the decrease in fusion at higher incident energies is attributed to a "low- $\ell$  window," i.e., a failure of the target and projectile to fuse for the lower incident partial waves.

\* Los Alamos Scientific Laboratory, Los Alamos, New Mexico.

<sup>†</sup> University of Maryland, College Park, Maryland.

<sup>‡</sup> Oak Ridge National Laboratory, Oak Ridge, Tennessee.

<sup>§</sup> Lawrence Berkeley Laboratory, Berkeley, California.

### C. HIGH ANGULAR MOMENTUM STATES IN NUCLEI

The study of very-high-spin states in nuclei represents a new frontier in nuclear-structure studies. Our efforts have focused on yrast traps and discrete states at or near the yrast line. The yrast line assumes special importance, because it is the locus of least excitation energy as a function of spin. Furthermore, properties of the yrast line are not extracted from continuum  $\gamma$ -ray studies, from which information concerning nuclei with high spin is usually obtained. Experiments in our study have been conducted with the MP Tandem at Chalk River, the FN Tandem at Argonne, and, in December 1978, the Argonne superconducting-linac booster. As the booster becomes operational in 1979, most of the research will be conducted at Argonne.

#### a. Yrast Traps Near the Closed Neutron Shell N = 82

T. L. Khoo, R. K. Smither, B. Haas,\* H. R. Andrews,\* O. Häusser,\* and D. Ward\*

An extensive search for yrast traps, conducted at GSI in collaboration with the Niels Bohr Institute group, revealed an island of high-spin isomers near  $N \sim 82$ . We have performed followup experiments by bombarding  $^{120,122,124}\text{Sn}$  and  $^{120,122}\text{Te}$  with pulsed beams of  $^{32}\text{S}$  both at Chalk River and at Argonne. High-spin isomers have been identified in  $^{148,149,150,151,152}\text{Dy}$ ,  $^{148}\text{Tb}$ ,  $^{147}\text{Gd}$ ,  $^{153}\text{Er}$ , and  $^{150}\text{Ho}$ . Half-lives, energies, spins (only approximately in some cases) and decay schemes of the isomers have been determined. In a number of cases, ( $^{12}\text{C},\text{xn}$ ) studies performed at Argonne have been indispensable in making isotopic assignments.

The isomers discussed above are of considerable interest in their own right since they may be related to the oblate yrast traps predicted by Bohr and Mottelson. From an experimental point of view, they open up the possibility of studying high-spin states above the isomers by means of delayed coincidence techniques. These techniques which we have developed make it possible to isolate both discrete and continuum  $\gamma$  rays

---

\* Chalk River Nuclear Laboratories, Chalk River, Ontario, Canada.

feeding into the isomers. Furthermore, isotopic identification of these  $\gamma$  rays is usually possible by exploiting the different lifetimes of the isomers.

b. Very-High-Spin States in  $^{152}\text{Dy}$

T. L. Khoo, R. K. Smith, B. Haas,\* O. Häusser,\* H. R. Andrews,\* D. Horn,\* and D. Ward\*

We have used the ( $^{32}\text{S}, 4n$ ) reaction with  $^{32}\text{S}$  beams to populate high-spin states in  $^{152}\text{Dy}$ . A very extensive set of  $\gamma$ -spectroscopic experiments have been performed, including measurements of: prompt and delayed  $\gamma$  rays; prompt  $\gamma$ - $\gamma$  coincidences both in and out of beam; and delayed  $\gamma$ - $\gamma$  coincidences to identify  $\gamma$  rays feeding and deexciting isomers. Excitation function and angular-distribution measurements of  $\gamma$  rays feeding isomers were made with the requirement that these  $\gamma$  rays must be followed by at least one delayed event in an array of four 3 in.  $\times$  3 in. NaI detectors.

We have observed states with spins of up to 36 or 37  $\hbar$ , higher than have ever been observed before. Three of these states are isomers with half-lives in the ns range. For  $I \geq 14$ , on the average the yrast energies can be written as  $E \sim E_0 + (\hbar^2/2J) I(I + 1)$ . The energy fluctuations about this average indicate that the yrast angular momenta are generated by aligning the spins of a few nucleons. The effective moment of inertia  $J$  has a value 18% larger than for rigid-sphere rotation. For a Fermi gas this moment of inertia is that of a rigid body with the same density distribution. Thus the large value of  $J$  for  $^{152}\text{Dy}$  may suggest an oblate deformation.

---

\* Chalk River Nuclear Laboratories, Chalk River, Ontario, Canada.

c. Recoil-Distance-Lifetime and Linear-Polarization Measurements of  $^{152}\text{Dy}$

B. Haas,\* H. R. Andrews,\* O. Häusser,\* D. Horn,\* J. F. Sharpey-Schafer,\* P. Taras,\* W. Trautmann,\* D. Ward,\* T. L. Khoo, and R. K. Smither

Following our observation of very-high-spin states in  $^{152}\text{Dy}$ , we have measured the lifetimes of many states using the Doppler-shift recoil-distance method. We have also determined the angular distribution and linear polarization of  $\gamma$  rays deexciting very-high-spin states. In both sets of measurements,  $\gamma$  rays feeding a 60 ns isomer were enhanced relative to the background by recording  $\gamma$  spectra in delayed coincidence with an array of four 3 in.  $\times$  3 in. NaI detectors. The deduced experimental transition probabilities are consistent with those for non-rotational nuclei, indicating that yrast angular momenta originate mainly from alignment of individual-particle spins.

d. High-Spin Yrast States in  $^{151}\text{Dy}$

T. L. Khoo, R. K. Smither, W. Kutschera, I. Ahmad,<sup>†</sup> C. N. Davids, S. Levenson, B. Haas,\* O. Häusser,\* H. R. Andrews,\* D. Horn,\* J. F. Sharpey-Schafer,\* P. Taras,\* and D. Ward\*

We have employed the  $(^{32}\text{S}, 5n)$  reaction and the extensive list of  $\gamma$ -ray spectroscopic experiments mentioned above (in connection with studies in  $^{152}\text{Dy}$ ) to identify states of  $^{151}\text{Dy}$  with spins of up to  $71/2$ . Sulfur beams with energies between 128 and 150 MeV were provided by the Chalk River MP Tandem Accelerator and the Argonne Tandem-Superconducting-Linac Booster. Two isomers were identified which had the following properties:  $E = 4905, 6033$  keV;  $I^\pi = 41/2^-$ ,  $49/2^+$ ;  $T_{1/2} = 6, 13$  ns. As in  $^{152}\text{Dy}$ , the yrast energies of  $^{151}\text{Dy}$  increase linearly with  $I(I + 1)$  on the average, for  $I \geq 25/2$ . Figure III-6 shows plots of  $E$  vs  $I(I + 1)$  for the yrast states of  $^{151}\text{Dy}$  and  $^{152}\text{Dy}$ . The effective moments of inertia,  $\mathcal{J}$ ,

\* Chalk River Nuclear Laboratories, Chalk River, Ontario, Canada.

<sup>†</sup> Chemistry Division, ANL.

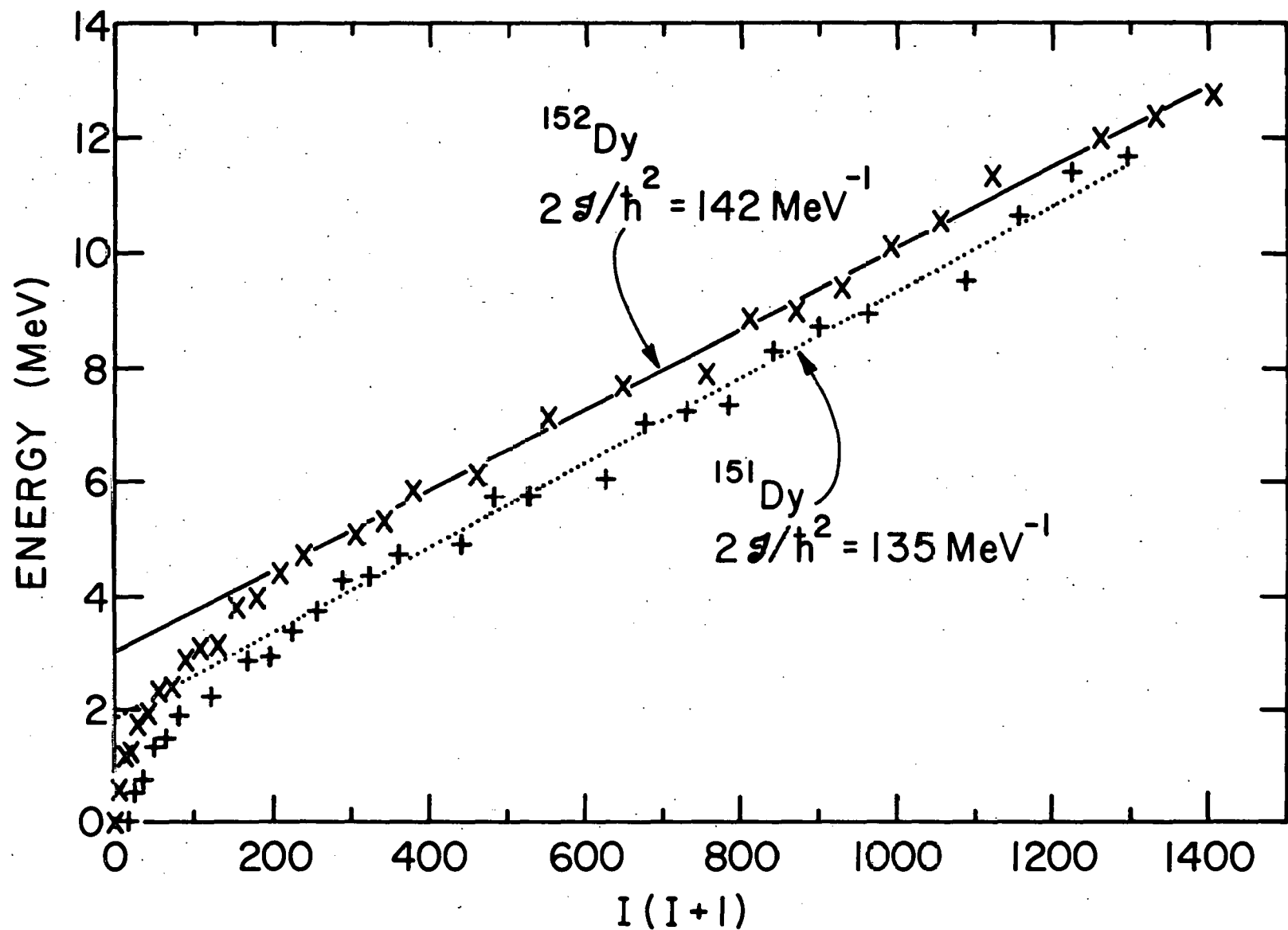


Fig. III-6. Plots of  $E$  vs  $I(I - 1)$  for the yrast states of  $^{151}\text{Dy}$  and  $^{152}\text{Dy}$ .

are 134 and 142 MeV<sup>-1</sup>, respectively. These are to be compared to the rigid-sphere value of 120 MeV<sup>-1</sup>. The excess over the rigid sphere value is due to either shell structure effects (high density of large-j valence orbits), or oblate deformation at high spin, or a combination of the two.

e. (<sup>12</sup>C, xn) Studies of <sup>151,152</sup>Dy

T. L. Khoo and R. K. Smither

In conjunction with the investigations of <sup>151,152</sup>Dy mentioned above, we have also performed experiments using the <sup>142</sup>Nd(<sup>12</sup>C, xn) and <sup>143</sup>Nd(<sup>12</sup>C, xn) reactions leading to <sup>151</sup>Dy and <sup>152</sup>Dy, with carbon beams from the Argonne FN Tandem accelerator. The results of these experiments aided in the isotopic assignment of  $\gamma$  rays to <sup>151</sup>Dy for which no level scheme previously existed. In addition, multipolarity assignments were made for many transitions deexciting isomers in both <sup>151,152</sup>Dy. In the <sup>32</sup>S-induced reactions the relaxation of the spin alignment in the isomeric states gave rise to isotropic angular distributions. With the <sup>12</sup>C beams used, there was significant side-feeding which by-passed the isomers, so that the relaxation problems are minimized.

f. High-Spin States in <sup>150</sup>Dy

W. Kutschera, I. Ahmad,\* C. N. Davids, T. L. Khoo, S. Levenson, R. D. McKeown, and R. K. Smither

To extend the systematics of the yrast line as a function of neutron number outside the N=82 closed shell, we have begun investigations of <sup>150</sup>Dy, using the <sup>122</sup>Sn(<sup>32</sup>S, 4n)<sup>150</sup>Dy reaction. The superconducting linac provided <sup>32</sup>S beams of 136 and 144 MeV. A number of isomers with half-lives around 3 ns have been observed in pulsed-beam measurements with a Ge(Li) detector by using the 20 ns beam-burst interval of the accelerator system. Figure III-7 shows  $\gamma$  rays from <sup>150</sup>Dy which are prompt and delayed with respect to the beam pulse. Figure III-8 shows the

\* Chemistry Division, ANL.

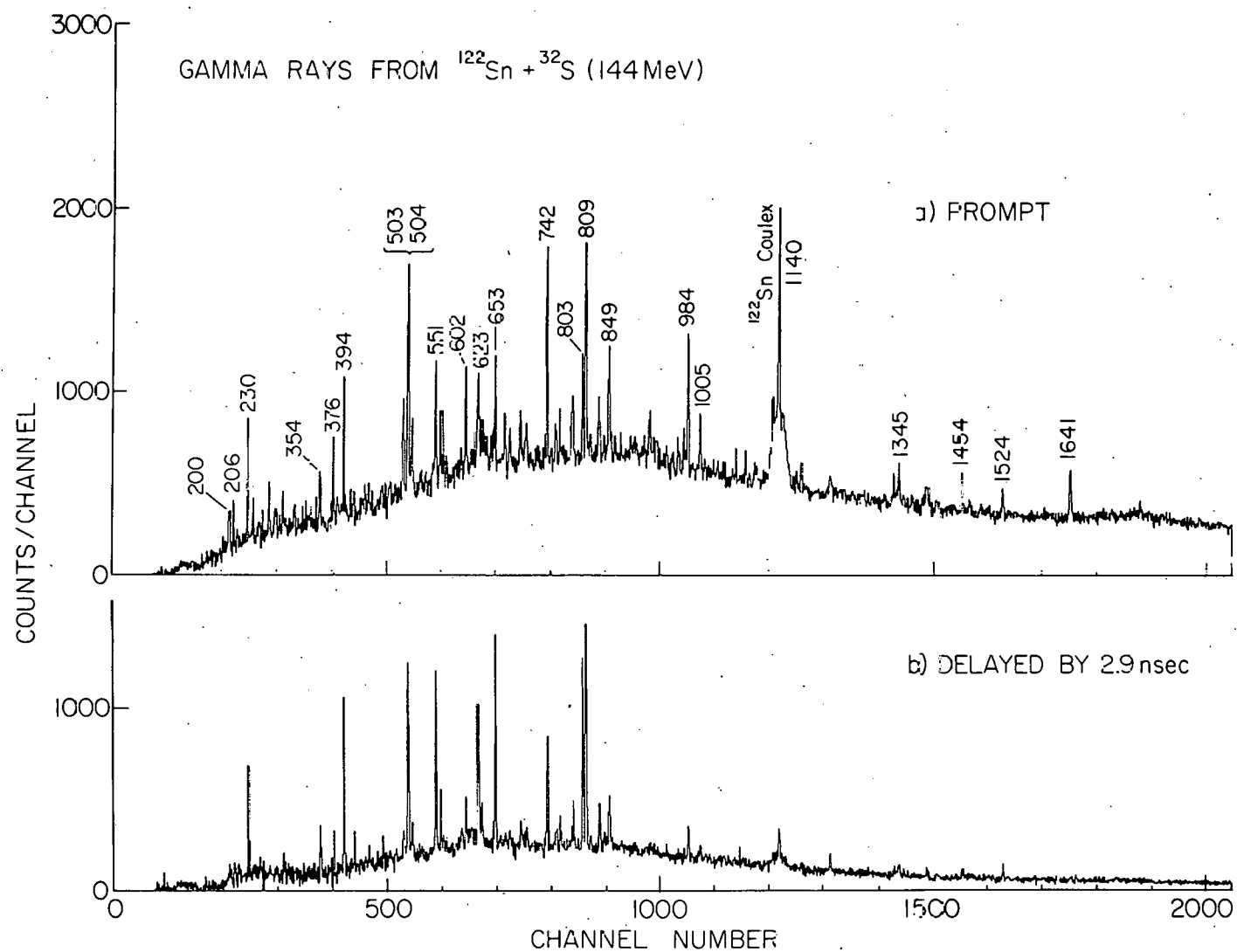


Fig. III-7. Gamma rays from bombardment of  $^{122}\text{Sn}$  with 144-MeV  $^{32}\text{S}$ .  $^{150}\text{Dy}$  is the principal product. (a) 2.5 ns wide prompt window; (b) 2.5 ns wide delayed window centered 2.9 ns after the prompt peak.

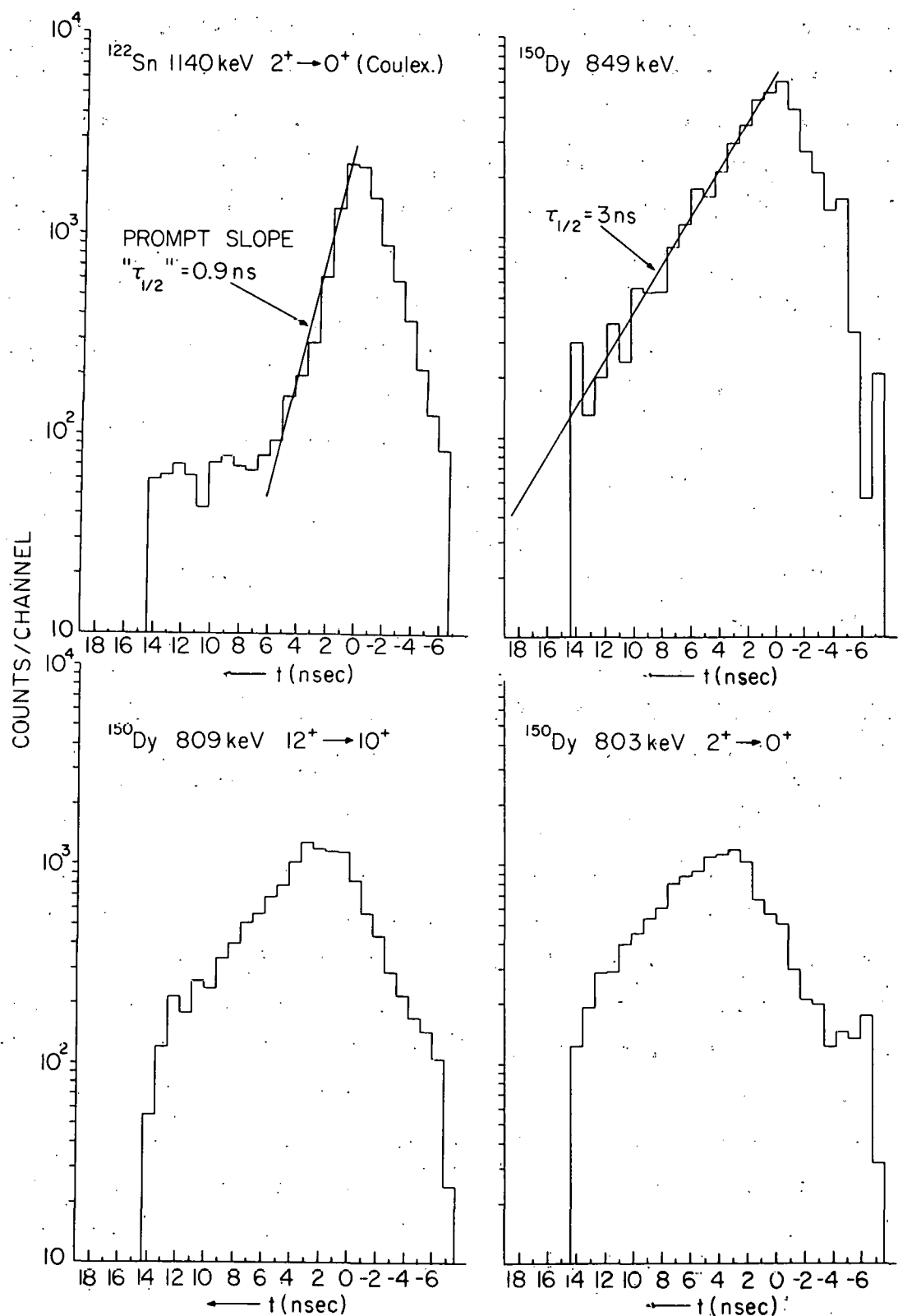


Fig. III-8. Time spectra (with respect to the beam pulse) for Coulomb excitation and  $^{150}\text{Dy}$  lines.

time spectra for a number of transitions. The time distribution for the line from Coulomb excitation demonstrates the experimental time resolution. The spectra for lines in Dy show a succession of isomers with lifetimes of around 3 ns (note the growth and decay character for the 803-keV  $2^+ \rightarrow 0^+$  transition). By virtue of the time structure associated with the linac beam, lifetimes as small as 1 ns can be easily observed in such time spectra. This is illustrated by the fact that  $\gamma$ -ray spectra in Fig. III-7 which are separated by 2.9 ns, clearly distinguish between prompt and delayed components.

In a delayed-coincidence experiment where the isomer decay was detected in an array of five 3 in.  $\times$  3 in. NaI detectors, we have identified many transitions (undoubtedly from very-high-spin states) feeding the isomers. Further experiments are in progress to establish the details of the  $^{150}$ Dy level scheme.

#### g. Spectroscopic Studies of High-Spin States in $^{148,149}$ Dy and $^{148}$ Tb

T. L. Khoo, I. Ahmad,\* C. N. Davids, W. Kutschera, S. Levenson, R. K. Smither, B. Haas,<sup>†</sup> H. R. Andrews,<sup>†</sup> O. Häusser,<sup>†</sup> P. Taras,<sup>†</sup> and D. Ward<sup>†</sup>

The distinction between spherical and deformed oblate shapes at high spin may be more clear-cut for nuclei with  $N = 82$  or very close to it. This is because the core excitations which are necessary for generating angular momentum are energetically unfavorable if the core remains spherical, leading to a steep yrast line. On the other hand, the gap above  $N = 82$  becomes smaller with deformation, so that the yrast line will not be so steep if the core becomes oblate at high spin. Study of yrast line systematics as a function of neutron number may thus yield important insights. We have recently initiated spectroscopic studies of very-high-spin states in  $^{148,149}$ Dy and  $^{148}$ Tb using the  $^{120}\text{Sn}(\text{<sup>32</sup>S}, \text{xn})$  and  $^{120}\text{Sn}(\text{<sup>32</sup>S}, \text{p3n})$  reactions, with sulfur beams from the Argonne

\* Chemistry Division, ANL.

<sup>†</sup> Chalk River Nuclear Laboratories, Chalk River, Ontario, Canada.

superconducting linac booster and the Chalk River MP Tandem. Gamma rays feeding 480 ns, 29 ns and 1.1  $\mu$ s isomers in  $^{148}\text{Dy}$ ,  $^{149}\text{Dy}$ , and  $^{148}\text{Tb}$ , respectively, have been identified. Prompt  $\gamma$ - $\gamma$  coincidences, followed by a delayed event in an array of five 3 in.  $\times$  3 in. NaI detectors, have been recorded. Analysis of the data is in progress.

## D. OTHER HEAVY-ION EXPERIMENTS

A variety of experiments is reported in this section: a careful study of inelastic heavy-ion scattering, the first charged-particle experiment with the linac booster, some precision straggling measurements with the bunching system, some developments in using the tandem system for radioisotope dating and the use of  $^{19}\text{F}$  beams in studying the profile of the hydrogen distribution in surface layers.

a. Energy Dependence of the Inelastic Scattering of  $^{16}\text{O}$  on  $^{40}\text{Ca}$

C. Olmer, W. Henning, D. G. Kovar, M. Paul, and S. J. Sanders

Our previous study [K. E. Rehm *et al.*, Phys. Rev. Lett. 40, 1479 (1978)] of inelastic scattering of  $^{16}\text{O}$  on  $^{40}\text{Ca}$  at  $E_{\text{lab}} = 60$  MeV provided information on the role multistep processes play in the excitation of the low-lying states in  $^{40}\text{Ca}$ . Publications of our data and analyses have prompted theoretical studies [R. Ascuitto *et al.*, Phys. Rev. Lett. 41, 1159 (1978)] by several other authors. From these analyses, specific dependence of the reaction behavior on incident energy is predicted. We have therefore extended our measurements to lower and higher energies ( $E_{\text{lab}} = 45$  MeV and 75 MeV) and measured angular distributions for the inelastic excitation of the lowest  $2^+$ ,  $3^-$ , and  $5^-$  states in  $^{40}\text{Ca}$ . Analysis of the data is well underway and indicates good agreement between the data and the coupled-channel calculations (CCBA) at the higher energy, as shown in Fig. III-9. However, as is shown in Fig. III-10, at the lower energy which is near the Coulomb barrier, some rather significant discrepancies exist. Work is in progress to understand this behavior in the energy dependence.

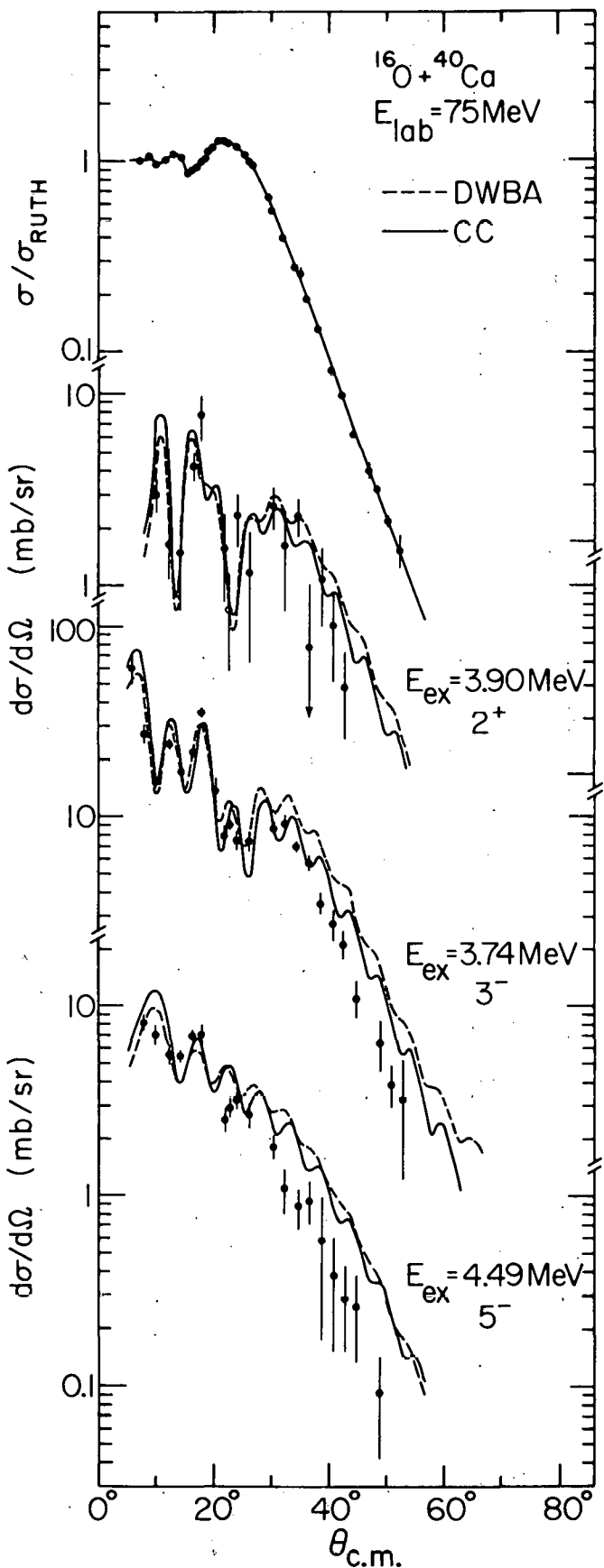


Fig. III-9. Angular distributions for elastic scattering of 75-MeV  $^{16}\text{O}$  by  $^{40}\text{Ca}$  and inelastic scattering to the lowest  $2^+$ ,  $3^-$ , and  $5^-$  states in  $^{40}\text{Ca}$ . The dashed lines are DWBA inelastic calculations using the code PTOLEMY; the solid lines are coupled-channel inelastic calculations using the code CHUCK. Both calculations produce similar results for the elastic scattering. The optical potential employed in the former calculations results from an energy-independent fit to the elastic scattering data at 45, 60, and 75 MeV; for the latter calculations, the same modification of the potential was done at each energy to correct for additional predicted elastic yield due to backfeeding from the inelastic into the elastic channel.

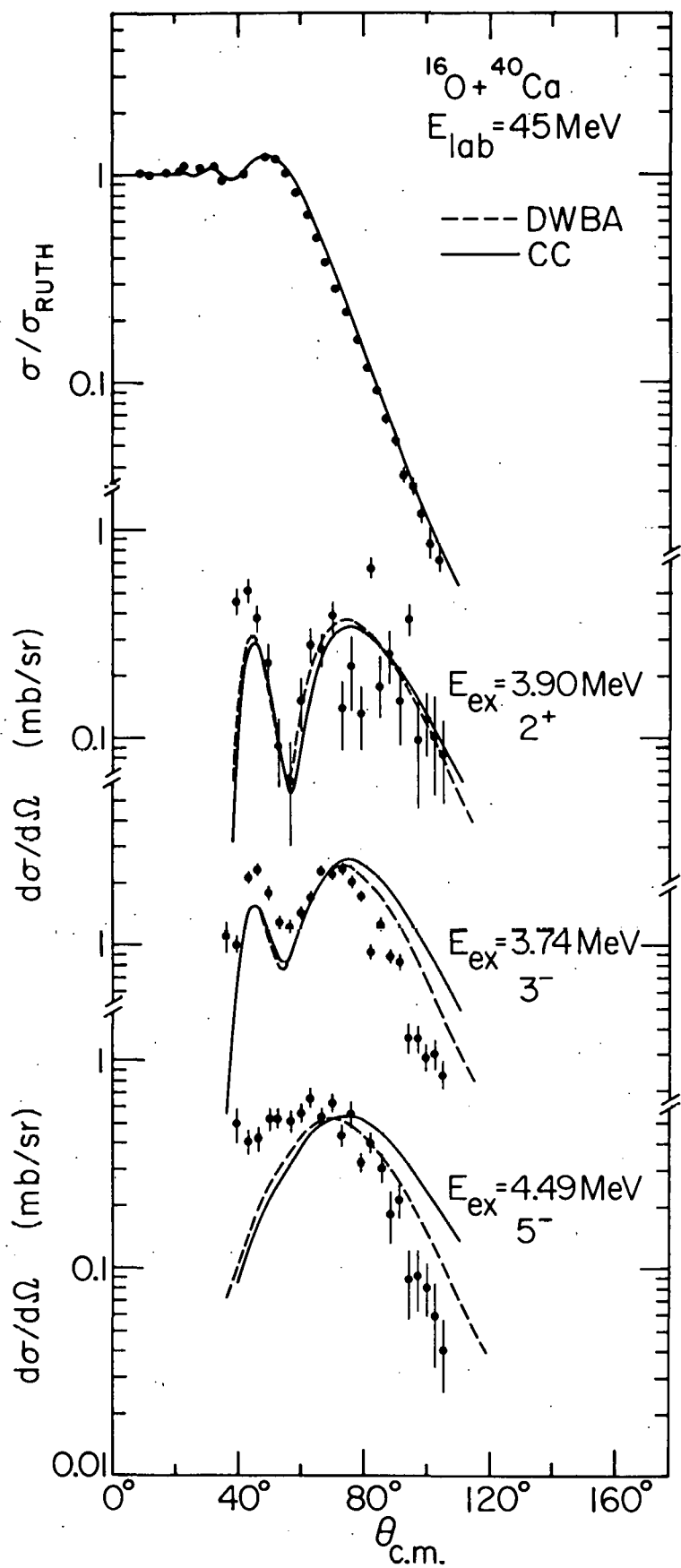


Fig. III-10. Angular distributions for elastic scattering of 45-MeV  $^{16}\text{O}$  by  $^{40}\text{Ca}$  and inelastic scattering to the lowest  $2^+$ ,  $3^-$ , and  $5^-$  states in  $^{40}\text{Ca}$ . The dashed lines are DWBA inelastic calculations using the code PTOLEMY; the solid lines are coupled-channel inelastic calculations using the code CHUCK. Both calculations produce similar results for the elastic scattering. The optical potential employed in the former calculations results from an energy-independent fit to the elastic scattering data at 45, 60, and 75 MeV; for the latter calculations, the same modification of the potential was done at each energy to correct for additional predicted elastic yield due to backfeeding from the inelastic into the elastic channel.

b. Interactions of  $^{32}\text{S}$  Beam from the Argonne Superconducting Post Accelerator with  $^{40},^{48}\text{Ca}$  Target Nuclei

B. Back,\* D. F. Geesaman, W. Henning, D. G. Kovar, A. Mignerey,\* C. Olmer, M. Paul, S. J. Sanders, J. P. Schiffer, and B. Zeidman

We have begun first experiments with the  $^{32}\text{S}$  beam available from the new superconducting booster at the Argonne FN tandem. The first study involved charged-particle measurements of the reaction products resulting from the interaction of 143-MeV  $^{32}\text{S}$  ions on  $^{40}\text{Ca}$  and  $^{48}\text{Ca}$  (Fig. III-11). This work is a natural extension to heavier projectiles of previous extensive studies at Argonne of  $^{16}\text{O}$  ions incident on various Ca isotopes. The objective of these studies is to determine the distribution of reaction strength in these medium-heavy systems and in particular to investigate whether nuclear structure aspects become apparent at the very high excitation energies involved in such reactions. Energy spectra and angular distributions for elemental yields were measured for the quasielastic and the more inelastic reactions. A preliminary analysis shows qualitative differences in the distribution of reaction strengths between  $^{32}\text{S} + ^{40}\text{Ca}$  and  $^{32}\text{S} + ^{48}\text{Ca}$ . Following a more detailed analysis, we plan to extend these measurements to other Ca target nuclei and to higher incident energies.

c. Energy-Loss Straggling Measurements for  $^{16}\text{O}$  and  $^{32}\text{S}$  Ions in Thin Carbon Foils

W. Henning and T. P. Wangler

While it is of considerable practical importance in the use of tandem stripper foils, not much is known experimentally about energy-loss straggling of heavy ions in thin foils at energies around 0.1 to a few MeV/nucleon. The major reason is that the required energy resolution cannot be easily obtained in a direct measurement.

\* Chemistry Division, ANL.

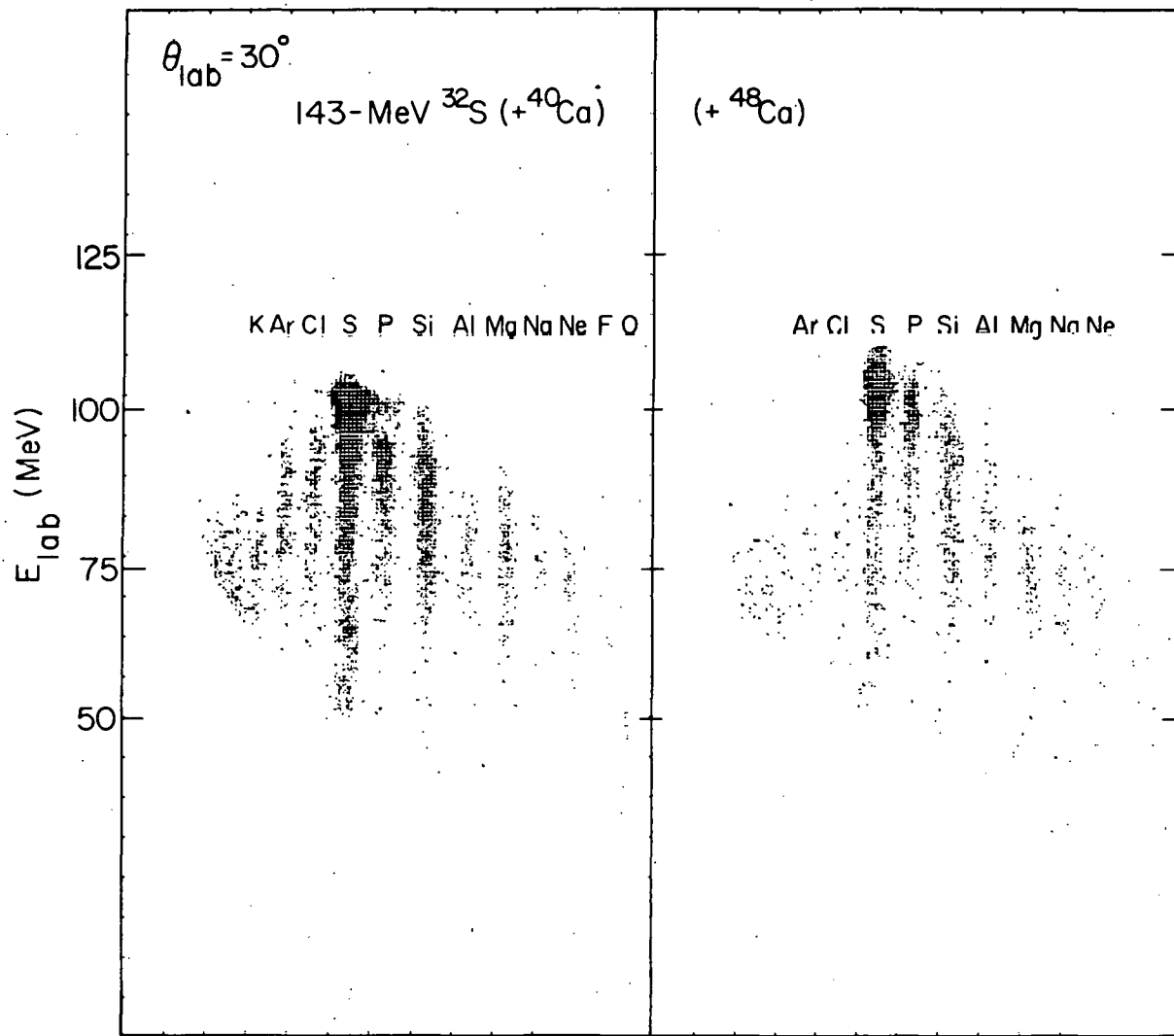


Fig. III-11. Contour plot of total energy  $E$  versus differential energy loss  $\Delta E$  for reaction products from  $^{32}\text{S} + ^{40,48}\text{Ca}$  at 143-MeV incident energy from the Argonne superconducting linac.

We have used the excellent time resolution of the ps-bunched beam from the booster bunching system to determine such energy straggling in time-of-flight measurements. The equivalent energy resolution obtained, approximately 5 keV, allowed energy-loss straggling measurements for  $^{16}\text{O}$  and  $^{32}\text{S}$  ions in single- and double-stripper configurations for thicknesses as low as  $2 \mu\text{g/cm}^2$ . We plan to use this extremely powerful system to extend these measurements to other ions and over the energy range available at the Argonne FN tandem.

#### d. Radioisotope Dating with the FN Tandem Accelerator

W. Kutschera, W. Henning, M. Paul, E. J. Stephenson, and J. L. Yntema

Due to intensive research in the field of nuclear reactions induced by heavy ions, high quality ion beams and sophisticated detector systems capable of identifying accelerated ions by mass and nuclear charge are available at accelerator laboratories. This has stimulated a new method of radioisotope dating by counting accelerated ions rather than their radioactive decays.<sup>1</sup> At the Rochester conference,<sup>2</sup> initial studies of  $^{14}\text{C}$  dating with accelerators were discussed. The need for dedicated facilities for precision work was emphasized. Such facilities for  $^{14}\text{C}$  will probably be tandem accelerators operating at low acceleration voltages. A tandem accelerator with higher voltage, on the other hand, has a broader range of applications for this new technique.<sup>3</sup>

We have started an investigation of radioisotope dating at the FN tandem (terminal voltage  $\leq 9$  MV). Our first measurements were

<sup>1</sup> R. A. Muller, Physics Today 32(2), 23 (1979) and references therein.

<sup>2</sup> Proceedings of the First Conference on Radiocarbon Dating with Accelerators, University of Rochester, April 20-21, 1978, edited by H. E. Gove (University of Rochester, N. Y., 1978).

<sup>3</sup> K. H. Purser, A. E. Litherland and H. E. Gove, Nucl. Instrum. Methods, to be published.

performed for  $^{14}\text{C}$  and  $^{32}\text{Si}$ . The recently upgraded FN tandem proved exceptionally stable and reproducible. Keeping all magnetic focusing elements at a fixed field level, various ion beams with identical magnetic rigidity were produced for tuning purposes by adjusting the tandem acceleration voltage. In the study of  $^{14}\text{C}^{4+}$ , ion beams of  $^{13}\text{C}^{4+}$  and  $^{18}\text{O}^{5+}$  were thus accelerated and found precisely focused. This accurate scaling with terminal voltage is attributed to negligible changes in electrostatic focusing from the new accelerator tubes, which have a straight electrode structure rather than the inclined field configurations often in use. No additional focusing elements are used in the accelerator.

To identify the accelerated ions by mass and atomic number, a standard heavy-ion detection system is used. It consists of an Enge split-pole magnetic spectrograph with an ionization chamber focal-plane detector.<sup>4</sup> A major objective was to develop a simple technique to discriminate against the isobaric background generally present in radio-isotope beams. This was achieved by utilizing the excellent momentum resolution of the spectrograph to accurately measure the energy loss dispersion from a uniform absorber (e.g., a stack of 15 aluminum absorber foils each  $100 \mu\text{g/cm}^2$  thick). The focal plane counter can also be physically shielded against the spatially separated strong background lines and provides unique identification of the accepted ions. The method has been tested for  $^{32}\text{Si}$  where a strong  $^{32}\text{S}$  background has to be eliminated. At present a detection limit of  $^{32}\text{Si}/^{28}\text{Si} \leq 10^{-14}$  has been achieved. A separation of  $^{36}\text{Ar}$  from  $^{36}\text{S}$  by energy loss dispersion in a gas cell and subsequent detection in a  $\Delta E - E$  telescope has been reported at the Rochester conference.<sup>5</sup>

---

<sup>4</sup> J. R. Erskine, T. H. Braid, and J. C. Stoltzfus, Nucl. Instrum. Methods 135, 67 (1976).

<sup>5</sup> T. S. Mast, in *Proceedings of the First Conference on Radiocarbon Dating with Accelerators*, University of Rochester, April 20-21, 1978, edited by H. E. Gove (University of Rochester, N.Y., 1978), p. 239.

For  $^{14}\text{C}$  detection the isobaric background from  $^{14}\text{N}$  is not present since  $^{14}\text{N}$  does not form stable negative ions. However, "tailing" from scattered  $^{12}\text{C}$  and  $^{13}\text{C}$  limits our  $^{14}\text{C}$  detection sensitivity to  $\leq 10^{-15}$ . First energy loss dispersion measurements indicate a substantial improvement in separating  $^{14}\text{C}$  from other ions. We are in the process of further investigating our method. Samples with varying radioisotope concentrations are being studied, including  $^{36}\text{Cl}$  as well as  $^{14}\text{C}$  and  $^{32}\text{Si}$ .

e.  $\text{Pd}(\text{O}_{16}, \text{xn})\text{Xe}$

R. K. Smither, A. M. Friedman,\* I. Ahmad,\* and D. L. Bushnell†

A change in the level structure (a sudden decrease in the level spacing in the ground-state band with increasing neutron number) at neutron number  $N = 62$  has been observed previously in the Cd and Te isotopes. The object of these experiments is to look for this structure change in the Xe isotopes. No new data were taken in 1978 but continued analysis of the 1977 data has yielded new level schemes for  $^{116}\text{Xe}$  ( $Z = 62$ ) and  $^{118}\text{Xe}$  ( $Z = 64$ ). The level structure change is observed between  $^{116}\text{Xe}$  and  $^{118}\text{Xe}$  with a resulting shift of the position of the  $6^+$  level of 109 keV as compared to a 13 keV shift observed between  $^{118}\text{Xe}$  and  $^{120}\text{Xe}$ . Data on the level scheme of  $^{114}\text{Xe}$  are sorely needed to complete this study. The yield of the  $^{102}\text{Pd}(\text{O}_{16}, 4n)^{114}\text{Xe}$  reaction is quite low, possibly because of competing charged-particle emission. A second series of experiments are planned for the coming year using the  $\text{Cd}(\text{C}_{12}, \text{xn})\text{Xe}$  reactions where the  $^{106}\text{Cd}(\text{C}_{12}, 4n)^{114}\text{Xe}$  reaction is expected to give more yield for the  $^{114}\text{Xe}$  isotope. Besides establishing the presence of this nuclear structure change in Xe, it is of interest to see if the structure change at  $N = 64$  is affected by the filling of the proton shell at  $Z = 50$ . The main change observed with the completion of the proton shell is an overall decrease in the energy scale. Thus all of the levels decrease by

\* Chemistry Division, ANL.

† Northern Illinois University, DeKalb, Illinois.

about 40% as  $Z$  goes from 46 to 54. Further work is planned for the Xe isotopes using heavier ions and the higher energies now available with the new superconducting booster to investigate higher spin states in these Xe isotopes and in the Ba isotopes. All of these isotopes are near closed shells or closed subshells for both protons and neutrons so a comparison with the new high-spin work of Khoo *et al.* (see Sec. III.C.g of this report) will be of considerable interest.

f. Heavy-Ion Coulomb Excitation in  $^{148,150,152,154}\text{Sm}$

R. K. Smither, D. L. Bushnell,\* A. M. Friedman,<sup>†</sup> and I. Ahmad<sup>†</sup>

The object of this work was to measure the  $B(E2)$  values of  $\gamma$  transitions from the second and third  $2^+$  states in  $^{148}\text{Sm}$  and to obtain more accurate determinations for the relative  $B(E2)$  values for transitions from the low-lying  $2^+$  states in the  $^{148,150,152,154}\text{Sm}$  isotopes. This improved accuracy is needed to make meaningful comparisons between the current phonon and rotor models that might be applicable. No new data were taken but continued analysis of earlier data has improved the accuracy of the results. The Coulomb excitation experiments were done with an  $^{16}\text{O}$  beam with energies from 35 to 55 MeV. Good data on the production of the second and third  $2^+$  states in  $^{148}\text{Sm}$  were obtained only at the highest energies,  $E_{\text{beam}} = 50-55$  MeV. At 55 MeV a significant amount of the yield comes from the interference between nuclear and Coulomb forces and detailed computer calculations were required to separate out the pure Coulomb cross section. The gamma-ray lines associated with these  $2^+$  states are strongly Doppler shifted and a computer analysis of the resultant line shapes yields approximate lifetimes for these states which can be used as a check on the cross-section measurements. The main result of this work was to obtain more accurate  $B(E2)$  values

---

\* Northern Illinois University, DeKalb, Illinois.

<sup>†</sup> Chemistry Division, ANL.

for the second and third  $2^+$  states in  $^{148}\text{Sm}$ . When these  $B(E2)$  values are compared with those from the other Sm isotopes, their relative values agree quite well with the predictions of the interacting boson model of Arima and Iachello. The old values for  $^{148}\text{Sm}$  were considerably different from the values established for the other Sm isotopes.

g. Radiation-Damage Enhanced Trapping of Hydrogen in Molybdenum

A. L. Hanson,\* D. H. Vincent,\* and C. N. Davids

Radiation-damage enhanced trapping of hydrogen in the near surface (first 2000 Å) region of single crystal molybdenum has been investigated. Hydrogen concentrations versus depth have been determined using the 16.44-MeV resonance of the reaction  $\text{H}(\text{F}^{19}, \alpha\gamma)^{16}\text{O}$  with  $\text{F}^{19}$  beams from the FN tandem. The hydrogen was introduced by implantation at 10, 15, and 20 keV. Some of the samples had been previously damaged with helium between 18 and 150 keV. The trapping of implanted hydrogen was used to study the damage processes in molybdenum.

h. Radiative Capture of  $^{12}\text{C}$  by  $^{12}\text{C}$  Near the Coulomb Barrier

T. J. Bowles, A. M. Nathan,<sup>†</sup> and A. M. Sandorfi<sup>‡</sup>

Recent studies of the electrofission of  $^{24}\text{Mg}$  and radiative capture of  $^{12}\text{C}$  by  $^{12}\text{C}$  have indicated that the structure of  $^{24}\text{Mg}$  plays a role in the coupling of resonances formed in the entrance channel of the  $^{12}\text{C} + ^{12}\text{C}$  system to quadrupole gamma decay into  $^{24}\text{Mg}$ . We have recently carried out studies at Argonne using the newly developed NaI spectrometers in order to study in detail the radiative capture of  $^{12}\text{C}$  by  $^{12}\text{C}$  near the Coulomb barrier. The good energy resolution ( $\sim 3.5\%$ ) of the NaI spectrometers at large solid angles ( $\sim 100$  msr) at high counting rates

\* University of Michigan, Ann Arbor, Michigan.

<sup>†</sup> University of Illinois, Urbana, Illinois.

<sup>‡</sup> Brookhaven National Laboratory, Upton, L.I., New York.

( $\sim 100$  kHz) in conjunction with good rejection of cosmic ray events ( $> 98\%$ ) was essential in order to measure the small cross sections (typically  $100 \text{ nb/sr}$ ) and to resolve decays to the first few excited states of  $^{24}\text{Mg}$ .

An excitation function at  $45^\circ$  was measured from  $19.5 \text{ MeV}$  to  $23 \text{ MeV}$  excitation energy in  $^{24}\text{Mg}$  and four resonances with widths  $\approx 250 \text{ keV}$  (and probably  $J^\pi = 2^+$  for three of the resonances) were observed. These are correlated to varying degrees in the decays to the ground, first, and second and third excited states in  $^{24}\text{Mg}$ . We are now trying to determine the relation of these resonances to resonances observed in other decay channels in the  $^{12}\text{C} + ^{12}\text{C}$  system.

## IV. CHARGED-PARTICLE RESEARCH

### INTRODUCTION

This activity encompasses a broad range of nuclear studies centered about the Dynamitron and Tandem Van de Graaff accelerators in the Physics Division. The scope of activity ranges from cross-section measurements of nuclear reactions of potential interest to thermonuclear nuclear-energy generation to fundamental aspects of the weak interactions as evidenced in nuclear-decay processes. Nuclear spectroscopy studies in the  $1f_{7/2}$  shell and in neutron-rich nuclei in the region  $50 \leq A \leq 70$  are also conducted. Studies of the parity violation in specific nuclear levels induced by the recently discovered neutral weak currents are being investigated.

The charged-particle research program in the Physics Division draws on the talents of a number of researchers in the Division, plus a very substantial interaction with researchers in the university community. The charged-particle research effort uses both the Dynamitron (30% of the available time) and the FN Tandem accelerator (25% of the available time).

## A. CHARGED-PARTICLE RESEARCH AT THE DYNAMITRON

This program has two principal components. The largest program in terms of ANL manpower is the ongoing investigation into exothermic reactions with light nuclei. The reactions to be studied are selected on the basis of their intrinsic interest to nuclear physics, astrophysics, and their potential use as a clean fuel in controlled thermonuclear research applications.

The other program is a continuation of the recently initiated research into studies of the fundamental aspects of weak interactions as observed in nuclei. Data have been taken on the  $\beta^{\pm}$ - $\alpha$  angular correlations in  $A = 8$  as a function of end-point energy. This allowed a very detailed test of CVC and was sensitive to the existence of axial-vector second-class interactions. The results support CVC and offer no evidence for the existence of a second-class current. A challenging experiment to measure the  $\Delta T=1$  parity mixing induced by the neutral weak current is now being readied to take data (in collaboration with a researcher from Stanford University).

### a. Interpretation of $d + ^6\text{Li}$ Reactions at Low Energies

A. J. Elwyn and J. E. Monahan

The systematic features of recent differential and total cross-section data relating to the  $^6\text{Li}(d, \alpha)\alpha$ ,  $^6\text{Li}(d, p)^7\text{Li}$ , and  $^6\text{Li}(d, n)^7\text{Be}$  reactions at deuteron energies between 0.1 and 1.0 MeV have been investigated in terms of the underlying reaction mechanisms. A paper has been accepted for publication in Physical Review C in which the above reactions are analyzed in terms of the Wigner-Eisenbud formalism with the R-matrix elements assumed constant, and includes, for the (d, p) and (d, n) reactions, an additional coherent direct-reaction contribution. The results, although they do not lead to a unique specification of parameters, give an indication of the magnitude of the direct component of these reactions, and also show that the observation of a resonance-like structure [in, e.g., the  $^6\text{Li}(d, \alpha)\alpha$  reaction at energies below 1 MeV] does not necessarily imply a corresponding state in the compound nucleus  $^8\text{Be}$ .

b. Absolute Cross Sections for Three-Body Breakup Reactions $^6\text{Li}(\text{d}, \text{n}^3\text{He})^4\text{He}$  and  $^6\text{Li}(\text{d}, \text{p}^3\text{H})^4\text{He}$ 

R. E. Holland, A. J. Elwyn, J. E. Monahan, C. N. Davids, L. Meyer-Schützmeister, and F. P. Mooring

Absolute cross sections were obtained for the reactions  $^6\text{Li}(\text{d}, \text{n}^3\text{He})^4\text{He}$  and  $^6\text{Li}(\text{d}, \text{p}^3\text{H})^4\text{He}$  for deuteron energies from 100 keV to 800 keV, as discussed in last year's Annual Review. The energy spectra of particles from these reactions are continua because of the three-body final state. Total cross sections as well as angular distributions were obtained with accuracies of 10 to 17 per cent. Comparisons of energy spectra were made to predictions of simple models. A paper with this title was prepared and has been published by Physical Review C.

c. The  $^6\text{Li}(\text{p}, \text{He})^4\text{He}$  and Other Reactions of Light Ions with  $^6\text{Li}$  at Low Energies

A. J. Elwyn, R. E. Holland, C. N. Davids, L. Meyer-Schützmeister, and F. P. Mooring

Over the past few years interest has been expressed in  $^6\text{Li}$ -H as an advanced fuel for the future generation of fusion-power devices. Previous measurements of the cross sections for the  $^6\text{Li}(\text{p}, \text{He})^4\text{He}$  reaction as well as for the important supplementary reaction  $^6\text{Li}(\text{He}, \text{p})$ , both of which provide the main portion of the data base necessary to evaluate the feasibility of this fuel, are in considerable disagreement. In the last Annual Review, we reported measurements for the  $^6\text{Li}(\text{p}, \text{He})^4\text{He}$  reaction at incident proton energies from 0.1 to 1.0 MeV. During the past year we have extended the differential cross-section measurements up to 3.0 MeV by a coincidence technique. Analyses of these data have led to the determination of total reaction cross sections accurate to better than 10%. The present results, together with those from our earlier studies, are shown in Fig. IV-1 compared to previous measurements. As seen, they provide a consistent set of  $^6\text{Li}(\text{p}, \text{He})^4\text{He}$  cross sections over

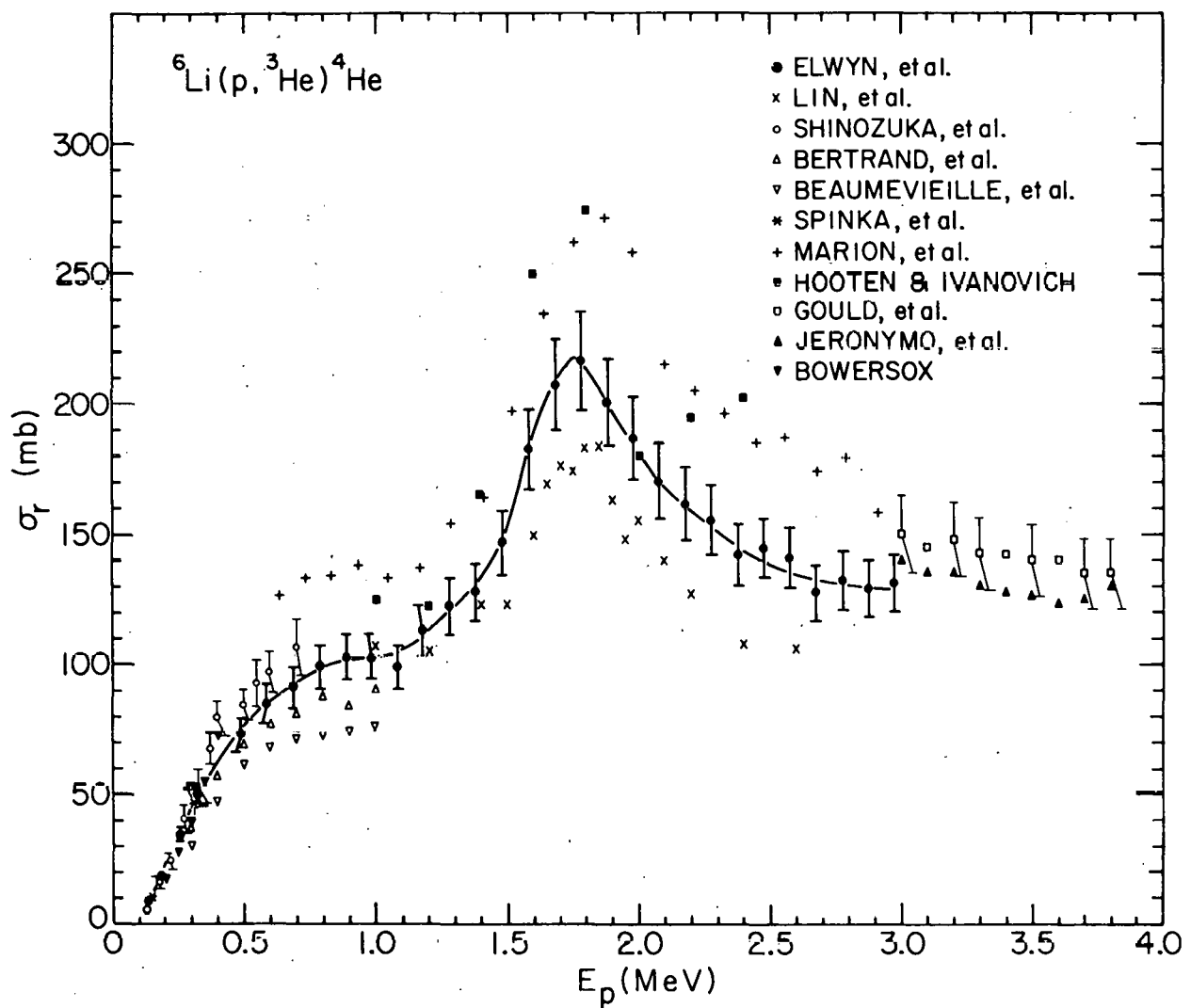


Fig. IV-1. Reaction cross section for the  ${}^6\text{Li}(\text{p}, {}^3\text{He}) {}^4\text{He}$  reaction compared to previous measurements. The present results are represented by the solid circles and the smooth curve is drawn to guide the eye.

a large portion of the energy region of interest to the thermonuclear studies. A paper describing these experiments is currently being prepared.

Measurements of the important  $^6\text{Li}(^3\text{He}, \text{p})$  reaction cross sections are discussed elsewhere in this Annual Review. Future experiments of light ions with  $^6\text{Li}$  will concentrate on the determination of the cross sections for elastic scattering of p, d, and  $\alpha$  particles at energies from below 1 up to 2 MeV. These data are not only of direct importance to CTR applications, but have intrinsic interest to basic studies of nuclear structure and reaction mechanisms.

d. Cross Sections for Three-Body Breakup in  $^3\text{He} + ^6\text{Li}$  Reactions at Low Energy

R. E. Holland, A. J. Elwyn, J. E. Monahan, C. N. Davids, L. Meyer-Schützmeister, and F. P. Mooring

Thermonuclear reaction rates arising from  $\text{d} + ^6\text{Li}$  and  $\text{p} + ^6\text{Li}$  reactions are expected to be influenced by contributions from the reactions of  $^3\text{He}$  with  $^6\text{Li}$ , since  $^3\text{He}$  is produced in these primary processes. We are investigating  $^3\text{He} + ^6\text{Li} \rightarrow 2 ^4\text{He} + \text{p}$  at bombarding energies from 0.5 to 2.0 MeV. This reaction proceeds through proton emission to the ground state of  $^8\text{Be}$ , as well as through the 2.94-, 16.63-, and 16.92-MeV excited states of  $^8\text{Be}$ . The appearance of the proton spectrum from this reaction also leads us to believe that direct three-body breakup occurs. (Contributions are also expected from sequential decay through states of  $^5\text{Li} + \text{a.}$ ) In the low-energy region of the spectrum of the outgoing particle one can also expect deuterons from transitions to  $^7\text{Be} + \text{d}$ , although no transition can occur to unbound levels of  $^7\text{Be}$  at our bombarding energies. Because the reaction cross section is small relative to the elastic scattering cross section, our first data were taken with absorber foils over surface barrier detectors, and allow the unambiguous determination of the cross section to the ground state of  $^8\text{Be}$  only. Other contributions to the total reaction cross section can only be obtained through more complicated experiments since the energy spectrum contains

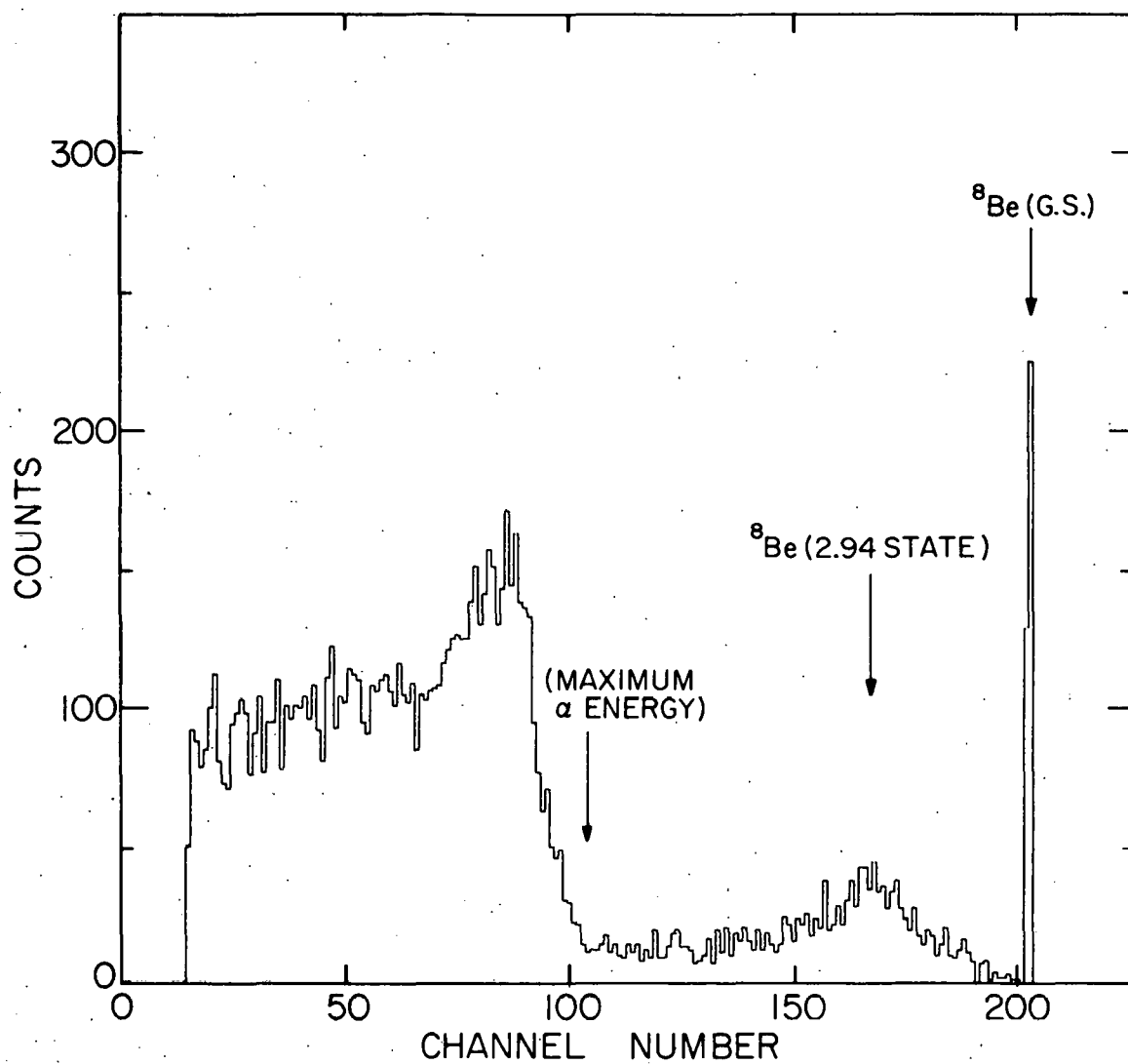


Fig. IV-2. Energy spectrum of particles from  ${}^6\text{Li} + {}^3\text{He}$  for  $E_{{}^3\text{He}} = 0.600 \text{ MeV}$ , and detector angle of  $135^\circ$ . An absorber foil of 2.4 mg of Al over the surface barrier detector prevented elastically-scattered  ${}^3\text{He}$  particles from entering the detector. Proton transitions to the ground state and first excited state of  ${}^8\text{Be}$  as well as the maximum  $\alpha$  energy are indicated on the figure.

protons, alpha particles, and deuterons. A typical energy spectrum of particles from  $^{6}\text{Li} + ^{3}\text{He}$  with a 2.4 mg Al foil over the detector is shown in Fig. IV-2. The absorber foil is thick enough to stop elastically-scattered  $^3\text{He}$  particles, so that the observed spectrum is caused by both protons and alpha particles. Since the partial cross section for decay through the ground state of  $^8\text{Be}$  can be cleanly extracted from the present data, we expect to use this cross section as a reference to allow us to normalize data from more complete experiments. Total cross sections and angular distributions for protons and alpha particles separately will be obtained from a time-of-flight measurement. This will also allow a check on our technique since the total cross section for  $\alpha$ -particle production must be twice that for proton production. We are not aware of any earlier measurements of total reaction cross section in this energy region.

e.  $^{8}\text{Li}(\beta^{-}, \alpha)$  and  $^{8}\text{B}(\beta^{+}, \alpha)$  Angular Correlations

R. D. McKeown and G. T. Garvey

A detailed study of the  $\beta^{\mp}$ - $\alpha$  angular correlations in the  $^{8}\text{Li}(\beta^{-})$  and  $^{8}\text{B}(\beta^{+})$  decays was performed. Since these decays proceed to the  $2\alpha$  continuum, detection of both alpha particles enabled determination of various correlations as functions of the final state energy.

Analysis of the spectrum of the difference in  $\alpha$ -particle energies in coincidence with  $\beta^{\mp}$  particles yields information on the  $^{8}\text{Be}^*$  recoil spectrum which in turn depends on the  $\beta\text{-}\nu\text{-}\alpha$  angular correlation. The data are consistent with pure Gamow-Teller decay throughout the region  $2 \text{ MeV} < E_x < 8 \text{ MeV}$ , where  $E_x$  is the final-state excitation energy in  $^{8}\text{Be}$ .

The  $\beta^{\mp}$ - $\alpha$  angular correlations are analyzed in the form  $W_{\mp}(\theta) = 1 + a_{\mp}(E, E_0) \cos(\theta) + p_{\mp}(E, E_0) \cos^2 \theta$ , where  $\theta$  is the angle between the  $\beta^{\mp}$  particle and an alpha particle. The coefficient  $a_{\mp}$  is predominantly kinematic in origin and serves as a useful check on the experimental

technique, whereas  $p_{\mp}$  contains information pertaining to the validity of CVC and the existence of second-class currents.

The quantity of interest for observing the effects of CVC and second-class currents is  $\delta^- = p_- - p_+$ , which can be expressed in terms of weak nuclear form factors enabling a model-independent analysis. These form factors can be completely determined from the beta-decay rate (ft value) and properties of the analog  $\gamma$  transition in  ${}^8\text{Be}$  assuming the validity of CVC and the absence of second-class currents. The finite isovector  $E2/M1$  mixing ratio in the analog  $\gamma$  transition implies that the result is sensitive to the effect of CVC at the second-forbidden level as well as the usual weak-magnetism term.

The experimental results for  $\delta^-$  show a small ( $\approx 15\%$  of weak magnetism) deviation from the CVC prediction which is dependent on the final-state energy. An effect of this size cannot be interpreted as convincing evidence for the presence of a second-class current or breakdown of CVC. However, the inclusion of the vector-second-forbidden terms in the nuclear weak current as predicted by CVC is crucial to obtain even approximate agreement with the experimental results.

#### f. Parity Violation in the 5.1-MeV $J=2$ Doublet of ${}^{10}\text{B}$

C. A. Gagliardi, S. J. Freedman,\* T. J. Bowles, A. R. Davis, G. T. Garvey, R. D. McKeown, and B. Myslek-Laurikainen

Since the discovery of the neutral weak current, there has been a great deal of experimental interest in defining its nature. To date, all of the semileptonic results are well described by the  $SU(2) \times U(1)$  gauge theory of Weinberg-Salam with mixing angle  $\sin^2 \theta_w \sim 0.2 - 0.25$ . Meanwhile, studies of the purely hadronic neutral current have been more ambiguous.

The only method available for studying the hadronic weak current is to measure parity-violating effects. Thus, it is natural to

---

\*Stanford University, Stanford, California.

describe it in terms of parity-violating amplitudes of definite isospin. When CP invariance is included, one finds that only the  $\Delta T=1$  component can have a one-pion exchange contribution.

The  $\Delta T=0$  and 2 currents arise from the exchange of multiple pions and heavier mesons, causing the associated parity-violating forces to have much shorter range. This makes results of calculations of the  $\Delta T=0$  and  $\Delta T=2$  effects unreliable since they are highly model dependent and the repulsive core of the nucleon-nucleon force is only poorly understood.

In addition to the fact that the  $\Delta T=1$  case is unencumbered by these theoretical uncertainties, the Cabibbo (charged) current contribution for  $\Delta T = 1$  is suppressed by a factor  $\sin^2 \theta_c$  relative to the neutral current. It is thus natural to attempt to observe the neutral weak current by studying cases of pure  $\Delta T=1$  parity violation.

Despite intensive efforts, previous experiments to measure  $\Delta T=1$  parity violation have merely set an upper limit on the size of the effect. We have undertaken a study of  $\Delta T=1$  parity violation in  $^{10}\text{B}$  by measuring mixing between the  $2^+$   $T=1$  state at 5.16 MeV and the  $2^-$   $T=0$  state at 5.11 MeV. The  $2^+$   $T=1$  state is produced via the  $^{6}\text{Li}(a, \gamma)^{10}\text{B}$  reaction, using a 1.2-MeV  $a$  beam from the Argonne Dynamitron. The total cross section is given by

$$\sigma = \sigma_0 (1 + \frac{1}{2} P_{zz} + FP_z),$$

where the  $z$  axis is along the  $a$ -beam direction. The quantity of interest is  $F$ , the helicity dependence of the rate. Preliminary measurements have shown that this experiment should be sensitive even to a purely charged (Cabibbo) contribution with reasonable counting times.

The polarized  $^6\text{Li}$  target for the experiment is now nearly complete. An intense  $^6\text{Li}$  atomic beam is collimated and then polarized using a pair of large gap (1.2 cm diameter), high field ( $\sim 12.5$  kG) sextupole magnets. The atomic polarization is then converted to nuclear polarization

using a weak-field rf-transition unit. The  ${}^6\text{Li}$  impinges on a hot ( $\sim 1100^\circ\text{C}$ ) oxidized tungsten surface in a holding field. The sitting time is such as to provide a monolayer target to a 50—100- $\mu\text{A}$  a beam with almost no depolarization. Subsequent  $\gamma$  decays are observed using a cylindrical NaI detector with a solid angle close to  $4\pi$ .

The final off-line tests are now in progress and should be completed by mid-summer. At that time, the polarized target will be installed on the Dynamitron for on-line testing, with data taking for the  ${}^6\text{Li}(a, \gamma){}^{10}\text{B}$  reaction beginning in the fall.

g. Measurement of the Direct Capture Reaction  ${}^2\text{H}({}^4\text{He}, \gamma){}^6\text{Li}$

T. J. Bowles, R. G. H. Robertson,\* R. A. Warner,\* P. Dyer,\* and R. C. Melin\*

We have completed a measurement of the excitation function of the direct capture reaction  ${}^2\text{H}({}^4\text{He}, \gamma){}^6\text{Li}$  from  $E_x = 3.4$  MeV to  $E_x = 9$  MeV in  ${}^6\text{Li}$ . The recoiling  ${}^6\text{Li}$  atoms were detected at  $0^\circ$  in the Enge split-pole spectrograph at Michigan State University. A stopping-gas proportional counter allowed particle identification of the  ${}^6\text{Li}$ . Measurement of the energy of the recoiling  ${}^6\text{Li}$  ions allows a determination of the entire angular distribution of the gamma decay due to the recoil momentum associated with the gamma ray. The direct capture cross section was measured to be  $\sim 20$  nb below 4-MeV excitation energy and rises with energy. A measurement at  $E_x = 4.3$  MeV is consistent with pure E2 decay.

The measurement is of astrophysical interest in determining the cosmic abundance of  ${}^6\text{Li}$ . This direct-capture cross section was the only unmeasured direct-capture reaction of light nuclei. Preliminary calculations indicate that the measured cross section is in agreement with accepted models which predict that  ${}^6\text{Li}$  is created primarily in spallation reactions.

---

\* Michigan State University, East Lansing, Michigan.

### h. Search for Neutral Currents in $^6\text{Li}$

T. J. Bowles, R. G. H. Robertson,\* R. A. Warner,\* P. Dyer,\*  
 R. C. Melin,\* A. B. McDonald,<sup>†</sup> G. C. Ball,<sup>†</sup> W. G. Davies,<sup>†</sup> and  
 D. Earle<sup>†</sup>

We are attempting to measure the parity-forbidden alpha decay of the  $0^+$ ,  $T=1$  level at 3.56 MeV in  $^6\text{Li}$ . The decay can occur only by mixing with a  $0^-$ ,  $T=0$  level at  $\sim 23$  MeV through a  $\Delta T=1$  weak hadronic current. This decay is predicted to be enhanced by a factor of  $\sim 100$  due to the presence of weak neutral currents as predicted by the Weinberg-Salam model.

The decay is measured via the inverse reaction  $^2\text{H}(\text{He},\gamma)^6\text{Li}$  using a spectrograph and stopping-gas proportional counter to identify the recoiling  $^6\text{Li}$  ions at  $0^\circ$ . A very preliminary measurement at Michigan State University using a cryogenically-pumped thin  $\text{D}_2\text{O}$  jet target set an upper limit of  $\Gamma_{\text{ad}} \approx 2 \times 10^{-8}$  eV with an uncertainty of a factor of  $\sim 5$ . A detailed calculation is now in progress at MSU.

We hope to reach the required level of sensitivity by using the Chalk River MP tandem and QDDD spectrograph with a pure- $\text{D}_2$  windowless-gas-jet target in 1-2 months of running time.

### i. Search for Neutral Currents in $^{20}\text{Ne}$

T. J. Bowles, R. G. H. Robertson,\* P. Dyer,\* and R. C. Melin\*

We are investigating the possibility of measuring the parity-forbidden alpha decay of the  $1^+$ ,  $T=1$  level at 11.26 MeV in  $^{20}\text{Ne}$ . This decay would be enhanced by a factor of  $\sim 100$  by weak neutral currents predicted by the Weinberg-Salam theory which would mix the  $1^+$ ,  $T=1$  level with a nearby  $1^-$ ,  $T=0$  level. The predicted parity-forbidden alpha width is  $\Gamma_a \approx 10^{-5}$  eV.

\* Michigan State University, East Lansing, Michigan.

<sup>†</sup> Chalk River Nuclear Laboratories, Chalk River, Ontario, Canada.

We are trying to determine accurately the energy of the  $T=1^+$ ,  $T=1$  level by looking for resonance absorption of gamma rays incident on a  $^{20}\text{Ne}$  gas target. The gamma rays are formed in the  $^{27}\text{Al}(p, \gamma)$  reaction using the intense  $\text{H}_2^+$  beam of the Argonne Dynamitron. We are using these studies to investigate the possibility of measuring the alpha width by the photodisintegration of  $^{20}\text{Ne}$ .

j. Measurement of the  $T=2$  Level in  $^{24}\text{Al}$

T. J. Bowles, R. G. H. Robertson,\*, A. Ledebuhr,\*, and L. Harwood\*

We have designed and built at Michigan State University a cryogenic He-jet target system connected to a particle detection system which allows measurement of beta-delayed particle emission of light nuclei. The activity from the target is transported to catcher foils which are stepped from the collection position to a detector system. This system allows measurement of the energy of the beta-delayed particle in a solid state detector; the direction in which the beta particle is emitted, and the time of flight of the recoiling daughter nucleus provide a rough determination of the mass of the daughter.

We are now measuring the energy of the  $T=2$  level in the  $T_z = -1$  nucleus  $^{24}\text{Al}$  by forming the  $T_z = -2$  nucleus in the target system via the  $^{24}\text{Mg}(\text{He}, 3n)$  reaction and looking for the superallowed beta decay to the  $T=2$  level in  $^{24}\text{Al}$ . We intend to complete the measurement in  $^{24}\text{Al}$  and to measure other  $T=2$  levels in  $T_z = -1$  nuclei in order to provide a more sensitive test of the isobaric multiplet mass equation.

---

\* Michigan State University, East Lansing, Michigan.

## B. CHARGED-PARTICLE RESEARCH AT THE TANDEM ACCELERATOR

The light-ion and nuclear-spectroscopy research carried out at the FN Tandem at the present time has two principal foci. Both bear on the nuclear spectroscopy of nuclear species sufficiently far from the valley of stability that little is known of their structure. The research into the properties of nuclei of interest to nucleosynthesis has focused on the properties of neutron-rich nuclei near iron to lay a foundation for more accurate production of ground-state properties of nuclei with a very large neutron excess. The other program is examining the spectroscopy of the low-lying levels of the proton-rich  $T=\frac{1}{2}$  nuclei in the 2p-1f shell. Very interesting state-dependent Coulomb energy shifts are seen in these spectra when compared to the neutron-rich member of the isospin multiplet. In some instances the electromagnetic lifetimes can be measured which allows an even more detailed comparison between the members of the  $T=\frac{1}{2}$  isospin multiplet. The availability of our recently-developed large-volume high-resolution NaI photon detectors makes a program to measure the radiative capture of  $\alpha$  particles appear very attractive.

### a. Coulomb Shifts in Mirror Nuclei of the $f_{7/2}$ Shell

L. Meyer-Schützmeister, G. Hardie, S. Gronemeyer, and A. J. Elwyn

The study of nuclear properties of  $^{45}\text{V}$  is of special interest since  $^{45}\text{V}$  is the mirror of the well-known  $^{45}\text{Ti}$  nucleus. The knowledge of its level scheme in combination with that of  $^{45}\text{Ti}$  offers the possibility of extracting Coulomb shifts for the mirror pair. Such shifts (which are obtained from data discussed in the following contribution) are found to vary for states of different  $J^\pi$ . This suggests the existence of charge-dependent effects which change as a function of the spin and parity of the nuclear level. Thus, examination of Coulomb shifts provides a means of testing nuclear wavefunctions in some detail.

As an example of such studies, we have found on the basis of an analysis of the Coulomb shifts associated with  $\frac{3}{2}^+$  states that the value of the interaction energy of a  $d_{3/2}$ -shell proton hole with a  $f_{7/2}$ -shell proton is the same in both the  $^{43}\text{Ti}-^{43}\text{Sc}$  and  $^{45}\text{V}-^{45}\text{Ti}$  mirror pairs. This is somewhat surprising since previous investigations of  $\frac{3}{2}^+$  states

for mirror pairs in  $f_{7/2}$ -shell nuclei  $A = 41, 43, 47$ , and  $51$  showed a mass dependence for the interaction energy. Since the  $A=43$  mirror pair are associated with  $A = 4n + 3$   $f_{7/2}$ -shell nuclei and the  $A=45$  nuclei are based on the  $A = 4n + 1$  series, the explanation may be that the variation of the  $d_{3/2}$ -proton hole— $f_{7/2}$ -proton interaction energy is different for the different series. Further investigation of this possibility in other  $f_{7/2}$  nuclei as well as the extension of these studies to other energy levels is planned during the coming year.

b. Gamma Decay in  $^{45}\text{V}$

S. Gronemeyer, L. Meyer-Schützmeister, G. Hardie, and A. J. Elwyn

In continuation of our studies of  $T=\frac{1}{2}$  mirror pairs in the  $f_{7/2}$ -shell nuclei,  $^{45}\text{V}$ , the mirror of the well-known  $^{45}\text{Ti}$  nucleus was investigated. Since hardly anything is known of  $^{45}\text{V}$ , the investigations began with a search for a 65-keV gamma ray, recently predicted for the  $\frac{5}{2}^- \rightarrow \frac{7}{2}^-$  transition. In our first attempt the reaction  $^{40}\text{Ca}(\text{Li},n)^{45}\text{V}$  was studied. Although a gamma of 56.4-keV energy, which was a good candidate for a  $^{45}\text{V}$  gamma transition, was observed, its intensity was too small to permit detailed investigations. Evaporation calculations indicated that the  $^{40}\text{Ca}(\text{Li},2n)^{45}\text{V}$  reaction might be more effective for the  $^{45}\text{V}$  production and indeed in this reaction the 56.4-keV gamma was easily observed. Prompt and delayed  $n-\gamma$  and  $\gamma-\gamma$  coincidences were studied. On the basis of the observed gamma cascades, the comparison with those known in the mirror nucleus  $^{45}\text{Ti}$ , and lifetime measurements for gamma transitions populating the  $^{45}\text{V}$  ground state, preliminary assignments were made for states in  $^{45}\text{V}$  as shown in Fig. IV-3. Since  $^{45}\text{V}$  is unstable against proton emission at an excitation energy larger than 1.62 MeV, only three more bound levels are expected (see Fig. IV-3). Two of them will be hard to observe since in  $^{45}\text{Ti}$  they either decay directly or predominantly to the ground state. The decay gamma rays of the third level have not been observed so far.

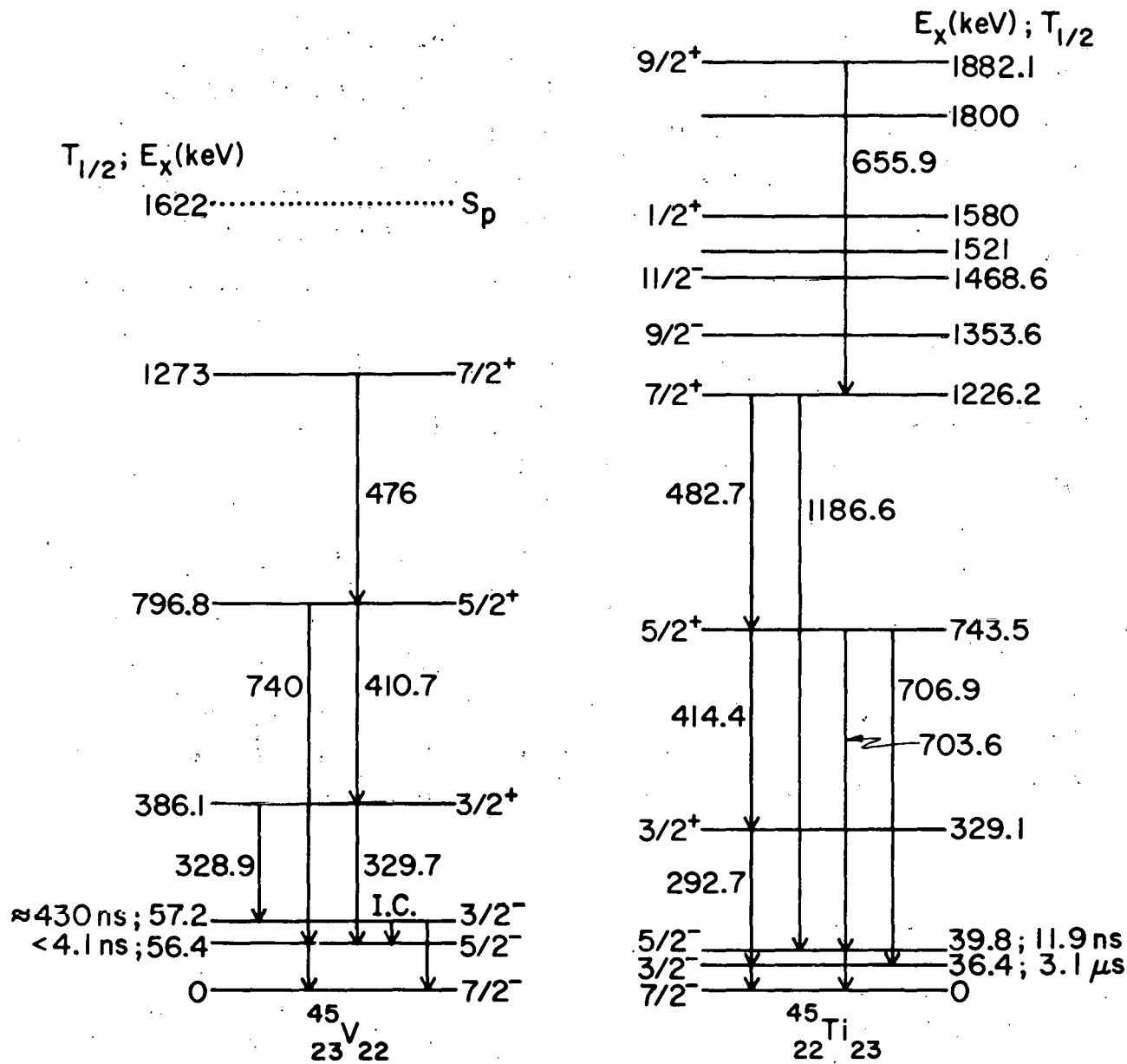


Fig. IV-3. Levels in the mirror pair  $^{45}V - ^{45}Ti$ .

c. States in  $^{47}\text{Cr}$

G. Hardie, A. J. Elwyn, S. A. Gronemeyer, and L. Meyer-Schützmeister

As part of our program with mirror pairs in  $f_{7/2}$ -shell nuclei we have begun a study of  $^{47}\text{Cr}$  since  $^{47}\text{V}$  is well known. We have used the  $^{40}\text{Ca}(\text{C}^{12}, \text{an})$  reaction in an attempt to populate states in  $^{47}\text{Cr}$ . Although  $^{47}\text{Cr}$  was only weakly produced, the first  $\frac{3}{2}^+$  state was detected at 472 keV. Analysis of the data is continuing. We will try the  $^{46}\text{Ti}(\text{He}, 2\text{n})$  reaction in the hope that it will be more satisfactory for this study.

d. Magnetic Moment of the First Excited State of  $^{99}\text{Mo}$

T. V. Ragland,\* R. J. Mitchell,\* R. P. Scharenberg,\* and R. E. Holland

We have measured the g factor of the  $\frac{5}{2}^+$  first-excited state of  $^{99}\text{Mo}$ . We obtained for this state, which has an excitation energy of 98 keV and a mean life of  $24.5 \mu\text{s}$ , a value  $g = -0.310 \pm 0.002$ . This result is consistent with the g factor observed for the  $d_{5/2}$  level in neighboring odd-neutron nuclei, and in approximate agreement with theoretical calculations. A paper has been written and published in Physical Review C.

e. Measurements of Astrophysical Interest

The program involving the study of new isotopes of interest to astrophysics is continuing. Properties of proton-rich and neutron-rich isotopes near iron are under investigation by means of  $\beta$ - and  $\gamma$ -ray spectroscopy. The resulting mass excesses,  $\beta$ -decay rates, and spins and parities of nuclear states are useful for calculations of nuclear abundances following explosive nucleosynthesis, as well as for checking mass predictions in this region of the periodic table.

Measurements of the production of the rare isotope  $^{180}\text{Ta}$  via the  $^{180}\text{Hf}(\text{p}, \text{n})^{180}\text{Ta}$  reaction were performed. The results indicate

\*Purdue University, West Lafayette, Indiana.

that this reaction is a possible source of  $^{180}\text{Ta}$  in stars. In collaboration with D. N. Schramm of the University of Chicago, consideration of r-process time scales has enabled constraints to be placed on the parameters of the astrophysical environment involved in the production of r-process nuclei. Studies of the  $0^+ \rightarrow 0^+$  Fermi-decay rates of N=Z nuclei in the f-p shell have begun with the first case,  $^{62}\text{Ga}$ , having a decay rate in good agreement with that from Fermi decays of lighter nuclei.

New Isotopes of Interest to Explosive Nucleosynthesis:

Neutron-Rich Isotopes. Neutron-rich isotopes are of interest to nucleosynthesis through their participation in neutron-capture processes in stars and by their possible existence in the crusts of neutron stars. We are searching for new isotopes near iron, in order to determine their  $\beta$ -decay properties and ground-state masses. This will enable comparisons with various mass predictions and provide information on nuclear systematics for extrapolation to large neutron excesses. Gamma-decay properties of states in the daughter nuclei are also obtained from these studies.

Proton-Rich Isotopes. Isotopes on the proton-rich side of  $\beta$  stability near iron are involved in low-density nucleosynthesis following a supernova explosion. Nuclides near the N=Z line are of prime importance.

(i)  $\beta^+$  Decay of  $^{67}\text{As}$

M. J. Murphy and C. N. Davids

As part of a study of nuclei far from  $\beta$  stability, the  $\beta^+$  decay of  $^{67}\text{As}$  has been investigated using gamma and beta spectroscopy. From the measured  $\beta^+$  endpoint the mass excess of  $^{67}\text{As}$  has been determined to be  $-56658 \pm 72$  keV. A decay scheme involving twenty-nine levels in  $^{67}\text{Ge}$  has been obtained, and upon completion of spin measurements for  $^{67}\text{Ge}$  excited states, an assignment or constraint to the ground-state spin and parity of  $^{67}\text{As}$  will be possible.

(ii) Level Structure of  $^{67}\text{Ge}$

M. J. Murphy and C. N. Davids

In conjunction with the study of  $^{67}\text{As}$ , and also to learn more about the structure of odd-A nuclei in the 1f-2p shell, the structure

TABLE IV-I.  $^{67}\text{Ge}$  low-lying levels and transitions.

$E_{\gamma}$	Transition	$I_i$	$I_f$	$\delta(E2/M1)$
104.4	$122.7 \rightarrow 18.2$	$\frac{3}{2}^-$	$\frac{5}{2}^-$	$0.73^{+2.17}_{-0.39}; 2.25^{+5.89}_{-1.65}$
122.7	$122.7 \rightarrow 0$	$\frac{3}{2}^-$	$\frac{1}{2}^-$	$-0.87^{+0.58}_{-0.48}; -0.34^{+0.23}_{-0.63}$
120.8	$243.6 \rightarrow 122.7$	$\frac{3}{2}^-$	$\frac{3}{2}^-$	$-1.28^{+0.50}_{-1.32}$
243.6	$243.6 \rightarrow 0$	$\frac{3}{2}^-$	$\frac{1}{2}^-$	$-0.58^{+0.53}_{-0.96}$
734	$752 \rightarrow 18.2$	$\frac{9}{2}^{+(a)}$	$\frac{5}{2}^-$	(Pure M2)

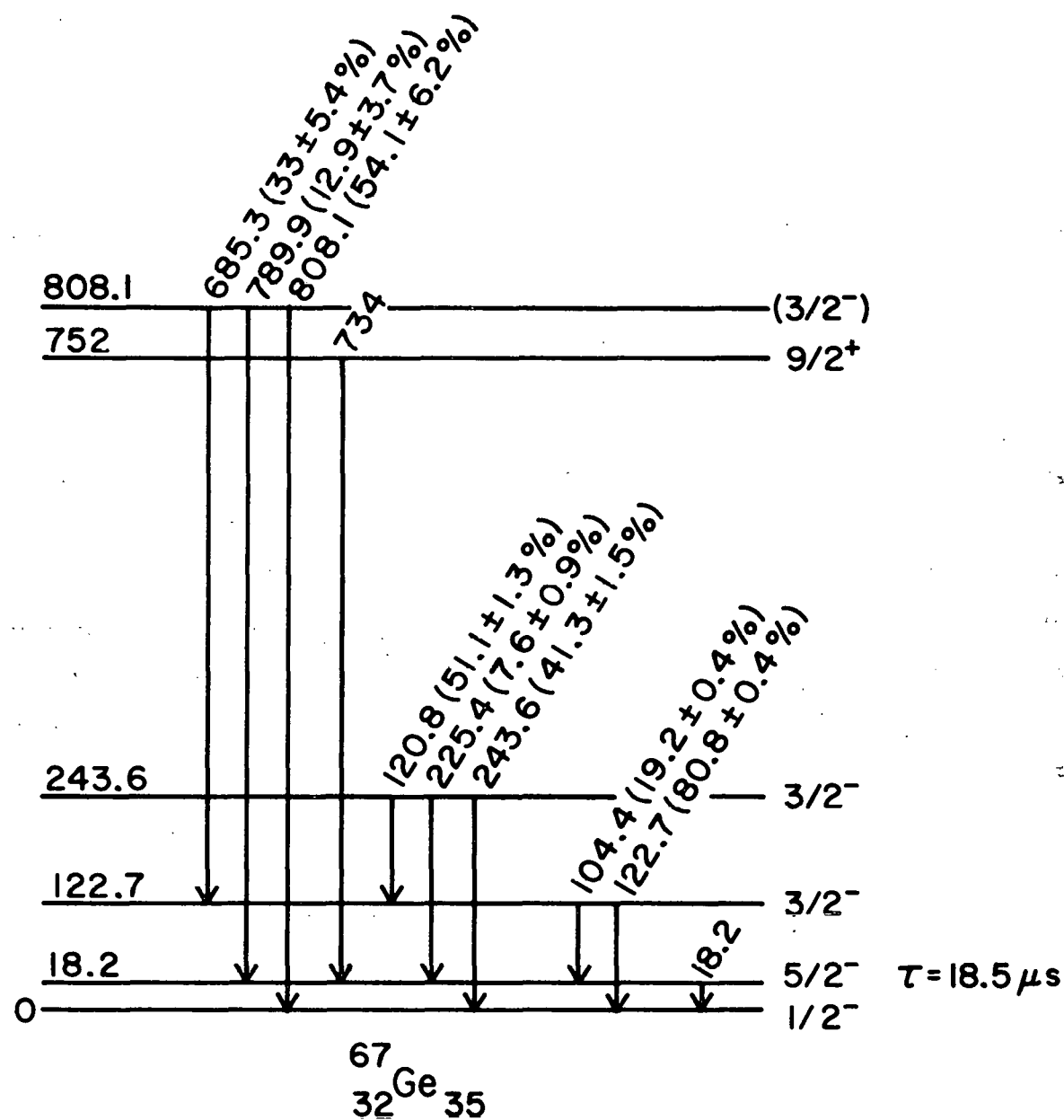
<sup>a</sup> Spin assignment by H. Bertschat *et al.*, Phys. Soc. Japan 34, 217 (1973).

of  $^{67}\text{Ge}$  has been studied via in-beam gamma-ray spectroscopy. Thirty-one excited states up to 2.6 MeV in  $^{67}\text{Ge}$  have been identified, and more than sixty gamma rays placed in the level scheme. The results of gamma-ray angular-distribution measurements have uniquely determined the spins of the lowest-lying states, and provided rough values for the E2/M1 mixing ratios of prominent gamma transitions of these states (see Table IV-I and Fig. IV-4). Directional-correlation data currently under analysis will more accurately determine these mixing ratios and provide spin/parity constraints on several higher energy levels.

### (iii) Production of $^{180}\text{Ta}$ by the $^{180}\text{Hf}(p,n)$ Reaction

E. B. Norman and T. R. Renner

It is generally believed that the great majority of the naturally-occurring nuclei heavier than iron are synthesized in stars via the slow (s-) and/or the rapid (r-) neutron-capture processes.  $^{180}\text{Ta}$  has a half-life greater than  $10^{13}$  years, and its abundance relative to  $^{181}\text{Ta}$  is  $1.2 \times 10^{-4}$ .

Fig. IV-4. Level scheme of  $^{67}\text{Ge}$ .

But  $^{180}\text{Ta}$  is bypassed in the s process, shielded from the r process by the stability of  $^{180}\text{Hf}$ , and from the conventional p process by the stability of  $^{180}\text{W}$ . In order to account for the observed abundance of  $^{180}\text{Ta}$ , several possible production mechanisms have been proposed: (a) proton-induced spallation reactions on abundant heavier nuclei, (b) the  $^{181}\text{Ta}(\gamma, n)^{180}\text{Ta}$  reaction, and (c) the  $^{180}\text{Hf}(p, n)^{180}\text{Ta}$  reaction. Measurements of the cross sections for each of these mechanisms would be useful but there is an added complication: an isomeric  $^{180}\text{Ta}^+$  state which  $\beta$  decays with a half-life of 8.1 hours. Any  $^{180}\text{Ta}$  formed in this isomeric state will not contribute to the observed abundance of  $^{180}\text{Ta}$ .

The thick target isomeric ratio from the (p, n) reaction on  $^{180}\text{Hf}$  has been measured at  $E_p = 8.00, 8.50$ , and  $9.00 \text{ MeV}$ . The  $^{180}\text{Ta}^m$  yield was deduced from measurements of the K x rays, and 93.3- and 103.6-keV  $\gamma$  rays emitted following the isomer  $\beta$  decay. Based on these measurements, a revised decay scheme for  $^{180}\text{Ta}^m$  has been constructed. The total (p, n) yield was estimated from previously-measured thick-target yields on a number of targets in this mass region. The  $^{180}\text{Ta}^g$  yield was calculated by subtracting the observed isomer yield from the interpolated (p, n) value. The thick-target  $^{180}\text{Ta}^g/^{180}\text{Ta}^m$  ratios at  $E_p = 8.00, 8.50$ , and  $9.00 \text{ MeV}$  are  $0.38 \pm 0.27, 0.31 \pm 0.26, 0.39 \pm 0.31$ , respectively.

#### (iv) On the Conditions Required for the r Process

Eric B. Norman and David N. Schramm\*

The astrophysical site for the production of the r-process nuclei is not presently known. Part of the reason for this lack of knowledge is that the range of conditions which enable the production of these nuclei has not been accurately determined. Dynamic r-process nucleosynthesis calculations provide a means by which limits can be placed on the range of initial conditions that can produce r-process nuclei. Such calculations have several important time scales inherent to them. By requiring the

\* University of Chicago, Chicago, Illinois.

time scales for neutron captures,  $\beta$  decays, hydrodynamic expansion, and seed-nucleus production to be mutually compatible, it has been found that constraints can be placed on the initial temperatures, densities, neutron/proton ratios, and chemical compositions that can produce the r-process nuclei. The allowed ranges of these parameters are presented along with the results of r-process calculations performed for several different sets of initial conditions.

(v) Superallowed  $0^+ \rightarrow 0^+$  Fermi Transitions

C. N. Davids, C. A. Gagliardi, W. Kutschera, M. J. Murphy, and E. B. Norman

The study of superallowed  $0^+ \rightarrow 0^+$   $\beta$  transitions between members of an isospin multiplet yields information on the weak vector-coupling constant  $G_V$ . The equality of the  $ft$  values for all such transitions, apart from small isospin corrections, is a necessary consequence of the conserved-vector-current hypothesis.

Much experimental effort has gone into precise measurements of the half-lives and total decay energies for the 18 or so known cases of  $0^+ \rightarrow 0^+$  transitions, ranging between  $^{10}\text{C}$  and  $^{62}\text{Ga}$ . We have begun a program to extend the masses involved up to  $A = 70$  by attempting to observe the  $\beta^+$  decays of  $^{62}\text{Ga}$ ,  $^{66}\text{As}$ , and  $^{70}\text{Br}$ . These nuclides are expected to have  $J=0^+$ ,  $T=1$  ground states, and thus will decay to the  $0^+$  ground states of the daughter nuclides by energetic positron emission. They are particularly interesting because the isospin-breaking electromagnetic interactions should cause observable effects.

The first case,  $^{62}\text{Ga}$ , was produced by the  $^{58}\text{Ni}(^{6}\text{Li}, 2n)^{62}\text{Ga}$  reaction using a 25-MeV  $^{6}\text{Li}$  beam. Positrons were observed with 2 separate detector systems, each a  $\Delta E$ -E telescope operated in fast coincidence. The first system consisted of a 4-cm $^2$  by 200- $\mu$ -thick Si surface-barrier detector placed before a 10-cm $^2$  by 11-mm deep high-purity Ge detector. A 0.76-mm-thick aluminum shutter was placed before the  $\Delta E$

detector to stop charged particles during the bombardment period and was rotated out of the way during the counting time. The second system consisted of a 2.54-cm-diam by 0.76-mm-thick NE 102 plastic scintillator, coupled to an RCA 8575 photomultiplier tube, and a 7.3-cm-diam by 5.8-cm-deep NE 102 plastic scintillator, coupled to an RCA 4524 photomultiplier tube. During the bombardment period the first dynode of each photomultiplier tube was shorted to the cathode.

The energy signal from the back detector and the time since the end of the bombardment were recorded on magnetic tape, and subsequently analyzed to yield the half-life and positron endpoint energy from the  $^{62}\text{Ga}$  decay.

In order to calibrate the energy detector, the  $\beta^+$  emitters  $^{28}\text{P}$ ,  $^{46}\text{V}$ ,  $^{50}\text{Mn}$ ,  $^{54}\text{Co}$ , and  $^{58}\text{Cu}$ , which have well-known endpoint energies ranging from 7.05 to 12.56 MeV, were produced by (p, n) reactions using 12 to 16.5 MeV protons and the appropriate targets. All experimental conditions remained constant except bombarding and counting times.

Figure IV-5 shows the time spectrum for  $\beta^+$  events having energies greater than 4.2 MeV. The solid curve is a fit to an exponential decay plus a constant background. The results of the  $^{62}\text{Ga}$  runs with the two detector systems were combined to yield the half-life value  $116.34 \pm 0.35$  ms. This is in excellent agreement with the two previous measurements.<sup>1,2</sup>

The total decay energy  $Q_{\text{EC}}$  for  $^{62}\text{Ga}$  was obtained by fitting the high-energy portion of the  $\beta^+$  spectrum with a spectral shape obtained from a similar decay with known decay energy. The energy calibration was obtained by fitting the five previously mentioned known decays by the same method. In each case the "standard" spectral shape was stretched or compressed on the energy axis. In Fig. IV-6 is shown a plot of  $Q_{\text{EC}}$  vs the stretch factors  $1/a$  obtained for the five known

<sup>1</sup> D. E. Alburger, Phys. Rev. C 18, 1875 (1978).

<sup>2</sup> R. Chiba et al., Phys. Rev. C 17, 2219 (1978).

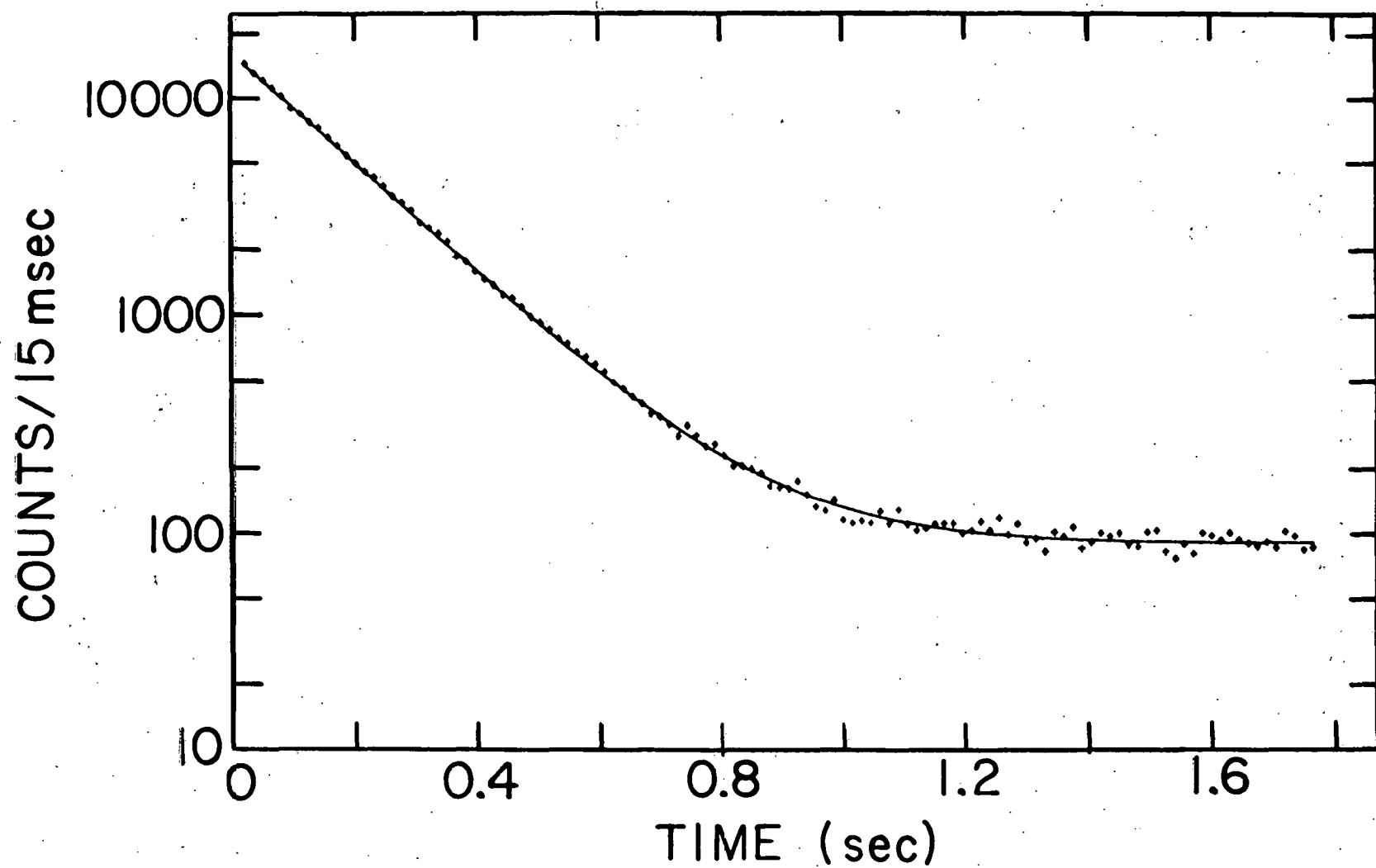


Fig. IV-5. Time spectrum for  $\beta^+$  events having energies greater than 4.2 MeV. The time dispersion is 15 ms/channel.

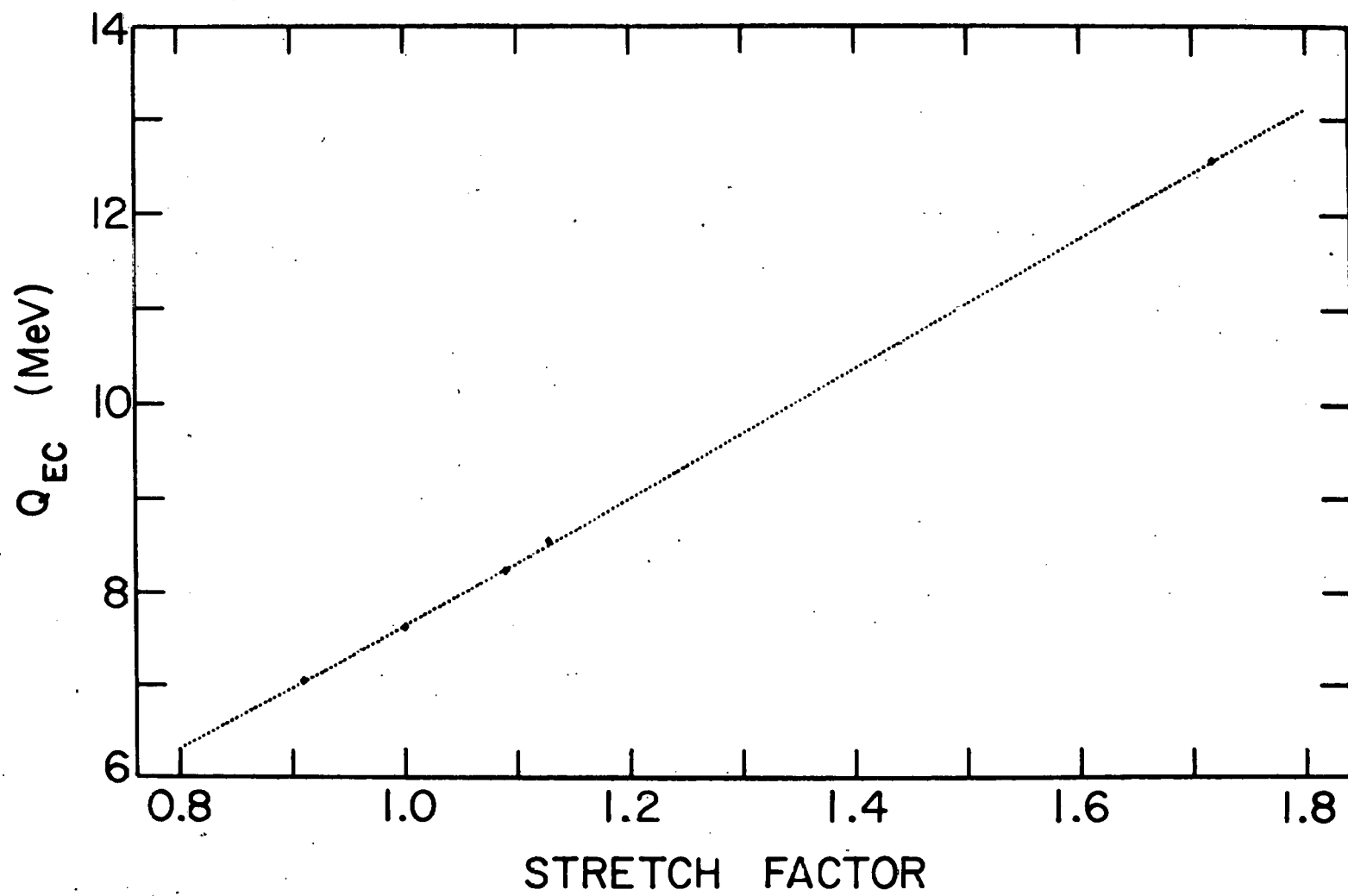


Fig. IV-6.  $Q_{EC}$  vs stretch factor for the 5 calibration spectra. Dotted line is linear least-squares fit to the points.

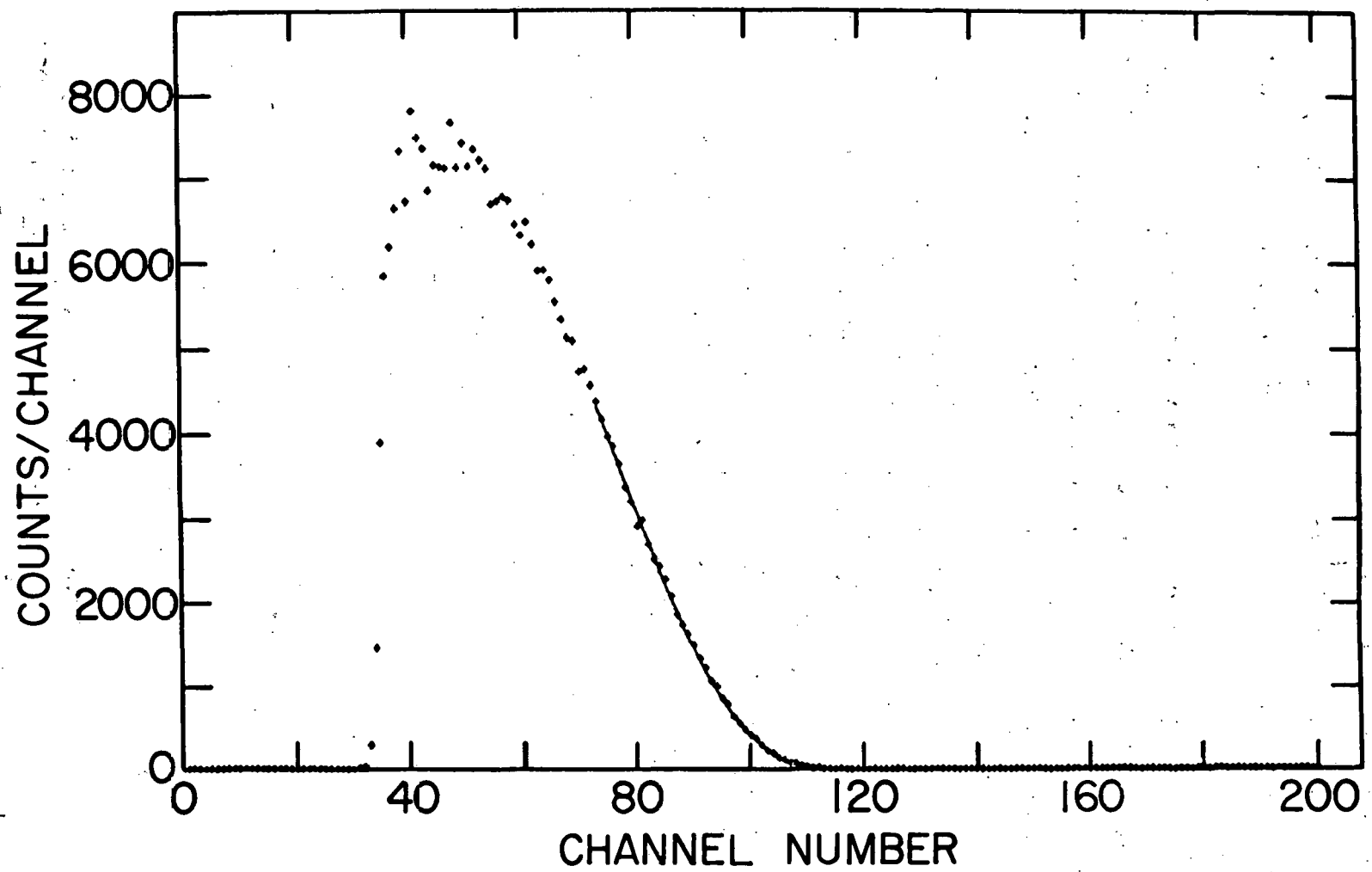


Fig. IV-7. Background-corrected  $^{62}\text{Ga}$   $\beta^+$  spectrum. Solid line is fit to data using the standard shape.

decays. The dotted line is a least-squares fit to a straight line, and the figure demonstrates the linearity and consistency of the fitting procedure. The RMS deviation of the points from the line is 25 keV. Using this technique on the background-corrected  $^{62}\text{Ge}$  spectrum yielded the fit shown in Fig. IV-7.

The procedure outlined above was followed a total of three times, using as standard spectra the decays of  $^{46}\text{V}$ ,  $^{50}\text{Mn}$ , and  $^{54}\text{Co}$ . All the results were consistent with one another, and the final value obtained for the  $Q_{\text{EC}}$  of  $^{62}\text{Ga}$  is  $9171 \pm 26$  keV. This is the average of runs using both detector systems.

After making small radiative and charge-dependent corrections, the "corrected"  $\mathfrak{f}_t$  value obtained for  $^{62}\text{Ga}$  is  $\mathfrak{f}_t = 3081 \pm 47$  s. This is in excellent agreement with the values obtained for the Fermi decays of  $14 < A < 54$  nuclei, i.e.,  $3082.5 \pm 2.0$  s<sup>3</sup> and  $3088.6 \pm 2.1$  s.<sup>4</sup>

The nuclides  $^{66}\text{As}$  and  $^{70}\text{Br}$  have been produced by the  $^{58}\text{Ni}(\text{<sup>10</sup>B}, 2n)$ ,  $^{66}\text{As}$  and  $^{58}\text{Ni}(\text{<sup>14</sup>N}, 2n)$ ,  $^{70}\text{Br}$  reactions. Preliminary results are summarized in Table IV-II.

TABLE IV-II. Preliminary half-lives and  $Q_{\text{EC}}$  values for odd-odd  $N=Z$  nuclides in the  $1f-2p$  shell.

Nuclide	Half-life <sup>a</sup> (ms)	$Q_{\text{EC}}$ (keV)	$\mathfrak{f}_t$ (sec)
$^{62}\text{Ga}$	$116.34 \pm 0.35$	$9171 \pm 26$	$3081.2 \pm 47.1$
	$115.95 \pm 0.30$ <sup>b</sup>		
	$116.4 \pm 1.5$ <sup>c</sup>		
$^{66}\text{As}$	$96.37 \pm 0.46$	$9550 \pm 50$	$3062 \pm 90$
	$95.78 \pm 0.39$ <sup>b</sup>		
$^{70}\text{Br}$	$80.20 \pm 0.82$ <sup>b</sup>	$9970 \pm 170$	$3118 \pm 295$

<sup>a</sup>Present work, unless otherwise noted.

<sup>b</sup>Reference 1.

<sup>c</sup>Reference 2.

<sup>3</sup>J. C. Hardy and I. S. Towner, Nucl. Phys. A254, 221 (1975); I. S. Towner, J. C. Hardy, and M. Harvey, Nucl. Phys. A284, 269 (1977).

<sup>4</sup>S. Raman, T. A. Walkiewicz, and H. Behrens, At. Data Nucl. Data Tables 16, 451 (1975).

## V. ACCELERATOR OPERATIONS AND DEVELOPMENT

### INTRODUCTION

The electrostatic tandem accelerator has operated well with the new set of NEC accelerator tubes and has begun to be used as the injector into sections of the superconducting linear post-accelerator. A number of minor problems associated with the coupling of a dc accelerator to an rf post-accelerator were corrected. The tandem operating efficiency was substantially improved by the installation of terminal valves which allow the accelerator tubes to remain under vacuum at all times. The installation of the NEC tubes resulted in better heavy-ion transmission and improved directional stability, but the maximum terminal voltage for stable operation is at this point somewhat lower than the one obtained with HVEC accelerator tubes.

## A. OPERATION OF THE TANDEM-LINAC ACCELERATOR

The Tandem-linac accelerator system supports both heavy-ion nuclear physics and charged-particle light-ion research.

Both the tandem and the booster are being systematically improved while continuing to support an energetic program of nuclear research. The main upgrading tasks on the tandem are now ongoing efforts to refine various subsystems of the working accelerator. At the booster, on the other hand, the main task is still to complete the installation of the planned 4-section system. The present 2-section system will be extended to 3 sections in mid-1979 and to 4 sections in 1980.

### 1. RECENT OPERATING EXPERIENCE FOR THE TANDEM

During 1978, the tandem operated on a 5-day week schedule until September. At that time, a 7-day/week schedule was resumed.

During the period 1 January 1978 to 31 December 1978, the accelerator operated 4314 hours. Of this time, 88% was used for the acceleration of  $^6\text{Li}$ ,  $^7\text{Li}$ ,  $^{10}\text{B}$ ,  $^{11}\text{B}$ ,  $^{12}\text{C}$ ,  $^{13}\text{C}$ ,  $^{14}\text{N}$ ,  $^{15}\text{N}$ ,  $^{16}\text{O}$ ,  $^{18}\text{O}$ ,  $^{19}\text{F}$ ,  $^{27}\text{Al}$ ,  $^{28}\text{Si}$ ,  $^{31}\text{P}$ ,  $^{32}\text{S}$ ,  $^{35}\text{Cl}$ , and  $^{58}\text{Ni}$  beams for the experimental program, 4% for the acceleration of protons and deuterons, and 8% for machine development and conditioning. The helium-ion source was not available for experimental use during this period of time, and this accounts for the unusually low percentage of time devoted to light-ion acceleration.

### 2. OPERATION OF THE SUPERCONDUCTING LINAC

The superconducting-linac heavy-ion-energy booster was operated in beam-acceleration tests in June, September, and December of 1978, a total of about 5 weeks of operation. About 14 weeks of operation are planned for 1979. Initially, the operation of the new machine has been carried out mainly by the staff members involved in its design.

Gradually, the operational responsibilities will be shifted to a unified team responsible for operation of the whole accelerator system.

### 3. UPGRADING OF THE TANDEM

J. L. Yntema, P. J. Billquist, and F. H. Munson

The FN tandem was substantially modified during the second half of 1977 with the primary objective of improving its characteristics as a heavy-ion injector for the superconducting linac. The modifications included the installation of the following: NEC accelerator tubes, a closed-corona voltage-distribution system for the accelerator tubes, a new terminal box, a new injection system, and a high-vacuum system. Throughout 1978, the various subsystems involved in these modifications were perfected and the quality of performance of the modified accelerator was tested.

The first full year of operation has demonstrated that the tandem modifications have substantially improved performance. The accelerator has operated well over the voltage range 2.75 to 9.0 MV. Even without a terminal lens, the beam transmission of the machine exceeds 60% for ions up to  $A = 58$  when the terminal stripping foil is  $10 \mu\text{g/cm}^2$  thick. With a  $5 \mu\text{g/cm}^2$  stripping foil, the measured transmission for  $^{32}\text{S}$  is 70%. The output beam is extremely stable both with respect to transit time and beam-spot position. The accelerator tube can accept an injected beam of at least  $4 \mu\text{A}$  of heavy ions, and beam currents on target are quite high—for example, more than  $1.6 \mu\text{A}$  of  $^{12}\text{C}^{4+}$ ,  $^{35}\text{Cl}^{8+}$ , and  $^{58}\text{Ni}^{10+}$ .

Details concerning the status and ongoing work on several of the subsystems are given below.

#### a. Ion Sources

The injection system has 3 ion-source positions. One position is occupied by the direct-extraction duoplasmatron, the second by the Li-exchange source, and the third by the 150-kV injection system, at which is mounted a sputter source of the type developed at Florida State University.

In 1978, the 150-kV injector was equipped with a 150-kV Deltatron power supply, which is stable to about 0.01%. This level of stability for the injected beam is important for good bunching.

A study of the size of the spot on the target cone from which negative ions from the FSU source originate indicates that about 60% of the negative ions come from a spot of about 2 mm diameter. This indicates that the source will be usable for the production of beams from isotopically enriched materials. It was found that the  $MgH^-$  beam was considerably enhanced if the Mg target was sandblasted immediately preceding installation in the cone wheel. A decrease in the distance between the ionizer and the target improved the  $CaH^-$  beam intensity by about a factor of 2. It appears that the production of  $CaH^-$  and  $MgH^-$  exceeds the production of  $CaH_3^-$  and  $MgH_3^-$  consistently. New power supplies which have greater stability and allow control from the tandem console were constructed for the source.

An NEC version of the Aarhus source (ANIS) has been purchased, and the construction of its control system has started. This source is expected to be especially useful for the production of ions such as Ti, V, and Zr.

#### b. Vacuum Systems

The conditioning of NEC tubes was investigated by measuring the partial pressures of gases released during conditioning. The conclusion was that moisture affects the acceleration system very adversely and that the best method of conditioning is to increase the terminal voltage quite slowly. Care has to be taken that the conditioning takes place uniformly along the accelerator structure and that x-ray production is kept at a low level. Under such conditions, voltage gradients in excess of 385 kV per section (compared to the 333 kV per section guaranteed by NEC) have been consistently obtained without damage to the accelerator tubes.

To avoid contamination by hydrocarbons, the turbomolecular pumps near the tandem have been replaced by cryopumps. Also, to eliminate a recurrent contamination of the ion pump at the low-energy end, the pump was replaced by one less susceptible to contamination.

c. Terminal Box

The 115-foil NEC foil changer in the terminal has recently been replaced by a 230-foil NEC changer. To avoid having to vent the accelerator tubes when foils are loaded, all-metal valves were designed and installed at each end of the terminal. These valves (modifications of a valve originally designed at Australian National University) allow the venting of the terminal box while keeping the vacuum in the accelerator tubes at  $10^{-8}$  Torr. After installation of the foils, the box is pumped down to the  $10^{-6}$  Torr range before opening the all-metal valves. This arrangement allows the tandem to be operated at 8.5 MV within 36 hours after a complete reloading of foils and it obviates the need for rebaking the accelerator tubes.

d. Stripping Foils

G. E. Thomas, P. Den Hartog, and J. L. Yntema

Stripping foils have short lifetimes under heavy-ion bombardment, and this has limited the usefulness of foil strippers in tandem terminals. During 1978, a group at Harwell has developed a new fabrication technique that appears to increase the lifetimes of carbon foils by an order of magnitude. Work along similar lines is in progress here. In addition, investigations of the characteristics of wrinkled foils and experiments with rotating discs are also underway.

e. Beam Bunching

The beam-bunching system described in previous years is an essential and major component of the tandem-linac accelerator system. During the last year, it has been used repeatedly to bunch the beam being injected into the linac.

Recently the bunching system has been exploited in a new application in which it serves as a refined time-of-flight energy spectrometer for measurements of energy straggling in stripping foils (see Sec. III. Dc of this report).

#### 4. INSTALLATION OF THE BOOSTER

The system now in operation consists of sections A and C, with a total of 8 high- $\beta$  resonators. This configuration will be operated through June 1979. Then, operation of the booster will be interrupted for several months while section D is installed. In a run tentatively scheduled for September 1979, the booster is expected to consist of three cryostats (ACD) containing at least 11 high- $\beta$  resonators and 1 low- $\beta$  resonator. Additional low- $\beta$  units will be added early in the coming year.

#### 5. PLANNED ACCELERATOR-SYSTEM IMPROVEMENTS

a. Tandem Improvements

J. L. Yntema, P. Billquist, and P. Den Hartog

The off-line test setup for ion source development has been reconstituted and work is in progress on further development of Ca and Mg beams from the inverted sputter source. The initial tests on beam production with ANIS will be followed by on-line tests of the energy

spread of the ions from this source using the slow and fast bunchers. The charge-exchange source will be rebuilt. Construction of a second 150-kV injection station will be started.

In the terminal, experiments on the use of a thin gas stripper prior to a foil stripper will be undertaken with the objective of reducing the magnitude of the Coulomb explosion following the dissociation of molecular ions. This technique is expected to increase the particle transmission and decrease the energy spread of beams that can only be injected in molecular form. Work on the terminal-communication system will continue.

Although the vacuum system in and immediately adjacent to the tandem is now satisfactory, the parts further downstream need to be upgraded.

Work on improving the controls of the injection system will continue.

#### b. Linac Improvements

Operation of the booster will be interrupted for several months in early 1980 in order to install a rebunching/debunching system on the output-beam line. The availability of this system will allow the pulsed-beam characteristic of the system to be used to full advantage.

The main task for the coming year is the fabrication and installation of section B. Since this section will consist mainly of low- $\beta$  resonators, it will greatly extend the mass range for which the booster is useful.

Effort will continue to be applied to the long-term task of perfecting the operation of the linac. This work will include: (1) efforts to increase the average accelerating fields of resonators, (2) installation of a low-loss liquid-nitrogen distribution system, (3) improvements in the beam-diagnostic system, and (4) development of the software system of the control computer.

## 6. EXPERIMENTAL FACILITIES DEVELOPMENT AT THE SUPERCONDUCTING-LINAC BOOSTER

Most of the activity in this area concerns the new target area for the linac booster. A short version of the  $0^\circ$  beam line has been implemented and beams were brought to two experiments involving the 18-in. scattering chamber and a small chamber for gamma-ray studies. Most of the remaining components of the  $0^\circ$  beam line will be completed during the coming year. Construction of a 65-in. scattering chamber is under way but its use is delayed until some elements of the  $20^\circ$  beam line become available in late 1979. The split-pole spectrograph will be mounted on its track during early 1979 in order to alleviate the very crowded conditions on the experimental floor. The development of the gamma-ray sum/multiplicity counter is proceeding and experiments should be starting with it during this year.

### a. New Beam Line for the Superconducting Linac Booster

To make use of the new heavy-ion beams from the superconducting linac booster, new beam lines and new experimental facilities are required. The effort has so far concentrated on installing a low-resolution zero-degree beam line. For this beam line the second stripper is located before the  $90^\circ$  analyzing magnet of the tandem which then acts as the charge-state selector. No debuncher/rebuncher is used after the booster. The quality of the beam in energy and time resolution is therefore not as good as it will be eventually. The beams during the booster test runs were brought into experimental equipment on this beam line. In the coming year we will implement the high-resolution  $20^\circ$  beam line with a debuncher/rebuncher and charge-state selecting magnet. A new 65-in. scattering chamber and an upgraded magnetic spectrograph will be installed on this beam line.

b. Layout and Installation of the Zero-Degree Beam Line in the New Experimental Area

D. G. Kovar, W. F. Evans, W. Henning, T. L. Khoo, J. Worthington, B. Zeidman, and J. Bicek

During the past year, effort has been spent in developing the new experimental area associated with the linac booster. At this time the layout of the zero-degree beam line has been completed and most of the components are constructed or purchased. A part of the beam line has been installed. An old 18-in. scattering chamber has been rehabilitated, particularly regarding its vacuum system, and it has been used in experimental studies with beams from the booster in runs in late 1978 and early 1979. An additional small gamma-ray chamber was also used in making measurements with the linac beams. During 1979, the zero-degree beam line will be further developed, to bring beams to a neutron time-of-flight chamber being constructed by the Chemistry Division and to an irradiation station which will be used to study delayed radioactivities with the aid of a fast rabbit and an He-jet system. Plans for a 20° beam line which will provide beams to the new 65-in. scattering chamber and the spectrograph are well underway and will start to be implemented late in 1979.

c. Beam Optics Calculations

B. Zeidman and D. G. Kovar

Calculations of beam optics for transport of beams to the 65-in. scattering chamber and the magnetic spectrograph have been extended. Essential features of the system are charge-state selection and maintenance of longitudinal phase space ( $\Delta E \Delta t$ ) so that sharp time foci are available at both target locations. This requires waists at the centers of bending magnets. The zero-degree-line triplet provides a waist at the center of the 20° bending magnet. A quadrupole generates a second waist at the center of the 20° switch magnet that directs the beam toward

the spectrograph. Quadrupole doublets in each of the beam lines enable well-focused beam spots to be produced at the target locations. The transport system introduces less than 20 ps total additional spread in the beam pulse on target with complete charge-state selection. For the zero-degree line, the extended calculations indicate <10% transmission for undesired charge states.

d. 65-in. Scattering Chamber in New Target Area

W. Henning, D. G. Kovar, and J. N. Worthington

The major components of the new general-purpose scattering chamber for experiments with beams from the superconducting linac have been constructed or are near completion.

The chamber body, consisting of a light-weight, low-cost structure, has been completed and successfully vacuum tested. Due to the polished stainless-steel surface, the chamber is easily brought into the  $10^{-7}$  Torr range within 1 hour of pumping with a 2000 l/sec cryopump. The aluminum wire metal seals work reliably on the grooveless, flat flanges of medium-ground finish. The interior support structure of the chamber is at present being equipped with drive gears and will soon be installed. In its first stage, the chamber is expected to be operational during 1979.

e. Split-Pole Spectrograph in the New Experimental Area

D. G. Kovar, F. P. Mooring, C. Bolduc, R. Kickert, and J. Worthington

Plans for installation of the Enge split-pole spectrograph from the ANL cyclotron in the new experimental area associated with the linac booster are well underway at this time. The spectrograph was moved in the area in 1978 and the support pad has been poured. The installation of the spectrograph into its position will be completed in early 1979. At the present time, it is planned to make the spectrograph

operational sometime in 1980 using a modified version of the Argonne focal plane detector system [J. R. Erskine, T. H. Braid, and J. C. Stoltzfus, Nucl. Instrum. Methods 135, 67 (1976)] to utilize the good timing properties of the linac beams.

f. Sum/Multiplicity Detector for  $\gamma$  Rays

I. Ahmad,\* C. N. Davids, T. L. Khoo, W. Kutschera, S. Levenson, R. McKeown, and R. K. Smither

In the gamma-ray facility for the booster, provisions are made for easy replacement of modules for different experiments and for a wide variety of coincidence measurements. Some of the target chambers and most of the beam line components are ready. Many experiments will be performed with a  $\gamma$ -sum-spectrometer/multiplicity filter. This consists of two 13 in.  $\times$  6 in. NaI crystals, each divided into four optically-separate quadrants. The total  $\gamma$  energy in a reaction is obtained by summing the output of all eight sectors, while a rough measure of the  $\gamma$  multiplicity is given by the number of sectors firing. When operated together, the two crystals should have a geometrical efficiency close to 90%, so that coincidence measurements with this device will proceed at near singles rates. The crystals have been delivered and we are in the process of preparing the system for use.

g. Nuclear Target Making and Development

G. E. Thomas and F. J. Karasek<sup>†</sup>

The Physics Division has a facility which produces very thin targets for experiments at the Tandem and Dynamitron accelerators, experiments for other members of the Division, and any other division at the Laboratory needing this service.

\* Chemistry Division, ANL.

<sup>†</sup> Materials Science Division, ANL.

This year, the target-making facility produced more than 800 targets varying in thickness from a few monolayers to several  $\text{mg/cm}^2$ . The different elements, isotopes or compounds evaporated, rolled, anodized or oxidized included Ag, Al,  $\text{Al}_2\text{O}_3$ , Au, B, C, <sup>40,42,44,48</sup>Ca, <sup>50</sup>Cr, <sup>63</sup>Cu, <sup>180</sup>Hf, Li, <sup>6,7,natural</sup>LiF, <sup>24,26,natural</sup>Mg, <sup>natural</sup>MgO, Mo, <sup>142,natural</sup>Nd, <sup>58,natural</sup>Ni, Pb, Si, <sup>144,natural</sup>Sm, <sup>120,122,124</sup>Sn, Ta, <sup>64</sup>Zn.

Unusual targets included a sandwich of Cu + Ni + <sup>6</sup>LiF + Cu which took advantage of the heat conductivity properties of Cu. A Mo target made use of its high melting point and good radiation characteristics.

Aluminum targets with 2, 10, 20, 50, and 100 monolayers of silicon were produced to be used as standards. Another target has been made using 42 carbon foils  $25 \mu\text{g/cm}^2$  thick stacked together with thin spacers between each one.

We have two vacuum storage systems for targets which oxidize readily, each having a 100 capacity. They are now both nearly filled with very select targets.

Our thin film evaporator system is continually being upgraded so that it will produce better targets of higher purity. Also, partially because of the increased value of separated isotopes, we are developing methods which use less source material for each target produced.

## 7. UNIVERSITY USE OF THE TANDEM ACCELERATOR

F. P. Mooring, J. P. Schiffer, J. L. Yntema, and P. J. Billquist

During the past year the accelerator improvement program and the development of the superconducting linac to be used as an ion-energy booster utilized a large fraction of the total tandem time. In spite of the limited time available, the use of the machine by outside users has remained high. In all instances they have chosen to collaborate with local

scientists. Of the total time available for physical research, 41% was assigned to experiments in which outside users participated.

A list of institutions from which visiting scientists came in the past year follows. Included in the list are the names of their Argonne collaborators, enclosed in parentheses, and the title of the research done.

- (1) Beloit College  
Development of a Focal-Plane Charged-Particle Detector for the Split-Pole Spectrometer  
J. C. Stoltzfus, (D. G. Kovar, C. Olmer, and M. Paul)
- (2) Hungarian Academy of Sciences, Institute of Nuclear Research  
Resonance Structures in the Excitation Function of the  $^{24}\text{Mg}(^{16}\text{O}, ^{12}\text{C})^{28}\text{Si}$  Reaction  
J. Cseh, (D. F. Geesaman, W. Henning, D. G. Kovar, C. Olmer, M. Paul, S. J. Sanders, J. P. Schiffer, and B. Zeidman)
- (3) The University of Illinois  
A Study of Excited States of  $^{24}\text{Mg}$  by Observing Gamma Rays from the Resonance Capture of  $^{12}\text{C}$  by  $^{12}\text{C}$   
A. M. Nathan, A. M. J. Sandorfi,\* and (T. J. Bowles)
- (4) University of Kansas  
A Study of the Fusion of  $^{15}\text{N}$  with  $^{27}\text{Al}$   
F. W. Prosser, (D. F. Geesaman, W. Henning, D. G. Kovar, C. Olmer, M. Paul, S. J. Sanders, and J. P. Schiffer)
- (5) University of Michigan  
A Determination of Hydrogen-Depth Profiles in Metals by Using Heavy Ions  
A. Hanson, D. Vincent, (C. N. Davids, M. J. Murphy, and E. B. Norman)
- (6) Stanford University  
A Study of Excited States of  $^{24}\text{Mg}$  by Observing Gamma Rays from the Resonance Capture of  $^{12}\text{C}$  by  $^{12}\text{C}$   
A. M. J. Sandorfi, A. M. Nathan,\* and (T. J. Bowles)
- (7) Tennessee Technological University  
Search for High-Spin States in  $^{152}\text{Dy}$   
R. L. Kozub, (I. Ahmad,<sup>†</sup> T. L. Khoo, and R. K. Smither)

\* Outside user from another institution.

<sup>†</sup> Chemistry Division, ANL.

## (8) Western Michigan University

(a) Investigation of States in  $^{45}\text{V}$ (b) The Level Structure of  $^{47}\text{Cr}$ 

G. Hardie, (C. N. Davids, A. J. Elwyn, S. A. Gronemeyer, and L. Meyer-Schützmeister)

The Resident Graduate Student Program continues to appeal to aspiring doctoral candidates. During the year two students finished their thesis research and have taken jobs elsewhere. Students participated in experiments which used 39% of the time allotted for physical research. The following is a list of students participating in the Resident Graduate Student Program who did research at the tandem during the past year. Their home institutions and local advisors are also given. Those who received their doctoral degree during the year are indicated by an asterisk.

(1) A. Davis, University of Chicago  
G. T. Garvey, adv.(2) K. Daneshvar, University of Illinois, Chicago Circle  
D. G. Kovar, adv.(3) S. A. Gronemeyer, Washington University  
L. Meyer-Schützmeister, adv.(4) M. J. Murphy, University of Chicago  
C. N. Davids, adv.(5) E. B. Norman,\* University of Chicago  
C. N. Davids, adv.(6) T. R. Renner,\* University of Chicago  
J. P. Schiffer, adv.

## B. DYNAMITRON OPERATIONS

The Physics Division operates a high-current 4.5-MV Dynamitron accelerator which has unique capability as a source of ionized beams of most atoms and many molecules. Among the unusual facilities associated with the Dynamitron are (1) a beam line capable of providing "supercollimated" ion beams permitting angular measurements to accuracies of 0.005 degree, (2) a beam-foil measurement system capable of measuring lifetimes of a few picoseconds, (3) an experimental system dedicated to measuring absolute nuclear cross sections at low energy, (4) a precise angular-correlation system for weak-interaction studies, and (5) a simultaneous irradiation system by which heavy ions from the Dynamitron and helium ions from a 2-MV Van de Graaff accelerator are focused on the same target. An advanced PDP-11/45 computer system is used for on-line data analysis and for the control of experimental systems.

During the past year, the Dynamitron has run well and it is heavily used in several research programs. Recently, we have completely modified a currently existing 150-kV test-bench facility to allow a more complete investigation of the properties of the various ion sources. In the coming year we plan, through operation of this test facility, to initiate a research program to develop ion beams of Li, Be, and B hydrides as well as usable currents of doubly-charged He ions ( $\text{He}^{++}$ ) with the new rf and Penning ion sources. The Dynamitron facility is presently well equipped with an on-line computer. In the past year, we have expanded the computer facility from its use to control experiments and on-line data acquisition and analysis, to a number of other operations by the addition of a microcomputer. Thus, we are presently using the microcomputer for running magnet scans to determine the masses of the various ion beams emerging from the accelerator. In the coming year we hope to extend its use to the automatic readout of the various meters on the accelerator control panel in order to more accurately and efficiently record the operating characteristics of the machine. It is planned that control and readout of ion-source parameters will also be implemented by use of a light-beam link to the high-voltage terminal of the accelerator.

### 1. OPERATIONAL EXPERIENCE OF THE DYNAMITRON

F. P. Mooring, D. S. Gemmell, A. J. Elwyn, R. L. Amrein,  
and A. E. Ruthenberg

Except for one major instance, the Dynamitron continued to perform well during the past year. The normal operating schedule was

twenty-four hours a day, five days a week. Very little running was done on weekends during calendar year 1978 for financial reasons.

During the year the accelerator was staffed a total of 5740 hours. Of this time 4683 hours (82%) were scheduled for experimental research during which a beam was provided to the experimenters 82% of the time. Machine preparation time used up 6% of the scheduled research time and machine malfunctions the remaining 12%. Scheduled accelerator improvements and modifications used a total of 1057 hours or 18% of the total available time.

The great versatility of the Dynamitron continued to be exploited by the research staff. Ion currents on target varied from less than a nanoampere to more than 170 microamperes with the ion energies ranging from 0.35 MeV to 4.0 MeV. A wide range of both atomic and molecular ions were delivered on target. They included  $^1H^+$ ,  $(^1H_2)^+$ ,  $^2H^+$ ,  $(^2H_2)^+$ ,  $^3He^+$ ,  $(^3He_2)^+$ ,  $^4He^+$ ,  $^4He^{++}$ ,  $(^4HeH)^+$ ,  $^7Li^+$ ,  $^{12}C^+$ ,  $(^{12}C_2^1H_2)^+$ ,  $(^{12}C^{16}O)^+$ ,  $(^{12}C^1H_4)^+$ ,  $(^{12}C^{16}O^1H)^+$ ,  $(^{12}C^{16}O_2)^+$ ,  $(^{12}C^{16}O_2^1H)^+$ ,  $^{14}N^+$ ,  $^{14}N^{++}$ ,  $^{16}O^{+4}$ ,  $(^{16}O^1H)^+$ ,  $(^{16}O^1H_2)^+$ ,  $(^{16}O^1H_3)^+$ ,  $(^{16}O_2)^+$ ,  $^{20}Ne^+$ ,  $^{20}Ne^{++}$ ,  $(^{20}Ne^4He)^+$ ,  $^{40}Ar^+$ ,  $^{51}V^+$ ,  $^{58}Ni^+$ , and  $^{84}Kr^+$ .

During the year a total of 67 principal investigators used the Dynamitron in some phase of their experimental research. Of these, 19 were from the Physics Division, 23 were from other Argonne research divisions, 19 were outside users (not temporary appointees) from other research facilities, and 6 were members of the Resident Graduate Student Program. Of the scheduled time 69% went to members of the Physics Division, 25% to other Argonne divisions, and 6% was exclusively assigned to outside users. However, outside users collaborated in experiments that used 23% of the total available time; and participants in the Resident Graduate Student Program worked on experiments that used 33% of the time.

The new accelerator tube, which was installed two years ago, has developed two tiny vacuum leaks in the highest energy section of

the twelve sections of the assembly. The leaks are easily sealed with a low vapor-pressure commercial sealant. However after a few months, they reopen. The leaks do not seem to be increasing in size, and seem to be in a ceramic-to-metal bond and not through the ceramic wall as were the disastrous leaks that developed in the previous short-lived tube. Since the leaks are only a minor irritant and do not seriously affect operations, there are no current plans to replace the faulty section.

During the latter half of August, serious arc damage occurred to the plexiglass main frame near the ground end. The surface of the insulating plastic was deeply eroded and charred, and the machine failed to hold voltage. The accelerator was stripped in the vicinity of the damage, and the surface was ground and sand-blasted to eliminate the shorts that had developed on the surface. The repair took ten days, and since its completion, the Dynamitron has performed as well as previously. No obvious reason for the failure could be found. Perhaps the surface of the main frame was allowed to collect sufficient deposits of one sort or another which caused a flashover leading to the intensive arcing. In the future the surfaces of the main frame and other insulators will be inspected periodically and cleaned where necessary. The solid-state rectifiers continue to function well. A simple test procedure has been developed and each rectifier is inspected every time the pressure vessel is opened. About once a month one or two of the 480 diodes in one of the 98 rectifier assemblies is found to be weak or has actually opened without affecting machine operations. Replacing faulty diodes is simple and can be done very quickly.

An Imsai 8080 microcomputer has been put on line to monitor, log, and control accelerator parameters. At present it records and/or controls the magnetic field of the main switching magnet, runs mass scans, and can be used to determine the required operating parameters of the magnet for any ionic species being accelerated. It is interfaced with a Camac crate to the various instruments that read the machine

parameters and control the magnet power supply. These include a picoammeter to read beam current, a voltmeter to determine the terminal voltage, a gauss meter to measure the magnetic field, and the controls for the magnet power supply. The results are displayed on an oscilloscope and printed out on a line printer. A plotter will be added in the near future. Plans also include using the computer to log and control all machine parameters that are now adjusted from the control console. In addition, future plans call for a light link to the terminal, and for the computer to directly monitor and control the ion-source parameters.

Operational experience with the radiation monitoring and interlock system revealed several operating conditions that overtaxed the original logic built into the system. These faults were caused in part by increasing the demands on the system to monitor the radiation conditions at four accelerators in the same general area. Most of these problems have been corrected. However, it is possible to start the Dynamitron with the system turned off. At present we recognize this situation exists and only run the Dynamitron if the radiation alarm system is functioning. To correct this fault in the logic is not simple; it will be corrected, however, as soon as possible.

## 2. UNIVERSITY USE OF THE DYNAMITRON

F. P. Mouring, D. S. Gemmell, A. J. Elwyn, and R. L. Amrein

The Dynamitron continues to attract users from outside the Laboratory, users who make special trips to Argonne to use the accelerator and its unique associated facilities while continuing their teaching or research activities at their home institutions. It is not only the availability of the hardware, but also the ability to collaborate with local personnel in research on problems of common interest that has attracted the visiting scientists.

Visitors from eleven research facilities including three foreign institutes came to use the Dynamitron during the past year. In all cases but one they have chosen to work jointly with Physics Division scientists. Of the total time scheduled for physical research, 23% was assigned to experiments in which outside users participated. A list of those institutions from which visitors have come, together with the title of the research done and the names of the principal investigators, is given below. The names of local collaborators are enclosed in parentheses.

- (1) University of Chicago  
Heavy Ion Beam Foil Spectroscopy  
R. DeSerio, (H. G. Berry, G. S. Gabrielse, T. J. Gay, and A. E. Livingston)
- (2) University of Frankfurt  
The Role of Excited Electronic States in the Interactions of Fast (MeV) Molecular Ions with Solids and Gases  
K. -O. Groeneveld, (D. S. Gemmell, E. P. Kanter, and B. J. Zabransky)
- (3) University of Liege  
Heavy Ion Beam Foil Spectroscopy  
H. P. Garnir, (H. G. Berry, G. S. Gabrielse, and T. J. Gay)
- (4) Marquette University  
Radiation Damage of Covalent Crystal Structures  
L. Cartz, T. Ehler, R. Fournelle, F. J. Karioris, C. H. Ma, K. Ramasami, and G. Sarkar
- (5) Michigan State University  
Resonance Absorption of Photons in  $^{20}\text{Ne}$   
P. Dyer, R. Melin, R. G. H. Robertson, and (T. J. Bowles)
- (6) Middlebury College  
The Role of Excited Electronic States in the Interactions of Fast (MeV) Molecular Ions with Solids and Gases  
P. J. Cooney, (D. S. Gemmell, E. P. Kanter, W. Pietsch, and B. J. Zabransky)
- (7) Northwestern University  
Test of the Response of Large NaI Crystals with Good Resolution  
R. E. Segel, (T. J. Bowles, D. F. Geesaman, and L. Meyer-Schützmeister)

(8) Stanford University  
Radiative Alpha Capture by  $^6\text{Li}$   
S. J. Freedman, (T. J. Bowles, C. A. Gagliardi, G. T. Garvey, and R. D. McKeown)

(9) University of Toledo  
Heavy Ion Beam Foil Spectroscopy  
L. J. Curtis, R. M. Schectman, (H. G. Berry, G. S. Gabrielse, T. J. Gay, and A. E. Livingston)  
Interaction of Fast Ions with Foil Surfaces and Thin Foils  
L. J. Curtis, R. M. Schectman, (H. G. Berry, G. S. Gabrielse, and T. J. Gay)

(10) Weizmann Institute  
The Role of Excited Electronic States in the Interactions of Fast (MeV) Molecular Ions with Solids and Gases  
Z. Vager, (D. S. Gemmell, E. P. Kanter, and B. J. Zabransky)

(11) Western Michigan University  
A Background Determination of an Intrinsic Germanium Detector with an Anticoincident NaI Annular Counter  
G. Hardie, (A. J. Elwyn, S. A. Gronemeyer, and L. Meyer-Schützmeister)

Members of the Resident Graduate Student Program used the Dynamitron in their research during the past year. Those that have done so are listed below, together with their home institution and their local thesis advisor. Those who have completed their research during the past year are indicated by an asterisk.

(1) G. S. Gabrielse,\* University of Chicago  
H. G. Berry, adv.

(2) C. A. Gagliardi, Princeton University  
G. T. Garvey, adv.

(3) T. J. Gay, University of Chicago  
H. G. Berry, adv.

(4) R. D. McKeown, Princeton University  
G. T. Garvey, adv.

(5) T. R. Renner, University of Chicago  
J. P. Schiffer, adv.

(6) S. A. Gronemeyer, Washington University  
L. Meyer-Schützmeister, adv.

These students participated in experiments that used 33% of the time scheduled for research.

THIS PAGE  
WAS INTENTIONALLY  
LEFT BLANK

## VI. NEUTRON AND PHOTONUCLEAR PHYSICS

### INTRODUCTION

A well-established research program centered around the Argonne threshold-photon facility uses high-precision measurements of  $(\gamma, n)$  reactions as reverse neutron-capture reactions to study the spectroscopy of excited nuclear states. The importance of the technique lies in its ability to reach regions of excitation in nuclei which are inaccessible by other traditional neutron-induced reactions and with a resolution and sensitivity which is unexcelled. In 1978 a major fraction of the program resources were devoted to construction of a new electron-beam transport system and expansion of the neutron-time-of-flight lines in detection areas. These new improvements will be exploited in work on several problems of immediate interest to the nuclear-science community.

Another phase of the photonuclear program is the high-resolution studies of photon scattering by medium- and heavy-weight nuclei. Photon scattering provides one of the simplest and most direct means of studying general features of nuclear matter, for example, the giant dipole resonance. Observation of elastic- and inelastic-photon scattering can resolve questions concerning the isospin character of the resonance and the nature of the coupling between it and collective modes of nuclear excitation. Unfortunately, observations of photon scattering in the past have been hindered by the difficulty in obtaining intense monochromatic beams. The only such sources available previously, photons from neutron capture, do not have sufficient energy to excite the GDR region in most nuclei. In the past year the Argonne group in collaboration with the University of Illinois completed a landmark experiment in which elastic and inelastic scattering from a spherical nucleus, in this case  $^{60}\text{Ni}$ , was measured directly for incident photons of precisely determined energies. Theoretical predictions based on currently accepted models bear little resemblance to our experimental results. It appears that our present understanding of photon excitations in nuclei must be reexamined. In view of these initial results, the Argonne group in collaboration with the staff of the University of Illinois MUSL-II electron microtron laboratory, plans to continue these measurements for an extensive range of nuclei in the coming year.

Traditionally, the Argonne neutron-physics program included vigorous activity in measuring fundamental properties of the neutron. This subject has re-emerged in importance recently with the intense interest in gauge theories of fundamental interactions of elementary particles. A careful determination of the electric-dipole moment of the neutron or a

correspondingly precise upper limit would provide a critical test of these theories, all of which have a breakdown of CP invariance at some level. The prospect of an intense pulsed neutron source at Argonne offers new possibilities in this area, and an ANL-University collaboration has begun development of an ultracold-neutron facility with the objective of a sufficiently sensitive measurement of the electric dipole moment. If preliminary design estimates are correct, the technique planned should provide the most sensitive measurement in its class. In view of the implications a new result will have, the Argonne staff will proceed as rapidly as circumstances permit.

### A. MEASUREMENT OF THE ELECTRIC DIPOLE MOMENT OF THE NEUTRON

V. E. Krohn, G. R. Ringo, J. M. Carpenter,<sup>\*</sup> T. O. Brun,<sup>\*</sup>  
T. W. Dombeck,<sup>†</sup> J. W. Lynn,<sup>†</sup> S. A. Werner,<sup>‡</sup> and J. W. Cronin<sup>§</sup>

The object of this project is to measure the electric dipole moment (EDM) of the neutron using stored ultracold neutrons (UCN). The EDM of the neutron, because it can be measured with such great sensitivity, has provided a useful challenge to fundamental particle theories. It has been instrumental in disposing of about 15 of these and at the moment is on the edge of testing the very successful Weinberg-Salam gauge theory of the weak interaction. In the currently popular model, which gives CP nonconservation, the EDM is calculated as  $1.6 \times 10^{-24}$  e-cm [S. Weinberg, Phys. Rev. Lett. 37, 657 (1976)]. The present measurements give an upper limit close to this value.

The sensitivity of the measurement to the length of time neutrons spend in the measuring apparatus makes the use of UCN stored in containers an attractive possibility for this measurement. These neutrons have velocities lower than 7 m/s and are totally reflected at all angles by the container walls. They can be stored for 100 seconds or more. By using a shutter on the container, opened only when the source is on, a pulsed source of UCN can give as large a number of stored neutrons as a steady state source with a flux equal to the peak flux of the pulsed source. Argonne has such a source in the ZING-P<sup>†</sup> project and calculations suggest it will give a higher density of UCN in a container than can the high-flux reactor at Grenoble where another EDM measurement is planned.

---

<sup>\*</sup>Solid State Science Division, ANL.

<sup>†</sup>University of Maryland, College Park, Maryland.

<sup>‡</sup>University of Missouri, Columbia, Missouri.

<sup>§</sup>University of Chicago, Chicago, Illinois.

At Argonne the UCN will be produced by reflection of 400 m/s neutrons from ZING-P' by a synthetic mica crystal on a 200 m/s rotor synchronized to the (30/s) pulses from the source. The UCN will be stored in a container which will be placed in a combined magnetic and electric field and the precession rate measured with the electric field parallel and antiparallel to the magnetic. If a density of more than 3 UCN/cc can be achieved, and it appears quite possible, the accuracy of the EDM measurement will be improved from the present  $3 \times 10^{-24}$  e-cm to about  $1 \times 10^{-25}$  e-cm. In all probability this will, however, require the further suppression of some significant sources of systematic errors below the levels that were tolerable in the present measurements (e.g., leakage currents from the electric field plates).

A UCN generator has been built and its rotor and shutter have been tested at their design speeds. Also, we have tested a considerable quantity of synthetic mica (fluor-phlogopite) for its neutron reflecting properties and a package of selected crystals has been assembled and observed to have a high efficiency for reflecting neutrons at the desired velocities and angles. There is a good possibility that the UCN facility will be useful in studies of neutron-surface interactions and perhaps in such fundamental studies as neutron lifetime measurements and observation of macroscopic quantum effects.

## B. PHOTONUCLEAR PHYSICS

a. NaI Spectrometers

T. J. Bowles, H. E. Jackson, and J. R. Specht

We have completed construction of two large NaI spectrometers which each consist of a 25-cm-diameter by 30-cm-long NaI crystal viewed by 7 photomultipliers. The NaI crystal is surrounded by 5 mm of  $^6\text{LiH}$  neutron shielding; this assembly is covered on the sides and front by 12 cm of plastic scintillator; and the whole is enclosed by 10 cm of cadmium saturated lead shielding. The  $^6\text{LiH}$  shield and cadmium-saturated lead shielding has reduced thermal-neutron backgrounds by a factor of  $\sim 20$  over that observed with lead shielding only. The best resolution observed to date is 2.3% at 17 MeV at low counting rates and we typically see better than 4% with counting rates in excess of 150 kHz. The gain has been stabilized dynamically to better than 1% by using a temperature controlled LED pulser. Timing resolution has been measured to be  $\sim 1$  ns. We are now working on improving the resolution at high counting rates.

The spectrometers have been used extensively in studies of pion reactions at LAMPF, in photon scattering at the University of Illinois, and in radiative-capture studies at Argonne.

b. Photon Scattering by the Giant Dipole Resonance

T. J. Bowles, R. J. Holt, H. E. Jackson, R. M. Laszewski, A. M. Nathan,\* J. R. Specht, and R. Starr\*

Elastic and inelastic scattering is one of the simplest and most rigorous probes of the properties of the giant dipole resonance (GDR) in nuclei. The basic photon interaction is well known. Elastic scattering is constrained by its connection to the photoabsorption cross

---

\* University of Illinois, Urbana, Illinois.

section through optical theorem and dispersion relations. Inelastic scattering provides a direct measure of the coupling between the giant-dipole excitation mode and other degrees of freedom such as collective surface and rotational excitations. In the past year, we observed elastic and inelastic scattering directly for the first time in an experiment in which the incident photon energy is measured and the elastic and inelastic scattering is resolved. The experiment was performed at the University of Illinois MUSL-II microtron, using the 100% duty factor electron beam to generate a "tagged" photon beam whose energy is known with a resolution of 150—200 keV. Scattered photons were detected in a large volume NaI(Tl) spectrometer system developed within the Physics Division in connection with programs in medium-energy and charged-particle physics. The  $120^\circ$  differential cross sections for photons scattering to the ground and first excited states of  $^{60}\text{Ni}$  were measured for excitations between 15 and 22 MeV. The scattering to the first-excited  $2^+$  state is weaker than anticipated over the full range of photon energies. Nowhere in this excitation region is the branching ratio of decay to the first excited state near the value of 0.3 typical of current widely discussed theories. Nor does the inelastic scattering show the rapid energy variation characteristic of the resonance shape calculated in the theory. A substantial effort to refine models of the interaction will be necessary to explain the present data. We have begun a sustained effort to extend this type of photon-scattering measurement to a range of nuclei.

### c. Photodisintegration of the Deuteron

H. E. Jackson, R. J. Holt, G. Mavrogenes,\* and J. R. Specht

The deuteron is the simplest nuclear system for testing various models of the nucleon-nucleon interaction. It is of particular interest because it is the one system for which the effects of meson-exchange currents and virtual isobar states can be calculated accurately. The

\* Chemistry Division, ANL.

photodisintegration of the deuteron is a particularly attractive reaction for probing the two-nucleon system since the basic interaction is so well understood. Until recently, it was generally accepted that the  $D(\gamma, n)$  reaction at moderate photon energies was understood with good precision in terms of potentials which have been determined from fits to two-nucleon scattering data, and corrections applied for meson-exchange currents.

However, recently measurements at Mainz<sup>1</sup> of the  $D(\gamma, n)$  reaction at  $180^\circ$  have shown a startlingly large—20 to 40 percent—discrepancy with all reasonable theoretical estimates of the photodisintegration amplitude. They highlight the importance of careful and comprehensive measurements of photoneutron angular distributions and polarizations over the region from threshold to 20 MeV. The existing data base is surprisingly limited.

Measurements at the ANL facility have focused on a determination of the angular distribution in the threshold region where the amplitude is particularly sensitive to mesonic effects. A precision of about 10% has been achieved, which is adequate to test the simple effective range theory. To date measurements have been limited to observation at  $90^\circ$ ,  $135^\circ$ , and  $155^\circ$ . It was evident from the data that a substantial improvement in precision would be possible only with measurements over the full angular range of photoneutron angles and with a direct means of calibrating the relative detection efficiency at each angle. To that end, a multidirectional photoneutron transport system was constructed in 1978. This system (shown in Fig. VI-1) provides bremsstrahlung beams on demand, vertically for efficiency calibrations, and horizontally in modes corresponding to angles of observation along our photoneutron flight lines in either the forward and backward hemisphere. More precise determination of photoneutron angular distributions over the full range of angles possible with this system will facilitate our search for interference effects which

---

<sup>1</sup> R. J. Hughes, A. Zieger, H. Wäffler, and B. Ziegler, Nucl. Phys. A267, 329 (1976).

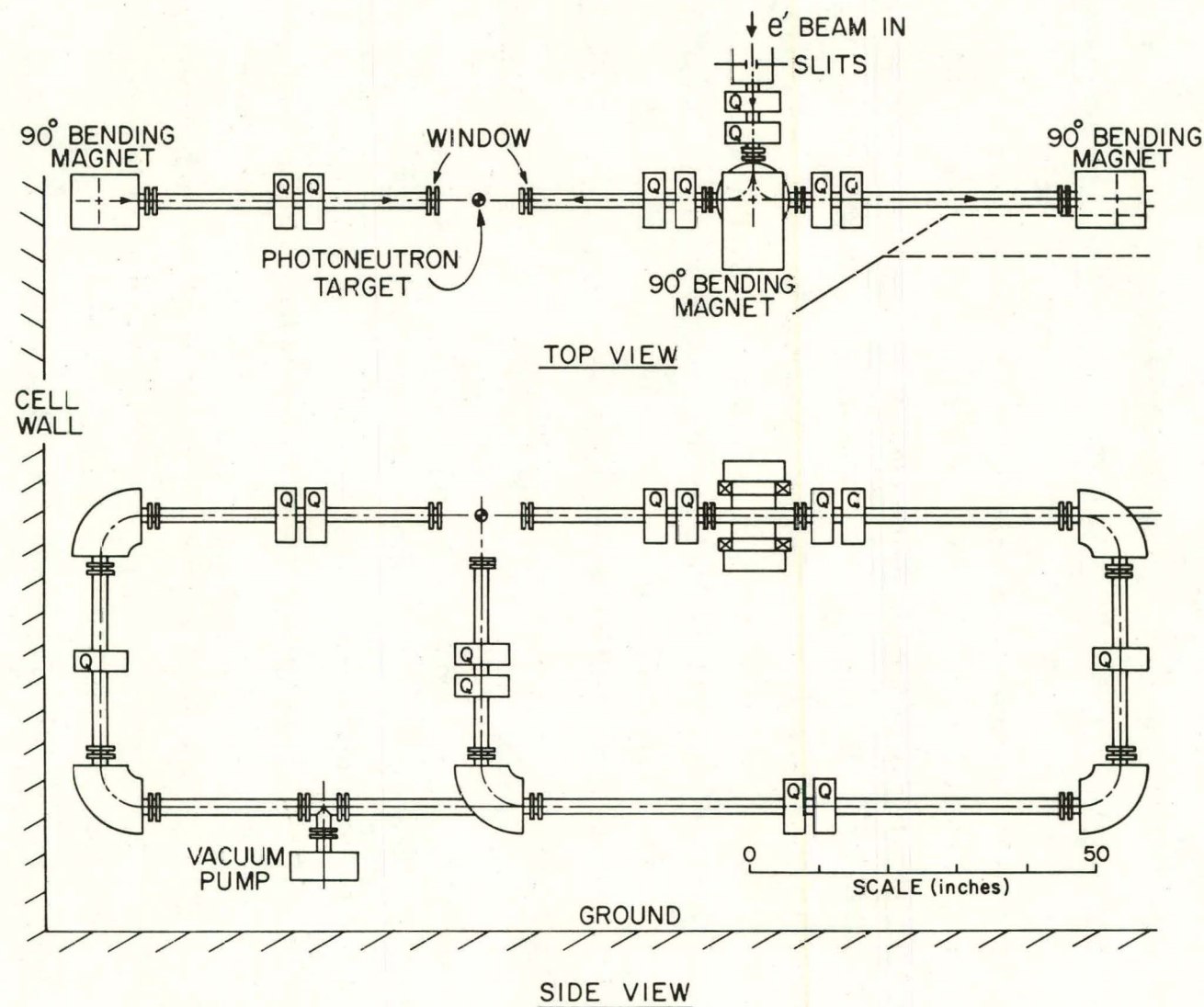


Fig. VI-1. Multidirectional beam transport system for photoneutron experiments.

are a signature of possible final-state interactions or momentum-dependent components in the nucleon potential.

d. R-Matrix Analysis of the  $^{13}\text{C}(\gamma, n_0) ^{12}\text{C}$  Reaction Below an Excitation of 9.3 MeV

R. J. Holt, H. E. Jackson, R. M. Laszewski, J. E. Monahan, and J. R. Specht

Electromagnetic transition rates in nuclei provide a particularly good test of nuclear-structure theories. The configurations of the  $\frac{3}{2}^+$  resonances at 7.7 and 8.2 MeV in  $^{13}\text{C}$  have been the subject of numerous theoretical calculations. These studies include the weak-coupling model, the Feschbach unified model, and full p-wave shell-model calculations. Unfortunately, the E1 ground-state radiative widths for these resonances have not been previously measured. This is due to the large resonant and nonresonant interference effects in this energy region. In order to extract accurate ground-state transition rates for these resonances, the observed high-resolution photoneutron cross section reported last year was interpreted in terms of a multilevel R-matrix analysis. In the analysis we have fully considered the well-known neutron scattering channel. The results of this analysis are compared with the data in Fig. VI-2. It appears that the channel capture widths of the 7.7- and 8.2-MeV resonances are large and their influence must be included in any comparison of the radiative widths with theory.

e. Effects of Channel and Potential Radiative Transitions in the  $^{17}\text{O}(\gamma, n_0) ^{16}\text{O}$  Reaction

R. J. Holt, H. E. Jackson, R. M. Laszewski, J. E. Monahan, and J. R. Specht

A general multilevel R-matrix analysis was performed for the observed  $^{17}\text{O}(\gamma, n_0) ^{16}\text{O}$  differential cross section. The ground-state radiation widths for resonances in the excitation-energy region 4.3—7 MeV were extracted from the data. The value of the radiation

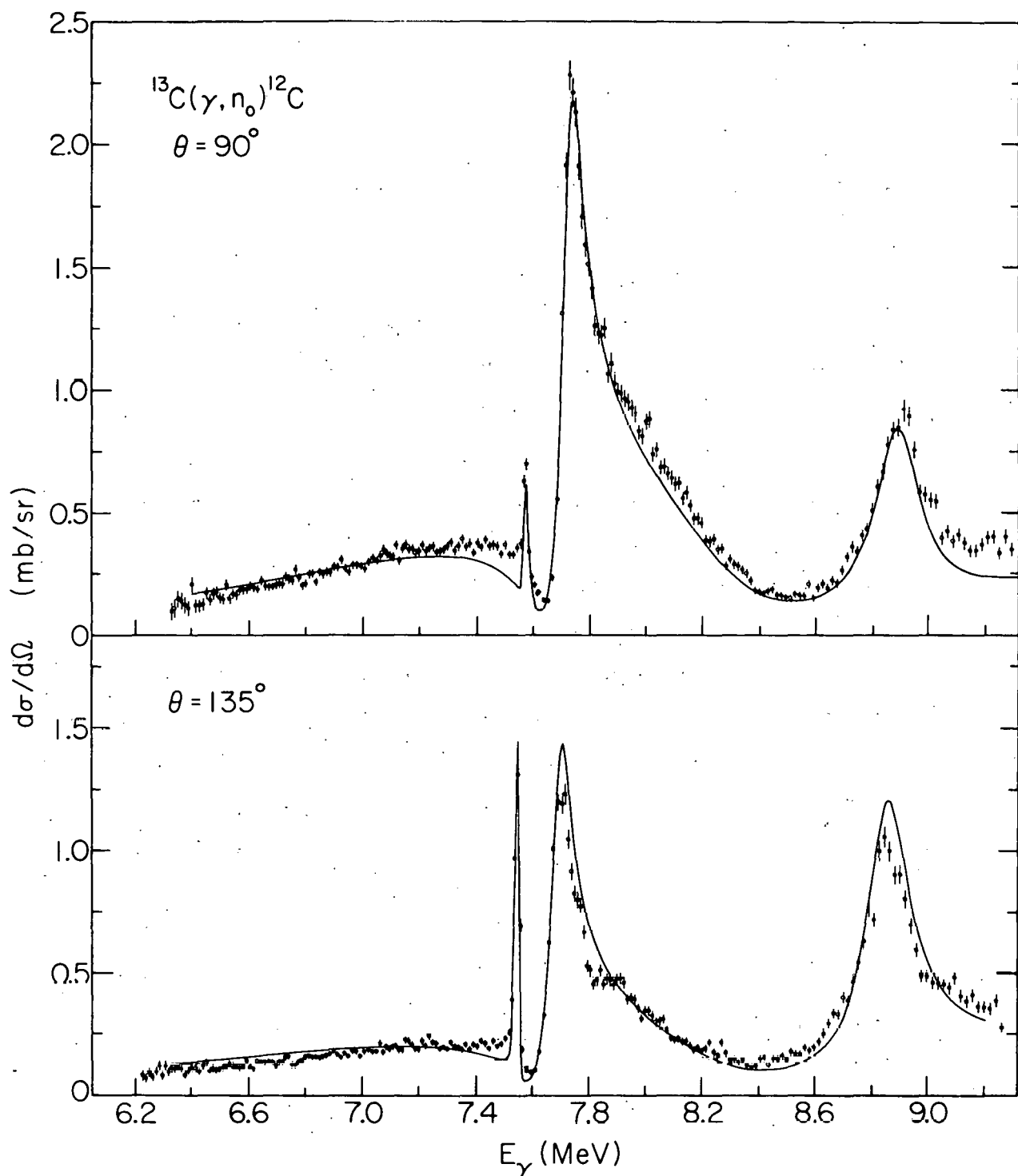


Fig. VI-2. The observed photoneutron cross section for the  $^{13}\text{C}(\gamma, n_0)^{12}\text{C}$  reaction at angles of  $90^\circ$  and  $135^\circ$ . The curves represent the R-matrix interpretation.

width for the  $d_{5/2} \rightarrow d_{3/2}$  spin-flip transition at 5.08 MeV was found to be approximately 1/3 of the value expected for a pure single-particle transition. The effects of potential radiative capture were observed directly in a photoneutron reaction for the first time. At the location of the 5.38-MeV,  $\frac{3}{2}^-$  resonance in  $^{17}\text{O}$ , a symmetric minimum was observed in the photoneutron cross section. This anomalous minimum was found to be due to a unique feature of channel capture within the framework of the Lane-Lynn theory of radiative capture. The neutron channel was defined by incorporating an R-matrix analysis of the  $^{16}\text{O}(n, n)^{16}\text{O}$  reaction into the present interpretation. The R-matrix theory was extrapolated into the keV region in order to estimate the neutron capture rate, a quantity of significance for studies of stellar nucleosynthesis. We found the capture rate, reported in the literature, to be underestimated by at least an order of magnitude. This is due to the fact that the early work ignored the natural width of the low-lying 440-keV resonance and the effects of direct capture. This work has been completed and published.

f. Doorway Resonances in  $^{29}\text{Si}$

R. J. Holt, H. E. Jackson, and J. R. Specht

In a recent study of the  $^{29}\text{Si}(\gamma, n_0)^{28}\text{Si}$  reaction near threshold, we found evidence for a doorway state with  $J^\pi = \frac{3}{2}^-$  near  $E_n = 750$  keV. Subsequent theoretical calculations supported the interpretation of this resonance as a doorway state. These calculations predict the existence of additional doorway resonances at higher energies. We have extended our measurements to higher excitation energies using the ANL picosecond photoneutron facility and the newly installed 25-m flight paths. Preliminary results suggest the existence of a localization of strength near 1.7 MeV. A doorway resonance at this energy is not consistent with the most recent theoretical models. Further experimental work will be necessary in order to extract accurate ground-state radiative widths.

g. The Giant M1 Resonance in  $^{119}\text{Sn}$

R. J. Holt, H. E. Jackson, R. M. Laszewski,\* and J. R. Specht

The observation of a broad resonance structure at 7.8 MeV has spurred the speculation that this resonance is due to collective proton spin-flip oscillations ( $g_{9/2} \rightarrow g_{7/2}$  proton transitions). Furthermore, the observed amount of transition strength almost exactly exhausts the M1 sum rule. One would expect that a resonance of this multipolarity would produce a polarization in the emitted photoneutron beam at a reaction angle of  $90^\circ$ . With the ANL threshold photoneutron polarimeter we observed the photoneutron polarization from the  $^{119}\text{Sn}(\gamma, n_0) ^{118}\text{Sn}$  reaction at  $90^\circ$  to be zero within the statistical error limits. In order to establish an upper limit for the magnitude of the M1-ground-state radiative width in this resonance structure, we also observed the differential cross section throughout the resonance region. From these results we estimated that the ground-state radiation width of the resonance structure is predominately (>75%) E1 in nature.

h. Absence of Large M1 Excitations in  $^{208}\text{Pb}$  Below 8.4 MeV

R. J. Holt, H. E. Jackson, R. M. Laszewski, and J. R. Specht

It has long been believed that the  $^{208}\text{Pb}$  nucleus should provide an ideal example of a collective M1 resonance in nuclei. Early  $(\gamma, n)$  angular distribution experiments at Livermore suggested that seven strong resonances, centered at approximately 7.9 MeV, exhausted more than half of the M1 sum rule. The threshold-photoneutron polarization studies performed at the ANL high-current electron linac showed that only one of these strong resonances at  $E_{\text{exc}} = 7.99$  MeV could be assigned as an M1 excitation. Many of these resonances were found to have a large s-d-wave admixture which would explain the incorrect parity assignments in the Livermore work.

\* University of Illinois, Urbana, Illinois.

In order to study this energy region, 7.5-8.4 MeV, in  $^{208}\text{Pb}$  in more detail, we performed a very high-resolution measurement of the  $^{208}\text{Pb}(\gamma, n_0) ^{207}\text{Pb}$  reaction using the unique picopulse and the newly-installed neutron flight paths at the electron linac facility. (See Fig. VI-3.) We discovered that the 7.99-MeV resonance ( $E_n = 610$  keV) exhibited a level-level interference pattern with the 7.98-MeV, E1 resonance in  $^{208}\text{Pb}$ . This constructive interference pattern is shown in greater detail in the inset figures for the resonances at  $E_n = 600$  and 610 keV. Thus, the last candidate for a strong M1 excitation was ruled out. This is somewhat disconcerting since all published theories predict that the giant M1 resonance should occur below 8.4 MeV. This work has led G. Brown to speculate that our thinking about the unperturbed energies used in the particle-hole model must change. Having used an effective nucleon mass to calculate the single-particle, Brown predicts that the giant M1 resonance should occur at a much higher energy ( $\sim 10$  MeV) than previously believed.

Oak Ridge has recently observed many weak M1 excitations between 7.4 and 7.7 MeV using the  $(n, n)$  and  $(n, \gamma)$  techniques. However, the reported transition strengths for  $^{208}\text{Pb}$  from the  $(n, \gamma)$  method seem to be consistently larger than those from the  $(\gamma, n)$  method. Fortunately, with the extended flight paths we have been able to calibrate the radiative widths in  $^{208}\text{Pb}$  relative to the well-known cross section for photodisintegration of the deuteron. This represents the first threshold  $(\gamma, n)$  measurement in  $^{208}\text{Pb}$  which is independent of some allegedly known radiative width from  $(n, \gamma)$  studies. We found that the  $(n, \gamma)$  method consistently overestimates the transition strengths by a factor of approximately 1.5 in  $^{208}\text{Pb}$ . Thus, the total known amount of M1 strength in  $^{208}\text{Pb}$  accounts for less than 10% of the M1 sum rule.

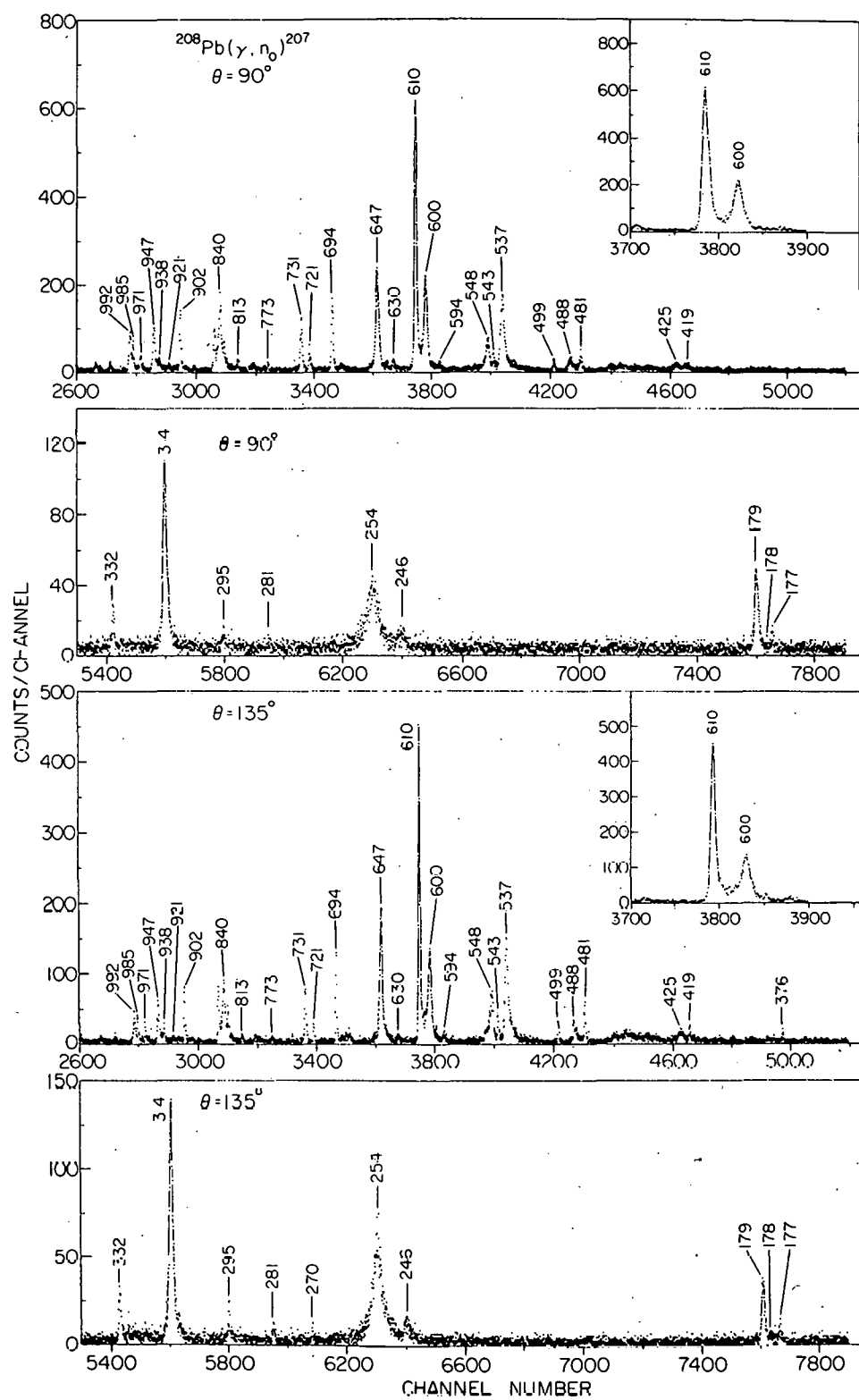


Fig. VI-3. The raw, high-resolution time-of-flight spectra for the  $^{208}\text{Pb}(\gamma, n_0)^{207}\text{Pb}$  reaction. The inset figures show the previously suspected giant M1 resonance region in detail.

i. Polarization in Nuclear Reactions Involving Photons

J. E. Monahan, R. J. Holt, and R. M. Laszewski\*

Published formulae for polarization phenomena in photo-nuclear reactions are beset with phase and normalization errors.

Expressions for the polarization tensors in reactions involving photons have been rederived. We found that our rederived coefficients for the differential photonucleon polarization are in agreement with those from the Stanford photonuclear group but differ in phase from those of Baldin *et al.* A paper describing these results was submitted for publication.

j. Background Photoneutrons from  $W(\gamma, n)$  at Radiation Therapy Centers

R. J. Holt, H. E. Jackson, and J. R. Specht

At the request of the radiological physics group at Stanford and with the understanding that numerous facilities for radiation therapy use 10-MeV electron sources, we have measured the yield of photoneutrons from natural W when irradiated with 10-MeV electrons from the ANL electron linac. At many medical electron-accelerator centers, the therapeutic radiation is derived from the bremsstrahlung process. Natural W is routinely used as a photon beam collimator or "hardener" at these facilities and represents a source of photoneutrons. The photoneutrons from W were observed using the ANL threshold photoneutron facility and associated time-of-flight spectrometer. The neutron yield per electron was measured as a function of the neutron energy. The results of this measurement are now under consideration by the Stanford group.

---

\* University of Illinois, Urbana, Illinois.

k. Study of the  $^6\text{Li} + \text{n}$  System Below 4 MeV

R. J. Holt, P. T. Guenther,\* A. B. Smith,\* and J. F. Whalen\*

This work was performed in collaboration with the Applied Physics Division. The neutron cross section for elastic and inelastic scattering was observed below 4 MeV using the Argonne fast-neutron generator. This work represents the first systematic study of the  $^6\text{Li} + \text{n}$  system in the MeV region. Even though the neutron cross section was found to be relatively large in this energy region, we found no definitive resonance structures. A multilevel, multichannel R-matrix analysis is in progress in order to understand the reaction mechanisms for the  $^6\text{Li} + \text{n}$  system.

l. Neutron Interaction with  $^{12}\text{C}$  in the Few-MeV Region

A. B. Smith,\* R. J. Holt, and J. F. Whalen\*

This work was performed in collaboration with the Applied Physics Division. Precision measurements of the neutron total and differential cross section for  $^{12}\text{C}$  were performed between 1.5 and 4 MeV using the fast-neutron generator at the ANL tandem-Dynamitron facility. Measurements of this precision should prove valuable for nuclear structure information and convenient standards for experimental studies of neutron induced processes. The experimental results were interpreted in terms of a multilevel R-function analysis. The experimental data available for the  $^{12}\text{C} + \text{n}$  system were reviewed and compared with the present R-function analysis. We found that the precision with which we measured the cross section renders  $^{12}\text{C}$  a suitable reference standard in experimental studies. The R-function interpretation provides a convenient description of neutron total and scattering cross sections of  $^{12}\text{C}$  as a function of both angle and energy. This work was completed and submitted for publication. These cross sections are now used routinely at the ANL fast-neutron generator facility as a secondary standard.

\* Applied Physics Division, ANL.

## VII. THEORETICAL PHYSICS

## INTRODUCTION

A. Heavy-Ion Direct Reactions at Nonrelativistic Energies.

The long-term objective of this work is, and has been for the past few years, to study heavy-ion direct reactions as a function of energy from the Coulomb barrier to the onset of strongly-damped processes and to develop the coupled-channel techniques and programs necessary for such studies. This year the main technical barriers to a multichannel approach to heavy-ion direct reactions have been removed; computational techniques have been developed that accelerate coupled-channel calculations by an order of magnitude beyond the previous state of the art.

B. Nuclear Shell Theory and Nuclear Structure. A variety of studies has been completed in which the best available nuclear-structure information is used to illuminate detailed properties of nuclear levels, transitions and interactions. These include systematic studies of E2 and other transition charge densities in 1p-shell nuclei, with applications to inelastic electron and pion scattering, and investigations of isospin-mixing and charge-dependent effects in light nuclei.

C. Nuclear Matter. Studies have been carried out of the validity of the Brueckner-Bethe hole-line expansion. The binding energy and saturation density of nuclear matter have been computed for various potentials with central and tensor components; two-, three- and four-hole-line contributions are included. The results are compared with the predictions of Monte-Carlo and variational calculations. (Spin-orbit forces are excluded because the Monte-Carlo and variational calculations cannot at present accommodate them.) These tests confirm the validity of the Brueckner-Bethe expansion and indicate that there is no significant discrepancy between Brueckner-Bethe and variational results.

D. Intermediate-Energy Physics and Pion-Nucleus Interactions. The long-term goal of this work is to describe the interaction of intermediate-energy pions and nucleons with nuclei in terms of a relativistic many-body quantum theory of pions, nucleons, and  $\Delta$ 's. The spirit here is radically different from most other theoretical work in intermediate-energy physics wherein the theory underlying relativistic particle interactions is assumed to be a field theory. A single Hamiltonian is sought that will govern nuclear structure (including pionic and  $\Delta$  degrees of freedom), nuclear reactions, and pion-nucleus reactions. Work has proceeded this year in two main areas. A detailed study of NN interactions up to 800 MeV (well above the pion threshold) has been carried out. The

interactions of pions with heavier nuclei have also been extensively studied; a formal relativistic particle theory has been developed and phenomenological calculations carried out for pion inelastic scattering on targets throughout the nuclear periodic table.

E. Dense Nuclear Matter and Classical Calculations of the High-Energy Collisions of Heavy Ions. Work has continued on classical equations-of-motion calculations of high-energy heavy-ion collisions; calculations have been carried out for the equal-mass systems  $A_{\text{proj.}} = A_{\text{tgt.}} = 20$  and 40 at laboratory energies of 117, 400, and 800 MeV/nucleon. Various phase-equivalent nuclear potentials were used and extensive results obtained on nucleon momentum distributions and on the qualitative evolution with time of the colliding systems. In a different area, the equation of state of nuclear matter has been studied in a mean-field theory with nonlinear interactions.

F. Radiative Transitions and Nuclear Resonance Reactions. Angular distributions and absolute cross sections for the reactions  $^{17}\text{O}(\gamma, n)^{16}\text{O}$ ,  $^6\text{Li}(d, n^3\text{He})^4\text{He}$ ,  $^6\text{Li}(d, p^3\text{H})^4\text{He}$ ,  $^6\text{Li}(d, a)_a$ ,  $^6\text{Li}(d, p)^7\text{Li}$ , and  $^6\text{Li}(d, n)^7\text{Be}$  at low energies have been interpreted in terms of the R-matrix theory of nuclear resonance reactions. A theory has also been developed for the phenomenon of quantum beats observed at Argonne in a study of the Mössbauer effect using a frequency-modulated source.

### A. HEAVY-ION DIRECT REACTIONS

Experimental studies of nonrelativistic heavy-ion collisions focus on the competition between two classes of direct reaction—peripheral and strongly-damped. Because of limitations on the type of ion that can be accelerated with present-generation accelerators, we have a clear picture only for systems wherein at least one of the heavy ions has a mass number less than 40. For such systems, the total reaction cross section  $\sigma_r$  close to the Coulomb barrier is dominated by peripheral reactions—elastic and inelastic scattering and few-nucleon transfer to very low-lying states. As the bombarding energy increases, the peripheral-reaction cross section quickly stabilizes and remains constant with increasing energy while the fusion reaction (compound-nucleus formation) rapidly increases in probability and soon dominates  $\sigma_r$ .

At a sufficiently high energy ( $E_{c.m.}/E_B \sim 1.5$  to 2), while the peripheral cross section stays roughly constant,  $\sigma_f$  suddenly stops increasing or even starts to decrease as more and more of the cross section goes into partial waves whose centrifugal content is too great to support a compound nucleus.

This energy region witnesses the onset of strongly-damped processes—direct reactions that leave the reaction products in highly-excited states. The picture for the collision of two very-heavy ions is not clear; it is likely however that fusion is of negligible probability and the competition between the two different sorts of direct reaction starts immediately above the Coulomb barrier.

The main challenge for theories of heavy-ion reactions, then, is to describe the relation between peripheral and strongly-damped processes. Are they basically distinct, with the strongly-damped processes to be described in statistical terms or by macroscopic dissipative models involving friction or viscosity? Or are the two classes of direct reactions merely names given to the extremes of what is in fact a continuum of direct reactions with no clear line of demarcation? The latter view is the one that underlies theoretical efforts—such as that in the Argonne Physics Division—that seek to describe heavy-ion reactions in terms of microscopic quantum-mechanical (or semiclassical) direct-reaction models. The hope is that, at least for bombarding energies up to some limit far enough above the Coulomb barrier to be of interest, peripheral and strongly-damped collisions can be described in terms of a multichannel reaction theory where the channels refer to energy-averaged giant resonances rather than to individual nuclear states. It remains to be seen, of course, whether the number of such 'channels' is small enough to be tractable and whether the known giant resonances suffice to provide the observed transfer of mass, charge, and energy.

During the past year, we have worked almost exclusively on techniques for carrying out coupled-channel calculations and on writing computer programs that implement them. Major progress has been achieved. New techniques have been developed in two main areas. A sequential-iteration method greatly accelerates the solution of the coupled equations within the range of nuclear reactions. Efficient methods for calculating multiple Coulomb excitation—always a significant source of computational difficulty in heavy-ion collisions—have been devised. We believe that these technical innovations accelerate coupled-channel calculations by an order of magnitude beyond the previous state of the art. With the computational barriers removed or at least weakened, work is now proceeding on studies of the evolution of heavy-ion direct reactions from below the Coulomb barrier to the onset of strongly-damped processes.

a. Heavy-Ion Coupled-Channel Calculations—Sequential Iteration

M. H. Macfarlane, S. C. Pieper, and M. J. Rhoades-Brown

Conventional coupled-channel programs solve the set of  $N$  coupled equations for each partial wave  $N$  times with different starting conditions in order to build solutions with appropriate asymptotic behavior at large distances. This  $N$ -fold waste of effort can be eliminated by use of a sequential-iteration method to solve the coupled radial equations within the range of nuclear interactions. It is found that sequential iteration diverges in many situations of physical interest for heavy-ion inelastic scattering. Direct application of the Padé method to the sequences of  $T$  matrices generated by iteration yields rapid convergence in all cases considered. On the average (over all partial waves for a given reaction), three- or four-figure accuracy in the  $T$  matrices can be attained in 3 steps of sequential iteration. A paper on these techniques is being prepared for publication.

b. Heavy-Ion Coupled-Channel Calculations—Coulomb Excitation

M. H. Macfarlane, S. C. Pieper, and M. J. Rhoades-Brown

The effects of Coulomb excitation in heavy-ion inelastic scattering can be very large and occur over a distance of several hundred fermis. Under such circumstances, direct integration of the coupled

radial equations is hopelessly inefficient. The region dominated by Coulomb excitation extends from an inner joining radius ( $\sim 20$  fm) just beyond the range of nuclear interactions to an outer radius (several hundred fm) beyond which the channel wave functions are pure Coulomb functions. The channel wave functions in the region of CE are expressed as products of Coulomb functions and modulating amplitudes; the modulating amplitudes vary slowly with  $r$ ; and, to a high degree of accuracy, satisfy a system of coupled first-order equations that can be solved very rapidly by a combination of the Born approximation and direct integration with large step-size ( $\sim 1$  fm). We solve the coupled radial equations in the interior region by the iterative method described above and join the interior solutions at the inner joining radius to solutions of the coupled Coulomb equations obtained in the manner just described. The interior and exterior parts of the solution of the coupled equations involve comparable amounts of computational labor.

c. Ptolemy: A Computer Program for Heavy-Ion Direct Reactions.  
Light-Ion Version

M. H. Macfarlane and S. C. Pieper

Earlier reports described the development of Ptolemy—a program that can perform optical-model calculations (including fits) for elastic scattering and DWBA calculations for inelastic scattering and transfer reactions. Work on Ptolemy during the past year was confined to routine maintenance and to the production of a revised edition of Ptolemy's documentation (Argonne Report ANL-76-11, Rev. 1). The version of Ptolemy described in this document is specialized in a variety of ways to the efficient treatment of heavy-ion-induced direct reactions. Work has begun, in collaboration with R. P. Goddard of the University of Wisconsin, on a version of Ptolemy appropriate for light-ion-induced reactions. The light-ion version will allow for spin-dependent potentials and permit the calculation of polarizations and analyzing powers.

d. Ingoing-Wave Boundary-Condition Model for Heavy-Ion Elastic Scattering

S. C. Pieper, U. Mosel,\* and R. Wolf\*

Attempts to interpret resonant structure in the 90° excitation function of  $^{16}\text{O} + ^{16}\text{O}$  elastic scattering in terms of an ingoing-wave boundary-condition model have been reported in the literature. The idea here is to use a conventional optical model for the interaction of the ions from infinity inward to a distance inside the optical-model radius and there to augment it by assuming ingoing-wave boundary conditions. Work on this model, in collaboration with U. Mosel and R. Wolf, was started during a two-week visit (partially supported by DOE) to the University of Giessen. Ptolemy was modified to permit calculations with the boundary-condition model and used to confirm Wolf's earlier conclusion that most previously-reported calculations with the model are incorrect. Attempts were made to vary the optical-model and boundary-condition parameters to fit the  $^{16}\text{O} + ^{16}\text{O}$  90° excitation function and angular distributions at various energies. Although the extra parameters introduced by the BC model permit a better fit to the data than is possible with the unmodified optical model, no satisfactory description of all the data has yet been found. R. Wolf is continuing this work at the University of Giessen.

e. The "Sensitive Radius" in Heavy-Ion Elastic Scattering

S. C. Pieper and M. H. Macfarlane

During the past few years, a number of studies of heavy-ion elastic scattering have led to the conclusion that the real part of the ion-ion potential is well determined at a definite radius—the sensitive radius. The basis of this conclusion is that when a given elastic angular distribution is fitted by a variety of Woods-Saxon potentials, the real parts of all such potentials come close to intersecting at a point; the radial coordinate of this "point" is determined to less than 0.1 fm and the corresponding

---

\* Institute für Theoretische Physik, University of Giessen, Giessen, West Germany.

potential to a few percent. The degree of radial localization apparently implied is highly suspicious, particularly in view of the fact that the wavelength of the relative motion in the reactions involved is typically about 1 fm. We have studied this matter in two ways--first by using analytic forms other than the Woods-Saxon for the real potential, second by treating the values of the real potential at a few fixed distances in the region of the nuclear surface as fitting parameters, completing the specification of the potential function by polynomial interpolation. Both approaches lead to the conclusion that the data do not determine the real part of the potential at any given radius to better than a factor of 2 although some weighted average of the real potential over an interval of one or two fermis in the nuclear surface is clearly well determined. Thus the conclusion that the data fixes the real part of the ion-ion potential at some specified sensitive radius is an artifact of the use of the Woods-Saxon form for the radial dependence of the potential.

## B. NUCLEAR SHELL THEORY AND NUCLEAR STRUCTURE

### a. Interpretive Model for $^{10}\text{B}$

D. Kurath

There are over 25 measured electromagnetic transitions and moments of M1 or E2 multipolarity involving the low-lying levels of  $^{10}\text{B}$ . A simplified model based on the dominance of [42] spatial symmetry in these levels has been developed which provides understanding of the general features of these transitions and contains a new selection rule. This selectivity is based on the near validity of the approximation that  $K_L$  is a good quantum number, the projection of orbital angular momentum on the nuclear symmetry axis. Strong E2 and M1 transitions are shown in Fig. VII-1, wherein the  $T=0$  levels are separated into two groups, those with  $K_L = 0$  on the left and  $K_L = 2$  in the center. In addition to selecting out the strong transitions, the  $L, K_L$  assignment also shows why certain M1 transitions are strongly inhibited. For example the  $20 \rightarrow 10$  transition is  $L$  forbidden and the  $30^* \rightarrow 30$  transition is  $K_L$  forbidden. A paper on this subject has been accepted for publication in Nuclear Physics.

### b. Transition Densities in the 1p Shell

D. Kurath

In calculating the matrix elements of one-body operators that occur for electromagnetic transitions or for inelastic scattering of pions or nucleons, one needs matrix elements (between nuclear states) of a particle and a hole coupled to angular momentum  $J$  and isospin  $T$ . These have been calculated for states connected to the ground states of 1p targets, using the Argonne shell-model programs. A further Speakeasy program was written to decompose these matrix elements into the LS representation, which helps to clarify the nature of a given excitation (i.e., whether the spin or spatial part of the operator dominates). Extensive use of this decomposition has been made in studying inelastic

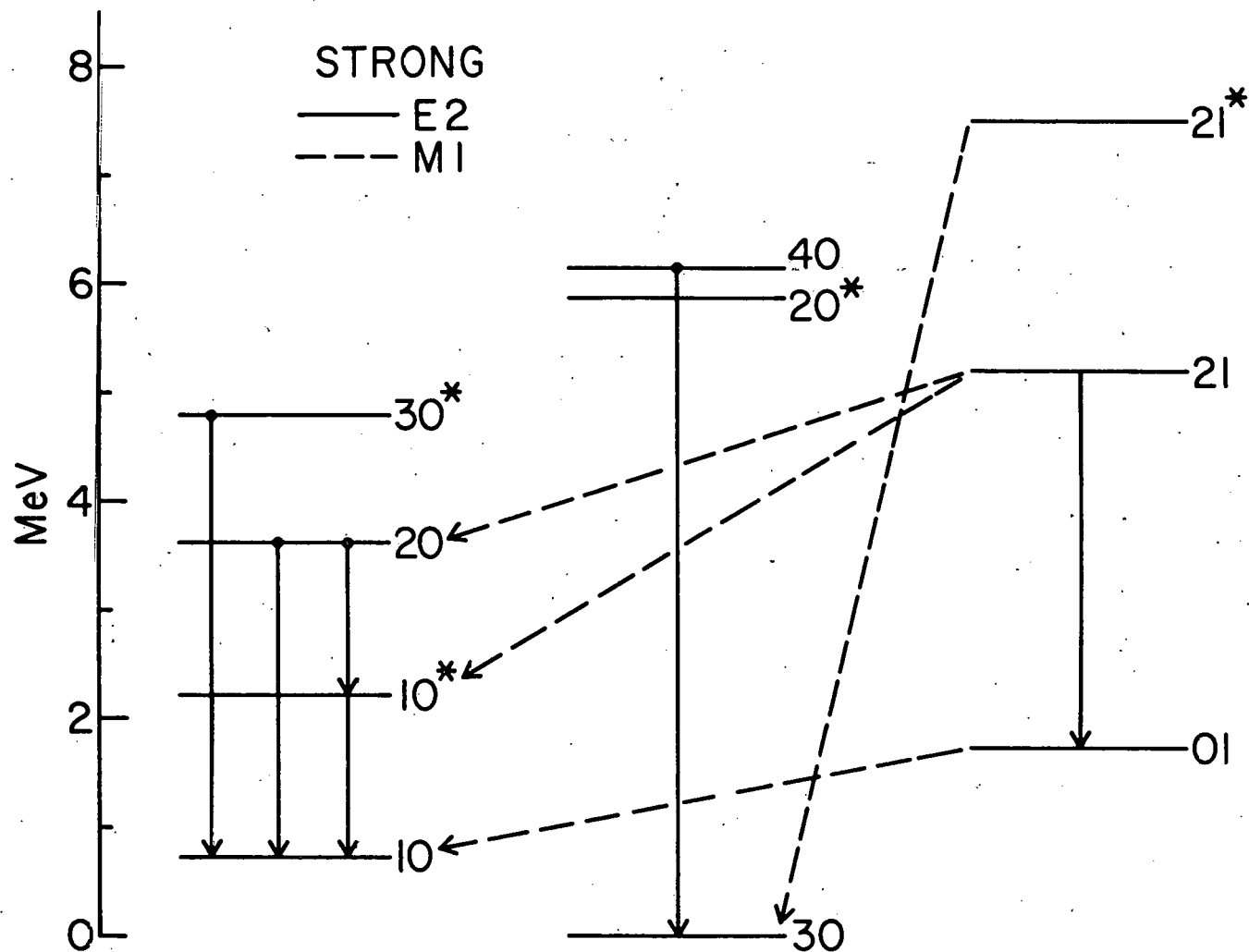


Fig. VII-1. Strong  $\gamma$  transitions between low-lying levels (identified by JT) of  $^{10}\text{B}$ . The selectivity can be understood in terms of the dominant  $(L K_L)$  values of the states. States on the left have  $K_L = 0$  with  $L = 2, 2, 2, 0$  in descending order. States in the center have  $K_L = 2$  with  $L = 3, 2, 2$  in descending order. States on the right have  $(L K_L)$  values  $(22), (20)$ , and  $(00)$ .

pion scattering in a DWIA approximation. Those results are described above in Sec. A.c.

c. Transverse E2 Form Factor for  $^{12}\text{C}(\text{e}, \text{e}')$

D. Kurath

In a recent experiment the contributions to excitation of the lowest  $2^+$  state of  $^{12}\text{C}$  have been separated to obtain the transverse part due to nuclear currents. There are two sources, one due to spin currents which dominate at higher momentum transfer, the other the convection current due to moving protons which is dominant at low momentum transfer. The convection contribution can be obtained from the longitudinal form factor (Coulomb term) by assuming the validity of the continuity equation between current and charge distributions. Alternatively it can be calculated directly, given a nuclear model.

For a pure 1p-shell configuration the calculated Coulomb transition probability is a factor of 2 to 3 less than observed, and the directly-calculated convection term is zero. A calculation has been carried out, going outside the 1p shell by projecting from Nilsson states containing  $2\hbar\omega$  components due to the effect of deformation. Relatively small admixtures permit a fit of the observed Coulomb form factor up to a momentum transfer of  $q = 2 \text{ fm}^{-1}$ . The transverse form factor resulting from these wave functions, using the continuity equation for the convection term, has the observed shape up to  $q = 2 \text{ fm}^{-1}$ , but is a factor of 3 too small in magnitude. Furthermore, direct calculation of the convection amplitude is a factor of 7 smaller yet, indicating that the continuity equation is not satisfied even in this enlarged shell model space.

d. Forbidden Beta Decay in  $^{205}\text{Tl}$

D. Kurath

The beta decay probability of the  $\frac{1}{2}^+$  state of  $^{205}\text{Tl}$  is relevant for interpreting a proposed experiment to study the flux of solar

neutrinos. An attempt was made to estimate this rate based on the systematics of similar observed decays for masses ranging from 125 to 128, and assuming reasonable nuclear configurations. Based on the results using four different sets of two-body interactions and the present empirical data, estimates of this probability are good to  $\pm 30\%$ .

e. The Isotensor Term in the Isobaric-Mass-Multiplet Equation

R. D. Lawson

Provided isospin is a good quantum number, the energies of states of a given isobaric multiplet with various values of  $T_z$  are related by the isobaric-multiplet mass equation

$$E = a + bT_z + cT_z^2.$$

The experimental values of  $c$  have been compared with the theoretical estimates obtained by using the "best-fit" p-shell nuclear eigenfunctions<sup>1</sup> and calculating the Coulomb interaction using Woods-Saxon wave functions. Even when  $(v/c)^2$  corrections and the effect of  $2\hbar\omega$  excitations are included, the experimental values of  $c$ , particularly for the seniority zero and one states, are larger than theoretical predictions. Moreover, the uncertainty associated with the difference in neutron and proton wave functions discussed in Sec. A.e above is mainly an isovector effect and contributes little to the isotensor coefficient  $c$ . On the other hand, when a charge-independence-breaking short-range interaction, whose strength is such that the (np) interaction is about 2% more attractive than the (nn) or (pp) potential, is introduced, theory and experiment for  $c$  can be brought into excellent agreement. This is approximately the same size as the charge-independence-breaking nucleon-nucleon interaction indicated by the free-nucleon scattering lengths and effective ranges.

---

<sup>1</sup>S. Cohen and D. Kurath, Nucl. Phys. 73, 1 (1965).

f. Isospin Mixing Between T=0 and T=1 States in the 1p Shell

R. D. Lawson

Experiments in the 1p shell indicate that there is a large off-diagonal matrix element between the yrast  $T=0$  and  $1^-$   $I=1^+$  states<sup>1</sup> in  $^{12}\text{C}$  and that the two  $2^+$  states in  $^8\text{Be}$  at 16.63 and 16.93 MeV are each 50%  $T = 0$  and  $T = 1$ . The off-diagonal matrix elements causing these mixings are larger than can be obtained from the Coulomb interaction alone and have been taken to imply the existence of a charge-symmetry breaking term in the nucleon-nucleon interaction. It has been shown that when different proton and neutron wave functions are used to evaluate matrix elements of a charge-independent nucleon-nucleon interaction, large off-diagonal matrix elements ( $\sim 150$  keV) can be generated in both  $^{12}\text{C}$  and  $^8\text{Be}$ .

Moreover, the magnitude of these matrix elements is extremely sensitive to the radial form of the wave functions.<sup>2</sup> Consequently until this wave function effect, which is of the same magnitude as the experimental off-diagonal matrix element, can be reliably calculated, it cannot be said that these 1p-shell experiments provide any evidence for a charge-symmetry breaking component in the specifically nucleon-nucleon interaction.

---

<sup>1</sup> J. M. Lind, G. T. Garvey, and R. E. Tribble, Nucl. Phys. A276, 25 (1977).

<sup>2</sup> R. D. Lawson, Phys. Lett. 78B, 371 (1978).

g. Isospin Mixing in  $^{19}\text{F}$

R. D. Lawson

Recent experimental beta-decay data<sup>1</sup> indicate that there is a small  $T=\frac{3}{2}$  component in the predominantly  $T=\frac{1}{2}$  yrast  $I=\frac{5}{2}^+$  state in  $^{19}\text{F}$ . Shell-model calculations have been undertaken to study whether this observation provides evidence for a charge-dependent term in the

---

<sup>1</sup> D. M. Perlman, L. Grodzins, and C. E. Thorn, Phys. Rev. C 18, 2333 (1978).

nucleon-nucleon interaction. When account is taken of the fact that the excitation energy of the  $s_{1/2}$  and  $d_{3/2}$  single-particle states is different in  $^{17}\text{F}$  and  $^{17}\text{O}$ , the magnitude of the observed mixing can be reproduced. Moreover, since the difference in the single-particle excitation energies can be explained by the Coulomb interaction alone,<sup>2</sup> these beta-decay data provide no evidence for an isospin-violating term in the nuclear interaction.

---

<sup>2</sup>J. A. Nolen, Jr., and J. P. Schiffer, Annu. Rev. Nucl. Sci. 19, 471 (1969).

#### h. The $f_{7/2}$ Nuclei

A. Müller-Arnke\* and R. D. Lawson

In Darmstadt during the summer of 1975 we wrote a program that was designed to study the  $f_{7/2}$  nuclei including the effect of one-particle excitation to the  $1f_{5/2}$ ,  $2p_{3/2}$ , and  $2p_{1/2}$  levels. During the summer of 1978 this program was used to explore the effect of one-particle excitation on the  $N=28$  nuclei with  $20 < Z < 28$ . The main excitation in this case was shown to involve neutrons; furthermore, the effect of such excitations on the properties of the  $f_{7/2}$ -proton nuclei can be taken into account by making a state-independent (proton-number independent) renormalization of the one and two-body proton operators. In addition, we were able to show that when mixing is permitted between the  $(\pi f_{7/2})^n I (\nu f_{7/2})^8$  states and all other configurations involving single-particle excitation, the only state, other than the predominantly  $(\pi f_{7/2})^n I (\nu f_{7/2})^8$  ones, that has appreciable  $(\pi f_{7/2})$  strength, is the most highly-excited state for given spin. Thus single nucleon transfer populates only the original  $(\pi f_{7/2})^n I (\nu f_{7/2})^8$  levels and a state at very high excitation energy. These results yield some understanding as to why the proton  $f_{7/2}$  nuclei look as pure in configuration as they do.

\*

Technische Hochschule, Darmstadt, Germany.

### C. NUCLEAR MATTER

The microscopic theory of nuclei as systems of interacting nucleons rests on our ability to determine adequate nucleon-nucleon potentials. Homogeneous nuclear matter is an important testing ground because the theory is mathematically well defined and its consequences are sensitive to features of the potentials that do not affect the observable properties of two-nucleon systems. For any density, the energy per particle can be calculated exactly from the amplitude for the excitation of two particles out of the Fermi sea, which must be obtained from the many body Schrödinger equation (coupled cluster equations) in a reliable approximation. The Brueckner-Bethe scheme ("hole-line expansion") is designed to produce such an approximation. Its validity depends on features of the potential and must be established by numerical tests. There has been a long-standing suspicion that the properties of a realistic tensor force, in particular its long-range features, require a modification of the Brueckner-Bethe scheme. Early attempts to calculate the binding energy of nuclear matter with the Reid potential by variational methods seemed to indicate the possibility of large errors in the Brueckner-Bethe scheme.

Numerical studies of model Bose gases have provided valuable insight. Specifically for Bose gases variational calculations are superior to approximate solutions of the coupled cluster equations. Our studies elucidate the reasons why this is so and why approximations different from the Brueckner-Bethe scheme are required. There is no indication that these reasons apply to Fermi gases.

It appears that reliable variational upper bounds for the energy of nuclear matter are available for sufficiently simple potentials, i.e., local potentials with possible spin-isospin dependence and tensor forces. Our recent efforts concentrated on potentials that are thus simplified for the benefit of variational calculations. For these potentials internal checks indicate that the Brueckner-Bethe scheme is satisfactory. There are no discrepancies with variational results.

#### a. Solution of the Three-Body Equations in Nuclear Matter

B. D. Day and F. Coester

The implementation of any method of solving the coupled-cluster equations such as the Brueckner-Bethe approximation, requires an accurate solution of the Bethe-Faddeev three-body equations. The three-body amplitudes are needed to make tests of the validity of the

scheme and, if the scheme proves valid, to calculate the resulting approximation to the energy.

In earlier work we have found that such calculations are feasible in momentum space. Tensor forces, spin-orbit forces, and all the other complexities of the nuclear force are properly treated in the three-body calculations. An angle-average approximation to the Pauli operator is used, and this causes uncertainties of 0.5—1.0 MeV at the empirical saturation density  $\rho_0$  and 2—3 MeV at  $2\rho_0$ . This accuracy is good enough to draw interesting conclusions and can be improved if necessary.

Two improvements in the three-body program have been implemented. First, we now use a perturbation method to achieve higher accuracy without any increase in the size of the matrices used. Second, we can now treat successive three-body correlations among different triplets, e.g., 1, 2, 3, then 1, 2, 4, then 2, 4, 5, etc. It has been suggested that this kind of chain effect might build up important long-range correlations.

As a first application, calculations have been made for the central potential  $v_2$  (defined as the central component of the Reid  $^3S-^3D$  potential allowed to act in all partial waves). In order to provide a stringent test, the calculations have been done at densities from the empirical saturation density  $\rho_0$  up to more than twice this value. At the highest density, the results are as follows.

(1) The two, three, and four-hole-line contributions to the energy are -30, -10, and +2 MeV, showing good convergence to this order.

(2) The sensitivity of the calculated energy to a shift  $\Delta$  in the single-particle energies of states above the Fermi sea has been studied. If  $D_2$  and  $D_3$  are the two and three-hole-line terms, respectively, then a necessary condition for the validity of the hole-line expansion is  $\partial D_2 / \partial \Delta \gg |\partial(D_2 + D_3) / \partial \Delta|$ . Our calculations give  $\partial D_2 / \partial \Delta = 0.27$  and  $\partial(D_2 + D_3) / \partial \Delta \approx 0.01$ , so that the desired condition is well satisfied.

(3) The chain effect is found not to build up appreciable long-range correlations. Hence there is no indication that this effect requires the hole-line expansion to be modified.

(4) For central potentials such as  $v_2$ , highly reliable upper bounds have been obtained by Kalos using Monte-Carlo integration. Our Brueckner-Bethe result lies 3 MeV below this upper bound.

Thus the results of these four tests are consistent with the validity of the Brueckner-Bethe hole-line expansion.

Similar calculations have been done for the potential  $v_6$  (Reid), which is derived from the Reid potential. It is spin and isospin dependent and has a strong tensor force but no spin-orbit coupling or  $\ell$  dependence. The results of tests 1—3 are similar to those for  $v_2$  and support the validity of the hole-line expansion for potentials with strong tensor forces. Test 4 involves Monte-Carlo variational calculations, which are not yet available for tensor forces. However, at densities from  $\rho_0$  to  $2\rho_0$ , the Brueckner-Bethe result lies 1—3 MeV below the variational result of Pandharipande.

In summary we draw two main conclusions from these calculations. First, the results of several different tests support the validity of the Brueckner-Bethe hole-line expansion, both for central and tensor forces. Second, there is no longer any significant discrepancy between Brueckner-Bethe and variational results.

These results have been reported at the Conference on "Recent Progress in Many-Body Theories," Trieste, October 1978. The conference proceedings will be published in a special issue of Nuclear Physics.

### b. Model Bose Gases

#### F. Coester

The formal properties of a homogeneous Bose gas of density  $\rho$  are like those of a Fermi gas of density  $\rho$  except that the "Fermi sphere" has zero radius. The equations for the coupled cluster amplitudes are

similar and simpler. The amplitude for the excitation of two particles is a function of the distance only. To calculate the energy we require this function only inside the range of the potential but there a high accuracy is required. On the other hand, this part of the function is quite sensitive to the behavior at large distances because of the coupled cluster equations. The difficulties in obtaining the long range behavior with sufficient accuracy have to do with the possibility of very low momentum excitations which are absent in Fermi gases. There are two conclusions. Not surprisingly for Bose gases, coupled-cluster calculations cannot compete with hypernetted-chain calculations. The study of Bose gases does not give any indication that the Brueckner-Bethe scheme for nuclear matter should fail.

#### D. INTERMEDIATE-ENERGY PHYSICS

The framework of our studies of intermediate-energy nuclear physics is relativistic many-body quantum mechanics for systems of nucleons,  $\Delta$ 's, and pions. There are two distinct aspects of this many-body problem, just as there are in the many-body theory of the nucleus as a system of nucleons. In building a many-body theory of systems of nucleons, the two distinct stages of the undertaking are (i) determination of the two-body nucleon-nucleon (N-N) interaction by fitting nucleon-nucleon scattering data and (ii) development of appropriate techniques for the solution of the many-nucleon problem from the phenomenological two-body interaction determined by study of the two-nucleon system.

The same two stages obviously occur in building a many-body theory of nucleons,  $\Delta$ 's, and pions. There is of course a greater number of basic interactions; these are taken to be (a)  $\pi N \rightleftharpoons \Delta$  in the resonant (3,3) channel of the  $\pi$ -N system, (b) direct two-body interactions in other  $\pi N$  channels, and (c) two-body interactions  $NN \rightleftharpoons NN$ ,  $N\Delta \rightleftharpoons N\Delta$ ,  $NN \rightleftharpoons N\Delta$  involving the nucleon and the  $\Delta$ .

These interactions are to be determined by studying pion-nucleon, nucleon-nucleon, and pion-deuteron scattering. In constructing a many-body theory from the elementary interactions, useful approximations depend on expansion in powers of the baryon (but not the pion) velocities and on the assumption that the interaction energies are small relative to the baryon masses. With these approximations the two-body Hamiltonian can be generalized to a many-body Hamiltonian.

Work is proceeding simultaneously on the two distinct stages of the N- $\Delta$ - $\pi$  many-body problem. We have previously fitted the pion-nucleon interactions to pion-nucleon scattering data. The construction of the baryon-baryon interactions is in progress.

Our approximations for the treatment of pion-nucleus reactions are based on the assumption that pion-nucleon scattering and the absorption mechanism  $\pi NN \rightarrow N\Delta \rightarrow NN$  dominate the reactions. At present we are examining nuclear structure information derived from recent elastic and inelastic-scattering data.

a. Phenomenological Determination of the Baryon-Baryon Interactions from N-N and  $\pi$ -d Scattering Data

M. Betz, F. Coester, and T. -S. H. Lee

We need to calculate NN scattering amplitudes both below and above the pion-production threshold. Multiple pion exchanges between N and  $\Delta$  as well as NN interactions in intermediate  $\pi$ NN states are expected to play a significant role. Since three-body intermediate states are involved in the NN scattering, numerical techniques appropriate to the three-body scattering problem must be employed. A computer code which implements these equations for NN scattering and determines the parameters of the baryon-baryon interactions by least-square fit to the phase shifts and inelasticity parameters has been written. Preliminary fits for the  $^1D_2$  NN partial wave have been obtained, neglecting NN interactions in  $\pi$ NN states but including multiple  $\pi$  exchanges between N and  $\Delta$ . These results indicate that the latter effect has little influence on the phase shifts but provides about 20% of the inelasticity in the energy region near 550 MeV.

b. Reaction Theory for Pion Nucleus Interaction

T. -S. H. Lee

Recent experimental data indicate that elastic scattering, quasielastic nucleon knockout and pion absorption make up the bulk of the total cross section. Inelastic scattering to low-lying excited states is important for the study of nuclear structure. For elastic and inelastic scattering we assume that in first approximation the pion interacts with one active nucleon, the other nucleons being passive spectators. Pion absorption involves two active nucleons which absorb the pion by the mechanism  $\pi$ NN  $\rightarrow$  N $\Delta$   $\rightarrow$  NN. With this mechanism, we can fit the  $\pi^+ + d \rightarrow pp$  data. The model accounts reasonably well for inclusive  $\pi^+ + {}^4He \rightarrow p + \dots$  cross sections for high-energy protons in the kinematical region where two-nucleon emission is dominant.

The absorption mechanism also contributes to the optical potentials  $U$  for elastic and inelastic scattering, i.e.,  $U = U^{(s)} + U^{(a)}$ , where  $U^{(s)}$  is the optical potential derived in the impulse approximation. We find that the absorption term  $U^{(a)}$  reduces the pion wave function inside the nucleus and affects the scattering cross section at large angles.

### c. Momentum-Space DWIA Studies of Pion-Nucleus Inelastic Scattering

T. -S. H. Lee, D. Kurath, R. Lawson, and S. Chakravarti

We have calculated pion-nucleus inelastic scattering in the distorted-wave impulse approximation (DWIA) for a wide range of nuclei. Our purpose was to check the extent to which this approximation can account for the data and to explore the nuclear-structure information that can be obtained from recent experiments. The distorted waves  $\chi_{\vec{k}'}^{(\pm)}$ , which are needed for the calculation of the inelastic scattering amplitude

$$\left\langle \chi_{\vec{k}'}^{(-)} | U_{fi}^{(s)}(E) | \chi_{\vec{k}}^{(+)} \right\rangle,$$

are calculated in momentum space from the optical potential  $U$  by solving a relativistic scattering equation. The optical potential  $U$  was adjusted to fit elastic scattering by changing the radius in  $U^{(s)}$ .

Calculations were carried out for 1p shell nuclei and for  $^{18}\text{O}$ ,  $^{24}\text{Mg}$ ,  $^{28}\text{Si}$ ,  $^{56}\text{Ni}$ , and  $^{208}\text{Pb}$ . In the study of 1p-shell nuclei the DWIA calculations are consistent with the new experimental data on inelastic excitation of  $^{12}\text{C}^{(2^+)}$  and  $^{9}\text{Be}^{(\frac{5}{2}^-, \frac{7}{2}^-)}$  provided the transition density resulting from the Cohen and Kurath calculation is enhanced by the same factor needed to fit  $B(E2)$  values in these cases. However, there is disagreement with the data on single-charge exchange  $^{13}\text{C}^{(\pi^+, \pi^0)} \text{N}^{(\text{g.s.})}$  and the ratio of cross sections for exciting the  $1^+ \text{T}=0$  and  $\text{T}=1$  states in  $^{12}\text{C}$ . In the study of  $^{18}\text{O}$ , it is shown explicitly that the isospin-dependent  $\pi\text{N}$  force plays an important role in the structure of the first  $2^+$  state in  $^{18}\text{O}$ . For  $^{18}\text{O}$ , both the ratio  $\sigma(\pi^-)/\sigma(\pi^+)$  and the absolute magnitudes of the cross sections can be reasonably described by the models of Lawson,

Serduke, and Fortune and the model of Zuker, Buck, and McGrory. The studies of the collective excitation of  $^{24}\text{Mg}$ ,  $^{28}\text{Si}$ ,  $^{58}\text{Ni}$ , and  $^{208}\text{Pb}$  indicate that the collective transition form factors which fit pion inelastic scattering are consistent with those resulting from inelastic electron scattering.

d. Momentum-Space Coupled-Channel Calculations of Pion-Nucleus Inelastic Scattering

S. Chakravarti and T.-S. H. Lee

Our studies of pion inelastic scattering from the 1p-shell nuclei show that the DWIA approximation fails when the coupling between neighboring excited states is strong. In the hope of exploring the nuclear structure in those regions, we are therefore solving the coupled-channel equations. The computer program for solving the coupled-channel equation in momentum space has been developed.

## E. DENSE NUCLEAR MATTER AND CLASSICAL CALCULATIONS OF THE HIGH-ENERGY COLLISIONS OF HEAVY IONS

Heavy-ion collisions of energies greater than about 100 MeV/nucleon are the only apparent possibility for obtaining transient hot dense nuclear matter. The study of such collisions may give information about the equation of state of nuclear matter at high densities and temperatures and about possible new states of nuclear matter. Because of the relatively large mean free path and associated large nonequilibrium phenomena, an adequate description of such collisions must in general be a microscopic one. We initiated and are continuing (with C. N. Panos and A. D. MacKellar) classical equations-of-motion (CEOM) calculations of high-energy heavy-ion (HF-HI) collisions for laboratory energies from about 100 MeV to about 1 GeV/nucleon. The CEOM method is a completely microscopic but classical approach whose essence is the simultaneous calculation of all nucleon trajectories using a two-body potential between all pairs of nucleons. The unique feature of the CEOM approach is that it is the only microscopic approach which includes finite-range interaction effects, in particular potential-energy effects, for realistic potentials and hence does not assume that nuclear matter is a dilute fluid as do the Boltzmann equation/cascade calculations.

### a. Nonrelativistic CEOM Calculations with Static and Momentum-Dependent Potentials

A. R. Bodmer, A. D. MacKellar, and C. N. Panos

We have continued our nonrelativistic calculations for equal mass projectile and target nuclei, with  $A_{\text{proj.}} = A_{\text{tgt.}} = 20$  and 40, and for laboratory energies of  $E_L = 117, 400$ , and 800 MeV/nucleon. The calculations have been made with a static nucleon-nucleon potential, with a repulsive core and attractive tail, which is fitted to NN scattering data by use of classical two-body trajectory calculations, and also for a phase-equivalent "transformed" potential. This latter is momentum dependent and gives the same two-body scattering as the static potential from which it is obtained by a canonical transformation due to Monahan, Shakin, and Thaler (unpublished). (It is also adjusted to give the same binding energy as the static potential.) Phase-equivalent potentials do not, however, give the same A-body scattering for dense conditions in which 3 or more

nucleons interact simultaneously; in effect they will be associated with different equations of state. Microscopic studies involving phase-equivalent potentials are only possible with the CEOM approach, and indicate the importance of potential-energy and finite-range interaction effects.

Extensive results have been obtained for the momentum distribution, or equivalently the inclusive nucleon cross section, as a function of time. These results illustrate the evolution of the dynamics of a collision, with the results at a late stage of the collision to be identified with the observable cross sections. We obtain fair agreement with the experimental data for  $A_{\text{proj.}} = A_{\text{tgt.}} = 20$  at  $E_L = 800 \text{ MeV/nucleon}$ , consistent with the expected limitations of the CEOM calculations.

To illustrate the evolution of collisions we summarize our results for central collisions. One can distinguish three stages. (1) An initial transparent stage when single NN scattering (quasifree scattering) is dominant, rather few high-momentum components have developed and the distribution is not too different from the initial one. (2) A relatively brief stage, of duration  $2-3 \text{ fm/c}$ , when the densities are quite high and during which multiple scattering becomes dominant with the development of appreciable high momentum components fairly close to their final distribution. The momentum distribution rapidly becomes approximately isotropic and much more equilibrated, especially at lower energies at which the mean free path is smaller. A peak which is at approximately the same energy for all angles develops. (3) A final expansion stage which begins when the densities are still quite large. As the expansion proceeds the common peak moves towards smaller energies in step with the increase of potential energy while simultaneously there is some steepening of the distribution above the peak. These developments seem to be associated with an approximate equilibration of the potential energy. There are quite large differences between the distributions for the phase-equivalent static and transformed potentials, closely correlated with corresponding differences in the potential energy. Consistent with a small

final potential energy for both cases (corresponding to well-separated nucleons), the final asymptotic ("observable") distributions are however effectively the same. The distributions also become more thermalized during the expansion, especially for the lower energies ( $E_L = 400$  and  $117$  MeV/nucleon) when the final distributions are almost completely thermalized without any final peaking. A striking feature of the collisions of heavier nuclei ( $A_{\text{proj.}} = A_{\text{tgt.}} = 40$ ) is the development of transverse peaking during the expansion, with the cross section larger perpendicular to the beam. This transverse peaking is reminiscent of some hydrodynamic results and must be considered as a collective effect.

Another property, of importance to the interpretation of experiments, is the dependence of the nucleon multiplicity distribution on impact parameter, since this will help in understanding the multiplicity as a signature of impact parameter. A study made for  $A_{\text{proj.}} = A_{\text{tgt.}} = 20$  and  $E_L = 800$  MeV/nucleon shows that the multiplicity is quite large and depends quite strongly on impact parameter if this is less than about a nuclear radius.

#### b. Programs to Analyze the Physical Content of the CEOM Calculations

A. R. Bodmer, A. D. MacKellar, and C. N. Panos

On the technical level, our analysis programs have been extended and developed, in particular for the calculation of two-nucleon correlations. A study of these has made it clear that to obtain useful information, much better statistics are required. This necessitates the use of much larger ensembles for our trajectory calculations with correspondingly large increases in computing time for the trajectory calculations.

Preliminary studies were made to improve the distributions representing the initial nuclei and at the same time to obtain more satisfactory two-body potentials.

c. Relativistic CEOM Calculations

A. R. Bodmer, A. D. MacKellar, and C. N. Panos

Trajectory and analysis programs have been further developed for relativistic calculations to  $O(v^2/c^2)$ . Such calculations seem to be the only ones which can give a consistent relativistic (Hamiltonian) particle description [to  $O(v^2/c^2)$ ], i.e., one which satisfies all the requirements of Lorentz covariance for both the interaction and for the trajectories. The most important new physics in such relativistic calculations is most probably due to the characteristic momentum dependence of the relativistic (retarded) terms in the potential rather than to the relativistic kinetic energy and the relativistic kinematics. In fact our results show that the relativistic kinematic effects are small compared to retardation effects. So far relativistic calculations have only been made for single distributions but not for complete ensembles of distributions of initial nuclei.

d. Macroscopic and Microscopic Descriptions of High-Energy Heavy-Ion Collisions

A. R. Bodmer

A review article on this subject is being written. It is an extension of an earlier review presented at the Topical Conference on Heavy-Ion Collisions (Fall Creek Falls State Park, Tennessee, June 1977). The emphasis is on the assumptions, limitations, and relations of different theoretical descriptions of He-HI collisions, especially the "a priori" descriptions, namely, hydrodynamics, Boltzmann equation/cascade calculations, and the CEOM calculations.

e. Dense Nuclear Matter

A. R. Bodmer and J. Boguta

The present investigations arose from our earlier interests in "collapsed" (superdense) nuclei. These were subsequently continued in a study of nuclear matter and the nuclear surface using a phenomenological

relativistic mean-field approach involving (linear) vector-meson and rather general nonlinear scalar-meson interactions. These studies have been extended to permit unequal numbers of neutrons and protons, leading in particular to studies of neutron matter and an investigation of implications for the structure of neutron stars. The equation of state has been calculated for nonzero temperatures. The general structure of mean-field theories with nonlinear interactions and their implications for the existence of abnormal states have been examined. Finite nuclei are being studied with a Thomas-Fermi approach with both the nonlinear model and the linear Walecka model.

## F. RADIATIVE TRANSITIONS AND NUCLEAR RESONANCE REACTIONS

a. A Theoretical Description of Quantum Beats of Recoil-Free Gamma Radiation

J. E. Monahan and G. J. Perlow

A theory has been developed for the phenomenon of quantum beats observed at Argonne<sup>1</sup> in a study of the Mössbauer effect using a frequency-modulated source. Consider radiation of unperturbed frequency  $\omega_0$  from a vibrating source that is transmitted through an absorber containing a resonance at frequency  $\omega_0'$ . The transmitted intensity  $I(\omega_0 - \omega_0', t)$  is obtained as a function of  $\omega_0 - \omega_0'$  and of the laboratory time  $t$ .

For fixed values of  $\omega_0 - \omega_0'$ , this intensity exhibits interference between different frequency components when considered as a function of  $t$ . See Fig. VII-2. The harmonic content of this beat phenomena is sensitive to the value of  $\omega_0 - \omega_0'$  and can be used for the precise measurements of small energy shifts. A comparison with the method of switching between the steepest points of an absorption "line" (as used in gravitational red-shift measurements) shows that the variances (counting statistics only) are comparable for the two methods.

As shown in Fig. VII-3 for particular values of  $\omega_0 - \omega_0'$  and  $t$ , the transmission sample actually enhances the intensity of the transmitted radiation. This can be attributed to a storage phenomenon in which the intensity at a particular time is due to an accumulation over previous times. It is the temporal equivalent of spatial diffraction.

Perturbation of  $I(\omega_0 - \omega_0', t)$  due to source inhomogeneities (both static and dynamic) have been calculated. These results are being used to optimize the present method for measurements of small energy shifts.

A paper describing these results is being prepared for publication.

<sup>1</sup> G. J. Perlow, Phys. Rev. Lett. 40, 896 (1978).

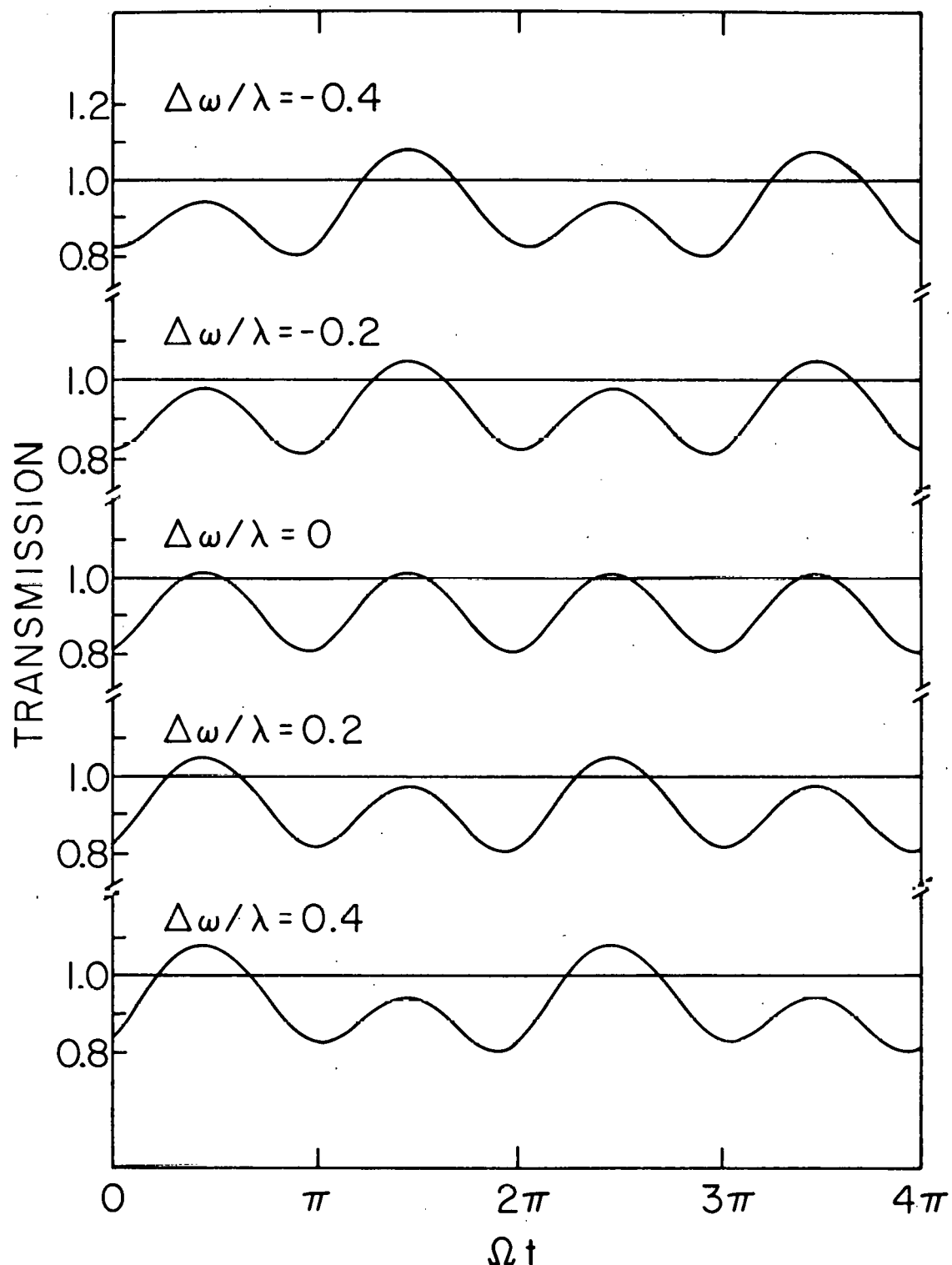


Fig. VII-2. Calculated quantum beats. The transmitted intensity  $I(t, \Delta\omega)$  plotted, at various fixed values of  $\Delta\omega = \omega_0 - \omega_0'$ , as a function of laboratory time. Here  $\lambda^{-1}$  is the mean lifetime of the decaying state of the source and  $\Omega$  is the frequency of vibrations of the source. Note the growth of the odd harmonics as  $|\Delta\omega|$  increases.

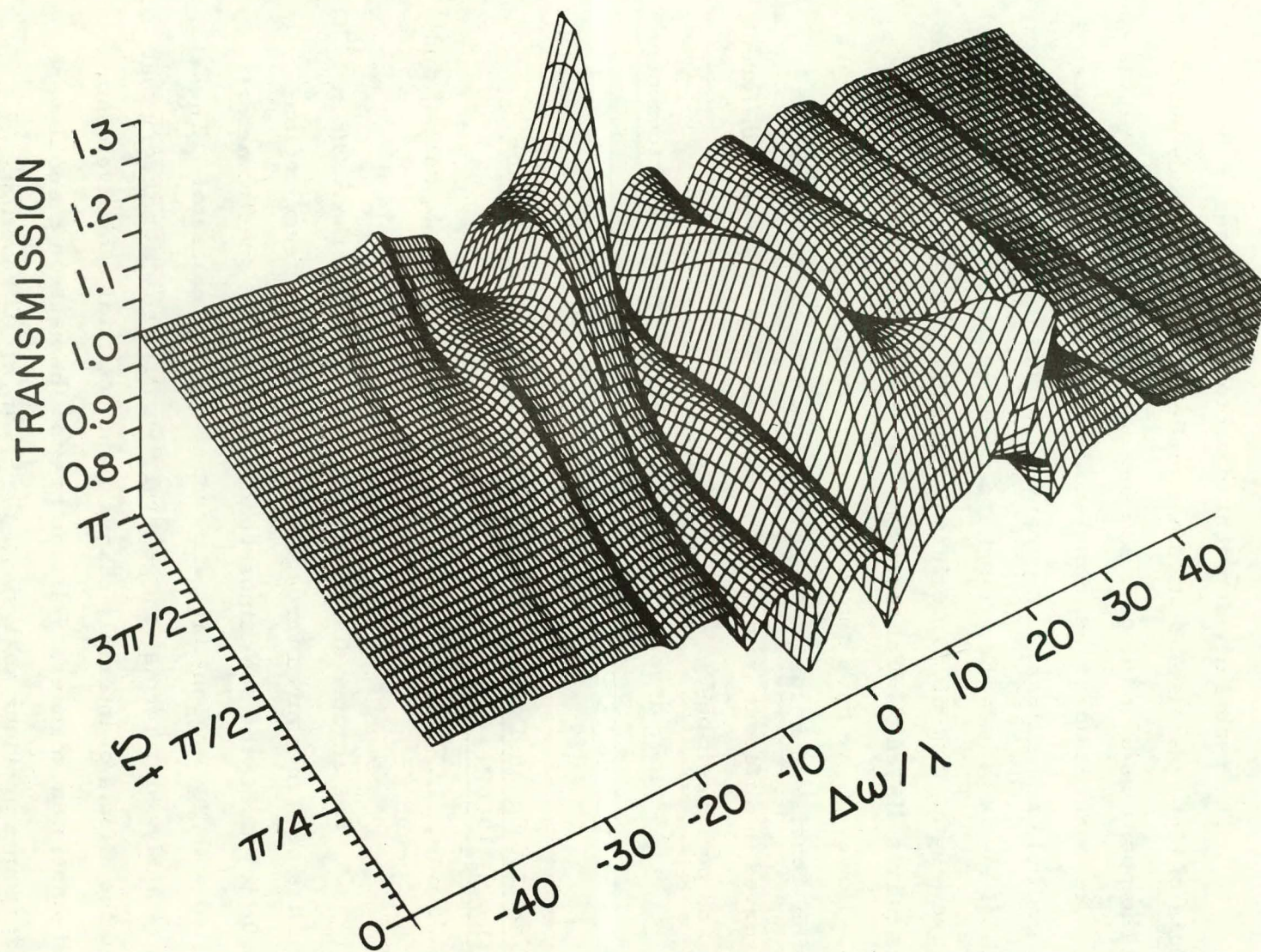


Fig. VII-3. The surface  $I(t, \Delta\omega)$ . The region from  $\Omega t = \pi$  to  $\Omega t = 2\pi$  (not shown) may be obtained by reflection in the plane perpendicular to the  $\Omega t$  axis at  $\Omega t = \pi$ .

b. Resonance Peak Shapes in Molecular Photoionization Mass Spectroscopy

J. H. D. Eland, J. Berkowitz, and J. E. Monahan

The recent development of photoionization mass spectrometers of high optical resolution has made possible the study not only of the positions of autoionizing resonances but also of their widths and shapes. Resonances observed in molecular photoionization are almost always multiple transitions, i. e., many rotational levels and often several vibrational levels of both the ground and excited states are involved at each wave length. Complex interference phenomena are thus introduced and this makes difficult any theoretical description of the resonance shapes. However, we have shown that a relatively simple parameterization yields consistent resonant energies and widths when resonances are observed in different fragment-ion channels with apparently different shapes and peak positions.

A paper describing the application of this result to recent Argonne data is being prepared for publication.

c. Effects of Channel and Potential Radiative Transitions in the  $^{17}\text{O}(\gamma, n_0)^{16}\text{O}$  Reaction

R. J. Holt, H. E. Jackson, R. M. Laszewski, J. E. Monahan, and J. R. Specht

The angular distribution of neutrons from the  $^{17}\text{O}(\gamma, n_0)^{16}\text{O}$  reaction has been measured throughout the excitation energy region 4.3—7.0 MeV using the sub-nanosecond time-of-flight spectrometer associated with the Argonne high-current electron accelerator. These data were analyzed in terms of a general R-matrix reaction theory that included the effects of internal, channel, and potential radiative capture in a self-consistent manner. Parameters for the neutron channel were obtained from a previous analysis of the  $^{16}\text{O}(n, n)^{16}\text{O}$  reaction. The effects of channel capture were observed directly in a photoneutron reaction for the first time. Anomalous minima in the energy spectra at 5.38 MeV were shown to be the result of a unique feature of channel capture.

The radiation width for the  $d_{5/2} \rightarrow d_{3/2}$  spin-flip transition at 5.08 MeV was found to be approximately 1/3 of the value expected for a pure single-particle transition. This would seem to indicate that nuclear structure effects or meson exchange corrections have an important effect on magnetic dipole transitions.

A description of these results has been published [Phys. Rev. C 18, 1962 (1978)].

#### d. Nuclear Mass Relations

J. E. Monahan and F. J. D. Serduke

The derivation of a set of nuclear mass relations, each member of which gives a prediction for the unknown mass of a particular nuclide, has been described previously.<sup>1</sup> An important feature of this set is that it allows an estimate not only of the mean value but also of the standard error of a predicted mass. Because the individual predictions are not statistically independent, the usual prescriptions for error estimates do not apply. We have examined this problem and we find that the corrections are less serious than was anticipated. Nevertheless, the numerical calculations necessary to obtain estimates for a single nucleus are inconvenient and consideration is being given to the generators of a table listing the mean values and associated standard errors for an appropriate range of "unknown" masses.

---

<sup>1</sup> J. E. Monahan and F. J. D. Serduke, Phys. Rev. C 15, 1080 (1977); Phys. Rev. C 17, 1196 (1978).

#### e. Absolute Cross Sections for Three-Body Breakup Reactions

$^6\text{Li}(d, n ^3\text{He}) ^4\text{He}$  and  $^6\text{Li}(d, p ^3\text{H}) ^4\text{He}$

R. E. Holland, A. J. Elwyn, C. N. Davids, F. J. Lynch, L. Meyer-Schützmeister, J. E. Monahan, F. P. Mooring, and W. Ray, Jr.

Absolute cross sections for the reactions  $^6\text{Li}(d, n ^3\text{He}) ^4\text{He}$  and  $^6\text{Li}(d, p ^3\text{H}) ^4\text{He}$  have been measured at the Argonne 4-MV Dynamitron

accelerator<sup>1</sup> for deuteron energies between 100 and 800 keV. Spectra were obtained for each of the particles emitted in these reactions. In an attempt to understand the mechanism of these three-body reactions, a comparison of the measured distributions  $d\sigma/dE_x d\Omega_x$  (where  $x$  is the observed particle) with predictions of simple models of final-state interactions has been made. For example, the reaction leading to a neutron in the exit channel may proceed partly through the ground state of  $^5\text{He}$  which then decays into a neutron and  $^4\text{He}$ . At the relatively low energies involved in these reactions, we find that the Coulomb interaction tends to dominate any resonant final-state interaction. For the reaction leading to  $n + ^3\text{He} + ^4\text{He}$ , the observed neutron distribution is reproduced for all but the lowest values of  $E_n$  when the Coulomb interaction between  $^3\text{He}$  and  $^4\text{He}$  is taken into account. With three charged particles in the exit channel the situation is less clear; however, there are preliminary indications that, if the Coulomb interaction between all pairs are considered, reasonable agreement with the observed distributions over most of the relevant energy interval is obtained.

A description of these results is scheduled for publication in a forthcoming issue of *Phys. Rev. C*.

#### f. Low-Energy $d + ^6\text{Li}$ Reactions

A. J. Elwyn and J. E. Monahan

Differential and total cross sections for the reactions  $^6\text{Li}(d, a)a$ ,  $^6\text{Li}(d, p)^7\text{Li}$ , and  $^6\text{Li}(d, n)^7\text{Be}$  (to the ground and first-excited states of  $^7\text{Li}$  and  $^7\text{Be}$ ) have been measured at the Argonne 4-MV Dynamitron accelerator<sup>1</sup> for deuteron energies between 0.1 and 1.0 MeV. The energy dependence of the integrated yields in the various outgoing channels can be accounted for solely in terms of the R-matrix s-wave surface functions

---

<sup>1</sup>A. J. Elwyn, R. E. Holland, C. N. Davids, L. Meyer-Schützmeister, J. E. Monahan, F. P. Mooring, and W. Ray, Jr., *Phys. Rev. C* 16, 1744 (1977).

in the incident channel at least for deuteron energies up to  $\sim 500$  keV. This suggests that the structure observed in these reactions at energies below 1 MeV, which has been interpreted in terms of resonances in  ${}^8\text{Be}$ , may simply be a manifestation of the energy dependence of the surface functions. Calculations of the differential cross sections, based on the assumption that there are no resonances in  ${}^8\text{Be}$  in the energy interval of interest, give reasonably good fits to the measured values and thus tend to confirm this conjecture.

A description of these results is scheduled for publication in a forthcoming issue of Phys. Rev. C.

THIS PAGE  
WAS INTENTIONALLY  
LEFT BLANK

# EXPERIMENTAL ATOMIC AND MOLECULAR PHYSICS RESEARCH

## INTRODUCTION

The atomic and molecular physics program in the Physics Division consists of six basic research projects as follows:

- A. Dissociation and Other Interactions of Energetic Molecular Ions in Solid and Gaseous Targets (D. S. Gemmell)
- B. Beam-Foil Research and Collision Dynamics of Heavy Ions (H. G. Berry)
- C. Photoionization-Photoelectron Research (J. Berkowitz, J. H. D. Eland)
- D. Spectroscopy of Free Atoms (W. J. Childs, L. S. Goodman, S. A. Lee)
- E. Mössbauer Effect Research (G. J. Perlow, S. L. Ruby)
- F. Monochromatic x-Ray Beam Project (S. L. Ruby)

A seventh basic research project to study the interactions of energetic atoms and ions with solid surfaces is carried out in conjunction with a larger applied physics research effort. That work is reported in Sec. IX.

THIS PAGE  
WAS INTENTIONALLY  
LEFT BLANK

## VIII. EXPERIMENTAL ATOMIC AND MOLECULAR PHYSICS

## A. DISSOCIATION AND OTHER INTERACTIONS OF ENERGETIC MOLECULAR IONS IN SOLID AND GASEOUS TARGETS

The Argonne 4-MV Dynamitron accelerator is used to study the dissociation and other interactions of fast (0.3-4.0-MeV) molecular ions incident upon thin ( $\sim 100 \text{ \AA}$ ) foils and gaseous targets. When such a molecular ion enters a solid, its binding electrons are stripped off within a few atomic layers of the solid's surface. Its constituent atomic ions are then driven apart by their mutual Coulomb repulsion. While the ions are moving through the solid, their "Coulomb explosion" is modified by the polarization oscillations induced by the passage of the fragment ions through the solid. A few femtoseconds later, at the rear surface of the foil target, the ion fragments may capture one or more electrons, further modifying their Coulomb explosion. By examining the angular distribution and energy spectra of these ion fragments in high resolution ( $\sim 0.005^\circ$  and  $\sim 300 \text{ eV}$ ) one can construct a rather detailed picture of the interaction of the ions with the solid and, also, extract information on the initial state of the ion beam and on the importance of various final-state interactions near the rear surface of the target. Studies of molecular-ion fragmentation in gas targets yield similar, though complementary information.

The work has two major objectives: (a) a general study of the interactions of fast charged particles with matter, but with the emphasis on those aspects that take advantage of the unique features inherent in employing molecular-ion beams (e.g., the feature that each molecular ion incident upon a solid target forms a tight cluster of atomic ions that remain correlated in space and time as they progress through the target) and (b) a study of the structures of the molecular ions that constitute the incident beams. Precise measurements on the energies and angles of the breakup fragments produced when fast molecular ions dissociate in foils and gases offer exciting possibilities as a new method for determining molecular-ion structures.

These two aspects of the work are mutually interdependent. In order to derive structure information about a given molecular ion, one needs to know details about the way the dissociation fragments collectively interact with the target in which the dissociation occurs. Similarly, a knowledge of the structure of the incident molecular ions is important in understanding the physics of their interactions with the target.

Our initial work involved detailed studies of the collision-induced dissociation of such simple diatomic molecular ions such as  $H_2^+$ ,  $HeH^+$ , and  $He_2^+$  in both solid and gaseous targets, with particular emphasis on the polarization oscillations induced by these ions as they move through solids. More recently, we have focused on the phenomenon of the transmission of molecular ions through thin foils and its relation to the much more probable dissociation of such ions. Another major project during the past year has been the design and construction of an apparatus to extend our work to the study of coincidences between fragments from individual molecular-ion projectiles.

The main effort in the past year has been invested into (i) the first detailed studies on the dissociation of fast molecular ions in gases and (ii) the design and construction of an apparatus that will enable extension of our work to the study of coincidences between fragments from individual molecular-ion projectiles.

#### a. Dissociation of Fast Molecular Ions in Gases

D. S. Gemmell, P. J. Cooney, E. P. Kanter, K. -O. Groeneveld, W. J. Pietsch, and Z. Vager

Joint distributions in energy and angle have been measured for fragments arising from the dissociation of 1.2-MeV  $H_2^+$  and 3.0-MeV  $HeH^+$  beams in  $H_2$ , He,  $N_2$ , Ar,  $CO_2$ , Xe, and  $SF_6$  at pressures in the range 1—500 mTorr. These studies employed a specially developed differentially pumped gas cell, 10 cm long with a 2-mm diameter entrance aperture and a 2  $\times$  6-mm exit slit. The measured distributions are ring-like and in addition are dominated by large central peaks. The intensity around the rings is uniform, as is to be expected in the absence of wake effects. These distributions are in marked contrast with those previously measured for foil-induced dissociation. We have used the foil data to derive the distributions of internuclear separations for projectiles in the incident beams. With these distributions we have then been able to analyze the gas data and have established that excited electronic states of the projectiles play a significant role in the dissociation. For  $H_2^+$ , most of the dissociations proceed via the  $2p_{\pi_u^+}$  (10%) and the Coulomb (90%) states. For  $HeH^+$  many excited electronic states are involved. The measured

distributions do not depend noticeably on the species of target gas. The results obtained on the central peaks in the measured distributions have led us to an explanation for the phenomenon of molecular-ion transmission through solids. Central peaks arise from dissociative collisions in which the projectile's initial internuclear separation is large and in which only one of the emerging fragments is charged. We believe transmission occurs when a similar projectile dissociates in a foil and then at the exit captures one or more binding electrons to reform a molecular ion. A lengthy paper describing much of our recent molecular-ion work has been completed and submitted for publication.

#### b. Modifications to the Apparatus

D. S. Gemmell, P. J. Cooney, E. P. Kanter, and B. J. Zabransky

Following our measurements on the structures of  $H_3^+$ ,  $CO_2^+$ , and  $N_2O^+$ , it has become apparent that our techniques offer new and unique possibilities for determining the structures of many molecular ions. These structures (unlike those for neutral molecules) are extremely difficult to measure using "normal" techniques. For all but the simplest projectiles (e.g., diatomics and homonuclear polyatomics) our method requires the detection of fragments in coincidence. Discretionary funds became available during the second half of 1978, and we have therefore invested a large effort into design and construction work, modifying our apparatus to permit high-resolution coincidence measurements. The beam-line section downstream from the target chamber has been replaced with a 20-in. diameter magnetically shielded stainless-steel flight tube followed by a 20-in. gate valve and a vacuum manifold that holds two movable detectors. This new experimental arrangement for the measurement of coincidences between fragments from collision-induced dissociation of fast molecular ions is shown in Figs. VIII-1 and VIII-2. Our electrostatic analyzer is coupled to the rear of this chamber. The two movable detectors are remotely controlled via a microcomputer slaved to the on-line PDP 11/45

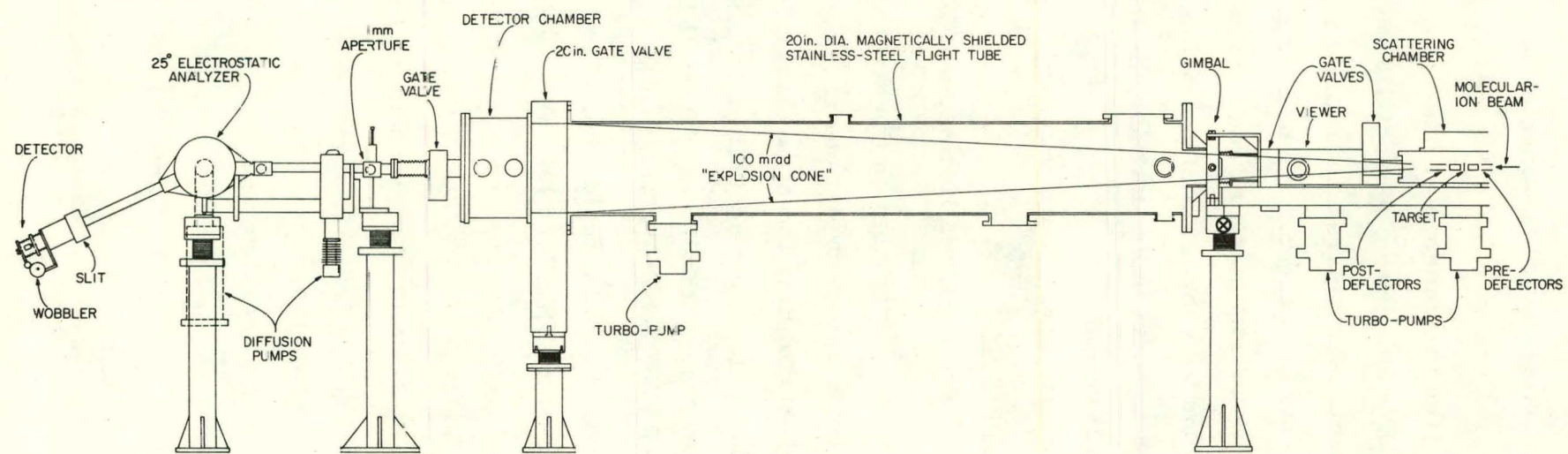


Fig. VIII-1. The newly constructed beam-line section downstream from the target chamber.

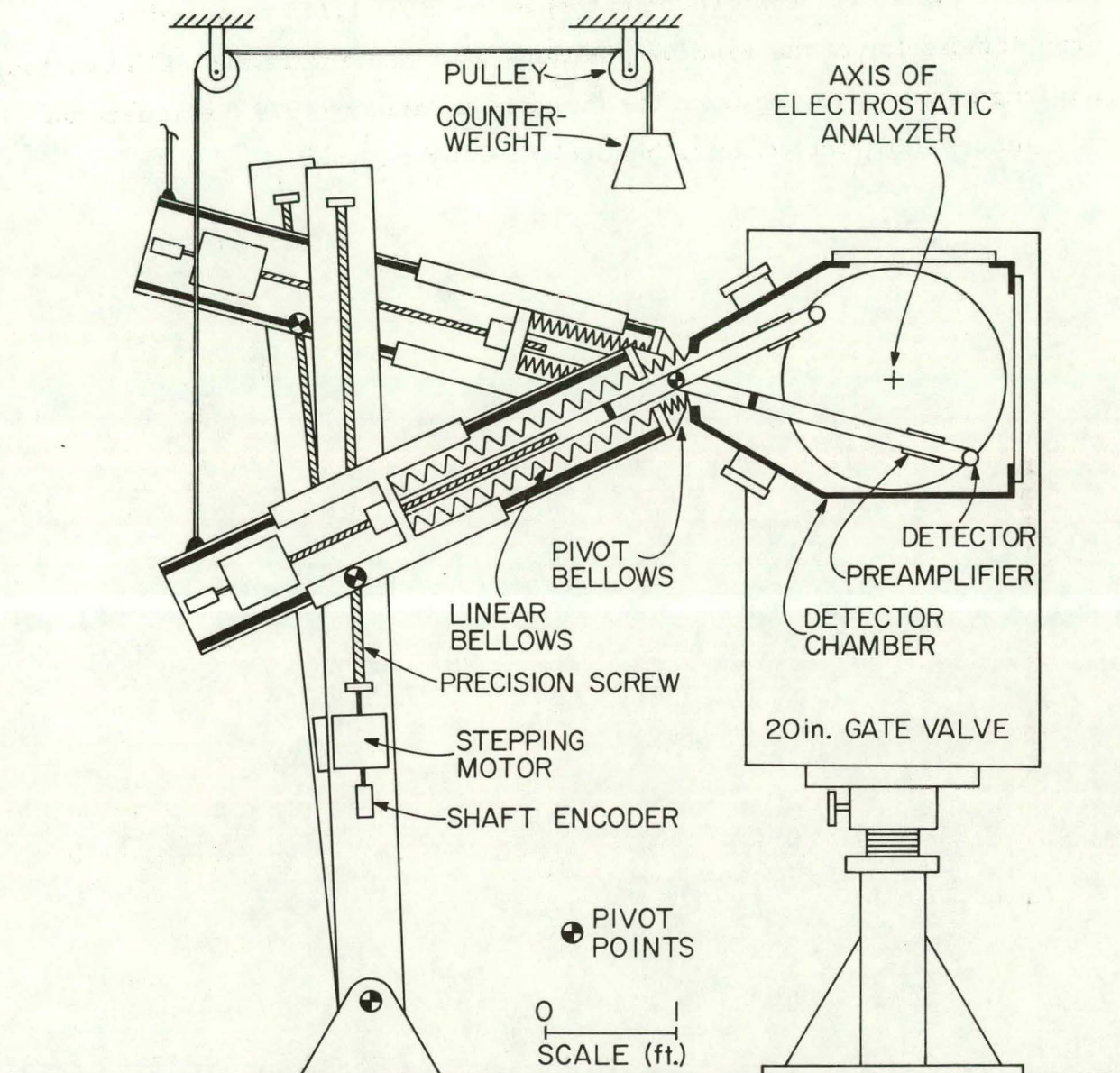


Fig. VIII-2. Cross section showing the computer-controlled movable detector systems.

data-acquisition computer and can be positioned to an accuracy of about 0.001 in. anywhere on a 20-in. diam. circular area that subtends an angle of 100 mrad at the target position. A commercial color TV has been interfaced (also via a microcomputer) to the PDP 11/45 to permit a graphics display of the relative positions of the detectors and of the various ion fragments emerging from the target. In January 1979 the apparatus was successfully tested using beams of 3-MeV  $H_2^+$  and  $H_3^+$ .

## B. BEAM-FOIL RESEARCH AND COLLISION DYNAMICS OF HEAVY IONS

Our present fast ion beam atomic physics program consists of four major parts, two of which are investigations in atomic structure, and two of which involve collision physics.

(1) Atomic Structure in Highly Stripped Ions of Two and Three Electrons. We are pursuing various tests of basic atomic calculations of relativistic and quantum electrodynamic effects in atoms of only a few electrons. One major technical objective of this program has been to improve the precision of wavelength measurements using the beam-foil technique on fast beams. We have reported accuracies of the order of 15 ppm and believe there is room for further improvement, even with very weak light sources. Recent atomic structure work includes observations of the resonance lines of 3 electron chlorine, the triplet resonance lines of 2 electron chlorine, and the quartet resonance lines of the multiply-excited systems of three-electron carbon, nitrogen, and oxygen. Our work is stimulating a number of theoretical studies to derive a consistent relativistic treatment of systems of more than one charged particle.

(2) Atomic Structure and Lifetimes of Heavy Ions. We have made a thorough analysis of the Cu I-like ion Kr VIII. This simple (one electron outside a closed 3d shell) system provides a good test of the possible experimental precision of atomic structure and lifetime measurements using the beam-foil technique. Various calculations including relativistic Hartree Fock and nonrelativistic theories with core polarization show and expect to have reasonable agreement ( $\sim 10\%$ ), while previous experimental values are widely different. We show that correct analysis of beam-foil decay curves, using both correlated cascades decay analysis and multiexponential fitting techniques can yield experimental transition probabilities in agreement with theory.

We expect to extend these techniques to other ionic systems such as: (i) the Zn I isoelectronic sequence, which has two electrons outside the closed 3d shell, and for which theoretical results are much more uncertain than for the Cu I sequence. (ii) We have made preliminary observations of +5 to +10 ions in the iron group Ti through Ni and expect to be able to apply the analysis using correlated decay curves to the K I and Ca I isoelectronic sequences.

(3) Foil Interaction with Fast Ions. As part of our continuing program of analyzing the beam-foil interaction primarily by optical polarization observations of light emitted from excited ions, we have verified a foil temperature dependence of the interaction. We interpret this dependence as due to changes in the rate of emission of secondary electrons from the final surface during the beam-foil interaction.

Systematic measurements of alignment and orientation produced in  $n^1,3^3P$  and  $1,3^3D$  states of He I ( $n = 3-8$ ) as functions of beam energy and foil tilt angle have been completed. Initial interpretations of these data in terms of the secondary electron flux and the dipole interaction between the solid and the moving ion are being made.

To help further analysis, we are planning a series of similar measurements in ultrahigh vacuum using different material foils evaporated in situ. A quantitative comparison with grazing angle surface scattering will also be possible.

(4) Ion-Ion Charge Exchange Cross Sections. Low-energy symmetric charge-changing cross sections have recently become relevant to the inertial fusion energy program; such cross sections determine the limit of storage times and beam-transport properties of GeV energy ions used to impinge on the fusion producing pellet. Theoretical work on these cross sections, especially at low energies (10 keV/nucleon or less), is in a primitive stage and experimental comparisons are needed to compare several different calculational models.

In an initial step of this program, we have measured the charge-exchange and ionization cross sections for  $Xe^+$  at 25-100 keV on  $Xe^0$ . Work is proceeding on a colliding beams experiment of singly and multiply charged xenon ions in the same energy range.

#### a. Excitation of Hydrogen by a Thin Carbon Foil

H. G. Berry and G. Gabrielse\*

Foil excitation of hydrogen creates coherence of opposite parity states (e.g., 2s-2p states) which can be measured as a change in phase of the Lamb shift quantum beat when a longitudinal electric field is reversed in sign. An automated field-reversal technique was used. The complete analysis including hyperfine structure and cascade effects of the decay process yields absolute cross sections and coherence amplitudes for the 2s and 2p system over an energy range of 0.02 to 1.5 MeV per proton.

This work constitutes part of G. Gabrielse's Ph. D. thesis.

---

\* Thesis Student, University of Chicago, Chicago, Illinois.

b. An Analysis of the Time Evolution of Atomic Observations

G. Gabrielse\*

A general analysis has been developed for the time evolution of atomic parameters in terms of a Hermitian unit tensor basis. This basis shows explicitly the symmetry properties of time reversal and spatial invariances of the various atomic properties. It has been applied to the particular cases of the anisotropy and polarization of emitted electric dipole photons, including the effect of external fields, and to the time evolution which occurs during atomic collisions. This basis provides a framework particularly useful for describing recent electron-hydrogen and foil-hydrogen excitation measurements.

This work constitutes part of G. Gabrielse's Ph. D. thesis.

c. Temperature Dependence of Alignment Production in HeI by Beam-Foil Excitation

T. J. Gay\* and H. G. Berry

We have measured the dependence upon target foil temperature of the linear polarization fraction (M/I) of the  $2s\ ^1S - 3p\ ^1P$ , 5016 Å transition in HeI for ion energies between 60 and 180 keV. The thin carbon exciter foils were heated externally by nichrome resistance elements. The energy and current dependences of M/I are the same assuming correspondence between beam heating and external heating. We also observe that  $\gamma$ , the number of secondary electrons produced per incident ion, decreases with increasing foil temperature. These two effects, in conjunction, offer a plausible explanation for the variation of polarization with beam current density. The temperature of the foil is shown to depend on beam current to the one-fourth power, indicating that radiation is the primary energy loss mechanism.

---

\* Thesis Student, University of Chicago, Chicago, Illinois.

d. Fine Structure of Doubly-Excited States of 3-Electron Ions

A. E. Livingston and H. G. Berry

We have resolved for the first time the fine structure of the lowest  $^4P^0 - ^4P$  transition in the three electron ions C IV, N V, and O VI. These results provide the first direct test of the calculation of the Coulomb-Breit relativistic interaction in the framework of a relativistic Hartree-Fock theory. Such calculations by K. T. Cheng (RER Division, ANL) show good agreement with our experiment. In addition, differential metastability of the fine structure components is observed for the upper  $^4P$  state. Recent calculations by Bhalla (Kansas State University) show fair agreement with our results.

e. Lamb Shift and Fine Structure of n = 2 in Cl XVI

H. G. Berry, R. DeSerio,\* and A. E. Livingston

Using 80-MeV chlorine beams from the Argonne tandem, ionized and excited by thin carbon foils, we have made precision measurements (20 ppm accuracy) of the wavelengths of the 2s-2p transitions of this two-electron ion. The Lamb shift comprises 0.5% of these transitions and hence, after accounting for nonrelativistic and relativistic structure contributions, we are able to deduce an experimental Lamb shift of  $\pm 0.3\%$  accuracy for Z = 17. The measurement verifies the Lamb shift calculation of Muhr which disagrees with the earlier theoretical work of Erickson and Yennie.

f. Spectroscopy of 3-, 4-, and 5-Electron Ions

H. G. Berry and R. DeSerio\*

We have measured the wavelength of the resonance transition of LiI-like chlorine to a precision of 50 ppm. By a careful comparison of this result and other measurements of LiI-like ions for Z = 3 to 27 with

\* Thesis Student, University of Chicago, Chicago, Illinois.

a  $1/Z$  expansion calculation of the nonrelativistic part and a  $(Za)$  expansion for the relativistic part of the energy, we can deduce the Lamb shift contribution to the three-electron system. This work is part of our program of investigating relativistic effects on atomic structure for atoms of a few electrons.

In the same spectra, yrast transitions of high  $(n, \ell)$  have been observed. We expect them to provide precise measurements of the dipole and quadrupole polarizabilities of these systems.

g. Energies and Lifetimes of Excited States of Kr VIII

A. E. Livingston, H. G. Berry, L. J. Curtis,\* and R. M. Schectman\*

The spectrum of Kr VIII has been observed between 180 Å and 2000 Å using foil excitation of 2.5—3.5-MeV krypton ions. Nineteen new transitions have been classified and eleven new excited-state energies have been determined within the  $n = 4—7$  shells. The excited-state energies and fine structures are compared with recent relativistic Hartree-Fock calculations. The 4p-state lifetime has been measured by performing a simultaneous analysis of decay data for the 4p level and for its dominant cascade-repopulating levels. The lifetime is found to be 30% shorter than previously-measured values and is in excellent agreement with the result of a recent multiconfiguration Hartree-Fock calculation.

h. Charge-Changing Cross Section of Xe on Xe

H. G. Berry, T. J. Gay,<sup>†</sup> and B. Filippone

In an initial experiment, we have measured the charge-exchange and ionization cross sections for singly ionized Xe on a target xenon gas, at ion energies of 25—100 keV. Where comparable, the results agree well with recent measurements by Beuhler *et al.* (Brookhaven National Laboratory).

\* University of Toledo, Toledo, Toledo, Ohio.

<sup>†</sup> Thesis Student, University of Chicago, Chicago, Illinois.

An experiment to measure the charge-changing cross sections for  $Xe^{+n}$  on  $Xe^+$  is in preparation. This crossed beam experiment involves one high intensity  $Xe^+$  beam (of about 1  $\mu$ A) at 80 keV, crossed by a 20—200-keV  $Xe^{n+}$  beam of intensity 1  $\mu$ A or less. The ultrahigh vacuum target chamber and second accelerator are nearing completion. The first colliding beam experiment will measure the total charge exchange and ionization cross sections for the n=1 beam.

#### IN THE COMING YEAR

Atomic Structure of Highly Stripped Ions. We intend to improve our precision of the two- and three-electron chlorine 2s-2p transition wavelengths to below the 10 ppm level. These results will provide significant challenges for the development of a consistent relativistic theory of atoms.

Such measurement will also be attempted for ions of Si (Z = 14) and S (Z = 16), and Ti (Z = 22) which will require use of the linac booster.

Atomic Structure and Lifetimes of Heavy Ions. We have recently shown it possible to accelerate appreciable beams of the iron group elements (about 200 nAmps on target) using an rf ion source at the Dynamitron accelerator. We shall try to extend the technique of our recently successful correlated decay wave analysis (see above) to measure accurate lifetimes in the K I and Ca I isoelectronic sequences of these ions.

Surface Interaction with Fast Ions. We have started experiments that should allow us to compare the atomic alignment and orientation production of fast ions passing through tilted thin foils and scattered from clean surfaces in an ultrahigh vacuum clean environment. Thin foil measurements with helium beams at 20—250 keV will be able to provide tests of Stark mixing theories and anisotropic electron pickup theories.

Ion-Ion Charge-Exchange Cross Sections. We expect to continue our collaboration with the Ion-Fusion Group and measure charge exchange cross sections for multicharged  $Xe^{n+}$  ( $n = 2-4$ ) on  $Xe^+$  in the energy range of 20-300 keV. Depending on count rates of the detected scattered ions, we hope to be able to measure some double charge transfer cross sections.

### C. PHOTOIONIZATION-PHOTOELECTRON RESEARCH

Our photoionization research program is aimed at understanding the basic processes of interaction of light with molecules, the electronic structures of molecules and molecular ions, and the reactions of molecular ions, both unimolecular and bimolecular. The processes and species we study are implicated in a wide range of chemical reactions, and are of special importance in outer planetary atmospheres and in interstellar clouds. Our work also provides fruitful tests for theories of electronic structure, which help in the evaluation of widely applicable models for multielectron systems. Most of this work is of a fundamental nature, but we also use the precise methods developed here to determine thermochemical quantities (heats of formation and ionization potentials) directly relevant in, e. g., reactions with ozone in the stratosphere and possible side reactions in a magnetohydrodynamic generator. Our experimental studies utilize five pieces of apparatus—two photoionization mass spectrometers and three photoelectron energy analyzers—each with special features.

(1) A three-meter normal-incidence vacuum-ultraviolet monochromator combined with a quadrupole mass spectrometer. This apparatus is capable of the highest resolution currently achieved in photoionization studies. It is also convenient for investigations of wavelength-dependent photoelectron spectra.

(2) A one-meter normal-incidence VUV monochromator mated with a magnetic-sector mass spectrometer. This apparatus has higher mass resolution, is less discriminatory in relative ion-yield measurements, and can be used to study metastable ions. Higher intensity for weak signals can also be achieved.

(3) Two cylindrical-mirror photoelectron-energy analyzers, which accept a large solid angle of photoelectrons, close to the "magic angle" of  $54^{\circ}44'$ . One has been extensively used for determining the photoelectron spectra of high-temperature species in molecular beams, and the other has recently been mated with the three-meter monochromator for studies of photoelectron spectra as a function of wavelength.

(4) A hemispherical electron-energy analyzer incorporated in a chamber which permits one to rotate the analyzer over a substantial fraction of  $4\pi$ . This device is intended for angular-distribution measurements, and also enables us to study very-high-temperature species.

An ArF excimer laser has recently been acquired, and will soon be used in studies of multiphoton ionization and as a tool for the preparation of short-lived intermediates.

Specific current activities include the following.

(1) The study of atoms and metal-containing molecules by photoionization and photoelectron spectroscopy. Of the 100 or so elements, atoms of only about 12 elements have been investigated by photoionization, because of technical difficulties with the high temperatures needed for sample vaporization. We propose to undertake the study of many additional elements using the new oven and analyzer; we are currently measuring the spectra of some atomic and molecular systems previously inaccessible.

(2) The reactions of species in selected states. Knowledge of such reactions is needed for modeling of many systems, e.g., planetary atmospheres. We achieve state selection by photoelectron-photoion coincidence techniques, and have extended such measurements to higher-energy states than have heretofore been studied, using line sources out to 40.8 eV.

(3) Photoelectron spectroscopy with a tunable light source. The characteristics of photoionization on and across resonances, rather than in the pure continuum are poorly understood; their investigation should reveal details of electron-electron interactions responsible for the shape of the observable spectra.

## 1. ONE-METER PHOTOIONIZATION MASS SPECTROMETER

### a. Photoionization Mass Spectrometry of UF<sub>6</sub>

J. Berkowitz

We have obtained the photoionization mass spectrum of <sup>238</sup>UF<sub>6</sub>. At 600 Å ≡ 20.66 eV, the relative ionic abundances are: UF<sub>6</sub><sup>+</sup>, 1.4; UF<sub>5</sub><sup>+</sup>, 100; UF<sub>4</sub><sup>+</sup>, 17; UF<sub>3</sub><sup>+</sup>, ~0.7; UF<sub>2</sub><sup>+</sup>, very weak; UF<sup>+</sup>, very weak; U<sup>+</sup>, essentially zero. The UF<sub>6</sub><sup>+</sup> signal is surprisingly high compared to other hexafluorides, e.g., SF<sub>6</sub> and XeF<sub>6</sub>. The adiabatic ionization potential for UF<sub>6</sub> determined in this experiment (13.897 ± 0.005 eV) is in very good agreement with a recent photoelectron spectroscopic determination (13.9 eV). The production of UF<sub>5</sub><sup>+</sup> begins at ~887 Å ≡ 13.98 eV, at which energy the UF<sub>6</sub><sup>+</sup> partial cross section abruptly declines and then levels off. This suggests the vague possibility of an isotope effect, whereby

a wavelength around 887 Å could be chosen and the relative ratios of  $\text{UF}_6^+$ / $\text{UF}_5^+$  from the two uranium isotopes could perhaps be different. The  $\text{UF}_4^+$  signal begins at  $\sim 725$  Å  $\equiv 17.10$  eV, at which energy the  $\text{UF}_5^+$  signal reaches a plateau value. The  $\text{UF}_5^+$  photoionization yield curve displays some autoionization structure from its threshold to  $\sim 750$  Å, which is probably related to Rydberg series converging upon the second, third, and fourth ionization potentials of  $\text{UF}_6$ .

b. Production of Doubly-Charged Ions in Vacuum-Ultraviolet Photoionization

J. H. D. Eland, J. Berkowitz, and J. A. Laramee

A high-resolution study of the production of doubly-charged ions by photon impact on molecules would give direct information on hitherto little known double-ionization thresholds, on the state of doubly-charged ion and on electron correlations. Such a study has never been made before, because the double-ionization thresholds mostly lie outside the convenient range of laboratory light sources, and outside the range where high resolution is available even with synchrotron sources. Three classes of molecules have recently been found to have low second ionization potentials, and to have abundant doubly-charged parent ions in their electron-impact mass spectra; they are the condensed ring aromatic hydrocarbons, zero-valent transition metal complexes, and transition-metal phthalocyanines. To assess the feasibility of using these molecules in a detailed study of photo double ionization, we have measured photoionization mass spectra of copper phthalocyanine and of ferrocene, using a directly heated sample oven in the source chamber of the 1-meter photoionization mass spectrometer. We find the doubly-charged ions to be much less abundant in photon-impact than in electron-impact mass spectra, but the ion signals were sufficiently intense to indicate that a detailed study would be possible after improvements in oven design and optimization of the light source. Preliminary photoionization-yield curves

for the doubly-charged ions were obtained. This work will be continued when time and manpower permit.

## 2. THREE-METER PHOTOIONIZATION MASS SPECTROMETER

### a. Collisional Ionization in Argon

J. Berkowitz

Photoion signals can be detected below the ionization threshold at pressures (ca.  $10^{-2}$ — $10^{-3}$  torr) where bimolecular collisions become significant. We have re-examined this behavior in the case of argon, where two competing ionization processes can be observed: (1)  $\text{Ar}^* + \text{Ar} \rightarrow \text{Ar}^+ + \text{Ar} + e$  (collisional ionization) and (2)  $\text{Ar}^* + \text{Ar} \rightarrow \text{Ar}_2^+ + e$  (associative ionization).

In both cases,  $\text{Ar}^*$  represents a highly excited (Rydberg) state of Ar. Process (1) requires additional energy, in the form of kinetic energy.

We find that the same Rydberg states are responsible for both processes. They are dipole-allowed ( $^1\text{P}$ ) states, predominantly  $\dots 3\text{p} [^5\text{P}_{3/2}] \text{nd}_{3/2}$  and  $3\text{p} [^5\text{P}_{3/2}] \text{nd}_{1/2}$ , whose convergence limit is the ground state of  $\text{Ar}^+$ ,  $^2\text{P}_{3/2}$ . Very near to threshold, process (1) dominates, but when the energy deficit approaches  $kT$ , process (1) declines exponentially, whereas process (2) remains significant. The cross section for formation of  $\text{Ar}_2^+$  surpasses that for  $\text{Ar}^+$  below  $n = 13$ , but it declines at very high- $n$  values, asymptotically vanishing at the ionization threshold. The above processes and their kinetics are relevant to the modeling of the performance of excimer lasers.

b. Comparison of Single-Photon and Multiphoton Ionization Near Threshold

J. H. D. Eland, A. D. Williamson,\* and R. N. Compton\*

If ionization potentials, which are usually more than 10 eV could be precisely measured by multiphoton rather than single photon ionization, the need for vacuum monochromators and differentially-pumped vacuum uv light sources would be avoided. It has generally been thought that multiphoton ionization cross sections must be dominated by discrete spectral structure resonant at the energy of one or two photons, well below the ionization limit, rather than by the structure in the ionization continuum. We have demonstrated that in pyrrole ionization this is not the case; the yield of pyrrole ions by both two-photon and three-photon ionization closely mimics the single-photon ionization yield curve as a function of wavelength near threshold. Even the vibrational structure just above threshold is apparent in the multiphoton ionization yield, though there is broadening due to the high gas pressures. With further development for improved sensitivity, this method may make it possible to obtain ionization information at much higher resolution than is currently available from vacuum monochromators. The results of this study have been published<sup>1</sup> and the Argonne involvement in it is concluded.

\* Oak Ridge National Laboratory, Oak Ridge, Tennessee.

<sup>1</sup> A. D. Williamson, R. N. Compton, and J. H. D. Eland, *J. Chem. Phys.* 70, 590 (1979).

c. Detailed Study of Molecular Autoionization

J. H. D. Eland, J. Berkowitz, and J. E. Monahan

The shapes and intensities of autoionizing resonance features in molecular photoionization spectra are often different when observed in the intensities of different fragment ions, particularly for resonances which interact strongly with the underlying continuum. We have found notable examples of this behavior in the photoionization of

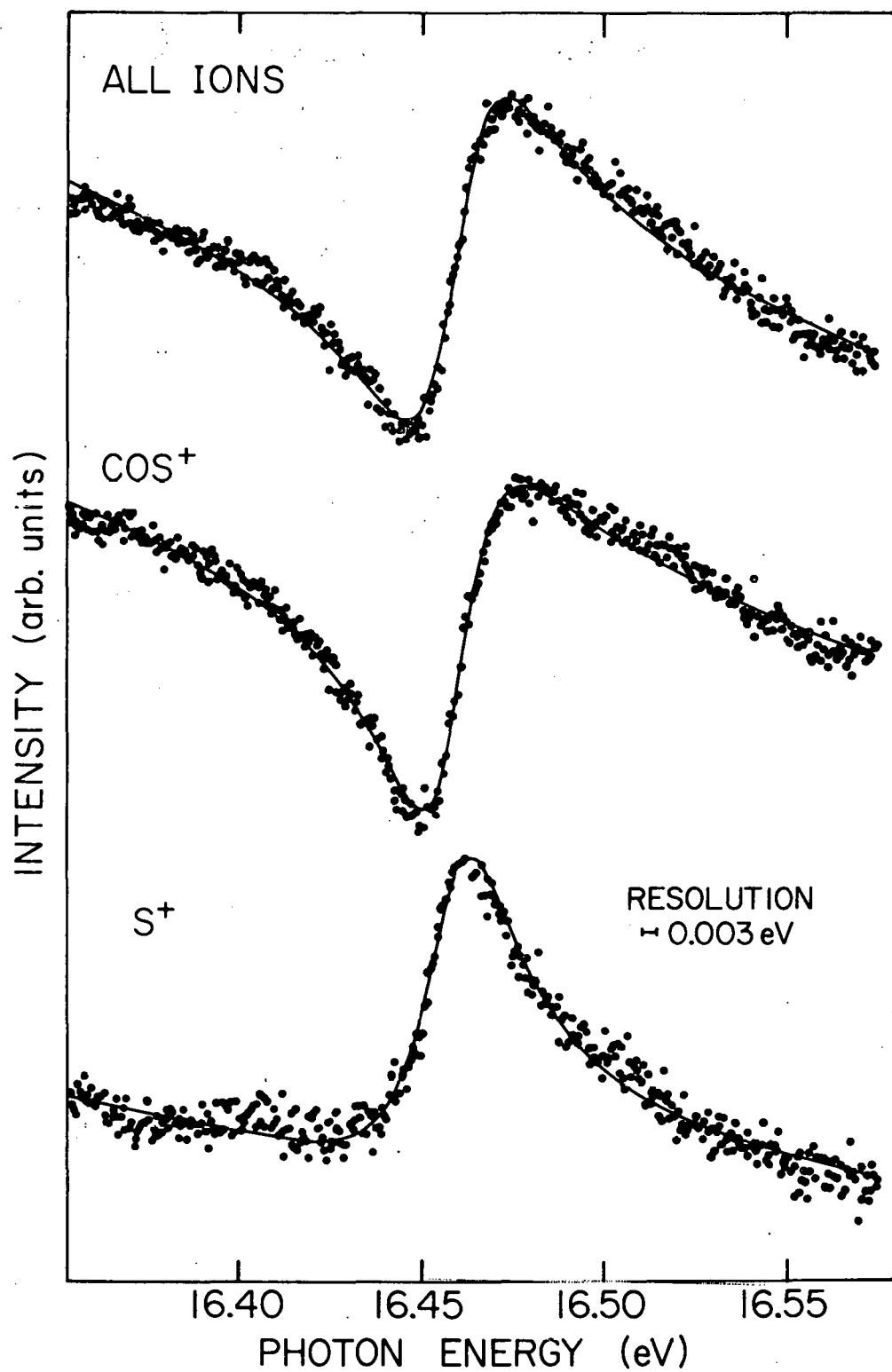


Fig. VIII-3. Photoionization yield curves over a resonance of COS, showing an inflection in the total photoionization cross section, a dip in the COS<sup>+</sup> yield and a peak in the S<sup>+</sup> yield. The solid lines are fits to Fano profiles.

$\text{CO}_2$ ,  $\text{CS}_2$ ,  $\text{N}_2\text{O}$ ,  $\text{COS}$  (see Fig. VIII-3) and a counter-example in neopentane, where peak shapes characteristic of strong interaction are the same in different channels despite intensity differences over two orders of magnitude. A formal theory of the phenomena involving many resonances and many continua is available, but is too complex to apply to the present data. We have evolved a simplified model for a single resonance interacting with several continua; while our previous results are compatible with this model, they cannot be used to test it thoroughly, because single fragment ions do not constitute single final channels in the sense of this (and other) theories. It is necessary to measure partial cross section for single final states by an electron energy analysis at each incident wavelength. Such experiments, while much more difficult to carry out, are now being attempted using the three meter monochromator-light source combination with the cylindrical-mirror electron spectrometer.

### 3. PHOTOELECTRON SPECTROSCOPY

#### a. Photoelectron Spectroscopy of Higher Temperature Vapors

J. Berkowitz and C. H. Batson

We initiated the study of the photoelectron spectra of volatile materials in this laboratory about 8 years ago. Many systems inaccessible for study by conventional instruments were investigated here. An insight was thereby gained into the bonding and electronic structure of many simple inorganic molecules, particularly ionic ones. The cylindrical-mirror analyzer and its molecular-beam source were found to experience severe problems at  $T \sim 1000^{\circ}\text{K}$ . Other laboratories have subsequently encountered similar difficulties.

The new apparatus which we have recently put into operation relieves some constraints imposed by the earlier apparatus, and incorporates additional measurement capabilities. The electron-energy analyzer

is of hemispherical design. A lens system at its entrance both retards and focuses incoming electrons onto the (virtual) entrance slit of the analyzer. The properties of this lens system (so-called "zoom" lens) minimize the transmission loss as one retards. The entire analyzer + lens system rotates in both  $\theta$  and  $\phi$  (longitudinal and azimuthal) directions about the center of the vacuum chamber, which is the source of photoelectrons. Hence, we now have the capability of measuring the angular distribution of photoelectrons from high-temperature species.

A rather complicated oven system is mounted from the bottom of the chamber. It consists of a bottom oven component surmounted by a narrow, tubular "upper oven." Each is heated radiatively by a noninductively wound, resistive tungsten filament. The noninductive feature of each filament minimizes, but does not eliminate magnetic fields. However, by bucking the two residual magnetic fields the resultant field has an insignificant effect upon analyzer performance. The oven system is capable of achieving temperatures in excess of  $2000^{\circ}$  K, although we have not yet tested the analyzer under these extreme conditions.

Among various high-temperature systems which we hope to study with this new apparatus are many atoms. Heretofore, the noble gases and a handful of metallic systems (Hg, Cd, Zn, some alkaline earths and rare earths) have been studied by PES. Our double-oven capability should enable us to investigate such systems as Bi and Sn, which sublime as mixtures of molecular and atomic species, in addition to the more refractory materials which have been beyond the accessible temperature range.

Our initial test of the apparatus was made with the lithium halides. About 20—25 years ago, it was first realized that the alkali halides vaporized as mixtures of diatomic molecules (monomers), tetratomic molecules (dimers) and even more complex species. The fraction of dimer (and higher polymeric forms) increased in the sequence  $\text{CsX-RbX-KX-NaX-LiX}$ , where X is a halogen. For lithium halides, the dimer composed at least

50% of the saturated vapor. Earlier studies (at this laboratory and elsewhere) focused on the photoelectron spectra of the monomers. The features of these spectra were conveniently explained with an ionic model incorporating spin-orbit splitting. Such dimer as was detected in PES provided more confusion than insight. In these earlier experiments, the lithium halides were avoided. However, we recognized that a determination of the PES of "pure" dimer could provide a clue to a more general understanding of molecular structure. The spectrum we obtain characterizes the valence band. We would like to know the extent of this valence band as the complexity of the molecule increases, and also its first ionization potential. Does it increase or decrease as one goes from monomer to dimer? If we can rationalize this behavior with some model, can we extend it to more complex species, and ultimately to a system that has the properties of the bulk crystal? Several photoemission studies on bulk crystals have already been performed, but they are inconsistent and fraught with difficulties characteristic of insulators—charging up of the sample, and an ill-defined energy scale.

We have now succeeded in obtaining spectra of each of the lithium halides under two conditions: (1) a vapor composition approximating the saturated vapor and (2) a super-heated system that strongly enhances the monomer.

By appropriate subtraction of the two spectra, we can deduce essentially pure monomer and dimer spectra. In each system, the dimer has a higher first ionization potential; the difference in IP's between dimer and monomer decreases in the sequence F, Cl, Br, I. The extent of the valence band in the dimer appears to be a property of the halogen. An example of the raw data, and the pure monomer and dimer spectra deduced therefrom, is given in Fig. VIII-4 (a—e) for the case of lithium iodide. Some further work on the other alkali halides is being undertaken, and a molecular calculation using the X-a, discrete variational method, has been performed to help interpret the available data.

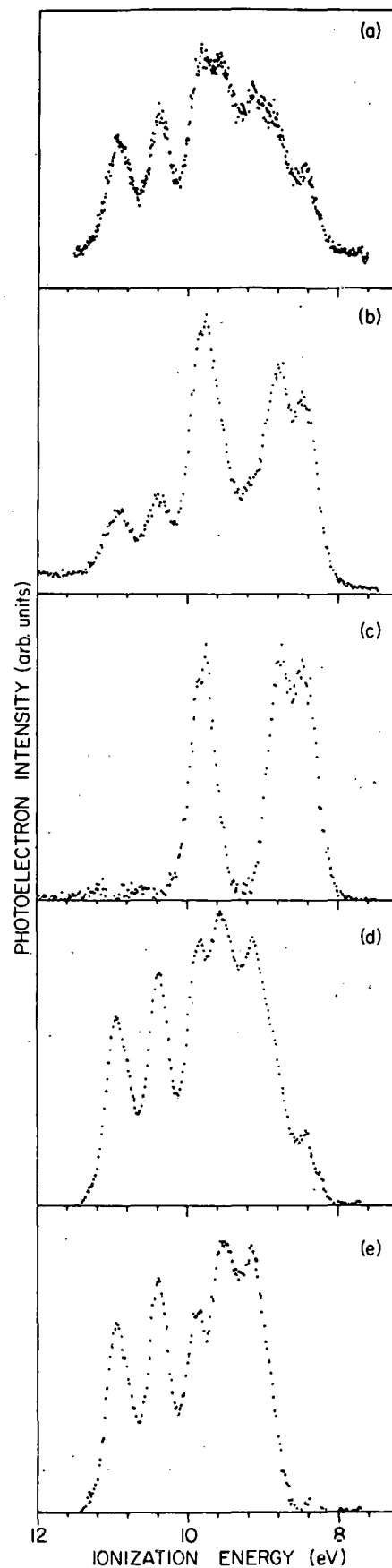


Fig. VIII-4. (a) He I photoelectron spectrum of LiI without superheating,  $T \cong 800^{\circ}\text{K}$ ; (b) He I photoelectron spectrum of LiI with superheating,  $T \cong 800^{\circ}\text{K}$ ; (c) "pure" monomer LiI spectrum, obtained by subtracting (a) from (b), after background subtraction and normalization at dimer band; (d) spectrum with 50% of the monomer subtracted, to demonstrate the effect of reduction on the various peaks; and (e) "pure" dimer ( $\text{Li}_2\text{I}_2$ ) spectrum, obtained by subtracting (c) from (a), after normalization at monomer band.

Preliminary data have also been obtained for one member of the rare earth halides, erbium triiodide. It appears perfectly feasible to study enough representative members of this class to elucidate the influence of 4f electrons from the rare earth on bond formation.

b. Partial Photoionization Cross Sections of Atomic Iodine: Irreducible Tensor Analysis of Intensities

J. Berkowitz and G. L. Goodman\*

The He I photoelectron spectrum of atomic iodine has been obtained from a thermal source. The relative intensities are compared with recent data<sup>1</sup> on Cl and Br. The major difference is an inversion in the relative intensities of  $^3P_0$  and  $^1S_0$  between Cl and I. An irreducible tensor algebra calculation of the angular factors for these intensities in intermediate coupling, combined with spectroscopic mixing parameters, reproduces this inversion quantitatively, and in addition adequately describes the entire intensity pattern for all three halogens. The strong implication is that angular factors and mixing parameters are the dominant features in determining relative intensities, and radial integrals and "anisotropic electron-ion interactions"<sup>2</sup> are much less important.

Furthermore, the latter calculations have not been performed properly.

\* Consultant, Physics Division, ANL.

<sup>1</sup> K. Kimura, T. Yamazaki, and Y. Achiha, Chem. Phys. Lett. 58, 104 (1978).

<sup>2</sup> D. Dill, A. F. Starace, and S. T. Manson, Phys. Rev. A 11, 1596 (1975); A. F. Starace and L. Armstrong, Jr., Phys. Rev. A 13, 1850 (1976).

c. Photoelectron Spectroscopy of Phthalocyanine Vapors

J. Berkowitz

The 21.2-eV photoelectron spectra of metal-free phthalocyanine and some metal-containing phthalocyanines MPc (M = Mg, Fe, Co, Ni, Cu, and Zn) have been obtained for the gaseous molecules.

Comparison of these spectra reveals that the uppermost occupied orbitals are ring-like, and not metal-3d-like, in all cases. Identification of some features in the 1487.6-eV photoemission spectra of thin films of phthalocyanines with similar features in the gas phase spectra enables one to establish an absolute energy scale for the thin film work, and to locate the ionization energies of the 3d-like orbitals. The experimental results and inferences are compared with recent ab initio calculations, and indicate that the X- $\alpha$  local density method is a promising one for describing the electronic structure of these large molecules and the generically related biological systems, chlorophyll and hemoglobin. In some spectra, phthalonitrile was identified as an impurity, and verified by obtaining the 21.2- and 40.8-eV photoelectron spectra of this molecule.

This completed study has been accepted for publication in the *Journal of Chemical Physics*.

d. Photoelectron Spectroscopy of Trinuclear Metal Complexes

J. Berkowitz and W. C. Trogler\*

Metal-cluster complexes, their synthesis and reactivity, comprise an important area of research in inorganic chemistry. These compounds have been shown to catalyze a variety of important chemical processes, and to serve as models for reactions which occur at metal surfaces. We have attempted to elucidate the electronic structure of small metal-cluster complexes using the technique of gas-phase photoelectron spectroscopy.

The compounds  $\text{Re}_3\text{X}_9$  ( $\text{X} = \text{Cl, Br}$ ) exhibit strong metal-metal bonding, as evidenced by their chemical reactivity and the results of x-ray diffraction. We have measured the photoelectron spectra of these species, and find support for these conclusions in the large splittings of the metal-localized d orbitals. To formulate a precise electronic structural model, we are currently comparing our spectra with the predicted ionization potentials from an X- $\alpha$  calculation.

\* Northwestern University, Evanston, Illinois.

Metal carbonyl cluster complexes of ruthenium and osmium have also been studied. Complete He I and He II photoelectron spectra of  $\text{Ru}_3(\text{CO})_{12}$  and  $\text{Os}_3(\text{CO})_{12}$  have been measured. Striking similarities exist between the spectra. Calculations by the X- $\alpha$  discrete variational method are in progress to aid in the spectroscopic assignments.

e. Photoelectron Spectroscopy of Sulfur Nitrides

J. Berkowitz and E. H. Appelman\*

An allotropic form of sulfur nitride, designated  $(\text{SN})_x$ , has been found to have some interesting properties bordering on superconductivity. Mass spectrometric studies of the vapor generated by heating  $(\text{SN})_x$  and the more common allotrope are sufficiently different to indicate that different vapor species are formed. The more common allotrope is generally believed to volatilize to a cyclic  $\text{N}_4\text{S}_4$  molecule.

We have undertaken a photoelectron spectroscopic study to characterize the valence ionizations of  $\text{N}_4\text{S}_4$  and the other related species that can be generated, i. e.,  $\text{N}_2\text{S}_2$ , NS and the ill-characterized species produced from  $(\text{SN})_x$ . To date, we have obtained the spectrum of  $\text{N}_4\text{S}_4$ . Here again, molecular calculations of the X $\alpha$  discrete variational method type are being planned to help in the interpretation of the data.

---

\* Chemistry Division, ANL.

**4. PHOTOELECTRON-PHOTOION COINCIDENCE SPECTROSCOPY**

a. Improved Apparatus for Fixed Wavelength Photoelectron-Photoion Coincidence Spectroscopy

J. H. D. Eland and C. H. Batson

Photoelectron-photoion coincidence spectroscopy is a technique for the study of reactions of molecular ions prepared in selected states. In fixed wavelength photoelectron-photoion coincidence spectroscopy

there is normally a degradation of electron energy resolution due to the continuous ion-drawout field applied across an ionization region of finite width. A technique has been devised to overcome this limitation by use of a pulsed drawout field. Essential features of the new method are a pulse repetition rate whose period is less than the mean time between the formation of detectable ions, and detection of electrons only during periods when the field is off. The use of timing information from the applied pulse edges (rather than electron detection times) to define the time scale for coincidence counting allows the mass resolution as well as the energy resolution to be improved.

Because this technique leads to a structured background of accidental coincidences, it was also necessary to develop electronic methods for the precise and automatic subtraction of false coincidences. Substantial improvements in electron-energy resolution and also in ion-mass resolution have been demonstrated, and the results published.<sup>1</sup>

The new technique will be used in future photoelectron-photoion coincidence work in the Laboratory.

---

<sup>1</sup>J. H. D. Eland, Rev. Sci. Instrum. 49, 1688 (1978).

b. Predissociation of  $C_2H_2^+$ ,  $H_2S^+$ , and  $D_2S^+$  Ions

J. H. D. Eland

Indirect evidence has suggested that molecular ions of acetylene and hydrogen sulphide dissociate without prior randomization of internal electronic excitation energy to vibrational energy, contrary to the assumptions of the statistical theory of mass spectrometry in its "strong" or strict form. The characteristics of these molecular-ion fragmentations from selected states were therefore examined directly by the photoelectron-photoion coincidence method. It was found that the reaction  $C_2H_2^+ \rightarrow C_2H^+ + H$  has its onset near 17.3 eV in the  $\tilde{\Lambda}^2\Sigma_g^+$  state of  $C_2H_2^+$  in agreement with earlier work, and in addition, that the products are formed there with zero kinetic energy, even though the

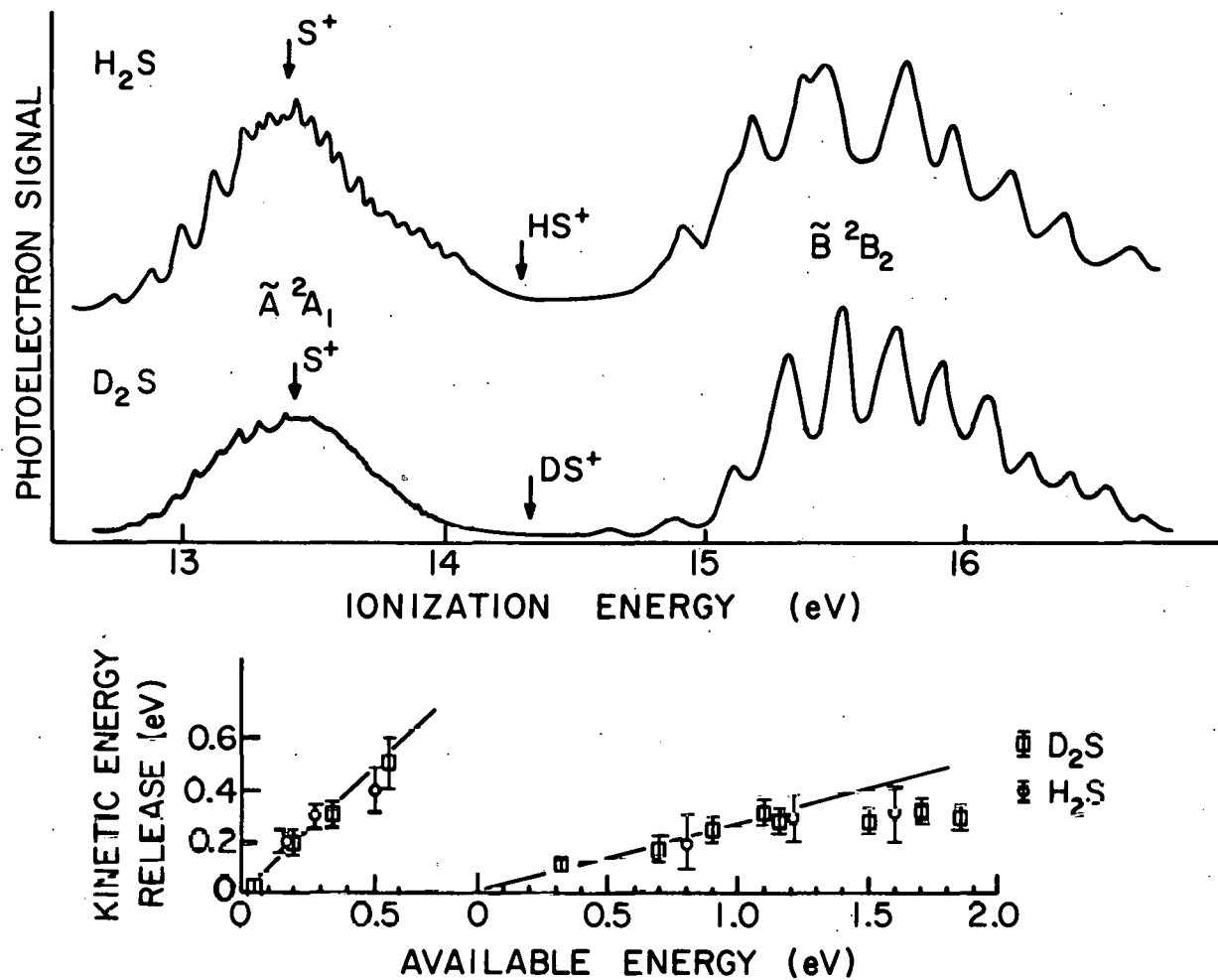


Fig. VIII-5. Photoelectron spectra of  $\text{H}_2\text{S}$  and  $\text{D}_2\text{S}$ , with the kinetic energy releases in their ionic dissociation at each energy. Only  $\text{S}^+$  is observed from the  $\tilde{\text{A}}^2\text{A}_1$  states, and only  $\text{HS}^+$  or  $\text{DS}^+$  from the  $\tilde{\text{B}}^2\text{B}_2$  states. Unit slope of the kinetic energy release plots for  $\text{S}^+$  products implies 100% conversion of available energy into kinetic energy of the products.

dissociation asymptote probably lies 0.5 eV lower in energy. At energies above 17.3 eV, one-fifth of the additional excess energy appears as kinetic energy, a fraction consistent with statistical energy partitioning. The results are explicable if  $C_2H^+$  product ions are formed from  $C_2H_2^+$  exclusively in an excited state. The dissociation of hydrogen sulphide ions from the  $\tilde{A}^2A$  state, on the other hand, yields  $S^+ + H_2$  products exclusively in their lowest electronic and vibrational states and with little, if any, excitation of  $H_2$  rotation. When the  $\tilde{B}^2B_2$  state of  $H_2S^+$  is populated, a different reaction occurs yielding  $HS^+ + H$ , with a roughly "statistical" fraction of the excess energy appearing as kinetic energy of the products. The observations are summarized in Fig. VIII-5. These three observations demonstrate that the statistical theory of mass spectra, involving complete energy randomization, is not valid for these molecular ions, and their reactions must be examined individually on the basis of individual potential energy surfaces for each electronic state.

### c. Angular Distributions of Photoelectrons from Orientated Molecules

J. H. D. Eland

The angular distributions of photoelectrons ejected from molecules which are fixed in space would contain detailed information on the molecular wavefunctions, and if known could provide a means of determining the orientations of molecules adsorbed on surfaces. In the course of a photoelectron-photoion coincidence study of the diatomic interhalogens  $I_2$ ,  $ICl$  and  $IBr$ , fragment-ion distributions which are anisotropic with respect to the ejected electron direction have been discovered. If an atomic-fragment ion is ejected along the molecular axis in a time short compared to a rotation period, its angular distribution is the same as the orientation of molecular ions detected in coincidence with electrons ejected into a small, fixed solid angle. This is closely related to the photoelectron angular distribution which would be observed for a space-fixed molecule. Anisotropic angular distributions were also

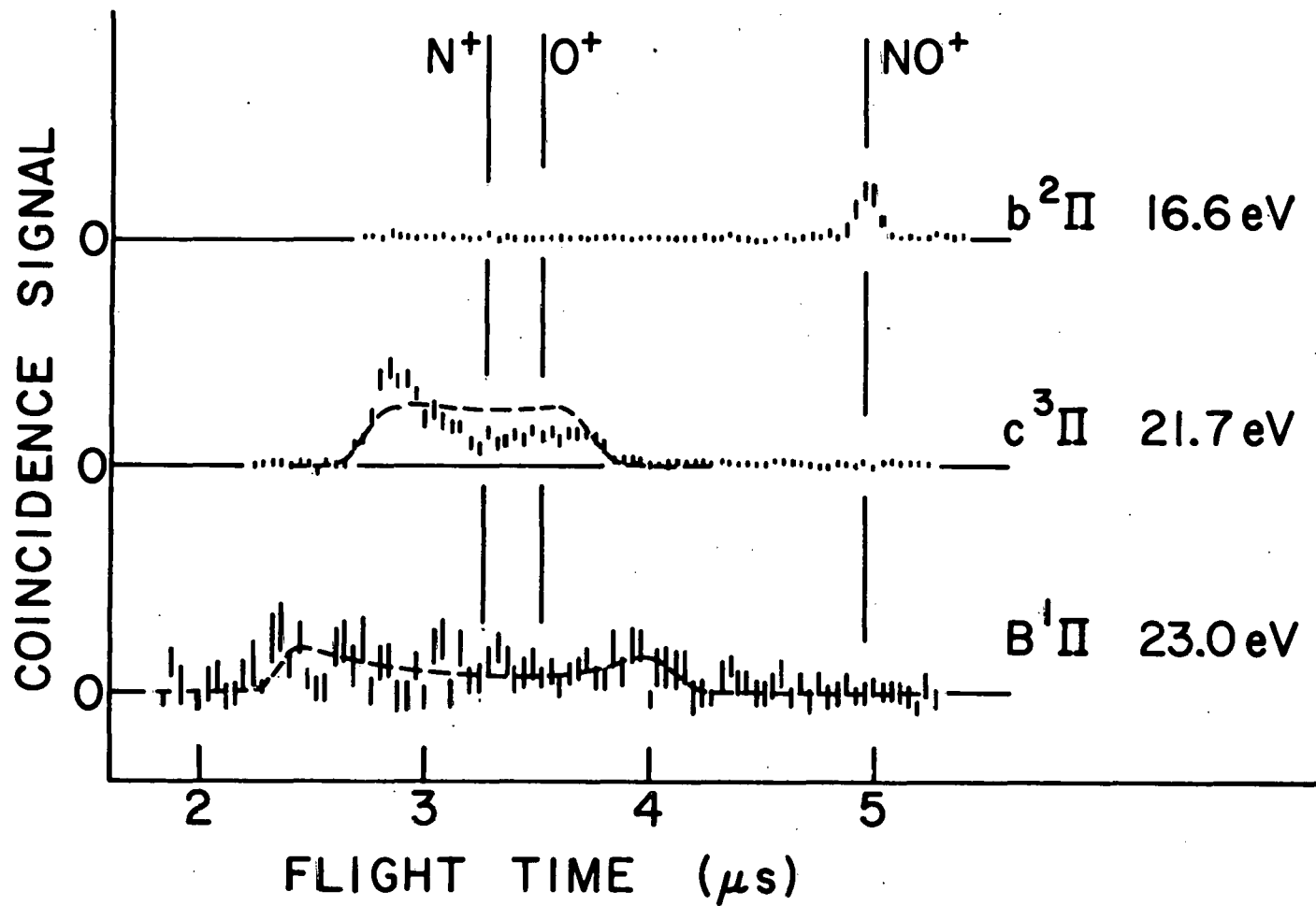


Fig. VIII-6. Coincidence time-of-flight distributions showing  $\text{NO}^+$  and  $\text{N}^+$  ions produced from different initial states of  $\text{NO}^+$  populated by photoionization at 30.4 nm (He IIa). The dashed lines are profiles computed on the basis of the known energy releases, with isotropic angular distributions of fragments. The marked deviation between theory and observation for  $\text{NO}^+$   $c^3\Pi$  dissociation is attributed to an effect of anisotropy.

found in ionic dissociations of  $O_2^+$  and  $NO^+$ ; the experiments involved the first coincidence measurements ever made using a He IIa (30.3 nm) light source. An example is shown in Fig. VIII-6, which also demonstrates how the angular anisotropy was inferred from the observed time-of-flight distribution.

This effect has important implications for the interpretation of photoelectron-photoion coincidence measurements and ion-photodissociation experiments, as well as possible applications to orientation and structure determinations. A theoretical analysis is being made at Argonne, and further experiments are being considered.

## D. SPECTROSCOPY OF FREE ATOMS

### 1. HIGH-RESOLUTION SPECTROSCOPY WITH TUNABLE LASERS AND ATOMIC BEAMS

The field of laser spectroscopy is expanding very rapidly as is clear from the increasingly large role such work plays in atomic physics meetings. Although much of the work concentrates on the laser aspects involved, our own interest is in the increased understanding of atomic structure that these new techniques can bring.

In the last year our use of the new laser-rf double-resonance technique to make extremely high precision measurements of the hyperfine structure (hfs) of atomic levels in vanadium and uranium has demonstrated the great power of the new technique for atomic structure studies. Our uranium work is also of potentially great value for laser isotope separation of uranium.

In the laser-rf double-resonance technique, a tunable, c.w. single-frequency dye laser is used to deplete the population of a particular magnetic substate of an atomic level by orthogonally illuminating an atomic beam at the resonance frequency. When light of the same wavelength is used to probe the atomic beam further from its source, little fluorescence is observed unless the depleted state is repopulated by inducing rf transitions in the space between the two laser-atomic-beam interaction regions. Since the linewidth of the observed rf transition depends only on the flight-time of the atom through the rf region, it can be thousands of times sharper than the laser-induced fluorescence lines. Six papers based on double-resonance research carried out during 1978 have been accepted for publication, and some of these experiments will be described separately below.

#### a. High-Precision Studies of the hfs of $^{51}\text{V}$

W. J. Childs, L. S. Goodman, and O. Poulsen

The well-known inability of conventional techniques to distinguish between hfs due to core polarization and that due to the direct contact contribution of the s electron in  $^N\text{L}$  s configurations has been a problem encountered by many people over the years. This was overcome in  $^{51}\text{V}$  by application of the laser-rf double-resonance technique to selected

highly excited states. Analysis of the results showed that the best ab initio calculations are rather good for the s-electron part, but entirely inadequate for the core-polarization part of the hyperfine structure; a more sophisticated theoretical approach to this aspect of the atomic structure is therefore called for. The vanadium experiment was of particular interest because of the extraordinarily large "second-order" hfs, i.e., that due to hfs interactions between two atomic states as opposed to the normal or first-order, which is simply the effect of the interaction within a single state. Because of the extremely high precision made possible by the double-resonance technique, we were able to use the measured second-order hfs to determine separately the two forms of contact hfs present.

b. Ultrahigh Precision Measurements of the hfs of Several Levels of  $^{235}\text{U}$

W. J. Childs, L. S. Goodman, and O. Poulsen

For fifteen years intensive efforts have been made at many laboratories around the world to achieve high-resolution measurement of the hfs of the ground and other low-lying atomic levels of  $^{235}\text{U}$ . Our work (published in January and February of 1979) has finally succeeded, and the values are 10,000 times more precise than even the most recent (1978) experiments performed elsewhere.

Figure VIII-7 shows a portion of the absorption line  $\lambda 5915.4 \text{ \AA}$  from the ground state as exhibited in laser-fluorescence, while Fig. VIII-8 demonstrates the high precision attainable with the laser-rf double resonance technique in measurements of the hfs of the initial state of the optical transition.

Table VIII-I compares the new double-resonance results for several ground-state hyperfine intervals in  $^{235}\text{U}$  with values determined in the present experiment from laser-fluorescence techniques. It should be noted that even these latter values are several times more precise than anything in the literature.

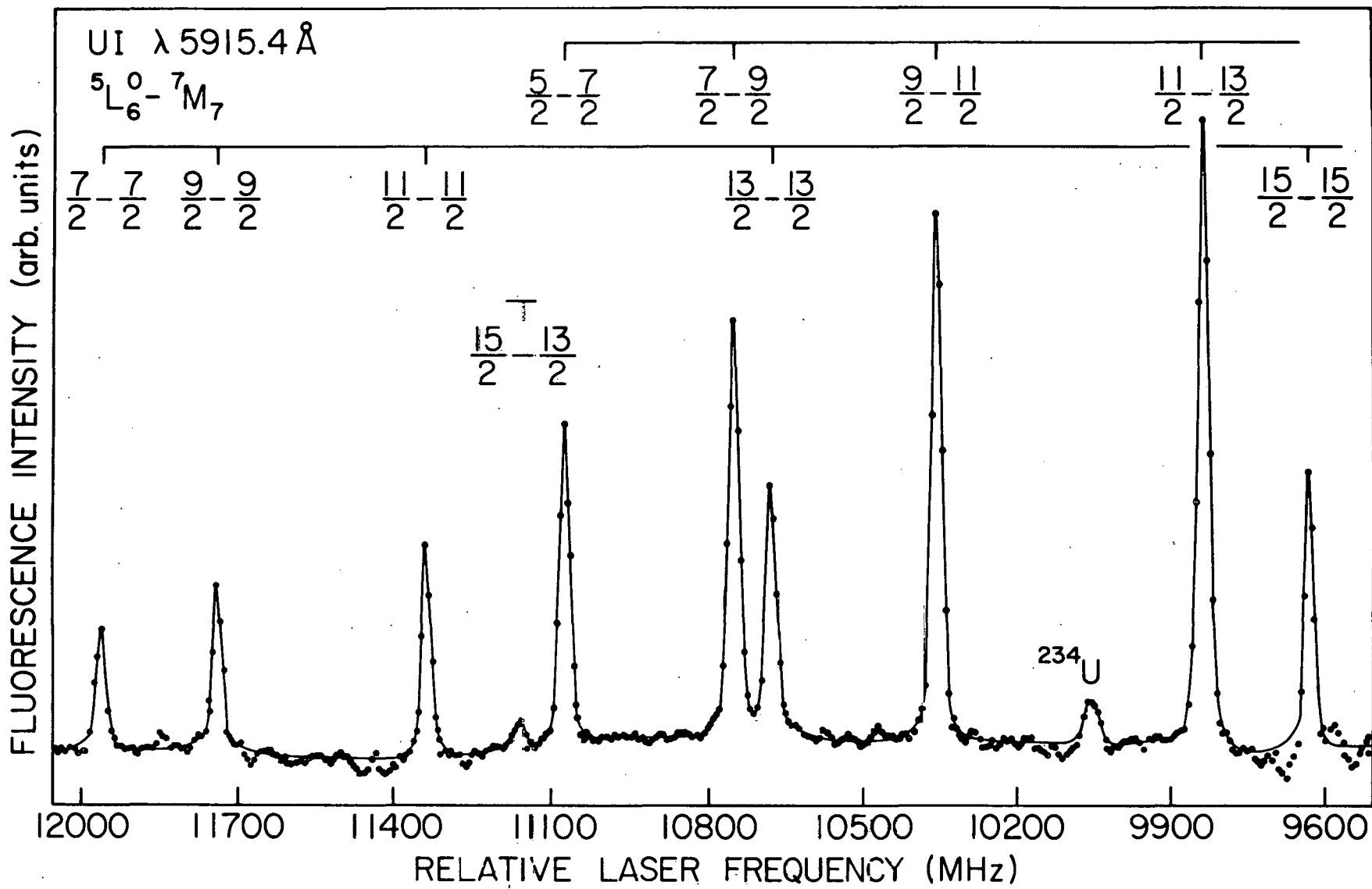


Fig. VIII- 7. A portion of the absorption line of  ${}^{235}\text{U}$  at  $\lambda 5915.4 \text{ \AA}$  as exhibited in laser-fluorescence measurements. In the best optical spectroscopy measurements published before this data was taken, these individual line components were completely unresolved.

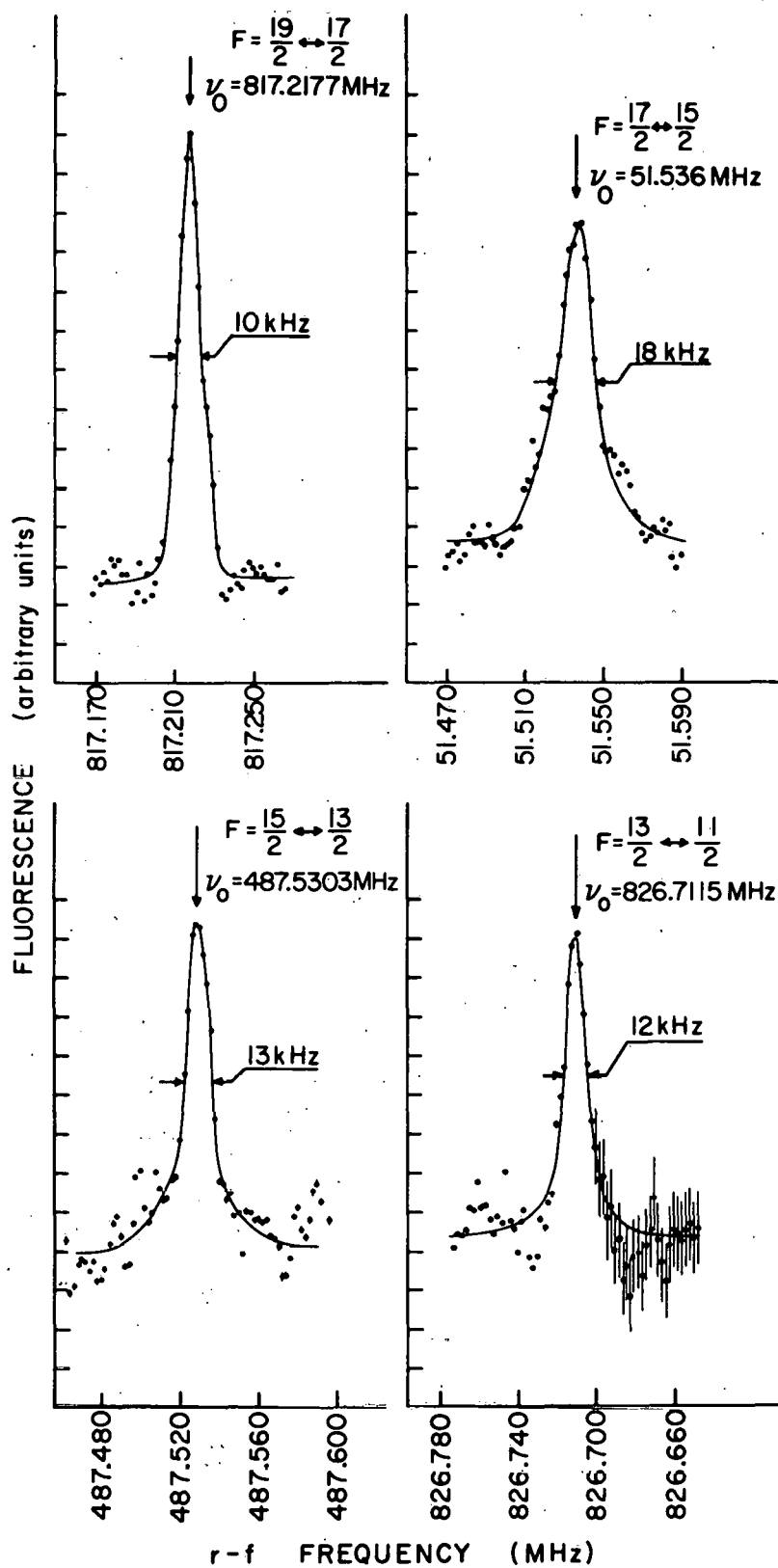


Fig. VIII-8. Laser-rf measurements of the hfs of the  $^5L_6^0$  ground state of  $^{235}\text{U}$ .

TABLE VIII-I. Measured values of the zero-field hyperfine intervals in the  $^{235}\text{U}$  atomic ground state as determined by laser fluorescence and laser-rf double resonance.

Hfs interval $F \leftrightarrow F'$	Measured value (MHz)	
	By laser	By laser-rf
	fluorescence	double resonance
19/2-17/2	816 $\pm$ 2	817.2177 $\pm$ 0.001
17/2-15/2	53 $\pm$ 2	51.536 $\pm$ 0.001
15/2-13/2	-486 $\pm$ 2	-487.5303 $\pm$ 0.001
13/2-11/2	-827 $\pm$ 2	-826.7115 $\pm$ 0.001
11/2-9/2	-992 $\pm$ 2	
9/2-7/2	-1009 $\pm$ 2	
7/2-5/2	-910 $\pm$ 2	

The hfs was measured in several levels, and the work established that our techniques could be applied with very high precision to measure details of the hfs and isotope shifts for all levels up to at least  $10,000 \text{ cm}^{-1}$ . A detailed theoretical analysis of the results showed that while the observations can be understood qualitatively, the complexity of the heavy uranium atom is so great that a quantitative understanding would require further substantial theoretical effort. In addition to their value for the understanding of the structure of the uranium atom, the results achieved could well prove to be of great importance for laser-isotope separation of atomic uranium.

### c. Enhancement of Isotope Separation Efficiency

W. J. Childs, L. S. Goodman, and O. Poulsen\*

Methods that have been suggested for laser-atomic-beam isotope separation all suffer from poor efficiency because of the difficulty

\*Institute of Physics, University of Aarhus, Denmark.

of exciting atoms from more than one hyperfine level with the sharp-line laser used for isotope selectivity. The techniques developed in the laser-rf double resonance studies of  $^{235}\text{U}$ , and the high-precision data itself, can be applied to improve laser-atomic-beam isotope separation methods by about a factor of five.

This suggestion has been published in *Optics Communications* 28, 309 (1979).

d. Identification of Previously Unclassified Spectral Lines in Terbium

W. J. Childs and L. S. Goodman

Ultrahigh resolution study of a number of spectral lines in terbium has shown that the completely resolved hyperfine structure can be used to identify the upper and lower levels of each transition uniquely. The resulting identifications show that some of the previous assignments were in error due to their dependence on much lower resolution studies. Surprisingly, one of the lines newly identified is the first line in the visible region of the spectrum known to connect to the atomic ground state. Such information, especially when combined with precise absolute wavelength determinations, will be of great value for extending our systematic understanding of the structure of complex atoms to higher excitation energies.

**2. STUDY OF HIGH-RYDBERG ATOMS**

Siu Au Lee and Frank Tomkins\*

Studies have been carried out to determine the effect of a strong magnetic field and a weak electric (stark mixing) field on the quasi-Landau levels of barium. A modified conventional heatpipe oven with shielded electrodes was used. Using a  $\text{H}_2$  discharge lamp as light source, the Zeeman spectrum of the high Rydberg states of Ba at a

---

\* Chemistry Division, ANL.

magnetic field of 50 kG was taken on photographic plates using the 30 ft Paschen-Runge grating spectrometer. When an electric field of 100 V/cm was also applied, no detectable change in the Zeeman spectrum was observed.

Increasing the electric field strength resulted in discharges in the oven. Attempts to further shield the electrodes or using different buffer gas to eliminate the discharge were unsuccessful.

To solve this discharge problem, future studies will be undertaken using an atomic beam instead of the heat pipe. The atomic beam interaction region is to be fitted into the bore of a superconducting magnet. Since the atomic beam has a much reduced atom number density, the previous absorption light source will not give enough signal strength. We are currently investigating the use of a frequency-doubled,  $N_2$ -laser-pumped dye laser as the light source.

We have also investigated the pressure shift and broadening of the high Rydberg states due to buffer gas. The preliminary results are in qualitative agreement with the Fermi line broadening theory. We plan to do a more quantitative study of the pressure effects. Particularly interesting will be to look at the interplay between the collisional and diamagnetic mixing of these levels.

## E. MÖSSBAUER EFFECT RESEARCH

In the twenty-one years since its discovery, the Mössbauer effect has become a mature field with many applications. The program here remains mainly the exploration of new and potentially important extensions of the discipline. In the special ambience of this laboratory, this approach has proved productive over the years. The present thrust is threefold.

- (1) Radio-frequency techniques in Mössbauer spectroscopy.
- (2) Gamma-ray coherence phenomena.
- (3) Studies of specialized solids.

The first category includes the use of radio-frequency fields to obtain precise hyperfine measurements, and to study the production of delayed ultrasound in low-temperature metals. An outgrowth of this work has been the second category,  $\gamma$ -ray optics of resonant media. This arose through consideration of the time structure of frequency-modulated, recoil-free,  $\gamma$  rays after transmission through an absorber. It has occupied center stage during the past year. The third category includes work on intercalation compounds of graphite, an interest of long standing in this laboratory, and also work by S. L. Ruby and collaborators on mixed valence iodine compounds, reported herein.

### 1. GENERATION OF DELAYED ULTRASOUND IN LOW-TEMPERATURE COPPER

G. J. Perlow and W. Potzel

The Mössbauer effect is a very sensitive detector of high-frequency acoustic signals. An emitter in motion at 10 MHz gives an easily discernible signal for particle amplitudes of  $10^{-10}$  cm. An experiment on the production of ultrasound in a copper foil carrying a high frequency (700 MHz) current had led to the observation of sound amplitudes several orders of magnitude larger than expected. Further investigation had shown an incubation period between the application of the pulse and the observation of the sound. The peak sonic amplitude occurs typically 100 microseconds after a short burst of rf power. The power pulse is in the order of 1 watt for 2 microseconds. The foil is a few microns

thick, and doped with  $^{57}\text{Co}$ , and the acoustic motion is detected by the change in the transmission of the 14.4-keV  $\gamma$  ray of  $^{57}\text{Fe}$  through a resonant absorber. The change is caused by the frequency modulation of the gamma ray by the ultrasonic motion of the source via the Doppler effect. The effect was found to be strongly temperature dependent. It is very large when the foil is immersed in superfluid helium, is still quite dramatic in 4.2 K helium liquid, is somewhat smaller in the vapor above the liquid surface and diminishes greatly as the gas is increased in temperature to 20 K. A crucial point in the experiments is whether the motion is in the plane of the foil or perpendicular to it. The latter would be relatively uninteresting. Early experiments, made by tilting the foil, indicated planar motion. We now believe that the effect is connected with the heat flow instabilities (well known but by no means well understood) in low-temperature helium. An additional experiment remains to be performed to test again for planar motion under conditions in which the direction of the gravitational force does not possibly predetermine the result. This requires an additional design of cryostatic equipment and rf resonator.

## 2. QUANTUM BEATS OF RECOIL-FREE $\gamma$ RAYS

When recoil-free radiation is emitted by a source that is vibrating at high enough frequency, the radiation spectrum is observed to have frequency-modulation sidebands. If the radiation is counted with fast-timing techniques and the time interval between the count and some reference phase is recorded and accumulated, no time structure is observed. If on the other hand, part of the spectrum is altered in amplitude or phase by passage through a resonant absorber, the resulting intensity displays a time dependence. It is caused by interference between the different energy components of the photon amplitude. The counting rate contains the vibration frequency and its harmonics. The harmonic constitution depends sensitively on the energy difference between the source and absorber resonances. Only even harmonics appear if the difference is zero, while odd harmonics appear if there is any shift. The ratio of fundamental to second harmonic may be used as a sensitive

measure of such a shift. It is an alternative to velocity spectrometry for this purpose and for small shifts is superior. A report below by Potzel and Perlow and Monahan describes a measurement of second-order Doppler shift by this technique.

An additional feature of the quantum-beat phenomenon shows up if instead of accepting counts during the entire vibration cycle, one records only those in some particular phase interval. With these, one now performs traditional Mössbauer velocity spectroscopy. The velocity spectrum is observed to be strongly distorted from the symmetric frequency modulation case seen in the absence of time selection. In particular each line contains both absorption and dispersion components. The dispersion results in a symmetric steepening of the line profile and an increase of counting rate above background at certain parts of the spectrum, depending on just which phase interval is chosen to be counted. The enhanced intensity is balanced by reduced intensity during other parts of the vibration cycle.

A report by Monahan and Perlow (see Sec. VII.F.a of this report) describes a classical optical theory of the quantum-beat phenomena including the dispersion. Two publications are being prepared. That by Monahan and Perlow on the theory of the process has been submitted to Phys. Rev. A. A paper by Potzel, Perlow, and Monahan on measurement of the second order Doppler shift in iron-beryllium by the harmonic variation in the quantum beats (abstracted below) is in preparation.

Future plans for these investigations: The applications of the quantum-beat phenomena are likely to be numerous. The harmonic ratio method of measurement of small shifts is applicable to problems in solid state physics and to chemistry. Effects which change the lattice parameters even quite slightly will cause a change in isomer shift and can be seen by the technique. Hydrostatic strain is one such. Phase transitions are another. With the aid of an undergraduate student, Anita L. Glover, and aid from a summer visitor, L. E. Campbell, a study is to be made of the energy shift accompanying the Zeeman effect in an applied magnetic field. A preliminary test has given evidence for such a shift, presumably associated with interactions depending on the square of the magnetic field.

A number of theoretical problems remain. While the general solution to the problem as an exercise in classical optics of resonant media has been stated, it is quite complicated. The problem for a thin absorber however has a considerably simpler solution. In ordinary Mössbauer spectroscopy one usually uses the thin absorber approximation for the transmission problem, and alters the parameters describing the (Lorentzian) line shape to get a phenomenological fit to the case of the thick absorber.

It remains to be seen whether a similar approach can prove effective for the quantum beam problem. It can be tested by computer simulation, after the general solution has been programmed for numerical calculation.

Measurement of the Second-Order Doppler Shift in Beryllium Doped with Iron by the Method of Harmonic Ratio of Gamma-Ray Quantum Beats

W. Potzel, G. J. Perlow, and J. E. Monahan

The second-order Doppler shift in Mössbauer spectroscopy dates back to papers of 1960 by B. Josephson, and by Pound and Rebka. They pointed out that, although the mean velocity of a nucleus in a solid averages to zero, its square does not. There is a time dilatation associated with the thermal motion and hence a relativistic temperature effect. It has been studied before in a number of substances, and in particular in Be-Fe. Typically the sample is placed in a temperature controlled enclosure and velocity spectra taken over a range of 500 or more degrees with points perhaps 50 K apart. The shift between points is readily seen. We were interested in a test of the method of harmonic ratios, and repeated the measurement with a total range of 80 K, and points spaced somewhat less than 10 K apart. At each point the ratio of fundamental (5.71 MHz) to second-harmonic amplitude of the counting rate was determined by a least-squares fit; the source was at room temperature and the absorber in a controlled enclosure was varied in temperature above and below it. A temperature change of about 2 K could be determined in about 12 hours of counting. The harmonic ratio could be calibrated in velocity units in a separate experiment involving an absorber moving at any of several fixed velocities. With the calibration, a shift of  $0.625 \text{ m/}^{\circ}\text{K}$  was obtained. It is in reasonable agreement with earlier work. It was not the aim of the project however to refine the earlier data, but rather to determine whether the harmonic-ratio method is capable of measuring small shifts practically. From this experiment, the answer emerges affirmatively.

### 3. IODINE IN UNIDIMENSIONAL, MIXED-VALENCE SOLIDS

There are a variety of stacked organic (or metallorganic) crystalline solids which can be prepared with and without iodine. Structural evidence from x-ray data indicates that the iodine forms a linear array extending through the unit cells. The crystals with iodine have much higher electrical conductivities than those without. We have added  $^{126}\text{I}$  Mössbauer techniques to x-ray, infrared, conductivity, and chemical preparation techniques to help clarify the local structure of the iodine. We find clear evidence that the iodine chain is not formed of a mixture of  $\text{I}_2$  and  $\text{I}^-$  ions. In two categories of metal organic crystals, the  $\text{I}_3^-$  ion appears to form the links in the chain, while in an organic case, the links appear to have both  $\text{I}_3^-$  and  $\text{I}_2$  entities weakly coupled to each other. This last is distinguishable from the  $\text{I}_5^-$  ion links found with iodine in starch.

Three papers have been written concerning the above work. No further effort is planned here.

a. Charge Transfer and Partial Oxidation in the Conductive Hydrocarbon-Iodine Complex "2perylene·3I<sub>2</sub>"

Robert C. Teitelbaum,\* Stanley L. Ruby, and Tobin J. Marks\*

It has long been thought that the highly conductive complexes formed between iodine and various polycyclic aromatic hydrocarbons are molecular complexes, i.e., they contain iodine as  $\text{I}_2$ . In this communication we report resonance Raman and iodine-129 Mössbauer spectroscopic characterization of the form of the iodine in the most highly conductive of these materials: "2perylene·3I<sub>2</sub>." We find that this is not a molecular complex, but rather a partially oxidized, mixed-valence compound, the charge distribution of which can be approximately formulated as  $(\text{perylene})^{+0.4} (\text{I}_3^- \cdot 2\text{I}_2)_{0.4}^-$ .

---

\* Northwestern University, Evanston, Illinois.

b. Rational Synthesis of Unidimensional, Mixed-Valence Solids.

Structure-Oxidation State-Charge Transport Relationships in Iodinated Nickel and Palladium Bisbenzoquinonedioximates

Leo D. Brown,\* Davida Webster Kalina,\* Malcolm S. McClure,\* Steven Schultz,\* Stanley L. Ruby, James A. Ibers,\* Carl R. Kanneur,\* and Tobin J. Marks\*

The experiment consists of a detailed study of crystal structure, stoichiometry, oxidation state, and electron transport in the materials  $\text{Ni}(\text{bqd})_2$ ,  $\text{Pd}(\text{bqd})_2$ ,  $\text{Ni}(\text{bqd})_2\text{I}_{0.02}$ ,  $\text{Ni}(\text{bqd})_2\text{I}_{0.5}\cdot\text{S}$ , and  $\text{Pd}(\text{bqd})_2\text{I}_{0.5}\cdot\text{S}$ , where  $\text{bqd}$  =  $\text{o}$ -benzoquinonedioximato and  $\text{S}$  = an aromatic solvent. The compound  $\text{Pd}(\text{bqd})_2\text{I}_{0.5}\cdot0.52$   $\text{o}$ -dichlorobenzene has been shown by single crystal x-ray diffraction to crystallize in the tetragonal space group  $D_{4h}^2\text{-P}4/\text{mcc}$ , with four formula units in a cell of dimensions  $a = 16.048(7)$  and  $c = 6.367(3)$  Å. Full-matrix least-squares refinement gave a final value of the conventional R index (on F) of 0.052 for 1278 reflections having  $F_0^2 > 3\sigma(F_0^2)$ .

---

\* Northwestern University, Evanston, Illinois.

## F. MONOCHROMATIC X-RAY BEAM PROJECT

S. L. Ruby and P. A. Flinn

Our purpose was to verify experimentally some of the newly predicted phenomena associated with nuclear-resonant Bragg scattering of x rays, and then to use them to produce highly directional and monochromatic x-ray beams by selective reflection of synchrotron radiation. The frequency spread was expected to be six orders of magnitude sharper than any existing beam. Such beams would have angular divergence less than  $10^{-7}$  steradian and a coherence length of some 10 meters, making it possible to extend into the x-ray region the techniques which the laser has brought to visible light—namely, long-path-length interferometry, and eventually holography.

The coherence length of existing x-ray beams ( $<10^{-3}$  cm) is too short for interferometric or holographic experiments. But if a very narrow nuclear-resonant mirror could serve as the monochromator, rather than the usual Bragg-scattering mirror, coherence lengths of several meters would be possible. For adequate intensity in such narrow-energy bands, the new synchrotron storage rings like SPEAR must be used as x-ray sources. Our purpose was to demonstrate that such a nuclear-scattered beam could be extracted from the overwhelmingly more abundant electronically-scattered x rays.

The task for 1978 was to carry out an experiment at the Stanford Synchrotron Radiation Laboratory (SSRL), using crystalline iron which had been enriched to 85%  $^{57}\text{Fe}$  and prepared with 7% silicon. Single crystals of adequate size ( $1 \times 1$  cm) oriented on the [622] plane were cut. Preliminary x-ray measurements using a single reflection revealed only modest mosaic imperfections whose result would be merely to lower the signal calculated for perfect crystals by a factor less than five. For these crystals, an experiment based on the pulsed nature of the synchrotron was designed to ignore a large number of prompt electronically

scattered x rays and then measure the time spectrum of the nuclear scattered, delayed x rays. We built and installed at SSRL a remotely controlled two-crystal x-ray spectrometer for a double-reflection experiment, and a detector system suitable for fast timing at low pulse rates. The limiting problems were the quality of the crystals, after-pulsing in photomultipliers, and beam availability.

Our calculations, which included the final size of the delayed time window and the effects of mosaic spread, indicated a final delayed count rate in excess of 10 counts/sec. An auxiliary experiment at SSRL demonstrated that we could see 5 delayed counts/sec quite clearly above our background in a measurement only 30 minutes long. However, in the actual measurements, no delayed counts were seen. The problem was traced to the fact that the 7% silicon abundance was not uniform across the crystal face, but varied between 6.5 and 7.5%. Calculations based on the diffusion rate of silicon in iron had indicated that this spread should have been 100 times smaller, and the discrepancy is not now understood. Such concentration gradients result in very large intensity losses for the nuclear-scattered radiation and fully explain the missing effect.

No further work on this project is now planned. We would be interested in trying again when a better nuclear-resonant reflector can be developed. All the other known technical problems now appear to be manageable.

## APPLIED PHYSICS

### INTRODUCTION

Although the main business of the Physics Division is basic research, we are also conducting two research programs that are dedicated primarily to applied research goals.

- A. Interaction of Energetic Particles with Solids (M. Kaminsky). This applied research is carried out in conjunction with the basic research studies from which it evolved. The two are closely linked, and they are reported here as one scientific project.
- B. Scanning Secondary-Ion Microprobe (V. E. Krohn, G. R. Ringo)

THIS PAGE  
WAS INTENTIONALLY  
LEFT BLANK

## IX. APPLIED PHYSICS

## A. INTERACTION OF ENERGETIC PARTICLES WITH SOLIDS

This research project is designed to study specific atomic and molecular phenomena that occur when energetic ions (keV—MeV range) interact with both bulk and surfaces of solids. Particularly, fundamental studies of the mechanisms underlying (a) the release of atomic and molecular species from solid surfaces, and (b) the changes in the surface topography and in the microstructure of the implant region under energetic-particle impact are being conducted.

One main goal of these studies is to determine how well-characterized surface regions of lattices with (1) a defined low degree of lattice damage and low gas content, or with (2) a high degree of lattice damage and high gas content caused by trapping of incident ions (e.g.,  $H^+$ ,  $D^+$ ,  $^4He^+$ ) will affect the basic mechanisms of such fundamental atomic processes as ion/atom reflection, secondary ion and electron emission, atom/molecule release by sputtering, and energy-loss mechanisms and charge states of particles penetrating through a lattice. Information of this type is practically nonexistent for light-ion bombardment of solids. However, such information is of significant importance for (a) a better understanding of atomic collision processes, (b) analysis of older data which showed significant scatter and may have been influenced by lattice damage and incident-ion trapping, and (c) for such practical applications as fusion-plasma-impurity control and accelerator technology.

Furthermore, we are conducting studies in direct support of the national fusion-power development program (supported by OFE/DOE and Princeton University). These studies have the following four goals: (1) To identify and develop a sufficient understanding of the processes leading to plasma contaminant release, surface damage and erosion of candidate beam dump, beam limiter and first-wall materials in order to allow the selection of optimum designs. (2) To generate data on plasma contaminant release yields and the degree of surface damage and erosion of low-Z coatings and medium-Z claddings under irradiation conditions that will be meaningful for an assessment of their use for vacuum vessels, armor plates, beam limiters and calorimeters in both near-term and long-term machines. (3) To search for solutions for the control and reduction of plasma contaminant release and surface damage and erosion processes. (4) To conduct cooperative studies with major plasma laboratories in the USA and abroad in order to help in the identification of some of the major sources for, and types of plasma contaminants and surface erosion in existing plasma devices and in the next generation of devices. Some work

in pursuit of these goals was carried out with Princeton's Plasma Physics Laboratory, Lawrence Livermore Laboratory and with the Kurchatov Institute in Moscow.

Finally, experiments will be designed for a search of molecular ions formed by the simultaneous interaction of two independent ion beams (e. g.,  $H^+$  and  $D^+$  in the 10-keV—100-keV range) with solid films. Transmission and backscattering using both monocrystalline and polycrystalline films, will be studied.

The experiments are carried out with well-characterized surfaces of solids which are studied with scanning electron microscopy, transmission electron microscopy, and scanning Auger spectroscopy. The irradiations are being carried out with three different facilities.

One facility is a recently completed (1977) novel accelerator system which produces two ion beams simultaneously, and merges them on the same beam axis before permitting them to interact with solid targets at a chosen angle of incidence. This system allows (1) *in situ* sputtering-yield determination under ultrahigh-vacuum conditions, (2) a search for the formation of molecular species formed by the simultaneous interaction of ions of two different species (e. g.,  $H^+$ ,  $D^+$ ) with solids, and (3) a search for interactive surface effects on the release of target particles and on target surface damage and erosion.

The second facility consists of a low-energy ion accelerator (1 keV to 15 keV). This system allows *in situ* determination for low ion energies under ultrahigh-vacuum conditions. Calibrated sputter-depth profiling will be used to determine the sputter deposits *in situ*. The third facility, upgraded during 1977/78, produced high current densities of mass analyzed ions ( $\sim 10$  mA/cm<sup>2</sup>) in the 10-keV to 120-keV energy range and allows target irradiation in the ultrahigh-vacuum range.

1. THE EFFECT OF DOSE ON THE EVOLUTION OF CAVITIES  
IN 500-keV  $^{4}\text{He}^{+}$ -ION IRRADIATED NICKEL

G. Fenske, S. K. Das, M. Kaminsky, and G. H. Miley\*

While radiation blistering phenomena have been widely studied, the mechanism of blister formation is still not fully understood.<sup>1</sup> Studies on the depth distribution of dislocation damage and of cavities (voids or bubbles) in ion irradiated metals are of great importance in understanding the blistering mechanism and the physics of particle penetration in solids. The aim of the present study is to determine how the size, density and volume fraction of cavities (swelling) change as a function of dose during the initial stages of bubble formation.

Transmission electron microscopy has been used to investigate the effect of total dose on the depth distribution of cavities (voids or bubbles) in nickel irradiated at 500°C with 500-keV  $^{4}\text{He}^{+}$  ions. A transverse sectioning technique, which allows one to obtain the entire depth distribution of cavities and of damage from a single specimen, was utilized. The size, number density and volume fraction of bubbles or voids were measured from the micrographs taken from samples sectioned parallel to the direction of the incident beam.

Figure IX-1(a) and (b) shows typical bright field micrographs of the cavity and dislocation microstructures of nickel foils implanted with 500-keV  $^{4}\text{He}^{+}$  ions to a dose of  $1 \times 10^{21}$  ions/m<sup>2</sup>. The interface between the plating and the irradiated regions is clearly seen in these figures together with the cavities and dislocation damage.

Figure IX-1(a) shows a cavity-denuded-zone extending to a depth of ~0.15 to

\* University of Illinois, Urbana, Illinois.

<sup>1</sup> M. Kaminsky and S. K. Das, "Radiation Blistering—Recent Developments," in The Physics of Ionized Gases [IX Summer School and Symposium on the Physics of Ionized Gases (SPIG-78), Dubrovnik, Yugoslavia, 28 August-2 September 1978], edited by R. K. Janev (Institute of Physics, Beograd, Yugoslavia, 1979), pp. 401-426.

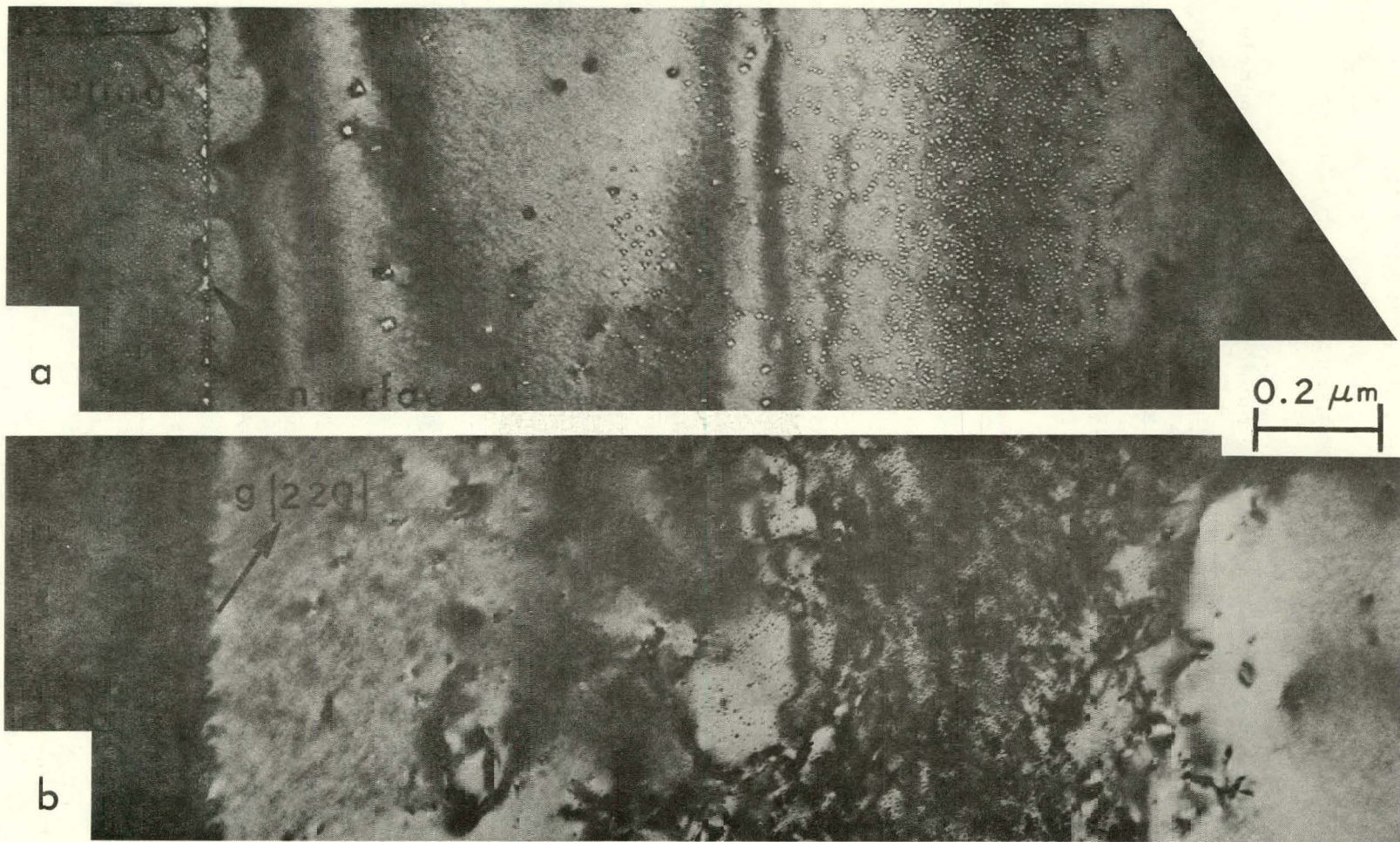


Fig. IX-1. The (a) cavity and (b) dislocation microstructure of nickel irradiated with 500-keV  ${}^4\text{He}^+$  ions at 500°C to a dose of  $1 \times 10^{21}$  ions/ $\text{m}^2$ .

0.2  $\mu\text{m}$  from the interface. A similar trend was also observed for the lower doses ranging from  $2 \times 10^{19}$  to  $1 \times 10^{21}$  ions/ $\text{m}^2$ . A large fraction of the cavities appears to have been heterogeneously nucleated at or near dislocations. This heterogeneous nucleation could be observed more readily for the lower dose range mentioned above.

The dislocation microstructure near the peak in the damage [Fig. IX-1(b)] consists of dense dislocation tangles with a few dislocations extending towards the interface. At depths beyond the peak, the dislocation density decreases more rapidly than the density in regions located between the interface and the peak. Figure IX-2(a)–(d) shows bright field micrographs of the cavities near the peak damage region of nickel irradiated at  $500^\circ\text{C}$  with 500-keV  ${}^4\text{He}^+$  ions to total doses ranging from  $2 \times 10^{19}$  to  $1 \times 10^{21}$  ions/ $\text{m}^2$ . Here, the increase in the cavity diameter and in the number density with increasing dose can be clearly seen.

Figure IX-3(a)–(d) shows quantitative results on the variations in the average cavity diameter and number density, and in the swelling due to cavities as a function of depth for nickel implanted at  $500^\circ\text{C}$  with 500-keV  ${}^4\text{He}^+$  ions, for doses ranging from  $2 \times 10^{19}$  ions/ $\text{m}^2$  to  $1 \times 10^{21}$  ions/ $\text{m}^2$ . For the lowest dose examined,  $2 \times 10^{19}$  ions/ $\text{m}^2$ , the average size is nearly independent of depth (within an experimental accuracy of  $\pm 0.5$  nm). However, as the dose is increased above  $2 \times 10^{19}$  ions/ $\text{m}^2$ , the size is no longer independent of depth. For doses above  $1 \times 10^{20}$  ions/ $\text{m}^2$ , it is observed that the diameters are largest near the surface. For the highest dose of  $1 \times 10^{21}$  ions/ $\text{m}^2$ , the size distribution becomes bimodal with a second peak occurring at a depth of  $\sim 1.15 \mu\text{m}$ , as shown in Fig. IX-2(d). Near the surface, the volume fraction increases slowly with increasing depth, it then increases rapidly beyond  $\sim 0.8 \mu\text{m}$  to maximum values between depths of  $\sim 1.07$  to  $\sim 1.2 \mu\text{m}$ , and then it drops off rapidly to zero at depths beyond  $\sim 1.4$  to  $1.5 \mu\text{m}$ . The solid and dashed curves in Fig. IX-3(a)–(d) show the depth distributions of the energy deposited into damage and of the projected range, respectively.

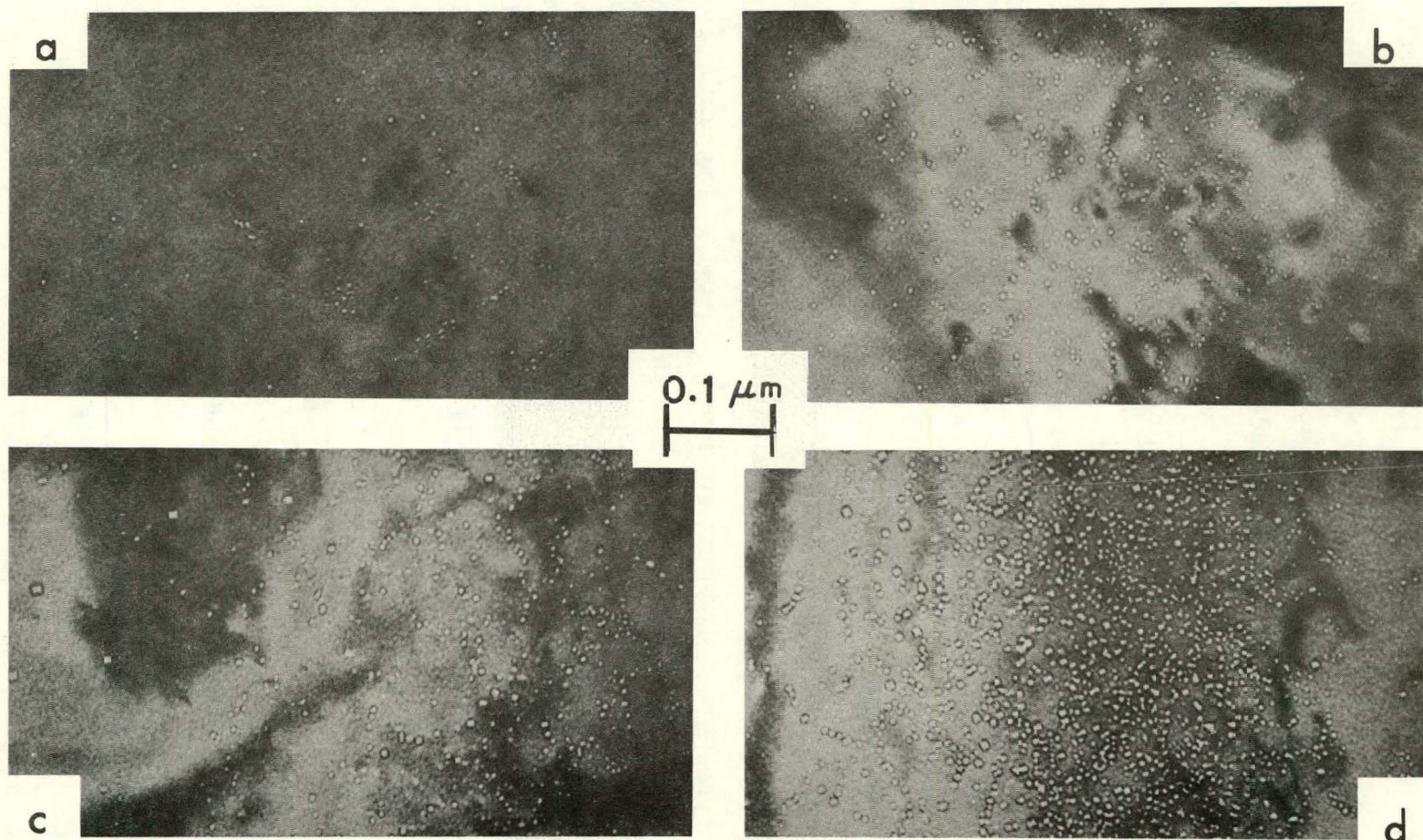


Fig. IX-2. The cavity microstructure near the peak swelling depths for nickel irradiated with 500-keV  ${}^4\text{He}^+$  ions at 500°C to doses of: (a)  $2 \times 10^{19}$  ions/m $^2$ , (b)  $1 \times 10^{20}$  ions/m $^2$ , (c)  $5 \times 10^{20}$  ions/m $^2$ , and (d)  $1 \times 10^{21}$  ions/m $^2$ .

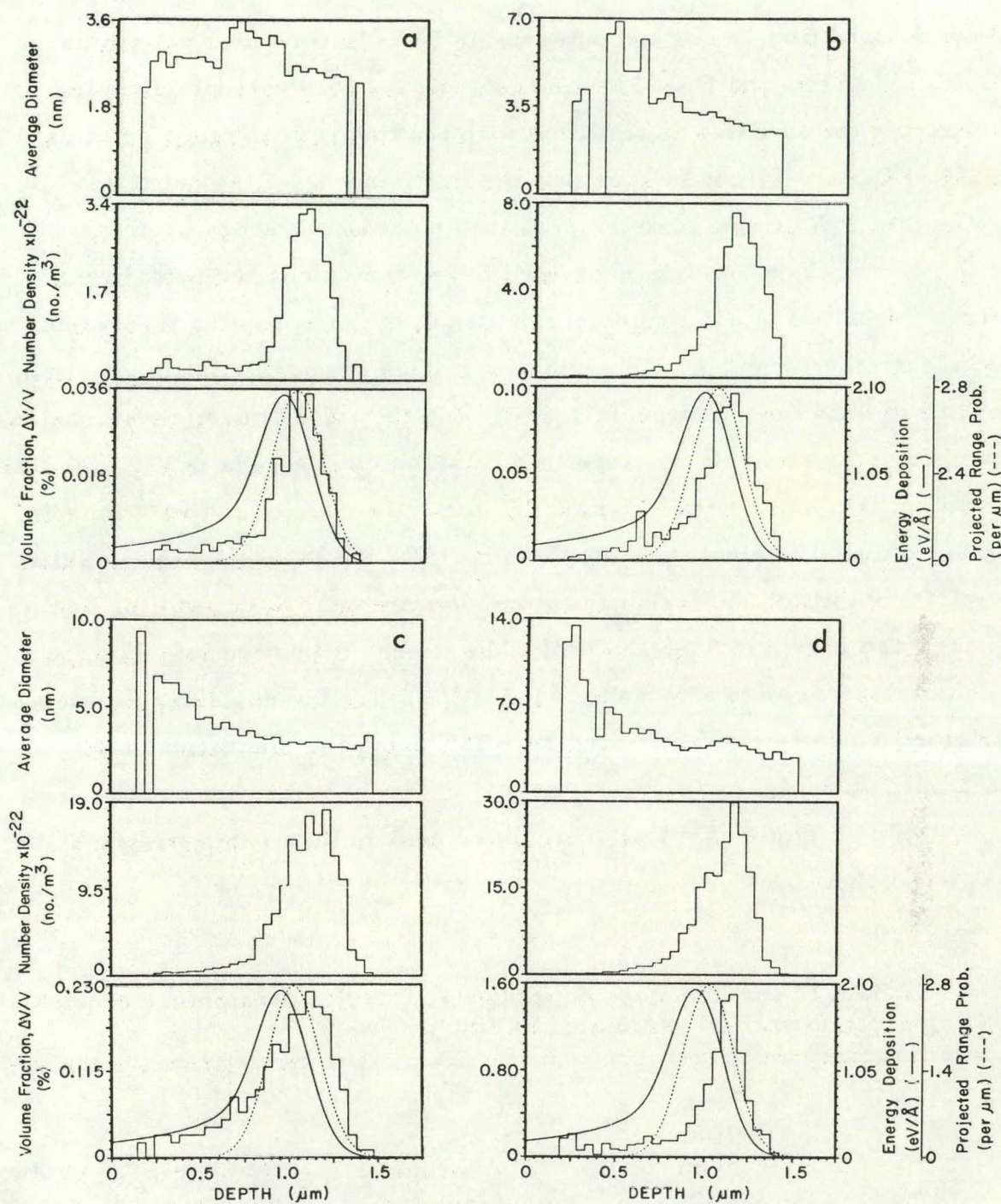


Fig. IX-3. The average diameter, number density, and volume fraction of cavities as a function of depth in nickel implanted at 500°C with 500-keV  ${}^4\text{He}^+$  ions to doses of (a)  $2 \times 10^{19}$  ions/ $\text{m}^2$ , (b)  $1 \times 10^{20}$  ions/ $\text{m}^2$ , (c)  $5 \times 10^{20}$  ions/ $\text{m}^2$ , and (d)  $1 \times 10^{21}$  ions/ $\text{m}^2$ . The plots of volume fraction vs depth include the calculated depth distribution of projected range (dashed curve) and energy deposited into damage (solid curve).

These distributions were computed using Brice's computer programs: COREL, RASE4, and DAMG2 with theoretical LSS electronic stopping. Comparing the swelling distribution with the theoretical range profiles in Fig. IX-3(a)–(d), it is seen that the maximum swelling occurs at depths 8 to 15% deeper than the peak in the projected range profile.

For the data presented here, the calculated peak in the energy deposited into damage occurs at  $\sim 0.95 \mu\text{m}$  assuming theoretical LSS electronic stopping. This underestimates the peak swelling position by 0.15 to  $0.25 \mu\text{m}$ . However, a shift of 0.15 to  $0.25 \mu\text{m}$  in these regions can change the swelling by more than 300% as can be seen in Fig. IX-3(d) for nickel implanted with 500-keV  $\text{He}^+$  ions to a dose of  $1 \times 10^{21} \text{ ions}/\text{m}^2$ . If one reduces the electronic stopping by 15%, the theoretical peak shifts to  $\sim 1.09 \mu\text{m}$  which corresponds to the experimental peak swelling depth for the case shown in Fig. IX-3(a). The energy deposited into damage at  $0.95 \mu\text{m}$  decreases to a value of  $\sim 1.5 \text{ eV}/\text{A}$ ; thus the dpa (displacements per atom) value is overestimated by  $\sim 33\%$  using the theoretical LSS electronic stopping.

Table IX-I lists calculated peak helium concentrations and peak dpa values.

TABLE IX-I. The dose dependence of cavity parameters at peak swelling depth for nickel irradiated at  $500^\circ\text{C}$ .

Dose (ions/ $\text{m}^2$ ) $\times 10^{20}$	Peak helium concen- tration (at. %)	Peak dpa	Average diameter (nm)	Number density (no./ $\text{m}^3$ ) $\times 10^{22}$	Volume fraction (%)
0.2	0.06	0.04	$2.5 \pm 0.5$	3.2	0.04
1.0	0.3	0.22	$2.8 \pm 0.5$	7.6	0.10
5.0	1.5	1.10	$3.0 \pm 0.5$	17.5	0.22
10.0	3.0	2.20	$4.1 \pm 0.5$	29.9	1.50

These studies will be continued to higher doses to allow a search for the onset dose for helium bubble coalescence.

## 2. SURFACE EFFECTS INDUCED BY SIMULATED PLASMA

### a. Temperature Dependence of the Relationship Between Blister Diameter and Blister Skin Thickness for Helium-Ion-Irradiated Nb

S. K. Das and M. Kaminsky

We have reported recently <sup>1,2</sup> the correlation of most probable blister diameter  $D_{mp}$  and blister skin thickness  $t$  for V, Nb, Ni, and Be irradiated at room temperature with  ${}^4He^+$  ions. These studies showed that the  $D_{mp}$ - $t$  relationship is strongly dependent on the type of metal studied and does not follow the relationship  $D_{mp} \propto t^{1.5}$  suggested by the lateral stress model. The aim of the present studies was to determine the temperature dependence of the  $D_{mp}$ - $t$  relationship for annealed polycrystalline Nb irradiated with  ${}^4He^+$  ions in the energy range 20 keV to 500 keV.

The blister diameter and blister skin thickness values were evaluated for only annealed polycrystalline niobium for irradiation at  $300^\circ C$  and at  $700^\circ C$ . The intermediate temperature range between  $300^\circ C$  and  $700^\circ C$  was avoided because this is the region where extensive coalescence of blisters and flaking of blister skin occurs. For the temperature range studied, it was observed that for a given projectile energy the blister skin thickness values did not change within the experimental error limits. Figure IX-4 shows a log-log plot of  $D_{mp}$  against mean blister skin thickness values for irradiation at room temperature, at  $300^\circ C$ , and  $700^\circ C$ . For room temperature irradiation, the  $D_{mp}$ - $t$  relationship is  $D_{mp} = 10.3 t^{1.22}$

<sup>1</sup> S. K. Das, M. Kaminsky, and G. Fenske, J. Nucl. Mater. 76 & 77, 215 (1978).

<sup>2</sup> M. Kaminsky and S. K. Das, J. Appl. Phys. 49, 5673 (1978).

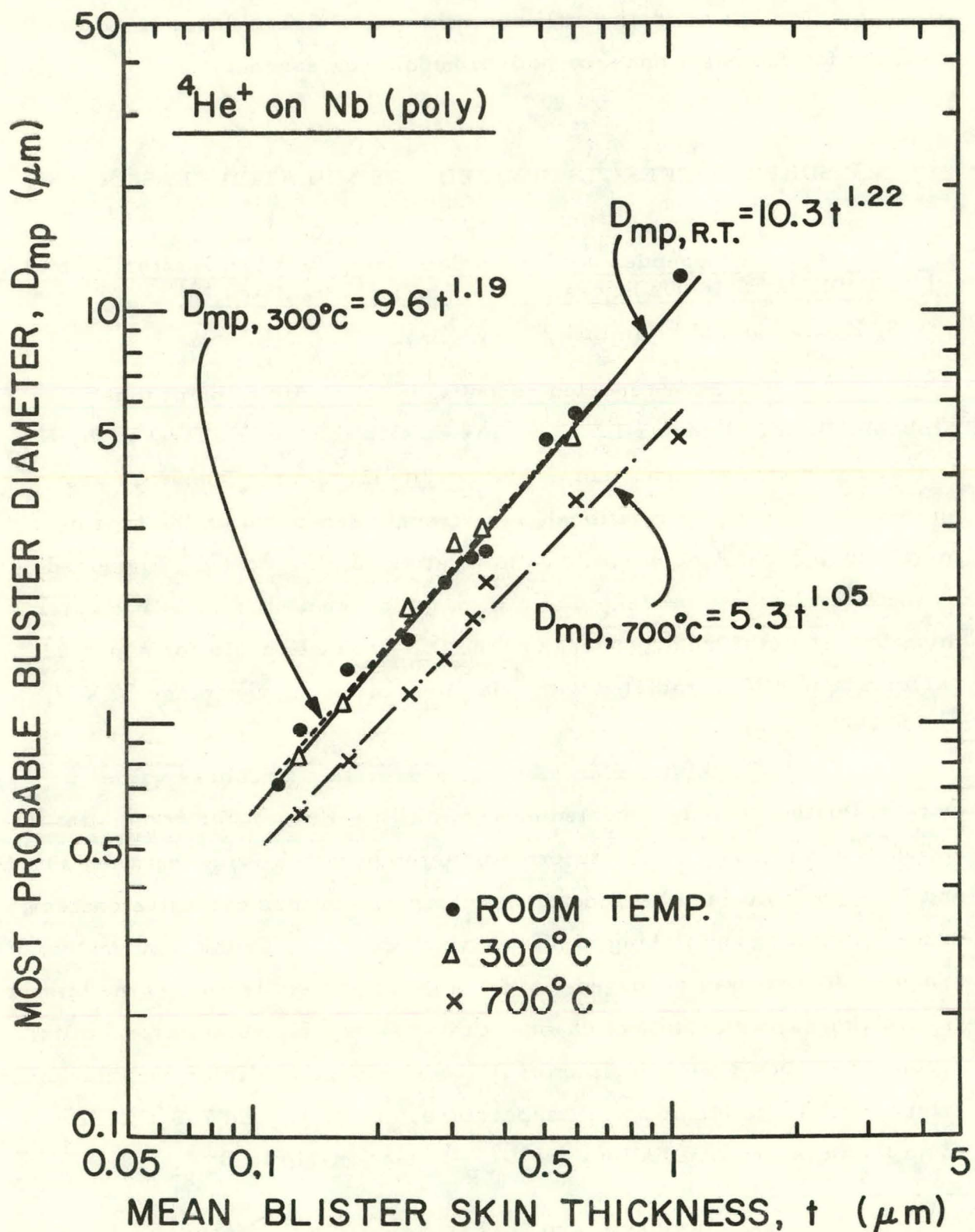


Fig. IX-4. A double logarithmic plot of most probable blister diameter against mean blister skin thickness for annealed polycrystalline Nb irradiated with  ${}^4\text{He}^+$  ions. The plot shows data for  $700^\circ\text{C}$ ,  $300^\circ\text{C}$ , and room temperature irradiation.

as has been given earlier.<sup>3</sup> For irradiation at 300°C a power curve fit through the data points gives the relationship  $D_{mp} = 9.6 t^{1.19}$ ,  $r^2 = 0.99$  (where  $r^2$ , the coefficient of determination, indicates the quality of the power fit), whereas for irradiation at 700°C, the relationship becomes  $D_{mp} = 5.3 t^{1.05}$ ,  $r^2 = 0.98$ , which is almost a linear relationship between the most probable blister diameter and mean blister skin thickness.

These results for niobium irradiated at different temperatures show that as the irradiation temperature is increased, the values for both the exponent and the pre-exponential factor in the D-t relationship decrease. These results are not consistent with the predictions of lateral stress models for blister formation.<sup>4</sup>

<sup>3</sup> S. K. Das, M. Kaminsky, and G. Fenske, *J. Appl. Phys.* (in print).

<sup>4</sup> E. P. Eer Nisse and S. T. Picraux, *J. Appl. Phys.* 48, 9 (1977).

b. Surface Damage of TFTR Protective Plate Candidate Materials by Energetic D<sup>+</sup> Irradiation

M. Kaminsky and S. K. Das

Experiments were conducted to determine the surface damage of ATJ graphite, V, Cu, and Type 316 stainless steel under 60-keV D<sup>+</sup> irradiation. These results are compared with our earlier studies on Mo and TZM alloy.<sup>1</sup> The irradiations were conducted in the pulsed mode, and the irradiation conditions were similar to those described earlier.<sup>1-3</sup>

Figure IX-5 shows scanning electron micrographs of polycrystalline materials irradiated with 60-keV D<sup>+</sup> for 2500 pulses (the total

<sup>1</sup> S. K. Das, M. Kaminsky, and P. Dusza, *J. Vac. Sci. Technol.* 15(2), 710-713 (1978).

<sup>2</sup> S. K. Das and M. Kaminsky, *Nucl. Metallurgy* 10, 240-254 (1973).

<sup>3</sup> S. K. Das and M. Kaminsky, Proceedings of the 5th Symposium on Engineering Problems of Fusion Research, IEEE Pub. No. 73CH0843-3-NPS (IEEE Nuclear and Plasma Sciences Society, New York, 1974), pp. 31-36.

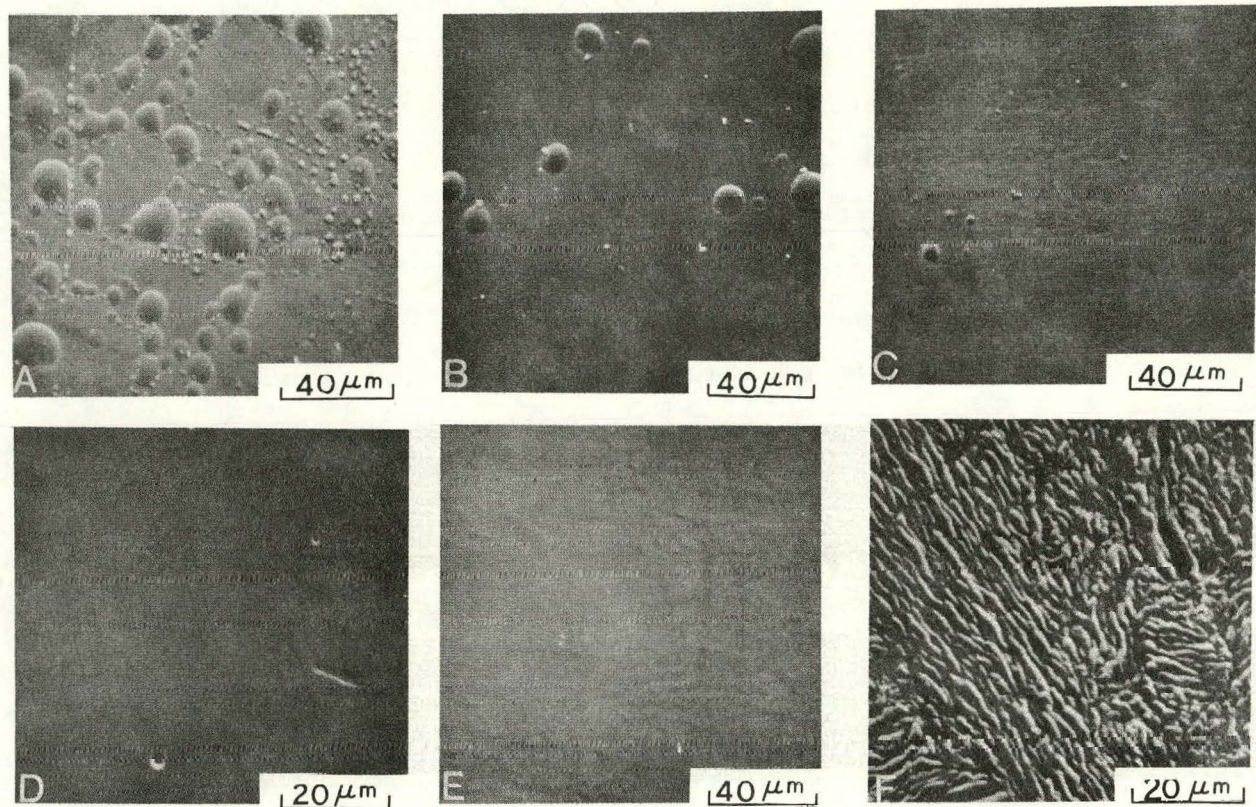


Fig. IX-5. Scanning electron micrographs of surfaces irradiated with 60-keV  $D^+$  for 2500 pulses (a) copper, (b) molybdenum, (c) TZM alloy, (d) type 316 stainless steel, (e) vanadium, and (f) ATJ graphite.

dose accumulated is  $8.1 \times 10^{18}$  ions/cm<sup>2</sup>). For this dose blisters can be readily seen for Cu [Fig. IX-5(a)], Mo [Fig. IX-5(b)], and TZM alloy [Fig. IX-5(c)] surfaces, but no blisters were observed on Type 316 stainless steel [Fig. IX-5(d)] and vanadium [Fig. IX-5(e)] surfaces. For the case of ATJ graphite, the surface damage was observed in the form of ridges and grooves [Fig. IX-5(f)]. In the case of copper, many large blisters with diameters ranging from 3.5  $\mu\text{m}$  to 46  $\mu\text{m}$  are observed in addition to some small ones (average diameter  $\sim 2 \mu\text{m}$ ).

For the case of Mo, the blister diameters range from 2  $\mu\text{m}$  to 17  $\mu\text{m}$ , whereas the largest blister observed for TZM is only  $\sim 9 \mu\text{m}$ . The blister density of the large blisters is the highest in the case of copper ( $1.1 \times 10^5$  blisters/cm<sup>2</sup>) and decreases to  $7.3 \times 10^4$  blisters/cm<sup>2</sup> for Mo and is  $< 3 \times 10^3$  blisters/cm<sup>2</sup> for TZM alloy. These observations of blister formation for Cu and Mo but not for stainless steel and V are related to the differences in the permeability of deuterium in these materials. For example, the data on the permeability of hydrogen through metals at 500°C show<sup>4</sup> that the permeation for V is four orders of magnitude higher than they are for Mo, and the one for Type 430 stainless steel to be two orders of magnitude higher than that for Mo. The reason for the difference in the degree of blistering between Cu, Mo, and TZM alloy is not quite clear, since permeability of hydrogen in Cu is about a factor of 2–8 higher than that for Mo in the temperature range of 200–600°C.<sup>5</sup> The difference may be partly due to the differences in the yield strength between Cu, Mo, and TZM alloy.

The results described so far are typical for pulsed irradiations. We have shown earlier<sup>1</sup> that the surface temperature of Mo irradiated with 60-keV D<sup>+</sup> in the continuous mode was 100–180°C higher than for

<sup>4</sup> L. D. Hansborough, *Technology of Controlled Thermonuclear Fusion Experiments and the Engineering Aspects of Fusion Reactors* (Technical Information Service, Springfield, Virginia, 1974), CONF-721111, p. 92.

<sup>5</sup> R. W. Roberts and T. A. Vanderslice, Ultrahigh Vacuum and Its Applications (Prentice-Hall, Englewood Cliffs, N.J., 1963), p. 110.

the pulsed mode. This difference in temperature causes a reduction in blistering for the continuous mode of irradiation. Furthermore, for 60-keV  $D^+$  irradiation of Mo held at  $300^\circ C$ , no blisters could be detected.

The ridges observed in the case of ATJ graphite (Fig. IX-5) have an average width of  $\sim 0.6 \mu m$  with a standard deviation of  $\sim 0.3 \mu m$ . An examination of the cross section of the ridges in fractured samples indicates that they are not hollow. The mechanism of formation of these ridges is not clear at present. Preliminary results indicate that even though there is considerable surface damage, the actual surface erosion may not be very severe for the irradiation conditions studied.<sup>6</sup> More detailed quantitative studies of the dependence of height and width of the ridges on  $D^+$  energy and dose are in progress.

<sup>6</sup> M. Kaminsky, S. K. Das, and J. Cecchi, to appear in 10th Symposium on Fusion Technology, Padova, Italy, 4-8 September 1978.

c. Damage of Niobium Surfaces Caused by Bombardment with  $^4He^+$  Ions of Different Energies Typical for T-20

M. I. Guseva,\* V. Gusev,\* Yu. V. Martynenko,\* S. K. Das, and M. Kaminsky

The first wall of a fusion reactor will be exposed to helium projectiles having a broad energy spectrum. Only a few studies of the surface damage of materials under helium ion impact at different energies have been conducted previously. These few existing studies were also performed by irradiating samples with monoenergetic helium ions sequentially at different energies, but over a small energy range. The authors reported<sup>1</sup> results on blistering of cold-worked niobium irradiated sequentially with  $^4He^+$  ions for the energy range of 3-500 keV to a total dose of  $1.0 C/cm^2$ . Wilson et al.<sup>2</sup> also studied a

\* Kurchatov Institute of Atomic Energy, Moscow, USSR.

<sup>1</sup> M. I. Guseva, V. Gusev, Yu. L. Krasulin, Y. V. Martynenko, S. K. Das, and M. Kaminsky, J. Nucl. Mater. 63, 245 (1976).

<sup>2</sup> K. L. Wilson, L. G. Haggmark, and R. A. Langley, Plasma Wall Interactions (Pergamon Press, Oxford, England, 1977), p. 401.

multiple energy sequential irradiation of stainless steel with  ${}^4\text{He}^+$  ions for the energy range of 3—20 keV. It should be noted that theoretical calculations of the energy spectrum of helium projectiles striking the first wall surfaces indicate that for near-term machines a substantial fraction of the helium projectiles will have energies up to 3.5 MeV.<sup>3,4</sup> Figure IX-6 shows a plot of the  $\text{He}$  ion spectrum (dashed line) per energy interval as a function of energy calculated<sup>4</sup> for the Tokamak T-20. The expression used for this calculation (as given in Fig. IX-6) has been discussed by the authors in an earlier publication,<sup>5</sup> where a preliminary attempt was made to simulate the calculated spectrum (up to 1.8 MeV) using monoenergetic irradiation. The actual energies used for the irradiations are shown by open squares. In the previous study<sup>5</sup> only annealed polycrystalline niobium targets were irradiated for total doses of 0.12 and  $1.12 \text{ C/cm}^2$ . The aim of the present studies was to study surface damage due to blistering of both annealed and cold-worked niobium (a candidate first wall material for T-20) irradiated sequentially with  ${}^4\text{He}^+$  ions with energies shown in Fig. IX-6 for a significantly larger total dose of  $5.0 \text{ C/cm}^2$ . This higher dose was chosen so that the critical dose for blister appearance is exceeded for many of the monoenergetic irradiations. The individual doses for each energy were chosen to match the calculated spectrum shown in Fig. IX-6 for T-20, and are listed in the following in parentheses in units of  $\text{C cm}^{-2}$  for a given energy in keV: 0.5(0.8), 1(0.886), 2(1.287), 3.5(0.725), 5(0.315), 8(0.052), 13(0.058), 29(0.063), 30(0.08), 45(0.1), 65(0.072), 90(0.072), 150(0.14), 200(0.03), 250(0.01), 300(0.025), 500(0.08), 1,000(0.11), 1,500(0.11), and 1,800(0.0084).

<sup>3</sup> W. Bauer, K. L. Wilson, C. L. Bisson, L. G. Haggmark, and R. J. Goldston, *J. Nucl. Mater.* 76 & 77, 396 (1978).

<sup>4</sup> V. M. Gusev, M. I. Guseva, Yu. L. Krasulin, Y. V. Martynenko, Kurchatov Institute of Atomic Energy Report No. IAE-2529 (1975), ANL Trans-993.

<sup>5</sup> S. K. Das, M. Kaminsky, V. M. Gusev, M. I. Guseva, Y. V. Martynenko, Yu. L. Krasulin, and I. A. Rozina, to appear in *Proceedings of 7th International Conference on Atomic Collisions in Solids*, Moscow, USSR, September 1977.

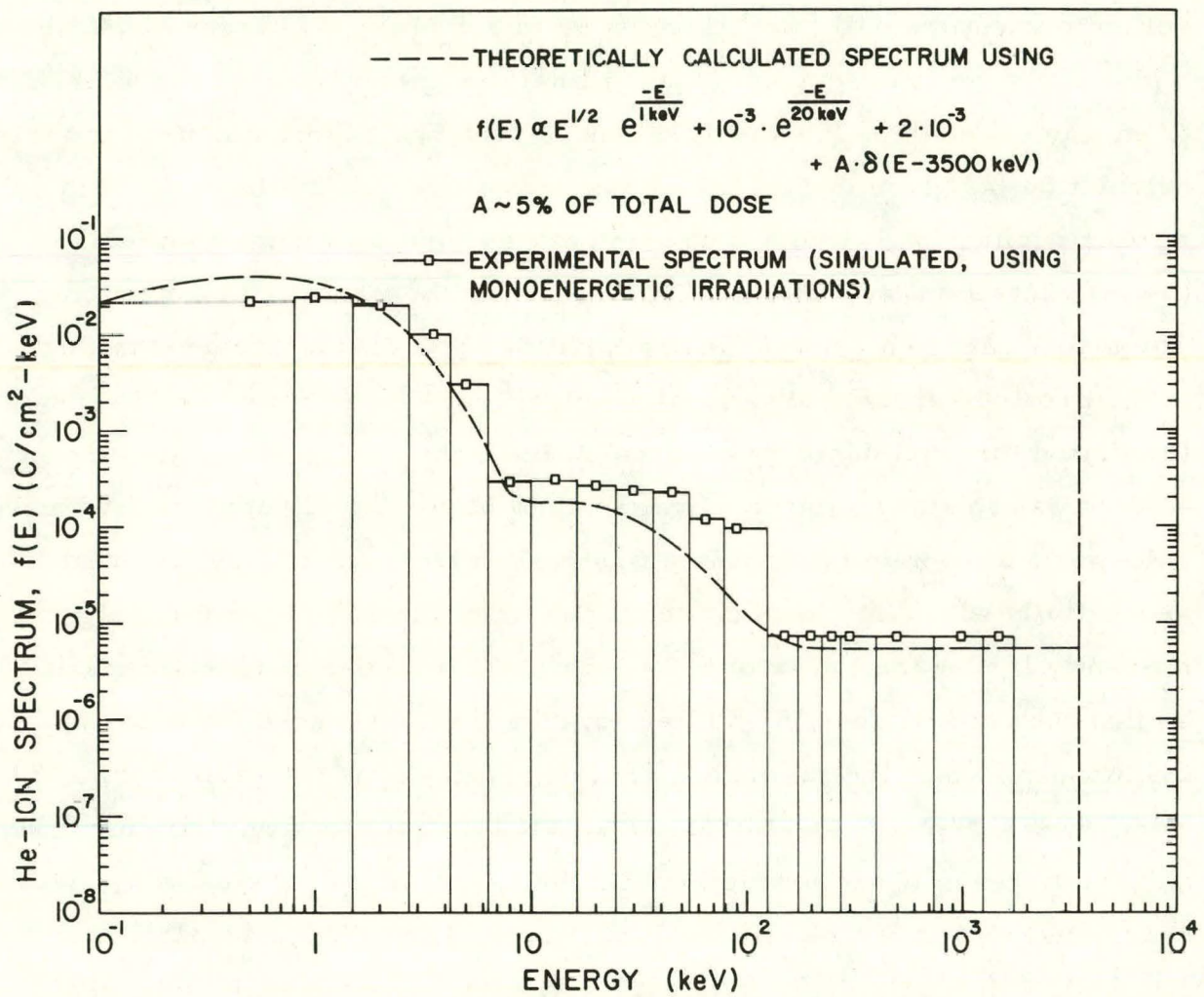


Fig. IX-6. Double logarithmic plot of He ion spectrum (dashed line) per energy interval as a function of energy calculated for Tokamak T-20 by Guseva et al.<sup>4</sup> Open squares show actual  $\text{He}^+$  energies used to simulate the theoretical spectrum.

### Irradiation of Cold-Worked Nb

Figure IX-7(A) shows a typical surface of cold-worked Nb after irradiations with  ${}^4\text{He}^+$  ions with increasing energy from 0.5 to 90 keV. Here the blister diameters range from 0.1  $\mu\text{m}$  to 3  $\mu\text{m}$  and most of the blisters have exfoliated. As in the case of annealed Nb, here also the blisters fall into several size classes, but the two most dominant ones have most probable blister diameters,  $D_{\text{mp}}$  of  $\sim 0.27 \mu\text{m}$  and  $\sim 2.0 \mu\text{m}$ . The skin thickness of the larger blisters ( $D_{\text{mp}} \sim 2.0 \mu\text{m}$ ) was measured to be  $\sim 0.23 \mu\text{m}$ , indicating that these blisters were most likely caused by the irradiation with the 45-keV  ${}^4\text{He}^+$  ions, a result which is similar to the one observed for the annealed target. Figure IX-7(B) shows the same area as in Fig. IX-7(A) but after irradiation with 150–1800-keV  ${}^4\text{He}^+$  irradiation for a higher dose of  $0.66 \text{ C/cm}^2$  than that used earlier for the annealed Nb target. In this case, the dose for the 150-keV  ${}^4\text{He}^+$  irradiation, which is the most dominant component in this energy range, was increased from 0.14 to  $0.3 \text{ C/cm}^2$ , a dose which is much higher than the critical dose for blister formation of cold-worked Nb for a single irradiation with 150-keV  ${}^4\text{He}^+$  ions.<sup>6,7</sup> This was intentionally done to see the effect of prior sequential irradiation (with 0.5–90-keV  ${}^4\text{He}^+$ ) on blister formation during subsequent irradiation with high energy ions (150–1800 keV). Now, a few additional blisters [marked by arrows in Fig. IX-7(B)] can be seen which were not present before [see Fig. IX-7(A)]. Figure IX-7(C) shows a cold-worked Nb surface which has been irradiated only with 150–1800-keV  ${}^4\text{He}^+$  ions (and not preirradiated with 0.5–90-keV  ${}^4\text{He}^+$  ions) for the same doses as the target shown in Fig. IX-7(B). By comparing Fig. IX-7(B) and IX-7(C), one can clearly see that prior irradiation with 0.5–90-keV  ${}^4\text{He}^+$  has helped in significantly reducing blistering.

<sup>6</sup> S. K. Das, M. Kaminsky, and G. Fenske, *J. Appl. Phys.* (in press).

<sup>7</sup> S. K. Das and M. Kaminsky, Radiation Effects on Solid Surfaces (Proceedings of the 170th Meeting of the American Chemical Society, Chicago, Illinois, 25–26 August 1975), edited by M. Kaminsky (American Chemical Society, 1976), p. 112.

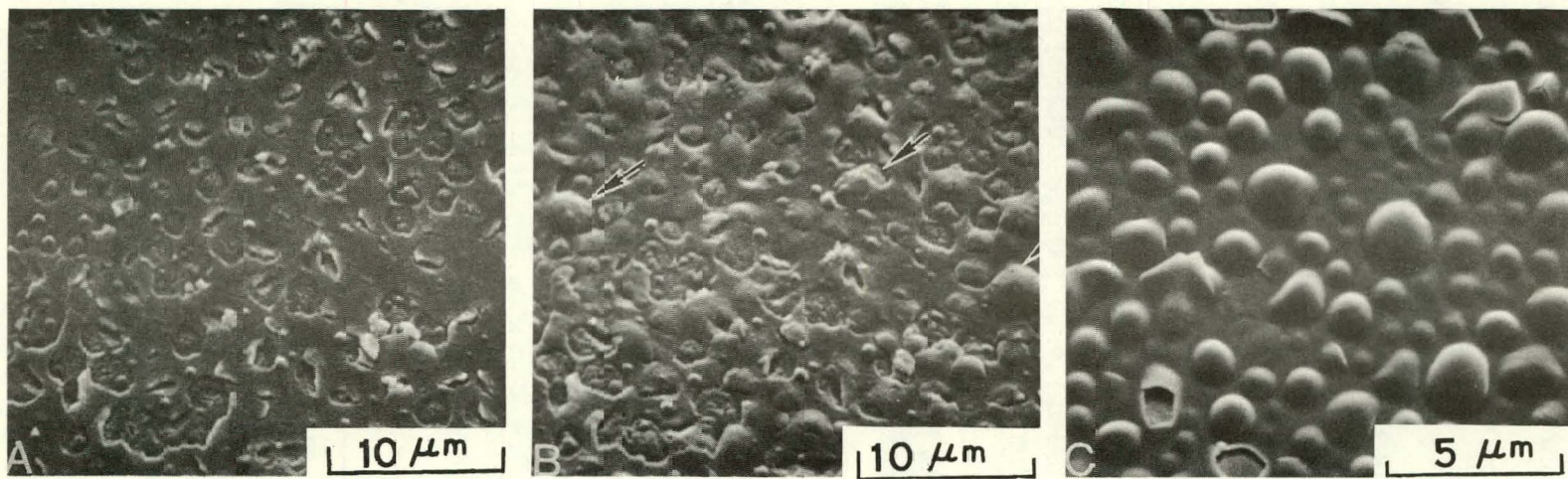


Fig. IX-7. SEMs of cold-worked Nb irradiated at room temperature (A) with 0.5–90-keV  ${}^4\text{He}^+$  ions for a dose of  $4.5 \text{ C/cm}^2$ ; (B) the same area as in (A) after further irradiation with 150–1800-keV  ${}^4\text{He}^+$  ions for a total dose of  $0.66 \text{ C/cm}^2$ ; (C) with only 150–1800-keV  ${}^4\text{He}^+$  ions for a dose of  $0.66 \text{ C/cm}^2$ .

For example, the blister density has been reduced to  $\sim 8 \times 10^5$  blisters/cm<sup>2</sup> for 0.5–1800-keV  $^4\text{He}^+$  irradiated sample as compared to  $3 \times 10^6$  blisters/cm<sup>2</sup> for the 150–1800-keV  $^4\text{He}^+$  irradiated sample. The largest blister diameter in the 0.5–1800-keV  $^4\text{He}^+$  irradiated sample is  $\sim 3 \mu\text{m}$ , whereas it is  $\sim 9 \mu\text{m}$  for the sample irradiated only with 150–1800-keV  $^4\text{He}^+$  ions.

In summary, the results presented here indicate that for sequential irradiation with  $^4\text{He}^+$  ions having an energy spectrum similar to that expected for the Tokamak T-20, most of the erosion due to blistering (for the dose range studied) is contributed by the 0.5–150-keV  $^4\text{He}^+$  ion component. For a total dose of 0.5 C/cm<sup>2</sup>, the erosion yield due to helium blistering of Nb ranges from  $(5.4 \pm 2.0) \times 10^{-3}$  to  $(1.5 \pm 0.7) \times 10^{-2}$  atoms/ion. For the cold-worked Nb target the results indicate clearly that the  $^4\text{He}^+$  implantations for the energy range from 0.5 to 90 keV help to reduce both the density and diameter of blisters formed by subsequent He-implantation for the energy ranging from 150 to 1800 keV.

## B. SCANNING SECONDARY-ION MICROPROBE

## MICROSCOPIC LOCATION OF TRACER ISOTOPES

V. E. Krohn and G. R. Ringo

The aim of this project is to improve the present ion-microprobe analyzer very significantly in space resolution and mass resolution to make it a more useful instrument, particularly in biology. The ion-microprobe analyzer generally uses a beam of primary ions focused to a point whose diameter determines the space resolution of the instrument and is at present 1 to 2  $\mu\text{m}$ . The primary beam is scanned over the specimen and a map of the distribution of an element or isotope of interest in the specimen is built up by detection of the secondary ions produced in the specimen and analyzed by a mass spectrometer of appropriate resolution, usually around 300.

We believe this instrument could be very useful in biology to map isotopes such as  $^{14}\text{C}$ ,  $^{17}\text{O}$ , etc. used as tracers. However, for full usefulness it will be necessary to identify all the interesting secondary ions (by resolving the various mass doublets).

To achieve high space resolution it is necessary to stop the beam down to a very small diameter to reduce the effect of lens aberrations. This means a very bright ion source is needed to get practical yields of secondary ions. We have developed such a source<sup>1</sup> which uses field evaporation of ions from liquid metals. Our source uses gallium and gives about  $10^6 \text{ A cm}^{-2} \text{ steradian}^{-1}$  at 21 kV.

The type of source which appears to be the most satisfactory considering such problems as stability of position and reliability of operation is one in which the gallium is fed on the surface of a tapered tungsten needle of about 5  $\mu\text{m}$  tip diameter.

<sup>1</sup>V. E. Krohn and G. R. Ringo, Int. J. Mass Spectry. Ion Phys. 22, 307 (1976).

Experiments with a heated source indicate liquid indium will be comparable to gallium in performance but tin will be much inferior.

THIS PAGE  
WAS INTENTIONALLY  
LEFT BLANK

## PUBLICATIONS FROM 1 APRIL 1978 THROUGH 31 MARCH 1979

The papers listed here are those whose publication was noted by the reporting unit of the Laboratory in the 1-year period stated above. The dates on the journals therefore often precede this period, and some dated within the period will be listed subsequently. The list of "journal articles and book chapters," which also includes letters and notes, is classified by topic; the arrangement is approximately that followed in the Table of Contents of this Annual Review. The "reports at meetings" include abstracts, summaries, and full texts in volumes of proceedings; they are listed chronologically.

A. PUBLISHED JOURNAL ARTICLES AND BOOK CHAPTERS

## 1. ELASTIC SCATTERING OF 162-MeV PIONS BY NUCLEI

B. Zeidman, C. Olmer, D. F. Geesaman, R. L. Boudrie,\*  
R. H. Siemssen,<sup>†</sup> J. F. Amann,<sup>‡</sup> C. L. Morris,<sup>‡</sup> H. A. Thiessen,<sup>‡</sup>  
G. R. Burleson,<sup>§</sup> M. J. Devereux,<sup>§</sup> R. E. Segel, and L. W.  
Swenson||

Phys. Rev. Lett. 40, 1316-1320 (15 May 1978)

Reprinted: Phys. Rev. Lett. 40, 1539-1542 (5 June 1978)

2. GAMMA-RAY STUDY OF PION-INDUCED REACTIONS ON THE  
NICKEL ISOTOPES

H. E. Jackson, S. B. Kaufman,<sup>¶</sup> D. G. Kovar, L. Meyer-  
Schützmeister, K. E. Rehm, J. P. Schiffer, S. L. Tabor, S. E.  
Vigdor, T. P. Wangler, L. L. Rutledge, Jr., \*\* R. E. Segel, \*\*  
R. L. Burman,<sup>‡</sup> P. A. M. Gram,<sup>‡</sup> R. P. Redwine,<sup>‡</sup> and M. A.  
Yates-Williams<sup>‡</sup>

Phys. Rev. C 18, 2656-2665 (December 1978)

\* University of Colorado, Boulder, Colorado.

<sup>†</sup> KVI, Groningen, Netherlands.

<sup>‡</sup> Los Alamos Scientific Laboratory, Los Alamos, New Mexico.

<sup>§</sup> New Mexico State University, Las Cruces, New Mexico.

|| Oregon State University, Corvallis, Oregon.

<sup>¶</sup> Chemistry Division, ANL.

\*\* Northwestern University, Evanston, Illinois.

3. QUADRUPOLE SCATTERING OF PIONS BY  $^9\text{Be}$   
 D. F. Geesaman, C. Olmer, B. Zeidman, R. L. Boudrie,\* R. H. Siemssen,† J. F. Amann,‡ C. L. Morris,‡ H. A. Thiessen,‡ G. R. Burleson,§ M. J. Devereux,§ R. E. Segel, and L. W. Swenson||  
*Phys. Rev. C* 18, 2223-2226 (November 1978)

4. PION DOUBLE-CHARGE EXCHANGE ON  $^{16}\text{O}$  AND  $^{18}\text{O}$   
 R. L. Burman,‡ M. P. Baker,‡ M. D. Cooper,‡ R. H. Heffner,‡ D. M. Lee,‡ R. P. Redwine,‡ J. E. Spencer,‡ T. Marks,¶ D. J. Malbrough,¶ B. M. Preedom,¶ R. J. Holt, and B. Zeidman  
*Phys. Rev. C* 17, 1774-1786 (May 1978)

5. CHANNELING OF POSITIVE AND NEGATIVE PIONS IN A SILICON CRYSTAL  
 T. H. Braid, D. S. Gemmell, R. E. Holland, W. J. Pietsch, A. J. Ratkowski, J. P. Schiffer, T. P. Wangler, J. N. Worthington, B. Zeidman, C. L. Morris,‡ and H. A. Thiessen‡  
*Phys. Rev. B* 19, 130-134 (1 January 1979)

6. BEAM BUNCHER FOR HEAVY IONS  
 F. J. Lynch,\*\*\* R. N. Lewis,\*\*\* L. M. Bollinger, W. Henning, and O. D. Despe\*\*\*  
*Nucl. Instrum. Methods* 159, 245-263 (1979)

7. COMPLETE FUSION OF  $^{16,18}\text{O}$  WITH  $^{24,26}\text{Mg}$   
 S. L. Tabor, D. F. Geesaman, W. Henning, D. G. Kovar, K. E. Rehm, and F. W. Prosser, Jr.††  
*Phys. Rev. C* 17, 2136-2143 (June 1978)

8. ELASTIC EXCITATION FUNCTION OF  $^{12}\text{C}$  ON  $^{40}\text{Ca}$  AT  $180^\circ$   
 T. R. Renner, J. P. Schiffer, D. Horn,‡‡ G. C. Ball,‡‡ and W. G. Davies‡‡  
*Phys. Rev. C* 18, 1927-1928 (October 1978)

\* University of Colorado, Boulder, Colorado.

† KVI, Groningen, Netherlands.

‡ Los Alamos Scientific Laboratory, Los Alamos, New Mexico.

§ New Mexico State University, Las Cruces, New Mexico.

|| Oregon State University, Corvallis, Oregon.

¶ University of South Carolina, Columbia, South Carolina.

\*\*\* Electronics Division, ANL.

†† University of Kansas, Lawrence, Kansas.

‡‡ Chalk River Nuclear Laboratories, Chalk River, Ontario, Canada.

9. SURFACE TRANSPARENCY IN  $^{12}\text{C}$  ELASTIC SCATTERING FROM  $^{40,42,48}\text{Ca}$   
 T. R. Renner  
 Phys. Rev. C 19, 765-776 (March 1979)  
 Ph.D. Thesis, University of Chicago, 1978

10.  $^{16}\text{O} + ^{40}\text{Ca}$  INELASTIC SCATTERING AND DIRECT-REACTION CALCULATIONS IN HEAVY-ION SCATTERING  
 K. -E. Rehm, W. Henning, J. R. Erskine, and D. G. Kovar  
 Phys. Rev. Lett. 40, 1479-1482 (5 June 1978)

11. RESONANT EFFECTS IN THE REACTION  $^{24}\text{Mg}(\text{O}, ^{12}\text{C})^{28}\text{Si}$   
 M. Paul, S. J. Sanders, J. Cseh, D. F. Geesaman, W. Henning,  
 D. G. Kovar, C. Olmer, and J. P. Schiffer  
 Phys. Rev. Lett. 40, 1310-1312 (15 May 1978)

12. ENERGY DEPENDENCE OF ELASTIC SCATTERING AND ONE-NUCLEON TRANSFER REACTIONS INDUCED BY  $^{16}\text{O}$  ON  $^{208}\text{Pb}$ . I  
 Steven C. Pieper, M. H. Macfarlane, D. H. Gloeckner, D. G. Kovar, F. D. Becchetti,\* B. G. Harvey,\* D. L. Hendrie,\* H. Homeyer,\* J. Mahoney,\* F. Pühlhofer,\* W. von Oertzen,\* and M. S. Zisman\*  
 Phys. Rev. C 18, 180-204 (July 1978)

13. ENERGY DEPENDENCE OF ELASTIC SCATTERING AND ONE-NUCLEON TRANSFER REACTIONS INDUCED BY  $^{16}\text{O}$  ON  $^{208}\text{Pb}$ . II  
 C. Olmer,\* M. Mermaz,\* M. Buenerd,\* C. K. Gelbke,\* D. L. Hendrie,\* J. Mahoney,\* D. K. Scott,\* M. H. Macfarlane, and S. C. Pieper  
 Phys. Rev. C 18, 205-222 (July 1978)

14. YRAST TRAPS AND VERY HIGH-SPIN YRAST STATES IN  $^{152}\text{Dy}$   
 T. L. Khoo, R. K. Smith, B. Haas,† O. Häusser,† H. R. Andrews,† D. Horn,† and D. Ward†  
 Phys. Rev. Lett. 41, 1027-1030 (9 October 1978)

15. OPTIMUM Q VALUE IN HEAVY-ION-INDUCED NEUTRON TRANSFER AT THE COULOMB BARRIER  
 W. Henning, Y. Eisen, H. -J. Körner, D. G. Kovar, J. P. Schiffer, S. Vigdor, and B. Zeidman  
 Phys. Rev. C 17, 2245-2247 (June 1978)

\* Lawrence Berkeley Laboratory, Berkeley, California.

† Chalk River Nuclear Laboratories, Chalk River, Ontario, Canada.

16. SEARCH FOR STRUCTURE IN THE FUSION OF  $^{16}\text{O} + ^{40}\text{Ca}$   
 D. F. Geesaman, C. N. Davids, W. Henning, D. G. Kovar,  
 K. - E. Rehm, J. P. Schiffer, S. L. Tabor, and F. W. Prosser, Jr.\*  
*Phys. Rev. C* 18, 284-289 (July 1978)

17. MASS AND  $\beta$  DECAY OF THE NEW ISOTOPE  $^{57}\text{Cr}$   
 C. N. Davids, D. F. Geesaman, S. L. Tabor, M. J. Murphy,  
 E. B. Norman, and R. C. Pardo  
*Phys. Rev. C* 17, 1815-1821 (May 1978)

18. MASS AND  $\beta$  DECAY OF THE NEW NEUTRON-RICH ISOTOPE  $^{60}\text{Mn}$   
 Eric B. Norman, Cary N. Davids, Martin J. Murphy, and  
 Richard C. Pardo  
*Phys. Rev. C* 17, 2176-2184 (June 1978)

19. POLARIZATION OF NEUTRONS FROM (p, n) REACTIONS ON  
 MEDIUM-WEIGHT NUCLEI AT ISOBARIC ANALOG RESONANCES  
 E. H. Sexton, R. E. Benenson, A. J. Elwyn, J. E. Monahan,  
 F. T. Kuchnir, F. P. Mooring, J. F. Lemming, and R. W. Finlay  
*Nucl. Phys.* A298, 269-284 (3 April 1978)

20. SEARCH FOR  $+\frac{1}{3}\text{e}$  FRACTIONAL CHARGES IN Nb, W, AND Fe  
 METAL  
 J. P. Schiffer, T. R. Renner, D. S. Gemmell, and F. P. Mooring  
*Phys. Rev. D* 17, 2241-2244 (1 May 1978)

21. MAGNETIC MOMENT OF THE FIRST EXCITED STATE OF  $^{99}\text{Mo}$   
 T. V. Ragland,† R. J. Mitchell,† R. P. Scharenberg,† R. E.  
 Holland, and F. J. Lynch  
*Phys. Rev. C* 18, 2494-2497 (December 1978)

22. POSITIVE-PARITY STATES IN  $^{43}\text{Ti}$   
 L. Meyer-Schützmeister, A. J. Elwyn, S. A. Gronemeyer,  
 G. Hardie, R. E. Holland, and K. E. Rehm  
*Phys. Rev. C* 18, 1148-1157 (September 1978)

23. LIFETIME AND  $\gamma$  DECAY OF THE ISOMERIC  $19/2^-$  STATE IN  $^{43}\text{Ti}$   
 L. Meyer-Schützmeister, A. J. Elwyn, K. E. Rehm, and  
 G. Hardie  
*Phys. Rev. C* 17, 1299-1307 (April 1978)

\* University of Kansas, Lawrence, Kansas.

† Purdue University, West Lafayette, Indiana.

24. NUCLEAR LEVELS IN  $^{238}\text{Np}$   
 V. A. Ionescu, \* Jean Kern, \* R. F. Casten, † W. R. Kane, †  
 I. Ahmad, ‡ J. Erskine, A. M. Friedman, ‡ and K. Katori  
 Nucl. Phys. A313, 283-306 (22 January 1979)

25. INHIBITED ELECTRIC-QUADRUPOLE TRANSITIONS IN ODD-  
 NEUTRON SPHERICAL NUCLEI  
 R. E. Holland, F. J. Lynch, and B. D. Belt  
 Phys. Rev. C 17, 2076-2079 (June 1978)

26. ABSOLUTE CROSS SECTIONS FOR THREE-BODY BREAKUP REA-  
 TIONS  $^6\text{Li}(\text{d},\text{n})^3\text{He}$   $^4\text{He}$  AND  $^6\text{Li}(\text{d},\text{p})^3\text{H}$   $^4\text{He}$   
 R. E. Holland, A. J. Elwyn, C. N. Davids, F. J. Lynch,  
 L. Meyer-Schützmeister, J. E. Monahan, F. P. Mooring, and  
 W. Ray, Jr.  
 Phys. Rev. C 19, 592-600 (March 1979)

27. STUDY OF THE  $^{12}\text{C}(\text{He},\text{a})^{11}\text{C}$  REACTION AT  $E = 36$  MeV  
 H. T. Fortune, D. J. Crozier, B. Zeidman, and M. E. Cobern §  
 Nucl. Phys. A303, 14-26 (26 June, 3 July 1978)

28. ISOVECTOR RADIATIVE DECAYS AND SECOND-CLASS CURRENTS  
 IN MASS 8 NUCLEI  
 T. J. Bowles and G. T. Garvey  
 Phys. Rev. C 18, 1447-1451 (September 1978)

29. MASS AND LOW-LYING LEVELS OF  $^{67}\text{Ge}$ ; TRENDS IN THE STRUC-  
 TURE OF  $^{63,65}\text{Ni}$ ,  $^{65,67}\text{Zn}$ , AND  $^{67,69}\text{Ge}$   
 M. J. Murphy, C. N. Davids, E. B. Norman, and R. C. Pardo  
 Phys. Rev. C 17, 1574-1582 (May 1978)

30. ENERGY LEVELS OF  $^{60}\text{Fe}$  POPULATED BY THE  $^{58}\text{Fe}(\text{t},\text{p})^{60}\text{Fe}$   
 REACTION  
 Eric B. Norman, Cary N. Davids, and Calvin E. Moss ||  
 Phys. Rev. C 18, 102-107 (July 1978)

31. MASS AND LOW-LYING ENERGY LEVELS OF  $^{69}\text{Cu}$   
 B. Zeidman and J. A. Nolen, Jr.  
 Phys. Rev. C 18, 2122-2126 (November 1978)

\* University of Fribourg, Fribourg, Switzerland.

† Brookhaven National Laboratory, Upton, L.I., New York.

‡ Chemistry Division, ANL.

§ University of Pennsylvania, Philadelphia, Pennsylvania.

|| Los Alamos Scientific Laboratory, Los Alamos, New Mexico.

32. TARGETS FOR HEAVY ION BEAMS  
 J. L. Yntema and F. Nickel\*  
Experimental Methods in Heavy Ion Physics, edited by  
 K. Bethge (Springer-Verlag, Berlin-Heidelberg, 1978),  
 pp. 206-235

33. EFFECTS OF CHANNEL AND POTENTIAL RADIATIVE TRANSITIONS  
 IN THE  $^{17}\text{O}(\gamma, n_0)^{16}\text{O}$  REACTION  
 R. J. Holt, H. E. Jackson, R. M. Laszewski, J. E. Monahan,  
 and J. R. Specht  
Phys. Rev. C 18, 1962-1972 (November 1978)

34. DIRECT OBSERVATION OF ELASTIC AND INELASTIC PHOTON  
 SCATTERING BY THE GIANT DIPOLE RESONANCE IN  $^{60}\text{Ni}$   
 T. J. Bowles, R. J. Holt, H. E. Jackson, R. M. Laszewski,  
 A. M. Nathan,<sup>†</sup> J. R. Specht, and R. Starr<sup>†</sup>  
Phys. Rev. Lett. 41, 1095-1097 (16 October 1978)  
 Erratum: Phys. Rev. Lett. 41, 1523 (20 November 1978)

35. ON THE CONDITIONS REQUIRED FOR THE  $\text{r}$ -PROCESS  
 Eric B. Norman and David N. Schramm<sup>‡</sup>  
Astrophys. J. 228, 881-892 (15 March 1979)

36. ENERGY DEPENDENT  $ft$ -VALUE AND  $B(M1)$  IN  $^8\text{Be}$   
 T. Tomoda<sup>§</sup> and K. Kubodera  
Phys. Lett. 76B, 259-262 (5 June 1978)

37. Erratum: FAMILY OF NUCLEAR MASS RELATIONS [Phys. Rev. C  
15, 1080 (1977)]  
 J. E. Monahan and F. J. D. Serduke  
Phys. Rev. C 17, 1519 (April 1978)

38. ISOSPIN MIXING BETWEEN  $T=0$  AND  $1$  STATES IN THE  $1p$  SHELL  
 R. D. Lawson  
Phys. Lett. 78B, 371-374 (9 October 1978)

---

\* Gesellschaft für Schwerionenforschung (GSI), Darmstadt, Germany.

<sup>†</sup> University of Illinois, Urbana, Illinois.

<sup>‡</sup> University of Chicago, Chicago, Illinois.

<sup>§</sup> University of Tokyo, Tokyo, Japan.

39. ALPHA TRANSFER TO  $^{18}\text{O}$  WITH EMPIRICAL WAVE FUNCTIONS  
 H. T. Fortune\* and D. Kurath  
 Phys. Rev. C 18, 236-238 (July 1978)

40. CURRENT STATE OF NUCLEAR MATTER CALCULATIONS  
 B. D. Day  
 Rev. Mod. Phys. 50, 495-521 (July 1978)

41. HC1 ROTATIONAL EXCITATION BY Ar IMPACT: QUASICLASSICAL CLOSE COUPLING APPROXIMATION FOR ATOM-DIATOMIC MOLECULE SCATTERING  
 Yehuda B. Band  
 J. Chem. Phys. 70, 4-13 (1 January 1979)

42. STRUCTURE EFFECTS SEEN IN THE DISSOCIATION OF 3.5-MeV BEAMS OF  $\text{CO}_2^+$  AND  $\text{N}_2\text{O}^+$  IN THIN FOILS  
 D. S. Gemmell, E. P. Kanter, and W. J. Pietsch  
 Chem. Phys. Lett. 55, 331-334 (15 April 1978)

43. EXPERIMENTAL DETERMINATION OF THE STRUCTURE OF  $\text{H}_3^+$   
 M. J. Gaillard,† D. S. Gemmell, G. Goldring,‡ I. Levine,‡  
 W. J. Pietsch, J. C. Poizat,† A. J. Ratkowski, J. Remillieux,†  
 Z. Vager, and B. J. Zabransky  
 Phys. Rev. A 17, 1797-1803 (June 1978)

44. MEAN-LIFE MEASUREMENTS FOR SOME FLUORINE TRANSITIONS IN THE QUARTZ REGION  
 E. H. Pinnington,§ D. J. G. Irwin,§ A. E. Livingston,§ J. A. Kernahan,§ R. N. Gosselin,§ and H. G. Berry  
 Can. J. Phys. 56, 517-521 (May 1978)

45. FINE STRUCTURE OF THE  $1s2s2p$   $^4\text{P}^0$  AND  $1s2p$   $^2\text{P}^4$  DOUBLY EXCITED STATES IN LITHIUMLIKE CARBON, NITROGEN, AND OXYGEN  
 A. E. Livingston and H. G. Berry  
 Phys. Rev. A 17, 1966-1975 (June 1978)

46. TEMPERATURE DEPENDENCE OF ALIGNMENT PRODUCTION IN He I BY BEAM-FOIL EXCITATION  
 T. J. Gay and H. G. Berry  
 Phys. Rev. A 19, 952-961 (March 1979)

\* Nuclear Physics Laboratory, Oxford England and University of Pennsylvania, Philadelphia, Pennsylvania.

† Université Claude Bernard, Lyon, France.

‡ Weizmann Institute of Science, Rehovot, Israel.

§ University of Alberta, Edmonton, Canada.

47. NE I-LIKE RESONANCE LINES AND Na I-LIKE SATELLITES IN ARGON AND CHLORINE  
 H. G. Berry, J. Desesquelles, K. T. Cheng,\* and R. M. Schectman  
 Phys. Rev. A 18, 546-551 (August 1978)

48. LAMB SHIFT AND FINE STRUCTURE OF  $n = 2$  IN  $^{35}\text{Cl}$  XVI  
 H. G. Berry, R. DeSerio,† and A. E. Livingston  
 Phys. Rev. Lett. 41, 1652-1655 (11 December 1978)

49. ACCURATE PHOTOIONIZATION THRESHOLDS BY MULTIPHOTON IONIZATION: PYRROLE  
 Ashley D. Williamson,‡ R. N. Compton,‡ and J. H. D. Eland  
 J. Chem. Phys. 70, 590-591 (1 January 1979)

50. PHOTOIONIZATION OF ARGON AT HIGH RESOLUTION: COLLISIONAL PROCESSES LEADING TO FORMATION OF  $\text{Ar}_2^+$  AND  $\text{Ar}^+$   
 K. Radler and J. Berkowitz  
 J. Chem. Phys. 70, 221-227 (1 January 1979)

51. PHOTOIONIZATION MASS SPECTROMETRY OF NEON USING SYNCHROTRON RADIATION: ANOMALOUS VARIATION OF RESONANCE WIDTHS IN THE NOBLE GASES  
 K. Radler and J. Berkowitz  
 J. Chem. Phys. 70, 216-220 (1 January 1979)

52. COMPARISON OF SYNCHROTRON AND LABORATORY DISCHARGE LIGHT SOURCES  
 K. Radler and J. Berkowitz  
 J. Opt. Soc. Am. 68, 1181-1183 (September 1978)

53. FLUORESCENCE QUANTUM YIELDS OF ISOTOPIC  $\text{CO}_2^+$  IONS  
 Sydney Leach, § Michal Devoret, § and John H. D. Eland  
 Chem. Phys. 33, 113-121 (1 September 1978)

54. RATES OF UNIMOLECULAR PYRIDINE ION DECAY AND THE HEAT OF FORMATION OF  $\text{C}_4\text{H}_4^+$   
 J. H. D. Eland, J. Berkowitz, H. Schulte, || and R. Frey ||  
 Int. J. Mass Spectry. Ion Phys. 28, 297-311 (November 1978)

\* Radiological and Environmental Research Division, ANL.

† University of Chicago, Chicago, Illinois.

‡ Oak Ridge National Laboratory, Oak Ridge, Tennessee.

§ Université de Paris-Sud, Orsay, France.

|| University of Freiburg, Freiburg, Germany.

55. MOLECULAR PHOTOELECTRON SPECTROSCOPY  
J. H. D. Eland  
J. Phys. E 11, 969-977 (1978)

56. IMPROVED RESOLUTION IN FIXED-WAVELENGTH PHOTOELECTRON-PHOTOION COINCIDENCE SPECTROSCOPY  
J. H. D. Eland  
Rev. Sci. Instrum. 49, 1688-1690 (December 1978)

57. ANGULAR DISTRIBUTIONS, ENERGY DISPOSAL, AND BRANCHING STUDIED BY PHOTOELECTRON-PHOTOION COINCIDENCE SPECTROSCOPY:  $O_2^+$ ,  $NO^+$ ,  $ICl^+$ ,  $IBr^+$  AND  $I_2^+$  FRAGMENTATION  
J. H. D. Eland  
J. Chem. Phys. 70, 2926-2933 (15 March 1979)

58. PES OF HIGH TEMPERATURE VAPORS. VIII. TRANSITION METAL DIHALIDES  
J. Berkowitz, D. G. Streets, and Andoni Garritz\*  
J. Chem. Phys. 70, 1305-1311 (1 February 1979)

59. PHOTOIONIZATION MASS SPECTROMETRIC STUDY OF  $KrF_2$   
J. Berkowitz and J. H. Holloway†  
J. Chem. Soc., Faraday Trans. II, 74(11), 2077-2082 (1978)

60. PHOTOIONIZATION OF  $CH_3OH$ ,  $CD_3OH$  AND  $CH_3OD$ : DISSOCIATIVE IONIZATION MECHANISMS AND IONIC STRUCTURES  
J. Berkowitz  
J. Chem. Phys. 69, 3044-3054 (1 October 1978)

61. PHOTOELECTRON SPECTROSCOPY OF ALKALI HALIDE VAPORS  
J. Berkowitz  
Chap. 5 in Alkali Halide Vapors: Structure, Spectra, and Reaction Dynamics, edited by P. Davidovits and D. L. McFadden (Academic, N. Y., 1979), pp. 155-188

62. PHOTOELECTRON SPECTROSCOPY OF PHTHALOCYANINE VAPORS  
J. Berkowitz  
J. Chem. Phys. 70, 2819-2828 (15 March 1979)

63. ENHANCEMENT OF  $^{235}U$  ISOTOPE SEPARATION WITH RADIO-FREQUENCY HYPERFINE TRANSITIONS  
L. S. Goodman, O. Poulsen, and W. J. Childs  
Opt. Commun. 28, 309-310 (March 1979)

\* Facultad de Quimica, U.N.A.M., Mexico.

† Chemistry Division, ANL.

64. LASER-rf DOUBLE-RESONANCE STUDIES OF THE HYPERFINE STRUCTURE OF  $^{51}\text{V}$   
 W. J. Childs, O. Poulsen, L. S. Goodman, and H. Crosswhite  
*Phys. Rev. A* 19, 168-176 (January 1979)

65. LASER-rf DOUBLE-RESONANCE SPECTROSCOPY IN THE SAMARIUM I SPECTRUM: HYPERFINE STRUCTURES AND ISOTOPE SHIFTS  
 W. J. Childs, O. Poulsen, and L. S. Goodman  
*Phys. Rev. A* 19, 160-167 (January 1979)

66. HIGH-PRECISION MEASUREMENT OF  $^{235}\text{U}$  GROUND-STATE HYPERFINE STRUCTURE BY LASER-rf DOUBLE RESONANCE  
 W. J. Childs, O. Poulsen, and L. S. Goodman  
*Optics Lett.* 4, 35-37 (January 1979)

67. HYPERFINE STRUCTURE OF EXCITED, ODD-PARITY LEVELS IN  $^{139}\text{La}$  BY LASER-ATOMIC-BEAM FLUORESCENCE  
 W. J. Childs and L. S. Goodman  
*J. Opt. Soc. Am.* 68, 1348-1350 (October 1978)

68. HIGH-PRECISION MEASUREMENT OF THE HYPERFINE STRUCTURE OF THE  $620\text{-cm}^{-1}$  METASTABLE ATOMIC LEVEL OF  $^{235}\text{U}$  BY LASER-rf DOUBLE RESONANCE  
 W. J. Childs, O. Poulsen, and L. S. Goodman  
*Optics Lett.* 4, 63-65 (February 1979)

69. ON THE STRUCTURE OF STARCH-IODINE  
 Robert C. Teitelbaum,\* Stanley L. Ruby, and Tobin J. Marks\*  
*J. Am. Chem. Soc.* 100, 3215-3217 (10 May 1978)

70. CORRELATION OF BLISTER DIAMETER AND BLISTER SKIN THICKNESS FOR HELIUM-BOMBARDED V  
 M. Kaminsky and S. K. Das  
*J. Appl. Phys.* 49, 5673-5675 (November 1978)

71. CELL SURVIVAL FOLLOWING MULTIPLE-TRACK ALPHA PARTICLE IRRADIATION  
 E. L. Lloyd,<sup>†</sup> M. A. Gemmell,<sup>†</sup> C. B. Henning,<sup>†</sup> D. S. Gemmell,  
 and B. J. Zabransky  
*Int. J. Radiat. Biology* 35(1), 23-31 (January 1979)

\* Northwestern University, Evanston, Illinois.

<sup>†</sup> Radiological and Environmental Research Division, ANL.

72. SUPERCRITICAL DENSITY MODIFICATIONS OF A LASER-PRODUCED PLASMA DUE TO RESONANT CAVITY FIELDS

Paul Probert,\* J. L. Shohet,\* and Albert J. Hatch

IEEE Trans. Plasma Sci. PS-7(1), 9-12 (March 1979)

B. PUBLISHED REPORTS AT MEETINGS

International Conference on Hyperfine Interactions Studied in Nuclear Reactions and Decay, Uppsala, Sweden, 10-14 June 1974. Contributed Papers, Vol. I, edited by E. Karlsson and R. Wäppling (Almqvist & Wiksell Int., Stockholm-New York, 1974)

1. HYPERFINE INTERACTION IN  $^{67}\text{ZnO}$  BY FREQUENCY MODULATION MÖSSBAUER SPECTROSCOPY

W. Potzel, G. J. Perlow, and H. De Waard

pp. 266-267

Understanding the Fundamental Constituents of Matter (Proceedings of the 1976 International School of Subnuclear Physics, Erice, Italy, 23 July-8 August 1976), edited by Antonino Zichichi (European Physical Society, Geneva, Switzerland, 1978)

2. CAN PEDESTRIANS UNDERSTAND THE NEW PARTICLES?

Harry J. Lipkin

pp. 179-254

Prospects for Strong Interaction Physics at ISABELLE (Proceedings of a Conference, Brookhaven National Laboratory, 31 March-1 April 1977), edited by D. P. Sidhu and T. L. Trueman (National Technical Information Service, Springfield, Va., 1977), BNL 50701

3. HIGH ENERGY SPECTROSCOPY

Harry J. Lipkin

pp. 177-221

Experimental Meson Spectroscopy 1977 (Proceedings of the Fifth International Conference, Northeastern University, Boston, Massachusetts, 29-30 April 1977), edited by Eberhard von Goeler and Roy Weinstein (Northeastern University Press, Boston, 1977)

4. THEORETICAL REVIEW OF STRANGE AND NONSTRANGE MESONS

Harry J. Lipkin

pp. 388-419

\* University of Wisconsin, Madison, Wisconsin.

Physics of Medium-Light Nuclei (Proceedings of the EPS International Conference, Florence, Italy, 7-10 June 1977), edited by P. Blasi and R. A. Ricci (Editrice Compositori, Bologna, 1978)

5. PROPERTIES OF THE  $d_{3/2}$ -HOLE STATES IN THE  $1f_{7/2}$  NUCLEI

R. D. Lawson and A. Müller-Arnke\*  
p. 433

Nuclear Structure Physics (Proceedings of the Eighteenth Scottish Universities Summer School in Physics, St. Andrews, 31 July-20 August 1977), edited by S. J. Hall and J. M. Irvine (SUSSP Publications, Edinburgh University, Edinburgh, Scotland, 1978)

6. MICROSCOPIC MODELS OF NUCLEI

M. H. Macfarlane  
pp. 1-95

Sixth Annual Conference of the International Nuclear Target Development Society, Lawrence Berkeley Laboratory, Berkeley, California, 19-20 October 1977

7. THIN CARBON FOIL BREAKAGE TIMES UNDER ION BEAM BOMBARDMENT

A. E. Livingston, H. G. Berry, and G. E. Thomas  
Proceedings of the Conference, compiled by Gordon Steers (National Technical Information Service, Springfield, Va., 1978), LBL-7950, pp. 149-157  
+ Program of the Conference, Abstract D2, p. 26

8. LIFETIMES OF CARBON STRIPPING FOILS

G. E. Thomas, P. K. Den Hartog, J. J. Bicek, and J. L. Yntema  
Proceedings of the Conference, pp. 17-25  
+ Program of the Conference, Abstract A2, p. 6

Fourth Annual Stanford Synchrotron Radiation Lab Users Group Meeting, Stanford, California, 27-28 October 1977, SSRL Report No. 77/11

9. THE INTERMEDIATE STATE IN BRAGG SCATTERING: AN EXAMPLE OF SUPER-RADIANCE

S. L. Ruby  
p. 30

---

\* Technische Hochschule Darmstadt, Germany.

Synchrotron Radiation Lab Users Group Meeting, Stanford, 27-28 October 1977 (cont'd.)

10. COHERENT NUCLEAR SCATTERING OF SYNCHROTRON RADIATION

G. T. Trammell,\* J. P. Hannon,\* S. L. Ruby, and Paul Flinn

p. 69a

Abstracts of Papers of the 144th National Meeting of the American Association for the Advancement of Science, Washington, D.C., 12-17 February 1978, edited by Arthur Herschman (American Association for the Advancement of Science, Washington, D.C., 1978)

11. PROGRESS ON A HIGH-RESOLUTION SECONDARY-ION MICROPROBE

G. R. Ringo and V. E. Krohn

pp. 22-23

Proceedings of the Symposium on Relativistic Heavy Ion Research, GSI Darmstadt, 7-10 March 1978, edited by R. Bock and R. Stock (Gesellschaft für Schwerionenforschung, Darmstadt, 1978), GSI-P-5-78

12. MACROSCOPIC AND MICROSCOPIC DESCRIPTION OF HE-HI COLLISIONS; CLASSICAL EQUATIONS OF MOTION CALCULATIONS

A. R. Bodmer

Vol. 2, pp. 347-364

175th American Chemical Society Meeting, Anaheim, California, 13-17 March 1978

13. STRUCTURAL STUDIES OF STARCH-IODINE BY RESONANCE RAMAN AND IODINE MÖSSBAUER SPECTROSCOPY

Robert C. Teitelbaum,† Tobin J. Marks,† and Stanley L. Ruby

Abstracts of Papers (Port City Press, Inc., Baltimore, Maryland, 1978), Abstract 42

Third International Conference on Plasma Surface Interactions in Controlled Fusion Devices, Abingdon, England, 3-7 April 1978

14. THE SIGNIFICANCE OF A CORRELATION OF BLISTER DIA-METER WITH SKIN THICKNESS FOR Ni AND Be FOR BLISTERING MODELS

S. K. Das, M. Kaminsky, and G. Fenske

J. Nucl. Mater. 76 & 77, 215-220 (1978)

\* Rice University, Houston, Texas.

† Northwestern University, Evanston, Illinois.

Plasma Surface Interactions in Controlled Fusion Devices, Abingdon,  
3-7 April 1978 (cont'd.)

15. DEPTH DISTRIBUTION OF BUBBLES IN  ${}^4\text{He}^+$ -ION IRRADIATED NICKEL AND THE MECHANISM OF BLISTER FORMATION

G. Fenske, S. K. Das, M. Kaminsky, and G. H. Miley\*  
J. Nucl. Mater. 76 & 77, 247-248 (1978)

16. SURFACE DAMAGE OF 316 STAINLESS STEEL IRRADIATED WITH  ${}^4\text{He}^+$  TO HIGH DOSES

M. Kaminsky and S. K. Das  
J. Nucl. Mater. 76 & 77, 256-257 (1978)

Proceedings of the First Conference on Radiocarbon Dating with Accelerators, University of Rochester, New York, 20-21 April 1978, edited by H. E. Gove (University of Rochester, New York, 1978)

17. TECHNICAL CONSIDERATIONS FOR DEDICATED SYSTEMS—THE CYCLOTRON

E. J. Stephenson  
pp. 187-195

American Physical Society, Washington, D.C., 24-27 April 1978

18. MASS DEPENDENCE OF PION DOUBLE CHARGE EXCHANGE

M. P. Baker,† R. L. Burman,† M. D. Cooper,† R. H. Heffner,† D. M. Lee,† R. P. Redwine,† J. E. Spencer,† M. A. Yates-Williams,† D. J. Malbrough,‡ T. Marks,‡ R. M. Freedman,‡ R. J. Holt, and B. Zeidman  
Bull. Am. Phys. Soc. 23, 592 (April 1978)

19. SUPERALLOWED  $\beta^+$  DECAY OF  ${}^{62}\text{Ga}$

C. N. Davids, M. J. Murphy, and E. B. Norman  
Bull. Am. Phys. Soc. 23, 573 (April 1978)

\* University of Illinois, Urbana, Illinois.

† Los Alamos Scientific Laboratory, Los Alamos, New Mexico.

‡ University of South Carolina, Columbia, South Carolina.

APS, Washington, D.C., 24-27 April 1978 (cont'd.)

20. PION INELASTIC SCATTERING AT 162 MeV  
 D. F. Geesaman, C. Olmer, B. Zeidman, R. L. Boudrie, \*  
 R. H. Siemssen, † C. L. Morris, ‡ J. Amann, ‡ H. A.  
 Thiessen, ‡ M. Devereux, § G. R. Burleson, § R. E. Segel, ||  
 and L. W. Swenson ‡  
 Bull. Am. Phys. Soc. 23, 593 (April 1978)

21. POSITIVE PARITY STATES IN  $^{43}\text{Ti}$   
 S. A. Gronemeyer, A. J. Elwyn, G. Hardie, R. E. Holland,  
 L. Meyer-Schützmeister, and K. E. Rehm  
 Bull. Am. Phys. Soc. 23, 521 (April 1978)

22. EFFECTS OF INTERNAL AND EXTERNAL RADIATIVE  
 CAPTURE IN THE  $^{17}\text{O}(\gamma, n_0)^{16}\text{O}$  REACTION  
 R. J. Holt, H. E. Jackson, R. M. Laszewski, and J. E.  
 Monahan  
 Bull. Am. Phys. Soc. 23, 507 (April 1978)

23. HIGH-SPIN ISOMERS WITH  $N \sim 82$   
 T. L. Khoo, R. K. Smith, H. R. Andrews, \*\* B. Haas, \*\*  
 O. Häuser, \*\* D. Horn, \*\* D. Ward, \*\* and M. Maynard ††  
 Bull. Am. Phys. Soc. 23, 627 (April 1978)

24. DETAILED STUDY OF THE  $\beta$ - $\alpha$  ANGULAR CORRELATION  
 IN  $^8\text{Li}$   $\beta$  DECAY  
 R. D. McKeown and G. T. Garvey  
 Bull. Am. Phys. Soc. 23, 500 (April 1978)

25. ELASTIC SCATTERING OF 162 MeV PIONS BY NUCLEI  
 C. Olmer, B. Zeidman, D. F. Geesaman, R. L. Boudrie, \*  
 R. H. Siemssen, † C. L. Morris, ‡ J. Amann, ‡ H. A.  
 Thiessen, ‡ M. Devereux, § G. R. Burleson, § R. E.  
 Segel, || and L. W. Swenson ‡  
 Bull. Am. Phys. Soc. 23, 592 (April 1978)

\* University of Colorado, Boulder, Colorado.

† K. V. I., Groningen, The Netherlands.

‡ Los Alamos Scientific Laboratory, Los Alamos, New Mexico.

§ New Mexico State University, Las Cruces, New Mexico.

|| Northwestern University, Evanston, Illinois.

¶ Oregon State University, Corvallis, Oregon.

\*\* AECL Chalk River Nuclear Laboratories, Chalk River, Ont., Canada.

†† Queens University, Kingston, Ont., Canada.

APS, Washington, D.C., 24-27 April 1978 (cont'd.)

26. COMPLETE FUSION OF  $^{15}\text{N}$  AND  $^{27}\text{Al}$   
 F. W. Prosser, Jr., \* R. A. Racca, \* D. F. Geesaman,  
 W. Henning, D. G. Kovar, K. E. Rehm, S. L. Tabor,  
 J. V. Maher, † and W. Jordan †  
 Bull. Am. Phys. Soc. 23, 503 (April 1978)

27. OBSERVATION OF THE RADIATIVE CAPTURE PROCESS  
 $^2\text{H}(\text{a}, \gamma)^6\text{Li}$   
 R. G. H. Robertson, ‡ R. A. Warner, ‡ P. Dyer, ‡ R. C.  
 Melin, ‡ and T. J. Bowles  
 Bull. Am. Phys. Soc. 23, 518 (April 1978)

28. DIFFUSENESS OF THE REAL NUCLEAR POTENTIAL FOR  
 $^{16}\text{O} + ^{40}\text{Ca}$  FROM FUSION AND ELASTIC SCATTERING DATA  
 S. E. Vigdor, § D. G. Kovar, P. Sperr, J. Mahoney, ||  
 A. Menchaca-Rocha, || C. Olmer, || and M. Zisman ||  
 Bull. Am. Phys. Soc. 23, 615 (April 1978)

Program of the American Ceramic Society, 80th Annual Meeting and  
 Exposition, Detroit, Michigan, 6-11 May 1978

29. SURFACE DAMAGE OF GRAPHITE UNDER  $^4\text{He}^+$  AND  $\text{D}^+$   
 IMPACT  
 M. Kaminsky, S. K. Das, and P. Dusza  
 American Ceramic Society Bulletin 57(3), 356 (1978)

---

\* University of Kansas, Lawrence, Kansas.

† University of Pittsburgh, Pittsburgh, Pennsylvania.

‡ Michigan State University, East Lansing, Michigan.

§ Indiana University, Bloomington, Indiana.

|| Lawrence Berkeley Laboratory, Berkeley, California.

Proceedings of the Third Topical Meeting on The Technology of Controlled Nuclear Fusion, Santa Fe, New Mexico, 9-11 May 1978, edited by J. R. Powell (National Technical Information Service, Springfield, Va., 1979), CONF-780508

30. THE ROLE OF PLASMA MATERIAL INTERACTION IN THE MAGNETIC FUSION PROGRAM

B. R. Appleton, \* W. Bauer, † K. L. Wilson, † S. A. Cohen, ‡  
R. W. Conn, § M. J. Davis, || F. L. Vook, || C. R.  
Finfgeld, ¶ D. M. Gruen, \*\* M. S. Kaminsky, and E. W.  
Thomas ††

Vol. 1, pp. 565-574

The 1978 IEEE International Conference on Plasma Science, Monterey, California, 15-17 May 1978 (IEEE Service Center, Piscataway, New Jersey, 1978), 78CH1357-3 NPS, Abstracts

31. SURFACE DAMAGE AND EROSION OF TFTR BEAM DUMP MATERIALS BY ENERGETIC D<sup>+</sup>-ION IRRADIATION

M. Kaminsky, S. K. Das, and P. Dusza  
p. 91

Twenty-Sixth Annual Conference on Mass Spectrometry and Allied Topics, St. Louis, Missouri, 28 May-2 June 1978 (American Society for Mass Spectrometry, 1978)

32. PHOTODISSOCIATIVE IONIZATION OF METHANOL

J. Berkowitz  
pp. 273-274

33. RATES OF UNIMOLECULAR PYRIDINE ION DECAY AND THE HEAT OF FORMATION OF C<sub>4</sub>H<sub>4</sub><sup>+</sup>

J. H. D. Eland, J. Berkowitz, H. Schulte, ‡‡ and R. Frey ‡‡  
pp. 267-269

---

\* Oak Ridge National Laboratory, Oak Ridge, Tennessee.

† Sandia Laboratories, Livermore, California.

‡ Princeton Plasma Physics Laboratory, Princeton, New Jersey.

§ University of Wisconsin, Madison, Wisconsin.

|| Sandia Laboratories, Albuquerque, New Mexico.

¶ U.S. Department of Energy, Washington, D.C.

\*\* Chemistry Division, ANL.

†† Georgia Institute of Technology, Atlanta, Georgia.

‡‡ University of Freiburg, Freiburg, Germany.

## Mass Spectrometry and Allied Topics, St. Louis, 28 May-2 June 1978 (cont'd.,

34. PHOTOIONIZATION MASS SPECTROMETRY OF NEON USING SYNCHROTRON RADIATION; ANOMALOUS VARIATION OF RESONANCE WIDTHS ON THE NOBLE GASES  
 K. Radler and J. Berkowitz  
 pp. 679-680

35. PHOTOIONIZATION OF ARGON AT HIGH RESOLUTION; COLLISIONAL PROCESSES LEADING TO FORMATION OF  $\text{Ar}_2^+$   
 K. Radler and J. Berkowitz  
 p. 681

## 1978 Annual Meeting of the American Nuclear Society, San Diego, California, 18-22 June 1978

36. DEPTH DISTRIBUTION OF BUBBLES IN 20-keV  ${}^4\text{He}^+$  IRRADIATED NICKEL  
 G. Fenske, S. K. Das, M. Kaminsky, and G. H. Miley\*  
 Trans. Am. Nucl. Soc. 28, 196-197 (June 1978)

Electron Microscopy 1978, Vol. I (Proceedings of the Ninth International Congress on Electron Microscopy, Toronto, Canada, 1-9 August 1978), edited by J. M. Sturgess (Microscopical Society of Canada, Toronto, 1978)

37. DEPTH DISTRIBUTION OF CAVITIES IN 20- AND 500-keV  ${}^4\text{He}^+$ -IRRADIATED NICKEL  
 S. K. Das, G. Fenske, and M. Kaminsky  
 pp. 398-399

The Physics of Ionized Gases [IX Summer School and Symposium on the Physics of Ionized Gases (SPIG-78), Dubrovnik, Yugoslavia, 28 August-2 September 1978], edited by R. K. Janev (Institute of Physics, Beograd, Yugoslavia, 1979)

38. SELECTED TOPICS ON SURFACE EFFECTS IN FUSION DEVICES: NEUTRAL-BEAM INJECTORS AND BEAM-DIRECT CONVERTERS  
 M. Kaminsky  
 pp. 717-736

---

\* University of Illinois, Urbana, Illinois.

The Physics of Ionized Gases, Dubrovnik, 28 August-2 September 1978  
 (cont'd.)

39. RADIATION BLISTERING—RECENT DEVELOPMENTS  
 M. Kaminsky and S. K. Das  
 pp. 401-426

40. GAS BUBBLE AND DAMAGE MICROSTRUCTURE IN HELIUM  
 IMPLANTED NICKEL  
 M. Kaminsky, S. K. Das, and G. Fenske  
 pp. 427-438

Fast Ion Spectroscopy (Proceedings of 5th International Conference on Beam-Foil Spectroscopy), Lyon, France, 5-8 September 1978

41. LAMB SHIFT AND FINE STRUCTURE OF  $n = 2$  IN  $^{35}\text{Cl}$  XVI  
 H. G. Berry, R. DeSerio,\* and A. E. Livingston  
 Suppl. J. Phys. (Paris) 40, C1-27—29 (Feb. 1979)

42. MEASUREMENT OF THE  $n=2$  DENSITY OPERATOR FOR HYDROGEN ATOMS PRODUCED BY PASSING PROTONS THROUGH THIN CARBON TARGETS  
 Gerald Gabrielse and H. G. Berry  
 Suppl. J. Phys. (Paris) 40, C1-338—339 (Feb. 1979)

43. TEMPERATURE DEPENDENCE OF THE BEAM-FOIL INTERACTION  
 T. J. Gay and H. G. Berry  
 Suppl. J. Phys. (Paris) 40, C1-298—300 (Feb. 1979)

44. ALIGNMENT, ORIENTATION AND THE BEAM FOIL INTERACTION  
 R. M. Schectman,<sup>†</sup> L. J. Curtis,<sup>†</sup> and H. G. Berry  
 Suppl. J. Phys. (Paris) 40, C1-289—294 (Feb. 1979)

45. DOUBLY EXCITED STATES OF THE LiI ISOELECTRONIC SEQUENCE  
 K. X. To,<sup>‡</sup> E. Knystautas,<sup>‡</sup> R. Drouin,<sup>‡</sup> and H. G. Berry  
 Suppl. J. Phys. (Paris) 40, C1-3—5 (Feb. 1979)

\* University of Chicago, Chicago, Illinois.

<sup>†</sup> University of Toledo, Toledo, Ohio.

<sup>‡</sup> Universite Laval, Quebec, Canada.

1978 Applied Superconductivity Conference, Pittsburgh, Pennsylvania,  
25-28 September 1978

46. DEVELOPMENT AND PRODUCTION OF SUPERCONDUCTING  
RESONATORS FOR THE ARGONNE HEAVY ION LINAC  
K. W. Shepard, C. H. Scheibelhut,\* P. Markovich,†  
R. Benaroya,† and L. M. Bollinger  
IEEE Trans. Magn. MAG-15(1), 666-669 (Jan. 1979)

American Physical Society, Division of Nuclear Physics, Asilomar,  
California, 1-3 November 1978

47. A HAMILTONIAN THEORY OF INTERMEDIATE ENERGY  
NN SCATTERING  
M. Betz and T.-S. H. Lee  
Bull. Am. Phys. Soc. 23, 963 (September 1978)

48. SUPERALLOWED  $\beta^+$  DECAY OF  $^{66}\text{As}$   
C. N. Davids, C. A. Gagliardi, and M. J. Murphy  
Bull. Am. Phys. Soc. 23, 930 (September 1978)

49. SEARCH FOR RESONANT STRUCTURES IN THE EXCITATION  
FUNCTIONS OF  $^{26}\text{Mg}(^{16}\text{O}, ^{14}\text{C})^{28}\text{Si}$  AND  $^{48}\text{Ca}(^{16}\text{O}, ^{14}\text{C})^{50}\text{Ti}$   
W. Henning, D. G. Kovar, R. L. Kozub, C. Olmer, M.  
Paul, F. W. Prosser, Jr., S. J. Sanders, and J. P.  
Schiffer  
Bull. Am. Phys. Soc. 23, 934 (September 1978)

50. ENERGY DEPENDENCE OF INELASTIC SCATTERING  
OBSERVED IN THE  $^{40}\text{Ca}(^{16}\text{O}, ^{16}\text{O})^{40}\text{Ca}$  REACTION  
C. Olmer, W. Henning, D. G. Kovar, M. Paul, and S. J.  
Sanders  
Bull. Am. Phys. Soc. 23, 941 (September 1978)

51. STUDIES ON THE  $^{24}\text{Mg}(^{16}\text{O}, ^{12}\text{C})^{28}\text{Si}$  AND  $^{24}\text{Mg}(^{16}\text{O}, ^{16}\text{O})^{24}\text{Mg}$   
REACTIONS  
M. Paul, J. Cseh, D. F. Geesaman, W. Henning, D. G.  
Kovar, R. L. Kozub, C. Olmer, F. W. Prosser, Jr.,  
S. J. Sanders, and J. P. Schiffer  
Bull. Am. Phys. Soc. 23, 934 (September 1978)

52. ITERATIVE SOLUTION OF COUPLED-CHANNEL EQUATIONS  
M. Rhoades-Brown, M. Macfarlane, and S. C. Pieper  
Bull. Am. Phys. Soc. 23, 946 (September 1978)

\* Engineering Division, ANL.

† Chemistry Division, ANL.

## APS, Asilomar, 1-3 November 1978 (cont'd.)

53. ANALYSIS OF THE ANGULAR DISTRIBUTIONS OF THE  
 $^{24}\text{Mg}(^{16}\text{O}, ^{12}\text{C})^{28}\text{Si}$  REACTION  
 S. J. Sanders, M. Paul, J. Cseh, D. F. Geesaman,  
 W. Henning, D. G. Kovar, R. L. Kozub, C. Olmer, and  
 J. P. Schiffer  
 Bull. Am. Phys. Soc. 23, 934 (September 1978)

54. PION INTERACTIONS IN NUCLEI  
 J. P. Schiffer  
 Bull. Am. Phys. Soc. 23, 932 (September 1978)

55. HIGH-SPIN YRAST STATES IN  $^{151}\text{Dy}$   
 R. K. Smith, T. L. Khoo, B. Haas,\* O. Hauser,\*  
 H. R. Andrews,\* D. Horn,\* and D. Ward\*  
 Bull. Am. Phys. Soc. 23, 944 (September 1978)

American Physical Society, Division of Electron and Atomic Physics,  
 Madison, Wisconsin, 29 November-1 December 1978

56. LAMB SHIFT AND FINE STRUCTURE OF  $n = 2$  IN  $^{35}\text{Cl}$  XVI  
 H. G. Berry, R. DeSerio, and A. E. Livingston  
 Bull. Am. Phys. Soc. 23, 1092 (November 1978)

57. Hfs OF EXCITED STATES OF  $^{51}\text{V}$  BY THE LASER-rf DOUBLE-  
 RESONANCE TECHNIQUE  
 W. J. Childs, O. Poulsen, L. S. Goodman, and H.  
 Crosswhite  
 Bull. Am. Phys. Soc. 23, 1092 (November 1978)

58. TEMPERATURE DEPENDENCE OF THE BEAM-FOIL  
 INTERACTION  
 T. J. Gay and H. G. Berry  
 Bull. Am. Phys. Soc. 23, 1099 (November 1978)

59. ENERGIES AND LIFETIMES OF EXCITED STATES IN  
 COPPER-LIKE KRYPTON  
 A. E. Livingston,<sup>†</sup> H. G. Berry, L. J. Curtis,<sup>‡</sup> and R. M.  
 Schectman<sup>‡</sup>  
 Bull. Am. Phys. Soc. 23, 1099 (November 1978)

\* AECL, Chalk River Nuclear Laboratories, Chalk River, Ont., Canada.

<sup>†</sup> University of Notre Dame, Notre Dame, Indiana.

<sup>‡</sup> University of Toledo, Toledo, Ohio.

APS, Madison, 29 November-1 December 1978 (cont'd.)

60. STUDIES OF THE BEAM-FOIL EXCITATION OF HeI  
 R. M. Schechtman,\* L. J. Curtis,\* and H. G. Berry  
 Bull. Am. Phys. Soc. 23, 1099 (November 1978)

American Physical Society, New York, 29 January-1 February 1979

61. MOMENTUM SPACE COUPLED-CHANNELS CALCULATIONS  
 OF INELASTIC PION-NUCLEUS SCATTERING  
 Soumya Chakravarti and T.-S. H. Lee  
 Bull. Am. Phys. Soc. 24, 62 (January 1979)

62. COLLISION-INDUCED DISSOCIATION OF MeV  $H_2^+$  AND  $HeH^+$   
 IN ATOMIC AND MOLECULAR GASES  
 P. J. Cooney, E. P. Kanter, D. S. Gemmell, K.-O. Groeneveld, Z. Vager, and B. J. Zabransky  
 Bull. Am. Phys. Soc. 24, 56 (January 1979)

63. THE PRODUCTION AND STORAGE OF ULTRA COLD NEUTRONS  
 AT THE ARGONNE PULSED NEUTRON SOURCE  
 T. Dombeck,<sup>†</sup> G. Hardekopf,<sup>†</sup> J. Lynn,<sup>†</sup> T. Brun,<sup>‡</sup> J. Carpenter,<sup>‡</sup> V. Krohn, R. Ringo, and S. Werner<sup>§</sup>  
 Bull. Am. Phys. Soc. 24, 44 (January 1979)

64. HYPERFINE STRUCTURE AND NUCLEAR MOMENT DETERMINATIONS FOR THE  $^{235}U$  ATOM  
 L. S. Goodman, W. J. Childs, and O. Poulsen  
 Bull. Am. Phys. Soc. 24, 17 (January 1979)

65. MEASUREMENT OF THE DISTRIBUTIONS OF INTERNUCLEAR SEPARATIONS IN 3.0-MeV  $H_2^+$  AND 3.63-MeV  $HeH^+$  BEAMS  
 E. P. Kanter, P. J. Cooney, D. S. Gemmell, and Z. Vager  
 Bull. Am. Phys. Soc. 24, 57 (January 1979)

66. VERY HIGH SPIN YRAST STATES IN NUCLEI  
 T. L. Khoo  
 Bull. Am. Phys. Soc. 24, 41 (January 1979)

\* University of Toledo, Toledo, Ohio.

<sup>†</sup> University of Maryland, College Park, Maryland.

<sup>‡</sup> Solid State Science Division, ANL.

<sup>§</sup> University of Missouri, Columbia, Missouri.

APS, New York, 29 January-1 February 1979 (cont'd.)

67. CHARGE-STATE EFFECTS OBSERVED IN THE COULOMB EXPLOSION OF 3.6-MeV  $O_2^+$  IONS

W. J. Pietsch, P. J. Cooney, D. S. Gemmell, and E. P. Kanter

Bull. Am. Phys. Soc. 24, 56 (January 1979)

68. GROUND STATE ALPHA DECAY OF THE ELECTRIC GIANT RESONANCES IN  $^{90}\text{Zr}$

R. E. Segel, L. L. Rutledge, Jr., \* K. Raghunathan, \* and L. Meyer-Schützmeister

Bull. Am. Phys. Soc. 24, 32 (January 1979)

American Physical Society, Chicago, Illinois, 19-23 March 1979

69. STRUCTURAL, ELECTRICAL AND SPECTRAL STUDIES OF SEVERAL MEMBERS OF THE CLASS OF CONDUCTIVE LOW-DIMENSIONAL MATERIALS—TTF·I<sub>x</sub>

T. J. Marks, \* R. C. Teitelbaum, \* M. S. McClure, \* C. R. Kannewurf, \* C. K. Johnson, † and S. L. Ruby

Bull. Am. Phys. Soc. 24, 233 (March 1979)

70. EXAFS STUDIES OF MATRIX ISOLATED ATOMS AND MOLECULES

P. A. Montano, ‡ G. K. Shenoy, § and S. L. Ruby

Bull. Am. Phys. Soc. 24, 505 (March 1979)

71. HIGHLY CONDUCTING COMPLEXES BETWEEN POLYCYCLIC AROMATIC MOLECULES AND IODINE—ARE THEY PARTIALLY OXIDIZED?

R. C. Teitelbaum, \* T. J. Marks, \* and S. L. Ruby

Bull. Am. Phys. Soc. 24, 355 (March 1979)

---

\* Northwestern University, Evanston, Illinois.

† Oak Ridge National Laboratory, Oak Ridge, Tennessee.

‡ West Virginia University, Morgantown, West Virginia.

§ Solid State Science Division, ANL.

C. PHYSICS DIVISION REPORT**PTOLEMY—A PROGRAM FOR HEAVY-ION DIRECT-REACTION CALCULATIONS**

M. H. Macfarlane and Steven C. Pieper

Argonne National Laboratory Topical Report ANL-76-11  
(Revision 1) (April 1978)

D. PATENT**OPTICAL CONTROL SYSTEM FOR HIGH-VOLTAGE TERMINALS**

John J. Bicek

U.S. Patent No. 4,107,519 (August 1978)

## STAFF MEMBERS OF THE PHYSICS DIVISION

The Physics Division staff for the year ending 31 March 1979 is listed below. Although the members are classified by programs, it must be understood that many of them work in two or more of the areas. In such cases, the classification indicates only the current primary interest.

In the period from 1 April 1978 through 31 March 1979, there were 36 temporary staff members and visitors (including 11 postdoctoral fellows), 22 graduate students, and 7 undergraduates. In these lists, the Temporary Scientific Staff are those with appointments for  $\geq 9$  months, while Visitors are on shorter appointments. Research Participants come to Argonne part-time for research while continuing their work at their own institutions.

## EXPERIMENTAL NUCLEAR PHYSICS

Permanent Scientific Staff

Ralph Benaroya, M.S., Case Institute of Technology, 1951

<sup>†</sup> Lowell M. Bollinger, Ph.D., Cornell University, 1951

<sup>‡</sup> Cary N. Davids, Ph.D., California Institute of Technology, 1967

<sup>§</sup> Alexander J. Elwyn, Ph.D., Washington University, 1956

<sup>||</sup> John R. Erskine, Ph.D., University of Notre Dame, 1960

<sup>¶</sup> Gerald T. Garvey, Ph.D., Yale University, 1962

---

<sup>†</sup> In charge of Superconducting Linac Project.

<sup>‡</sup> Full time at Argonne. Also Senior Visiting Research Associate at the Enrico Fermi Institute, University of Chicago.

<sup>§</sup> In charge of Dynamitron accelerator operations as of July 1978.

<sup>||</sup> Temporarily at D.O.E. Headquarters, Washington, D.C.  
(December 1977—December 1979).

<sup>¶</sup> Director of the Physics Division through February 1979; then Acting Associate Laboratory Director, Physical Research.

Donald F. Geesaman, Ph. D., State University of New York, Stony Brook, 1976

Walter Henning, Ph. D., Technical University, Munich, 1968

Robert E. Holland, Ph. D., University of Iowa, 1950

Roy J. Holt, Ph. D., Yale University, 1972

Harold E. Jackson, Jr., Ph. D., Cornell University, 1959

Teng Lek Khoo, Ph. D., McMaster University, 1972

Dennis G. Kovar, Ph. D., Yale University, 1971

Victor E. Krohn, Ph. D., Case Western Reserve University, 1952

<sup>†</sup> John J. Livingood, Ph. D., Princeton University, 1929

Luise Meyer-Schützmeister, Ph. D., Technical University of Berlin, 1943

F. P. Mooring, Ph. D., University of Wisconsin, 1951

G. Roy Ringo, Ph. D., University of Chicago, 1940

<sup>‡</sup> John P. Schiffer, Ph. D., Yale University, 1954

Kenneth W. Shepard, Ph. D., Stanford University, 1970

Robert K. Smither, Ph. D., Yale University, 1956

<sup>\*</sup> Thomas P. Wangler, Ph. D., University of Wisconsin, 1964

<sup>§</sup> J. L. Yntema, Ph. D., Free University of Amsterdam, 1952

Benjamin Zeidman, Ph. D., Washington University, 1957

#### Temporary Scientific Staff

Thomas J. Bowles, Ph. D., Princeton University, 1977

Walter Kutschera, Ph. D., University of Graz, 1965  
(From Technical University, Munich)

<sup>¶</sup> Ronald M. Laszewski, Ph. D., University of Illinois, 1975

Robert D. McKeown, Ph. D., Princeton University, 1979

Catherine Olmer, Ph. D., Yale University, 1975

<sup>\*</sup> No longer at Argonne as of 31 March 1979.

<sup>†</sup> Emeritus.

<sup>‡</sup> Associate Director of the Physics Division. Joint appointment with the University of Chicago.

<sup>§</sup> In charge of Tandem accelerator operations.

Michael Paul, Ph.D., Hebrew University of Jerusalem, 1973

Stephen J. Sanders, Ph.D., Yale University, 1977

Edward J. Stephenson, Ph.D., University of Wisconsin, 1975

Visitors

\* Jozsef Cseh, Ph. D., Kossuth University, Debrecen, 1977

(From Institute of Nuclear Research through the Exchange Program  
of the Hungarian Academy of Sciences, Debrecen, Hungary)

Thomas W. Dombeck, Ph.D., Northwestern University, 1972

(Research participant from University of Maryland)

\* Gerald Hardie, Ph. D., University of Wisconsin, 1962

(Research participant from Western Michigan University)

Raymond L. Kozub, Ph.D., Michigan State University, 1967

(Research participant from Tennessee Technological University)

Jeffrey W. Lynn, Ph.D., Michigan State University, 1972

(Research participant from University of Maryland)

Bogumila Myslek-Laurikainen, Ph. D., Warsaw University, 1974

(From Institute of Nuclear Research, Swierk, Poland)

\* Francis W. Prosser, Jr., Ph.D., University of Kansas, 1955

(From University of Kansas)

\* Brian B. Sabo, Ph. D., University of Minnesota, 1973

(Research participant from St. Olaf College)

Ralph E. Segel, Ph.D., Johns Hopkins University, 1955

(Research participant from Northwestern University)

Supporting Staff

John J. Bicek

Patric K. Den Hartog

William F. Evans

Joseph E. Kulaga

James W. Lamka

James R. Specht

George E. Thomas, Jr.

James N. Worthington

---

\* No longer at Argonne as of 31 March 1979.

Graduate Students

Tswei Chen (Northwestern University)

Kasra Daneshvar (University of Illinois, Chicago Circle Campus)

Alexandra R. Davis (University of Chicago)

Carl A. Gagliardi (Princeton University)

Suzanne A. Gronemeyer (Washington University)

\* Albert L. Hanson (University of Michigan)

Samuel M. Levenson (University of Chicago)

Martin J. Murphy (University of Chicago)

\* Eric B. Norman (University of Chicago)

\* Timothy R. Renner (University of Chicago)

## THEORETICAL PHYSICS

Permanent Scientific Staff

\* Yehuda B. Band, Ph.D., University of Chicago, 1973

† Arnold R. Bodmer, Ph.D., Manchester University, 1953

Fritz Coester, Ph.D., University of Zurich, 1944

Benjamin Day, Ph.D., Cornell University, 1963

Dieter Kurath, Ph.D., University of Chicago, 1951

Robert D. Lawson, Ph.D., Stanford University, 1953

Tsung-Shung Harry Lee, Ph.D., University of Pittsburgh, 1973

\* Malcolm H. Macfarlane, Ph.D., University of Rochester, 1959

James E. Monahan, Ph.D., St. Louis University, 1953

---

\* No longer at Argonne as of 31 March 1979.

† Joint appointment with the University of Illinois, Chicago Circle Campus.

‡ Joint appointment with the University of Chicago.

<sup>†</sup> Murray Peshkin, Ph. D., Cornell University, 1951

Steven C. Pieper, Ph. D., University of Illinois, 1970

<sup>\*</sup> Johann Rafelski, Ph. D., Johann Wolfgang Goethe University, 1973

#### Temporary Scientific Staff

Michel Betz, Ph. D., Massachusetts Institute of Technology, 1977

Mark J. Rhoades-Brown, Ph. D., University of Surrey, 1977

#### Visitors

Robert P. Goddard, Ph. D., University of Wisconsin, 1978  
(Research participant from University of Wisconsin)

<sup>\*</sup> Alan D. MacKellar, Ph. D., Texas A & M University, 1965  
(Research participant from University of Kentucky)

William D. Teeters, Ph. D., University of Iowa, 1968  
(Research participant from Chicago State University)

#### Graduate Students

Soumya Chakravarti (University of Chicago)

<sup>\*</sup> Constantine N. Panos (University of Illinois, Chicago Circle Campus)

## SPEAKEASY CENTER

#### Permanent Scientific Staff

<sup>\*</sup> Stanley Cohen, Ph. D., Cornell University, 1955

#### Temporary Staff

Monika A. Wehrenberg, M. A., School of the Art Institute of Chicago,  
1972

#### Visitor

<sup>\*</sup> Daniel F. X. O'Reilly, Ph. D., Stanford University, 1975  
(From Marquette University)

<sup>\*</sup> No longer at Argonne as of 31 March 1979.

<sup>†</sup> Associate Director of the Physics Division; Acting Director since  
February 1979.

Graduate Students

- \* Thomas P. Grace (University of Illinois)
- \* Steve G. Massaquoi (Harvard Medical School)
- \* Richard D. Schlichting (Cornell University)
- \* Gregory R. Vassmer (Northern Illinois University)

## EXPERIMENTAL ATOMIC AND MOLECULAR PHYSICS

Permanent Scientific Staff

- Joseph Berkowitz, Ph. D., Harvard University, 1955
- † H. Gordon Berry, Ph. D., University of Wisconsin, 1967
- William J. Childs, Ph. D., University of Michigan, 1956
- Santosh K. Das, Ph. D., University of California, 1971
- John H. D. Eland, D. Phil., Oxford University, 1966
- ‡ Donald S. Gemmell, Ph. D., Australian National University, 1960
- § Leonard S. Goodman, Ph. D., University of Chicago, 1952
- Manfred S. Kaminsky, Ph. D., University of Marburg, 1957
- Siu Au Lee, Ph. D., Stanford University, 1976
- || Gilbert J. Perlow, Ph. D., University of Chicago, 1940
- Stanley L. Ruby, B. A., Columbia University, 1947

Temporary Scientific Staff

- Patrick J. Cooney, Ph. D., State University of New York, Stony Brook, 1975  
(From Middlebury College)

\* No longer at Argonne as of 31 March 1979.

† Joint appointment with the University of Chicago.

‡ In charge of Dynamitron accelerator operations until July 1978.

§ Assistant Director of the Physics Division.

|| Joint appointment as Editor of the Applied Physics Letters.

\* Paul A. Flinn, Sc. D., Massachusetts Institute of Technology, 1952  
(From Carnegie-Mellon University)

Elliot P. Kanter, Ph. D., Rutgers University, 1977

Siu-Kwong Lam, Ph. D., College of William & Mary, 1975

Visitors

\* Ben Greenebaum, Ph. D., Harvard University, 1965  
(Research participant from University of Wisconsin—Parkside)

\* Karl-Ontjes E. Groeneveld, Ph. D., University of Frankfurt, 1966  
(From University of Frankfurt/M)

\* James P. Hannon, Ph. D., Rice University, 1966  
(Research participant from Rice University)

A. Eugene Livingston, Ph. D., University of Alberta, 1974  
(Research participant from University of Notre Dame)

\* Walter A. Potzel, Ph. D., Technical University of Munich, 1971  
(From Technical University of Munich)

\* Ove Poulsen, Ph. D., University of Aarhus, 1976  
(From University of Aarhus)

William C. Trogler, Ph. D., California Institute of Technology, 1978  
(Research participant from Northwestern University)

Bilin P. Tsai, Ph. D., University of North Carolina, 1975  
(Research participant from University of Minnesota)

\* Zeev Vager, Ph. D., Weizmann Institute of Science, 1960  
(From Weizmann Institute of Science)

Supporting Staff

Charles H. Batson

John A. Dalman

\* Peter J. Dusza

Robert W. Nielsen

Walter J. Ray

Bruce J. Zabransky

Graduate Students

\* David E. Brinza (California Institute of Technology)

---

\* No longer at Argonne as of 31 March 1979.

- <sup>†</sup> George R. Fenske (University of Illinois)
- <sup>\*</sup> Bradley W. Filippone (University of Chicago)
- <sup>\*</sup> Gerald S. Gabrielse (University of Chicago)
- Timothy J. Gay (University of Chicago)
- <sup>\*</sup> James A. Laramee (Purdue University)

#### ADMINISTRATIVE STAFF

- <sup>#</sup> Albert J. Hatch, M. S., University of Illinois, 1947

---

<sup>\*</sup> No longer at Argonne as of 31 March 1979.

<sup>†</sup> Transferred to Materials Science Division January 1979.

<sup>#</sup> Assistant Director of the Physics Division.

**Distribution for ANL-79-40****Internal:**

W. E. Massey  
 M. V. Nevitt  
 R. M. Adams  
 R. Avery  
 N. Beyer  
 L. Burris  
 S. A. Davis  
 P. M. Dehmer  
 R. E. Diebold  
 P. R. Fields  
 M. S. Freedman  
 A. Friedman  
 B. R. T. Frost  
 G. T. Garvey  
 D. Grahn  
 J. B. Hamilton  
 M. Inokuti  
 M. A. Kanter  
 A. B. Krisciunas (12)  
 J. J. Livingood  
 M. Novick  
 E. N. Pettitt  
 E. G. Pewitt  
 R. J. Royston  
 L. L. Rutledge  
 W. K. Sinclair  
 A. F. Stehney  
 D. Streets  
 J. F. Thomson  
 C. E. Till  
 J. W. Tippie  
 P. D. Vashishta  
 S. Wexler  
 C. H. Batson  
 R. Benaroya  
 J. Berkowitz  
 H. G. Berry  
 A. R. Bodmer  
 L. M. Bollinger

W. J. Childs  
 F. Coester  
 J. A. Dalman  
 C. N. Davids  
 B. Day  
 P. K. Den Hartog  
 J. H. D. Eland  
 A. J. Elwyn  
 J. R. Erskine  
 D. F. Geesaman  
 D. S. Gemmell  
 L. S. Goodman  
 A. J. Hatch  
 W. Henning  
 R. E. Holland  
 R. J. Holt  
 H. E. Jackson  
 M. S. Kaminsky  
 T. L. Khoo  
 D. G. Kovar  
 V. E. Krohn  
 J. E. Kulaga  
 D. Kurath  
 R. D. Lawson  
 S. A. Lee  
 T-S. H. Lee  
 M. H. Macfarlane  
 R. McKeown  
 L. Meyer  
 J. E. Monahan  
 F. P. Mooring  
 R. C. Pardo  
 K. M. Pemble  
 G. J. Perlow  
 M. Peshkin (75)  
 S. C. Pieper  
 G. R. Ringo  
 S. L. Ruby

J. P. Schiffer  
 K. W. Shepard  
 R. K. Smither  
 J. R. Specht  
 J. L. Stadelmann  
 G. E. Thomas  
 J. N. Worthington  
 J. L. Yntema  
 B. Zabransky  
 B. Zeidman  
 L. Arnellos  
 M. E. Betz  
 J. Borggreen  
 R. L. Brooks  
 S. Chakravarti  
 A. Davis  
 B. W. Filippone  
 T. Gay  
 G. Gagliardi  
 R. P. Goddard  
 C. M. Jachcinski  
 R. L. Kozub  
 W. Kutschera  
 S-K. Lam  
 S. Levenson  
 J. Lynn  
 P. Marikar  
 M. Murphy  
 B. Myslek-Laurikainen  
 I. Plessner  
 M. Rhoades-Brown  
 S. J. Sanders  
 R. E. Segel  
 K. E. Stephenson  
 W. C. Trogler  
 B. Botch  
 ANL Contract File  
 ANL Libraries (5)  
 TIS Files (5)

**External:**

DOE-TIC, for distribution per UC-34 (135)  
 Manager, Chicago Operations and Regional Office, DOE  
 Chief, Office of Patent Counsel, DOE-CH  
 President, Argonne Universities Association  
 Physics Division Review Committee:  
 B. Bederson, New York U.  
 H. G. Blosser, Michigan State U.  
 W. L. Brown, Bell Telephone Labs.

R. Middleton, U. Pennsylvania  
W. Haeberli, U. Wisconsin-Madison  
J. W. Negele, Massachusetts Inst. Technology  
H. B. Willard, Case Western Reserve U.  
F. Ajzenberg-Selove, U. Pennsylvania  
R. G. Allas, U. S. Naval Research Lab.  
J. D. Anderson, Lawrence Livermore Lab.  
Antioch College, Olive Kettering Library  
P. Axel, U. Illinois  
P. D. Barnes, Carnegie-Mellon U.  
H. H. Barschall, U. Wisconsin-Madison  
B. Bayman, U. Minnesota  
G. B. Beard, Wayne State U.  
G. L. Bennett, Div. Reactor Safety Res., USNRC  
C. H. Blanchard, U. Wisconsin-Madison  
R. L. Boudrie, Los Alamos Scientific Lab.  
T. J. Bowles, Los Alamos Scientific Lab.  
D. A. Bromley, Yale U.  
Brooklyn College, Dept. of Physics  
G. E. Brown, SUNY at Stony Brook  
S. B. Burson, Office of Nuclear Regulatory Res., USNRC  
D. L. Bushnell, Northern Illinois U.  
F. R. Buskirk, U. S. Naval Postgraduate School  
D. J. Buss, Illinois Benedictine College  
L. E. Campbell, Hobart & William Smith Colleges  
P. Caruthers, Los Alamos Scientific Lab.  
Catholic University of America, Keane Physics Research Center  
J. Cerny III, Lawrence Berkeley Lab.  
B-d. Chang, U. Rochester  
Chemical Abstracts Service, Columbus  
G. F. Chew, Lawrence Berkeley Lab.  
W. A. Chupka, Yale U.  
Cincinnati, U. of, Physics Library  
J. W. Clark, Washington U.  
C. M. Class, Rice U.  
T. B. Clegg, U. North Carolina  
H. Cohen, California State U., Los Angeles  
S. Cohen, Speakeasy Computing Corp., Chicago  
Colorado, U. of, Nuclear Physics Lab.  
P. J. Cooney, Middlebury College  
Cornell U., Library  
K. Daneshvar, U. Pennsylvania  
S. E. Darden, U. Notre Dame  
Dartmouth College, Library  
S. K. Das, Pratt and Whitney Aircraft Group, West Palm Beach  
P. T. Debevec, U. Illinois  
D. Dehnhard, U. Minnesota  
Denver, U. of, Physics Dept.  
R. M. DeVries, Los Alamos Scientific Lab.  
B. Donnally, Lake Forest College, Lake Forest, Ill.  
P. J. Dusza, Physics Equipment, Midlothian, Ill.  
G. N. Epstein, Massachusetts Inst. Technology  
U. Fano, U. Chicago  
H. J. Fischbeck, U. Oklahoma

P. A. Flinn, Intel Corp., Santa Clara  
Ford Aerospace and Communications Corp., Newport Beach, Calif.  
H. T. Fortune, U. Pennsylvania  
J. L. Fowler, Oak Ridge National Lab.  
W. A. Fowler, California Inst. Technology  
P. W. Gilles, U. Kansas  
N. K. Glendenning, Lawrence Berkeley Lab.  
D. H. Gloeckner, Pacific-Sierra Research Corp., Arlington, Va.  
H. Goldstein, Columbia U.  
H. E. Gove, U. Rochester  
S. A. Gronemeyer, Massachusetts General Hosp.  
W. Haeberli, U. Wisconsin  
I. Halpern, U. Washington  
M. Hamermesh, U. Minnesota  
S. S. Hanna, Stanford U.  
A. O. Hanson, U. Illinois  
R. R. Hart, Cambridge, Mass.  
B. G. Harvey, Lawrence Berkeley Lab.  
M. Hasan, Northern Illinois U.  
H. G. Heard, Woodside, Calif.  
D. W. Heikkinen, Lawrence Livermore Lab.  
R. G. Helmer, EG&G Idaho, Inc.  
E. M. Henley, U. Washington  
R. G. Herb, National Electrostatics Corp., Middleton, Wis.  
R. E. Honig, RCA Labs.  
J. T. Hood, Washington U.  
V. W. Hughes, Yale U.  
J. R. Huizenga, U. Rochester  
IIT Research Institute, Physics Library  
Illinois, U. of, Chicago Circle, Dept. of Physics  
Indiana U., Cyclotron Project  
M. Inghram, U. Chicago  
D. R. Inglis, U. Massachusetts  
Institute for Advanced Study, Physics Preprint Library, Princeton  
P. B. Kahn, SUNY at Stony Brook  
R. J. Kandel, Office of Basic Energy Sciences, USDOE  
E. P. Kanter, Rutgers U.  
A. K. Kerman, Massachusetts Inst. Technology  
B. B. Kinsey, U. of Texas at Austin  
E. A. Knapp, Los Alamos Scientific Lab.  
N. Koller, Rutgers U.  
F. T. Kuchnir, Elmhurst, Ill.  
R. O. Lane, Ohio U.  
A. Langsdorf, Jr., Schaumburg, Ill.  
R. M. Laszewski, U. Illinois, Urbana  
L. L. Lee, Jr., SUNY at Stony Brook  
A. E. Livingston, U. Notre Dame  
L. F. Long, U. Notre Dame  
G. D. Loper, Wichita State U.  
Louisiana State U., Dept. of Physics and Astronomy, Librarian  
Louisiana State U., Director, Nuclear Science Center  
A. P. Magruder, EG&G, Las Vegas, Nev.  
J. V. Maher, U. Pittsburgh  
M. Maier, Lawrence Berkeley Lab.

J. Margrave, Rice U.  
Marquette U., Physics Dept.  
J. V. Martinez, Office of Basic Energy Sciences, USDOE  
Maryland, U. of, Dept. of Physics and Astronomy, Preprint Lib.  
Massachusetts Inst. of Technology, Physics Reading Room  
D. A. McClure, Georgia Inst. Technology  
J. C. McDonald, Sloan-Kettering Inst.  
G. W. Meisner, U. North Carolina  
Michigan State U., Cyclotron Lab., Librarian  
Mississippi, U. of, Library  
A. Moen, Central College, Pella, Ia.  
C. F. Moore, U. of Texas at Austin  
H. T. Motz, Los Alamos Scientific Lab.  
A. I. Namenson, Naval Research Lab.  
H. Newson, Duke U.  
New York U. Medical Center, Environmental Medicine Lib., Tuxedo  
J. A. Nolen, Jr., Michigan State U.  
E. B. Norman, U. Washington  
C. Olmer, Indiana U.  
W. K. H. Panofsky, Stanford Linear Accelerator Center  
J. T. Park, U. Missouri-Rolla  
L. A. Parks, Florida State U.  
E. S. Pierce, Office of Basic Energy Sciences, USDOE  
R. E. Pollock, Indiana U.  
R. S. Preston, Northern Illinois U.  
F. W. Prosser, U. Kansas  
S. Raboy, Harpur College, SUNY, Binghamton  
J. L. Rainwater, Columbia U., Irvington  
A. J. Ratkowski, New York State Dept. of Health  
G. Reynolds, Palmer Physics Lab., Princeton U.  
Rochester U. of, Physics/Optics/Astronomy Lib.  
E. Rose, Princeton U.  
N. P. Samios, Brookhaven National Lab.  
R. P. Scharenberg, Purdue U.  
R. M. Schectman, U. Toledo  
P. D. Schnur, Charles B. Chrystal Co., New York City  
F. J. D. Serduke, Lawrence Livermore Lab.  
K. K. Seth, Northwestern U.  
S. M. Shafrroth, U. North Carolina  
R. Sherr, Palmer Physics Lab., Princeton U.  
C. G. Shull, Massachusetts Inst. of Technology  
H. Shwe, East Stroudsburg State College  
C. E. Skov, Monmouth College  
C. P. Slichter, U. Illinois  
H. E. Stanton, Oak Lawn, Ill.  
N. Stein, Yale U.  
P. H. Stelson, Oak Ridge National Lab.  
E. J. Stephenson, Indiana U.  
M. B. Sterns, Ford Scientific Lab.  
J. Stoltzfus, Beloit College  
W. G. Stoppenhagen, Ohio U., Lancaster  
R. V. Straz, North American Co., Chicago  
T. T. Sugihara, Texas A&M U.  
M. Svonavec, Purdue U., Calumet Center

S. L. Tabor, U. Maryland  
R. F. Taschek, Los Alamos Scientific Lab.  
C. C. Trail, Brooklyn College  
R. Vandenbosch, U. Washington  
S. E. Vigdor, Indiana U.  
C. M. Vincent, U. Pittsburgh  
D. H. Vincent, U. Michigan  
J. D. Walecha, Stanford U.  
T. P. Wangler, Los Alamos Scientific Lab.  
B. A. Watson, Stanford U.  
L. Weaver, Kansas State U.  
G. H. Wedberg, Gaithersburg, Md.  
M. J. Weiss, U. Nebraska  
V. Weisskopf, Massachusetts Inst. Technology  
K. J. Wetzel, U. Portland  
W. R. Wharton, Carnegie-Mellon U.  
M. G. White, Princeton U.  
E. P. Wigner, Princeton U.  
H. B. Willard, Case Western Reserve U.  
Wisconsin U. of, Physics Library, Madison  
G. T. Wood, Cleveland State U.  
C. S. Wu, Columbia U.  
O. K. Wu, Gould Inc., Rolling Meadows, Ill.  
A. J. F. Boyle, U. Western Australia, Australia  
J. O. Newton, Australian National U., Australia  
T. R. Ophel, Australian National U., Australia  
L. J. Tassie, Australian National U., Australia  
E. W. Titterton, Australian National U., Australia  
W. Kerber, Zentralbibliothek d. Physik Inst., Vienna, Austria  
Euratom, Central Bu. Nuclear Measurements, Library, Belgium  
Katholieke Universiteit Leuven, Inst. voor Theoretische Fysica, Belgium  
J. Vervier, U. Catholique de Louvain, Belgium  
Brasilia, Universidade de, Inst. Central de Fisica, Brazil  
Divisao de Estudos Avancados, San Jose dos Campos, Brazil  
O. Sala, Universidade de Sao Paulo, Brazil  
Sao Paulo, Universidade de, Nuclear Physics Lab., Pelletron Lab., Brazil  
Alberta, U. of, Nuclear Research Centre, Dept. of Physics, Canada  
G. A. Bartholomew, Atomic Energy Canada Ltd., Canada  
H. C. Evans, Queens U., Kingston, Canada  
T. J. Kennett, McMaster U., Canada  
J. D. Kurbatov, Victoria, B.C., Canada  
McGill U., Lib., Rutherford Physics Bldg., Montreal, Canada  
G. C. Nielson, U. Alberta, Edmonton, Canada  
W. V. Prestwich, McMaster U., Canada  
W. J. Romo, Carleton U., Canada  
J-s. Maa, National Tsing-Hua U., Republic of China  
P-K. Tseng, National Taiwan U., Republic of China  
A. Bohr, Inst. for Theoretical Physics, Copenhagen, Denmark  
L. T. Chadderton, Copenhagen U., Denmark  
C. J. Christensen, Danish AEC, Risø, Denmark  
B. R. Mottelson, Inst. for Theoretical Physics, Copenhagen, Denmark  
Niels Bohr Inst., The Library, Copenhagen, Denmark  
O. Poulsen, U. Aarhus, Denmark  
F. ElBedewi, Atomic Energy Establishment, Cairo, Egypt

M. ElNadi, Cairo U., Egypt  
I. Hamouda, Atomic Energy Establishment, Cairo, Egypt  
A. Osman, Cairo U., Egypt  
W. D. Allen, U. Reading, England  
Berkeley Nuclear Labs., Central Electricity Generating Bd., Librarian, England  
J. B. Birks, The University, Manchester, England  
D. R. Chick, Surrey, England  
Culham Lab., UKAEA, Librarian, England  
N. Daly, UKAWRE, Aldermaston, England  
A. T. G. Ferguson, AERE, Harwell, England  
M. Grace, Oxford U., England  
C. E. Johnson, U. Liverpool, England  
J. S. Lilley, Daresbury Lab., England  
G. C. Morrison, U. Birmingham, England  
R. S. Nelson, AERE, Harwell, England  
Sussex, U. of, Library, Brighton, England  
M. W. Thompson, U. Sussex, England  
University College London, Library, Dept. of Physics and Astronomy, England  
J. Walker, U. Birmingham, England  
J. C. Willmott, The University, Manchester, England  
K. V. Laurikainen, U. Helsinki, Finland  
A. Abragam, CEN Saclay, France  
P. Catillion, CEN Saclay, France  
CEA Saclay, Library, France  
Centre de Recherches Nucleaires, Strasbourg, France  
C.N.R.S., Centre de Physique Theorique, Marseille, France  
J. Delaunay, CEN Saclay, France  
H. Ekstein, C.N.R.S., Marseille, France  
Inst. de Physique Nucléaire, Lib., Div. de Physique Theorique, Orsay, France  
Institut des Sciences Nucleaires, Librarian, Grenoble, France  
Laboratoire de l'Accelerateur Lineaire, U. Paris, Orsay, France  
A. Michaudon, C.E.A., Centre d'Etudes de Bruyeres le Chatel, France  
H. Nifenecker, CEN Grenoble, France  
J. C. Poizat, U. Claude Bernard, Villeurbanne, France  
J. M. Remillieux, U. Claude Bernard, Villeurbanne, France  
R. Seltz, Centre de Recherches Nucleaires, Strasbourg, France  
J. C. Sens, Centre de Recherches Nucleaires, Strasbourg, France  
K. Bethge, Inst. f. Kernphysik, Universität, Frankfurt, Germany  
R. Bock, GSI, Darmstadt, Germany  
H. Bohn, Technische Universität, Munich, Germany  
Deutsches Elektronen-Synchrotron, Librarian, Hamburg, Germany  
K. A. Eberhard, U. Munich, Germany  
H. Ehrhardt, U. Kaiserslautern, Germany  
A. A. Forster, Techn. U. Munchen, Germany  
Gesellschaft für Schwerionen-forschung mbH, Bibliothek, Darmstadt, Germany  
K. Grabisch, Hahn-Meitner Inst., Berlin, Germany  
K-O. Groeneveld, Universität Frankfurt, Germany  
D. Habs, Max-Planck Inst. fuer Kernphysik, Heidelberg, Germany  
J. W. Hammer, U. Stuttgart, Germany  
P. Kienle, Technische Hochschule Munchen, Germany  
H. V. Klapdor, Max-Planck Inst. f. Kernphysik, Heidelberg, Germany  
H-J. Körner, Technische Universität Munchen, Germany  
L. Lassen, Universität Heidelberg, Germany  
N. Marquardt, Ruhr-Universität Bochum, Germany

C. Mayer-Börcke, Kernforschungsanlage Julich, Germany  
T. Mayer-Kuckuk, Universität Bonn, Germany  
U. B. Mosel, Universität Giessen, Germany  
A. Müller-Arnke, Technischen Hochschule, Darmstadt, Germany  
O. Osberghaus, Universität Freiburg, Germany  
W. J. Pietsch, U. Cologne, Germany  
W. Potzel, Technical U. Munich, Germany  
K. E. Rehm, Technische Universität, Munich, Germany  
A. Richter, Tech. Hochschule, Darmstadt, Germany  
R. Santo, U. Munchen, Germany  
O. W. B. Schult, KFA Julich, Germany  
P. Sperr, Technische Universität Munchen, Germany  
J. Speth, Inst. für Kernphysik der KFA, Julich, Germany  
U. Strohbusch, Inst. für Experimentalphysik Zyklotron, Hamburg, Germany  
Technischen Universität Munchen, Library, Physik Dept., Germany  
D. von Ehrenstein, U. Bremen, Germany  
S. Wagner, Physikalisch-Technische Bundesanstalt, Braunschweig, Germany  
G. Wortmann, Technical U. Munchen, Germany  
J. G. Zabolitzky, Ruhr-Universität, Bochum, Germany  
A. Katsanos, NRC Democritos, Greece  
J. Cseh, Inst. Nuclear Research Hungarian Ady. Sciences, Debrecen, Hungary  
N. Anantaraman, UEC Lab., Calcutta, India  
Bhabha Atomic Research Centre, Calcutta, India  
M. R. Bhiday, U. Poona, India  
N. Nath, Kurukshetra U., India  
S. P. Pandya, Physical Research Lab., Ahmedabad, India  
N. G. Puttaswamy, Bangalore U., India  
N. N. Raina, U. Kashmir, India  
I. Ramarao, Tata Inst. of Fundamental Research, Bombay  
A. P. Shukla, Indian Inst. of Technology, Kanpur, India  
P. C. Sood, Banaras Hindu U., India  
A. A. Azooz, U. Mosul, Iraq  
J. Alster, Tel Aviv U., Israel  
A. E. Blaugrund, Weizmann Inst. of Science, Israel  
Y. Eisen, Weizmann Inst. of Science, Israel  
A. Marinov, Hebrew U., Israel  
M. Moinester, Tel Aviv U., Israel  
Negev, U. of the, Physics Preprint Library, Israel  
M. Paul, Hebrew U., Israel  
B. Rosner, Technion — Israel Inst. of Tech., Israel  
Z. Vager, Weizmann Inst. of Science, Israel  
A. Weinreb, Hebrew U., Israel  
Weizmann Inst. of Science, Physics Library, Israel  
N. Zeldes, Hebrew U., Israel  
C. Coceva, C.N.E.N., Bologna, Italy  
Instituto di Fisica, Preprint Librarian, Torino, Italy  
Instituto de Fisica Sperimental, c/o Dr. M. Vadacchino, Torino, Italy  
Instituto Nazionale di Fisica Nucleare, Sezione di Pisa, Italy  
Instituto Superiore di Sanita, Laboratorio della Radiazioni, Rome, Italy  
M. Mando, Phys. Inst. of the University, Firenze, Italy  
C. Signorini, Istituto di Fisica, Padova, Italy  
Y. Abe, Kyoto U., Japan  
K. Hiida, U. Tokyo, Japan

T. Hirano, Hosei U., Tokyo, Japan  
K. Iwatani, Hiroshima U., Japan  
K. Katori, U. of Tsukuba, Japan  
Nagoya U., Dept. of Physics, Preprint Center, Japan  
G. Narumi, Hiroshima U., Japan  
H. Ohnuma, Tokyo Inst. Technology, Japan  
K. Sugiyama, Tohoku U., Japan  
Tokyo, U. of, High Energy Physics Lab., Japan  
Tokyo, U. of, Inst. for Nuclear Study, Lib., Japan  
Tokyo, U. of, Meson Science Lab., Japan  
K. Tsukada, Japan Atomic Energy Research Inst., Japan  
Y. S. Kim, Atomic Energy Research Institute, Seoul, Korea  
Instituto de Fisica, Theoretical Physics Grp., Preprint Lib., Mexico City, Mexico  
Instituto Politecnico Nacional Physics Dept. Lib., Mexico City, Mexico  
J. Blok, Free U., Amsterdam, The Netherlands  
J. de Jager, Bibliotheek V.U., Natuurkunde, Amsterdam, The Netherlands  
H. de Waard, Rijksuniversiteit, Groningen, The Netherlands  
P. F. A. Goudsmit, Inst. for Nuclear Physics Research, Amsterdam, The Netherlands  
Koninklijke Nederlandse Akademie van Wetenschappen, Library, Amsterdam, The Netherlands  
R. H. Siemssen, U. Groningen, The Netherlands  
A. Poletti, U. Auckland, New Zealand  
J. F. Williams, Queens U., Belfast, Northern Ireland  
Pakistan Inst. of Nuclear Science and Technology, Rawalpindi, Pakistan  
Quaid-e-Azam U., Dcpt. of Physics, Islamabad, Pakistan  
Q. O. Navarro, Philippine Atomic Research Center, Quezon City, Philippine Islands  
J. Kuzminski, Inst. of Physics, Katowice, Poland  
W. Zych, Inst. of Nuclear Research, Warsaw, Poland  
F. da Silva, Lab. de Fisica e Engenharia Nucleares, Sacavem, Portugal  
Institute for Physics and Nuclear Eng., Bucharest, Romania  
U. of Timisoara, Library, Romania  
D. Branford, U. Edinburgh, Scotland  
D. H. Pringle, Nuclear Enterprises Ltd., Edinburgh, Scotland  
F. D. Brooks, U. Cape Town, South Africa  
W. R. McMurray, Southern Universities Nuclear Inst., Faure, South Africa  
D. W. Mingay, Atomic Energy Board, Pretoria, South Africa  
D. Reitmann, Atomic Energy Board, Pretoria, South Africa  
J. P. F. Sellschop, U. of the Witwatersrand, South Africa  
O. Almen, Chalmers U. of Technology, Sweden  
I. Bergstrom, Nobelinstitut for Fysik, Stockholm  
M. Braun, Research Inst. of Physics, Stockholm, Sweden  
N. Ryde, Chalmers U. of Technology, Sweden  
Tandem Accelerator Lab., Uppsala, Sweden  
K. Kubodera, Swiss Inst. for Nuclear Studies, Villigen, Switzerland  
J. Rafelski, CERN, Geneva, Switzerland  
S. Ketudat, Chulalongkorn U., Bangkok, Thailand  
A. Saplakoglu, Ankara Nuclear Research and Training Center, Ankara, Turkey  
A. J. Kalnay, IVIC, Physics Section, Caracas, Venezuela  
Venezuela, Universidad Central de, Physics Dept., Caracas, Venezuela